ATMOSPHERIC TRANSPORT OF HYDROGEN SULFIDE FROM PROPOSED GEOTHERMAL POWER PLANT (UNIT 13)

Predictions by Physical Modeling
in a Wind Tunnel

by

R. L. Petersen**, J. E. Cermak*,
and Samir Ayad**

Prepared for

Aminoil USA, Incorporated
Santa Rosa, California

Fluid Dynamics and Diffusion Laboratory
Fluid Mechanics and Wind Engineering Program
Colorado State University
Fort Collins, Colorado
80523

April 1977

CER76-77RLP-JEC-SA51

*Director, Fluid Dynamics & Diffusion Laboratory
**Graduate Research Assistant, Department of Civil Engineering

EXECUTIVE SUMMARY

Tests were conducted in the Colorado State University Environmental Wind Tunnel Facility of the transport and dispersion of the H_2S plume emanating from a geothermal steam venting located near Anderson Springs, California. The wind tunnel tests were conducted with a terrain modeled to a scale of 1:1920 and also with scale models of a surface release and stack releases of varying exit velocity and height (0 and 30 m). For the surface release exit velocities were varied to simulate a 100 and 21 percent flow of steam to Unit 13. The effects of wind direction and wind speed upon the ground level H_2S concentrations for the various source configurations in the vicinity of Anderson Springs and Whispering Pines were established based on a constant source strength of 100 ppm. Data obtained include photographs and motion pictures of smoke plume trajectories and ground level tracer gas concentrations downwind of the source.

The results of the study can be summarized as follows:

- The maximum H_2S concentrations near Anderson Springs were observed to be 1) 49.8 ppb for a surface release, 250° wind direction, 9.4 m/s wind speed and 12.7 m/s exit velocity, 2) 2.2 ppb for a surface stack release, a 230° wind direction and a 9.4 m/s wind speed and 3) 104.2 ppb for a 30m stack release, 250° wind direction, 9.4 m/s wind speed and 20.6 m/s exit velocity.

- The maximum H_2S concentrations near Whispering Pines were observed to be 1) 12.5 ppb for a surface release, 210° wind direction, 6.2 m/s wind speed and 12.7 m/s exit velocity, 2) 9.8 ppb for a surface stack release, a 6.2 m/s wind speed, 210° wind direction and a 111.7

m/s exit velocity, and 3) 10.5 ppb for a 30 m stack release, 210° wind direction, 9.4 m/s wind speed and 111.7 m/s exit velocity.

- The use of stacks (30 m or less) and increased exit velocity as a modification to the existing steam venting (surface release) does not reduce the expected maximum H_2S ground level concentration for the wind directions studied. In some cases the modifications would increase concentrations.

- Curves are presented for the surface release which give a range of volume flow rates at given wind speed for which the 30 ppb limit will not be exceeded at locations studied in the wind tunnel. The curves show that 100 percent flow (816.2 m^2/s) is allowable for all wind speeds studied with a 210° wind direction. For the 230 and 250° wind directions the allowable flow rates varies with wind speed and is always below 100 percent.

- The added heat due to the steam venting increases plume rise and hence decreases the ground level concentrations. This affect is most noticeable at the low wind speeds.

ACKNOWLEDGMENTS

The support of Aminoil USA, Incorporated in carrying out this study is gratefully acknowledged. Construction of the building model was accomplished by personnel of the Engineering Research Center machine shop. Mr. James A. Garrison supervised construction of the terrain model and photographic recording of the flow visualizations. The authors also acknowledge the assistance of Mrs. Stephanie Allen in typing and organizing this report. The help of the following students throughout the research is appreciated: Mr. Stan Schwartz, Mr. Dave Graham, Mr. Tom Zook, Mr. Chris Leveroni, Mr. Jim DeCino, Mr. John Elmer, and Mr. Herb Riehl.

TABLE OF CONTENTS

LIST OF TABLES

LIST OF TABLES
(Continued)

LIST OF TABLES
(Continued)

LIST OF TABLES
(Continued)

LIST OF TABLES
(Continued)

LIST OF TABLES
(Continued)

LIST OF TABLES
(Continued)

LIST OF FIGURES

LIST OF FIGURES
(Continued)

LIST OF FIGURES
(Continued)

LIST OF FIGURES
(Continued)

LIST OF FIGURES
(Continued)

LIST OF FIGURES
(Continued)

LIST OF FIGURES
(Continued)

LIST OF SYMBOLS

Symbol	Definition	
D	Stack Diameter	(L)
D_e	Hydraulic Diameter	(L)
E	Gas Chromatagraph Response	(mvs)
Fr	Froude Number $\frac{v^2}{g(\frac{\Delta\rho}{\rho_a})\ D}$	(-)
g	Gravitational Constant	(L/T^2)
h	Stack Height	
H	Effective Ridge Height	(L)
k	von Karman Constant	(-)
K	Concentration Isopleth	(-)
L	Characteristic Length	
ℓ	Building Length	(L)
p	Pressure	$(M/T^2/L)$
Q	Source Strength	(M/T)
r^2	Correlation Coefficient	(L)
R	Exhaust Velocity Ratio V_s/V_a	(-)
R_c	Cold Resistance	(Ω)
R_e	Reynolds Number $\frac{VL}{\nu}$	(-)
R_n	Hot Resistance	(Ω)
U_*	Friction Velocity	(L/T)
V	Mean Velocity	(L/T)
W	Building Width	(L)
x,y,z	General Coordinates - Downwind, Lateral, Upwind	(L)
z_o	Surface Roughness Parameter	(L)

LIST OF SYMBOLS
(continued)

Symbol	Definition	
χ	Local Concentration	(M/L^3 or ppm)
τ	Sampling Time	(T)
θ	Azimuth Angle of Upwind Direction Measured from Plant North	(-)
σ	Standard Deviation of Either Plume Dispersion or Wind Angle Fluctuations	(L), (-)
Λ	Volumetric Flow	(L^3/t)
ν	Kinematic Viscosity	(L^3/T)
δ	Boundary Layer Thickness	(L)
γ	Density Ratio	$M(T^2L^2)$
ρ	Density	(M/L^3)
Ω	Angular Velocity	(1/T)
μ	Dynamic Viscosity	M/(TL)
$\Delta\Gamma$	Specific Weight Difference	M/(TL)

Subscripts

a	Free Stream
s	Stack
m	Model
p	Prototype
max	Maximum

1.0 INTRODUCTION

The purpose of this study was to determine the transport characteristics of hydrogen sulfide released in plumes emanating from steam releases at a proposed new geothermal power plant (Unit 13). The location of Unit 13 is shown in Figure 1.1 in relation to Anderson Springs and Whispering Pines.

Using a 1:1920 scale model of the source and surrounding topography in a wind tunnel capable of simulating the appropriate meteorological conditions, downwind ground-level H_2S concentrations were measured by sampling concentrations of a tracer gas (propane) released from the model. Overall plume geometry was obtained by photographing the plumes made visible by releasing smoke (titanium tetrachloride) from the modeled source. Source geometry corresponded to 1) a ground level release over a 2.4 m x 244 m area (hereafter referred to as "surface release"), 2) a circular ground level release with varying exit velocity (referred to as "surface stack release") and 3) a 30.5 m stack release with varying exit velocity (referred to as "stack release").

The primary focus of this study was on H_2S concentrations in the vicinity of Anderson Springs and Whispering Pines for neutral thermal stratification. Accordingly, studies of the upper-level winds were confined to three directions: 210°, 230°, and 250° azimuth. Figure 1.2 shows the wind rose which was obtained from a meteorological tower in the vicinity of the sites under study (see Figure 1.1 for relative location). Information from the meteorological station indicated that winds in the sector 210° to 250° occur approximately 40 percent of the time. Wind speeds of 3.1, 6.2, and 9.4 m/s were modeled to obtain representative concentrations under beneficial and adverse plume rise conditions.

A secondary objective was to relate wind speed at the proposed Unit 13 site to that at the meteorological station in the area and the upper-level (ambient) wind speed in the wind tunnel.

Included in this report are a brief description of the similarity requirements for atmospheric motion, and explanation of test methodology and procedures, results of plume visualization and concentration measurements, results of wind flow measurements, and a summary of the results.

This report is supplemented by a motion picture (in color) which shows plume behavior for the various wind speed and wind direction test scenarios. Black and white photographs as well as slides of each plume visualization further illustrate the material presented.

2.0 SIMULATION OF ATMOSPHERIC MOTION

The use of wind tunnels for model tests of gas diffusion by the atmosphere is based upon the concept that nondimensional concentration coefficients will be the same at corresponding points in the model and the prototype and will not be a function of the length scale ratio. Concentration coefficients will only be independent of scale if the wind tunnel boundary layer is made similar to the atmospheric boundary layer by satisfying certain similarity criteria. These criteria are obtained by inspectional analysis of physical statements for conservation of mass, momentum, and energy. Detailed discussions have been given by Halitsky (1963), Martin (1965), and Cermak, et al. (1966). Basically, the model laws may be divided into requirements for geometric, dynamic, thermic, and kinematic similarity. In addition, similarity of upwind flow characteristics and ground boundary conditions must be achieved.

For this study, geometric similarity was satisfied by an undistorted model of length ratio 1:1920. This scale was chosen to facilitate ease of measurements and to provide a representative upwind fetch.

When interest is focused on the vertical motion of plumes of heated gases emitted from stacks into a thermally neutral atmosphere, the following variables are of primary significance:

ρ_a = density of ambient air

$\Delta\Gamma = (\rho_a - \rho_s)g$ - difference in specific weight of ambient air and source exhaust

Ω = local angular velocity component of earth

μ_a = dynamic viscosity of ambient air

V_a = speed of ambient wind at meteorological tower height (10 m)

V_s = speed of gas emission

h = stack height

H = local difference in elevation of topography

D = stack diameter

δ_a = thickness of planetary boundary layer

z_o = roughness heights for upwind surface

Grouping the independent variables into dimensionless parameters with ρ_a, V_a and H as reference variables yields the following parameters upon which the quantities of interest must depend:

$$\frac{V_a}{H\Omega}, \frac{\delta_a}{H}, \frac{z_o}{H}, \frac{D}{H}, \frac{V_a \rho_a H}{\mu_a}, \frac{V_s}{V_a}, \frac{V_a^2}{g\gamma D}, \gamma$$

where $\gamma = \frac{\rho_a - \rho_s}{\rho_a}$.

Tables 2.1 and 2.2 summarize the pertinent dimensional and dimensionless parameters which were modeled in this study. The source volumetric emission rates and gas densities represent cooling tower source parameters and not a super heated steam. Appendix A includes a comparison of model test results using source parameters for superheated steam and those conditions given in Tables 2.1 and 2.2 (cooling tower parameters). The appendix shows that the ground level concentrations are less for the superheated steam release.

The laboratory boundary layer thickness $\frac{\delta_a}{H}$ was estimated to be nearly equal for model and prototype. Near equality (within a factor of two) of the surface parameter $\frac{z_o}{H}$ for model and prototype was achieved through geometrical scaling of the source and upwind roughness. The source parameter $\frac{D}{H}$ was equal for model and prototype.

The magnitude of the roughness parameter, z_o, for the model was calculated by using the logarithmic wind equation:

$$\frac{V}{U^*} = \frac{1}{\kappa} \ln \left(\frac{z}{z_o}\right)$$

The wind speed at heights 1.27 cm and 2.54 cm above the model terrain were substituted into the equation. With the resulting two equations, z_o (and U*) was calculated. The magnitude of z_o for the prototype was estimated by reference to a plot of z_o versus terrain type present in Cermak (1975).

Dynamic similarity is achieved in a strict sense if the Reynolds number, $\frac{\rho_a V_a H}{\mu_a}$, and Rossby number, $\frac{V_a}{H\Omega}$, for the model are equal to their counterparts in the atmosphere. The model Rossby number cannot be made equal to the atmospheric value. However, over the short distances considered (up to 5000m), the Coriolis acceleration has little influence upon the flow. Accordingly, the standard practice is to relax the requirement of equal Rossby numbers (Cermak, 1971).

Kinematic similarity requires the scaled equivalence of streamline movement of air over prototype and model. It has been shown in Halitsky, et al. (1963) that flow around geometrically similar sharp-edged buildings at ambient temperatures in a neutrally stratified atmosphere should be dynamically and kinematically similar when the approaching flow is kinematically similar. This approach depends upon producing flows in which the flow characteristics become independent of Reynolds number if a lower limit of the Reynolds number is exceeded. For example, the resistance coefficient for flow in a sufficiently rough pipe, as shown in Schlichting (1960, p. 521), is constant for a Reynolds number larger than 2×10^4. This implies that surface or drag forces are directly proportional to the mean flow speed squared. In turn, this condition is the necessary condition for mean turbulence statistics such as root-mean-square value and correlation coefficient of the turbulence velocity components to be equal for the model and the prototype flow.

Equality of the parameter $\frac{V_a^2}{g\gamma D}$ for model and prototype in essence determines the relationship between the atmospheric wind speed and the model wind speed once the geometric scale has been selected (1:1920 in this case). Often this criteria results in $(V_a)_m$ being too small to satisfy the minimum Reynolds number requirement. When this happens, the density ratio for the model $(\gamma)_m$ can be made larger than $(\gamma)_p$ to compensate for the effect of small geometric scale. However, this relaxes the equality of the density difference ratio for model and prototype. This equality ensures that the initial plume behavior where acceleration of the source gases is maximum will be modeled correctly. However, for this study, near field plume behavior is not important and relaxation of the density ratio equality is justified.

Using a wind speed of $(V_a)_p$ of 3.1 m/s at the meteorological tower height (10 m), a scale of 1:1920, and a density ratio of $\frac{\gamma_m}{\gamma_p} = 7.9$, the Froude number equality gives

$$\frac{(V_a)_m^2}{(V_a)_p^2} = \frac{1}{1920} \frac{(\gamma)_m}{(\gamma)_p} \text{ or}$$

$$(V_a)_m = \left(\frac{1}{43.8}\right) (7.9)^{1/2} (3.1) = 0.20 \text{ m/s.}$$

The corresponding representative model velocity at a height of .46 m (878 m prototype) is 0.34 m/s. Using this velocity as the free-stream velocity and a distance of 13.6 m from the beginning of the wind tunnel to the test site, the Reynolds number becomes

$$Re_L = \frac{0.34 \times 13.6}{15 \times 10^{-6}} = 3.1 \times 10^5.$$

Referring to Figure 2.1 from Cermak (1975) it can be seen that for a Reynolds number of 3.1×10^5 the surface length-roughness length ratio L/K_s must be less than 250 for the flow to be independent of Reynolds number. Thus K_s, the roughness length, must be greater than $\frac{13.6}{250}$ or 0.054 m. Taking the ridge height as the roughness height, K_s, results in $K_s = 0.06$ m, which is nearly equal to the critical value of 0.054. Consequently, the flow over the test section is Reynolds number independent.

The method used to increase the Reynolds number such that the flow was independent of Re was to increase the specific weight difference between model and prototype. Since $\frac{(\gamma)_m}{(\gamma)_p} = 7.9$ represented the maximum specific weight difference practically attainable, the greatest increase in the local Reynolds number was achieved using this difference. Since the minimum Reynolds number for the cases studied was 3.1×10^5, similarity of concentration distributions over the topographic surface can be assured for all wind speeds studied.

To summarize, the following scaling criteria were applied for the neutral boundary layer situation:

1. $Fr = \frac{V_a^2}{g\gamma D}$; $(Fr)_m = (Fr)_p$,
2. $R = \frac{V_s}{V_a}$; $R_m = R_p$,
3. $L/K_s > 250$ (implies Reynolds number independence),
4. $(z_o)_m = (z_o)_p$,
5. Similar geometric dimensions,
6. Similar velocity and turbulence profiles upwind.

3.0 TEST APPARATUS

3.1 Wind Tunnels

The Environmental Wind Tunnel (EWT) shown in Figure 3.1 was used for this neutral flow study. This wind tunnel, especially designed to study atmospheric flow phenomena, incorporates special features such as adjustable ceiling, rotating turntables, transparent boundary walls, and a long test section to permit adequate reproduction of micro-meteorological behavior. Mean wind speeds of 0.06 to 37 m/second (0.14 to 80 miles/hour) in the EWT can be obtained. In the EWT, boundary layers four feet thick over the downstream 12.2 meters can be obtained with the use of vortex generators at the test section entrance. The flexible test section roof on the EWT is adjustable in height to permit the longitudinal pressure gradient to be set at zero.

3.2 Model

The source was modeled to a scale of 1:1920. Four different source models were constructed: a 0.13 by 1.3 cm area source (2.44 by 24.4 m prototype) and three stacks of height 1.59 cm (30.5 m prototype) with diameters of 0.16 cm, 0.21 cm, and 0.37 cm. Surface stack releases were simulated by burying the stack in the styrofoam so that the stack top was flush with the surface. In this manner three gas release modes were studied: 1) surface release, 2) stack release and 3) surface stack release. The relevant building dimensions are given in Table 2.1 and a photograph of the models is shown in Figure 3.2-1.

Topography was modeled to the same scale by cutting styrofoam sheets of 0.6 cm and 1.27 cm thicknesses to match contour lines of a topographic map enlarged to the 1:1920 scale. The topography for the

210° wind direction is shown mounted in the wind tunnel in Figure 3.2-2. Sections of modeled topography for the three wind directions were constructed for regions upwind and downwind of the topography mounted on the 3.66-meter diameter turntable. In this way, rectangular regions could be fitted into the wind tunnel test section.

An array of sampling tubes was inserted into the model terrain to give a minimum of 34 representative sampling locations for each wind direction. The sampling locations for each wind direction are shown in Figures 3.2-3, 3.2-4, and 3.2-5 and enumerated in Table 3.2-1.

Metered quantities of gas were allowed to flow from the modeled source to simulate the exit velocity. The exit velocities simulated were 2.5 and 12.7 m/s (100 and 21% volume flow) for the area source and 20.6, 63.1, and 111.7 m/s (100% flow) for the three stacks. Helium, compressed air, and propane (the tracer) were mixed to give the highest practical specific weight. Fischer-Porter flow rotor settings were adjusted for pressure, temperature, and molecular weight effects as necessary. When a visible plume was required, the gas was bubbled through titanium tetrachloride before emmission.

3.3 Flow Visualization Techniques

Smoke was used to define plume behavior from the geothermal power plant complex. The smoke was produced by passing the air mixture through a container of titanium tetrachloride located outside the wind tunnel and transported through the tunnel wall by means of a tygon tube terminating at the source structure inlet. A schematic of the process is shown in Figure 3.3-1.

The plume was illuminated with arc-lamp beams and a visible record was obtained by means of pictures taken with a Speed Graphic camera.

Additional still pictures were obtained with a Hasselblad camera. Stills were taken with a camera speed of one second to identify mean plume boundaries. A series of color motion pictures were also taken with a Bolex motion picture camera.

3.4 Gas Tracer Technique

After the desired tunnel speed was obtained, a mixture of propane, helium, and air of predetermined concentration was released from the source tower at the required rate. Samples of air were withdrawn from the sample points and analyzed. The flow rate of propane mixture was controlled by a pressure regulator at the supply cylinder outlet and monitored by a Fischer and Porter precision flow meter. The sampling system is shown in Figure 3.4-1.

-Analysis of Data-

Propane is an exellent tracer gas in wind tunnel dispersion studies. It is a gas that is readily obtainable and of which concentration measurements are easily obtained using gas chromatography techniques.

The procedure for analyzing the samples was as follows:

1. A sample volume drawn from the wind tunnel of 2 cc was introduced into the Flame Ionization Detector.
2. The output from the electrometer (in millivolt seconds) was integrated and then the readings were recorded for each sample.
3. These readings were transformed into propane concentration values by the following steps:

$$\chi(\text{ppm}) = C(\text{ppm/mvs})E(\text{mvs})$$

where C was determined from a calibration gas of known concentration

$$C = (\text{ppm/mvs}) \text{ calibration gas.}$$

The values of the concentration parameter initially determined apply to the model and it is desirable to express these values in terms of the field. At the present time, there is no set procedure for accomplishing this transformation. The simplest and most straightforward procedure is to make this transformation using the scaling factor of the model. Since

$$1m|_m = 1920m|_p,$$

one can write

$$\frac{\chi V}{Q}\Big|_p(m^{-2}) = \frac{1}{1920^2}\frac{\chi V}{Q}\Big|_m(m^{-2}).$$

The sample scaling of the concentration parameter from model to field appears to give reasonable results. All data reported herein are in terms of the dimensionless value, $K = \frac{\chi V_a D^2}{Q}$ and in terms of H_2S concentration $\chi_p(H_2S) = \left(\frac{1}{1920}\right)\left(\frac{\chi V}{Q}\right)_m\left(\frac{Q}{V}\right)_p$.

-Errors in Concentration Measurement-

Each sample, as it passes through the flame ionization detector, is separated from its neighbors by a period during which nitrogen flows. During this time, the detector is at its baseline, or zero level. When the sample passes through the detector, the output rises to a value equal to the baseline plus a level proportional to the amount of tracer gas flowing through the detector. The baseline signal is set to zero and monitored for drift. Since the chromatograph used in this study features a temperature control on the flame and electrometer, there is very low drift. The integrator circuit is designed for linear response over the range considered.

A total system error can be evaluated by considering the standard deviation found for a set of measurements where a precalibrated gas mixture is monitored. For a gas of ~ 100 ppm propane ± 1 ppm, the average standard deviation from the electrometer was two percent. Since the source gas was premixed to the appropriate molecular weight and repetitive measurements were made of its source strength, the confidence in source strength concentration is similar. The flow rate of the source gas was monitored by Fischer-Porter flowmeters which are expected to be accurate to two per cent, including calibration and scale fraction error. The wind tunnel velocity was constant to ± 10 per cent at such low settings. Hence, the cumulative confidence in the measured values of $\frac{\chi V}{Q}$ will be a standard deviation of about ± 11 per cent, whereas the worst cumulative scenario suggests an error of no more than ± 20 per cent.

The lower limit of measurement is imposed by the instrument sensitivity and the background concentrations of hydrocarbons in the air within the wind tunnel. Background concentrations were measured and subtracted from all measurements quoted herein; however, a lower limit of 1 to 2 ppm of propane is available as a result of background methane levels plus previous propane releases. An upper limit for propane with the instrument used is 10 per cent propane by volume. A recent report on the flame ionization detector for sampling gases in atmospheric wind tunnels prepared by Dear and Robins (1974) arrives at similar figures.

-Test Results: Concentration Measurements-

Since the conventional point-source diffusion equations cannot be used for predicting diffusion near objects which cause the wind to be nonuniform and nonhomogeneous in velocity and turbulence, it is necessary to calculate gaseous concentrations on the basis of experimental data.

It is convenient to report dilution results in terms of a nondimensional factor independent of model to prototype scale.

In Cermak et al. (1966) and Halitsky (1963), the problem of similarity for diffusing plumes is discussed in detail. Considering this, the concentration measurements were transformed to K-isopleths by the formula

$$K = \left(\frac{\chi V_a d^2}{Q} \right)_m$$

where

χ_m = sample concentration (ppm)

D_m = cell diameter (m)

V_{a_m} = mean wind velocity at the meteorological station height (m/s)

Q_m = gas source release rate (ppm m^3/s)

Thereafter prototype H_2S concentrations were calculated assuming a 100 ppm H_2S prototype source strength with the following relation

$$\chi_p = \frac{K \Lambda \ 10^5}{V_{a_p} D_p^2}$$

where

Λ = Prototype volume flow rate (172.3 and 816.2 m^3/s)

χ_p = H_2S concentration (ppb)

When interpreting model diffusion measurements, it is important to remember that there can be considerable difference between the instantaneous concentration in a plume and the average concentration due to horizontal meandering. In the wind tunnel, a plume does not generally meander due to the absence of large-scale eddies. Thus, it is found that field measurements of peak concentrations which effectively

elimate horizontal meandering should correlate with the wind tunnel data (Hino, 1968). In order to compare downwind measurements of dispersion to predict average field concentrations, it is necessary to use data on peak-to-mean concentration ratios as gathered by Singer, et al. (1953, 1963). Their data is correlated in terms of the gustiness categories suggested by Pasquill for a variety of terrain conditions. It is possible to determine the frequency of different gustiness categories for a specific site. Direct use of wind tunnel data at points removed from the building cavity region may underestimate the dilution capacity of a site by a factor of four unless these adjustments are considered (Martin, 1965).

To estimate the equivalent prototype sampling time another dimensionless variable was derived by including time as one of the pertinent parameters. The relationship then exists

$$\left(\frac{\tau U_a}{L}\right)_m = \left(\frac{\tau U_a}{L}\right)_p$$

or,

$$\tau_p = \tau_m \left(\frac{L_p}{L_m}\right) \left(\frac{U_m}{U_p}\right) .$$

Since the model sampling time was approximately 30 s, then

$$\tau_p = \frac{30}{60} \left(\frac{1920}{1}\right) \left(\frac{7.2}{1920}\right)^{1/2} = 59 \text{ min.}$$

Since the prototype sampling time of interest is one hour, the data presented herein have not been corrected for sampling time.

3.5 Wind Profile Measurements

-Hot Wire Measurements-

Velocity measurements over the terrain model at various locations were obtained using hot wire anemometry techniques.

A constant temperature TSI hot wire anemometer* was used for measuring both the root-mean-square value and the mean of the wind speed in the wind tunnel model. Calibration over the model was carried out in small calibrated flow chambers. The calibration measurements were correlated to King's law and put in the following form:

$$\frac{E^2}{R_h(R_h-R_c)} = A + BU^n$$

where

R_h = hot resistance of the wire

R_c = cold resistance of the wire

E = the output signal of the wire (millivolts)

U = the velocity sensed (meters/second)

n, A and B = the constants of King's law

Although the power n was found to be close to 0.5 over the velocity range 1.8 m/s to 15.2 m/s, it was found to be equal to 0.6634 at the low velocity range 0.03 m/s to 1.2 m/s. The Kings's law constants are thus

A = 0.266955

B = 0.036573

n = 0.6694

To obtain the velocity measurements, a calibrated carriage was used, together with a digital voltameter. In this manner, the location of the hot-wire probe over the terrain could be adjusted from outside the tunnel.

---

*Detailed discussion on hot wire anemometry can be found in textbooks. Only those concepts that are essential to our measurements are presented here.

-Smoke-Wire Wind Profile Visualization-

The smoke-wire system was used to visualize instantaneous wind profiles. The smoke-wire probe (shown in Figure 3.5-2) is a tubular frame on which a nichrome wire 0.05 cm in diameter and approximately 66 cm long (1267 m-prototype) is held in a vertical position on insulated contacts. The wire, of about 325 ohm-per-foot resistance, is coated with a light oil, which, when heated, will rapidly evaporate and form a line of smoke which moves with the air stream and traces the velocity profiles instantaneously. The heating of the nichrome wire is accomplished by discharging a capacitor through it; the pulse of current from the capacitor (two micro-Farad) causes rapid heating of the wire and vaporization of the oil. The trigger control circuit is adjusted to 1000 volts. The electronic pulse is also used to start a time counter.

The visualizations presented herein were taken with a 0.5-second delay; the smoke wire probe was located at three different positions (denoted by S, A and M in Figure 32.3) at simulated elevations of 720, 793, and 976 m, MSL.

4.0 TEST PROGRAM RESULTS - SURFACE RELEASE

4.1 Plume Visualization

The test results consist of photographs and movies showing the surface release plume behavior for different wind directions and speeds. Of particular interest is the plume transport and dispersion in the vicinity of Anderson Springs and Whispering Pines.

The sequence of photographs in Figure 4.1-1 and 4.1-2 show plume behavior for the 250° and 210° wind directions, a 12.7 m/s exit velocity, and wind speeds of 3.1, 6.2, and 9.4 m/s for each direction. Photographs for the other cases studied are not presented because the smoke was not visible in the pictures. The plume behavior for each direction is generally the same. For the light wind speed cases (3.1 m/s) the plume tends to achieve more rise. However, as the wind speed increases, the plume altitude decreases, and for the high wind speed cases, the plume tends to follow along the terrain confluences.

Although the figures do not show the plume transport clearly, visual observations indicate the plume was transported over Anderson Springs for the 250° wind direction and over Whispering Pines for the 210° wind direction.

Complete sets of still photographs supplement this report. Color motion pictures have been arranged into titled sequences and the sets available are given by run number in Table 4.1-1.

4.2 Concentration Measurements

The diffusion of gaseous effluent emitted from the model surface release was studied for three wind directions (250°, 230°, and 210°

azimuth), three wind speeds for each direction (3.1, 6.2, and 9.4 m/s), and two exit velocities (2.5 and 12.7 m/s) for each wind speed. Propane concentrations at ground level were measured at distances from 1200 to 4000 meters downwind.

For each wind direction studied, thirty-four gas samples were collected at ground level. The sampling arrays for the three wind directions are shown in Figures 3.2-3, 3.2-4, and 3.2-5. The prototype locations for all sampling points are summarized in Table 3.2-1 with north and east as positive directions. The zero coordinate is the center of the terrain which was mounted on the turntable. This point is represented by the base of the wind direction arrow in all figures.

All concentration data have been reported as H_2S concentrations and as dimensionless coefficients as explained in Section 3.4.

The results for wind directions and speeds studied are presented in Tables 4.2-1 through 4.2-18. Sample locations in the tables are defined in Table 3.2-1 and Figures 3.2-3, 3.2-4, and 3.2-5.

In order to visually and quantitatively assess the effect of wind direction and wind speed on ground level concentration patterns, Figures 4.2-1 through 4.2-18 were prepared. These figures show isopleths of H_2S concentration for the wind directions and speeds studied. These figures show an increase in maximum ground level concentration with increased wind speed for the case with an 12.7 m/s exit velocity. The case with the 2.5 m/s exit velocity shows generally little change in maximum value with wind speed.

The highest H_2S concentration near Anderson Springs of 49.8 ppb was observed to occur with a 250° wind direction at 9.4 m/s. Figure 4.2-6 shows the isopleth pattern for this case. At this speed and

direction, it is evident that the plume is mixed rapidly to the ground after emission and follows the terrain confluences down through Anderson Springs. The highest H_2S concentration near Whispering Pines of 12.5 ppb was observed to occur with a 210° wind direction and 6.2 m/s wind speed. The isopleth patterns for this case are shown in Figure 4.2-17.

5.0 TEST PROGRAM RESULTS - STACK RELEASE

5.1 Plume Visualization

The tests results consist of photographs and movies showing stack release plume behavior for different wind directions and speeds. Three 1.6 cm stacks (30.5 m prototype) of different diameters were used to simulate exit velocities of 20.6, 63.1, and 111.7 m/s. Of particular interest was the plume transport and dispersion in the vicinities of Anderson Springs and Whispering Pines.

The sequence of photographs in Figure 5.1-1 through 5.1-9 show plume behavior for the 250°, 230°, and 210° wind direction, wind speeds of 3.1, 6.2, and 9.4 m/s for each direction, and exit velocities of 20.6, 63.1, and 111.7 m/s. The plume behavior for each direction is generally the same. For the light wind speed cases (3.1 m/s), the plume tends to rise over the underlying terrain. However, as the wind speed increases, the plume altitude decreases and for the high wind speed case tends to follow along the terrain confluences. Because of low model volume flow rates, plume behavior is not completely visible in the photographs. However, visual observations during the study confirm the above results.

The plume was observed to be transported over Anderson Springs for the 250° wind direction and over Whispering Pines for the 210° wind direction.

Complete sets of still photographs supplement this report. Color motion pictures have been arranged into titled sequences and the sets available are summarized by run number in Table 5.1-1.

5.2 Concentration Measurements

The diffusion of gaseous effluent emitted from the three stacks was studied for three wind directions (250°, 230°, and 210° azimuth),

three wind speeds for each direction (3.1, 6.2, and 9.4 m/s), and three exit velocities for each speed (20.6, 63.1, and 111.7 m/s). Propane concentrations were measured at distances from 1200 to 4000 meters downwind.

For each wind direction studied, thirty-four gas samples were collected at ground level. The sampling arrays for the three wind directions are shown in Figure 3.2-3, 3.2-4, and 3.2-5. The prototype locations for all sampling points are summarized in Table 3.2-1 with north and east as positive directions. The zero coordinate is the center of the terrain which was mounted on the turntable. This point is represented by the base of the wind direction arrow in all figures.

All concentration data have been reported as H_2S concentrations and as dimensionless concentration coefficients as explained in Section 3.4.

The results for the wind directions and speeds studied are presented in Tables 5.2-1 through 5.2-27. Sample locations in the tables are defined in Table 3.2-1 and Figures 3.2-3, 3.2-4, and 3.2-5.

In order to visually and quantitatively assess the effect of wind direction and wind speed on ground level concentration patterns, Figures 5.2-1 through 5.2-27 were prepared. These figures show isopleths of H_2S concentration for the wind directions, wind speeds, and exit velocities studied. These figures clearly show the increase in maximum ground level concentration with increased wind speed. Also shown is the decrease in maximum ground level value with increasing stack exit velocity. For all cases, the concentrations were low (> 2 ppb) for the light wind speed case.

The highest H_2S concentration near Anderson Springs of 104.2 ppb was observed to occur with a 250° wind direction at 9.4 m/s with a 20.6 m/s exit velocity. Figure 5.2-3 shows the isopleth pattern for this case. At

this speed and direction, it is evident that the plume is mixed rapidly to the ground after emission and follows the terrain confluences down through Anderson Springs.

The highest H_2S concentration near Whispering Pines of 12.4 ppb was observed to occur with a 210° wind direction at 6.2 m/s with an exit velocity of 111.7 m/s.

6.0 TEST PROGRAM RESULTS - SURFACE STACK RELEASE

6.1 Plume Visualization

The test results consist of photographs and movies showing the surface stack release plume behavior for different wind directions and speeds. Three exit speeds (20.6, 63.1, and 111.7 m/s) for the surface stack release were studied. Of particular interest was the plume transport and dispersion in the vicinity of Anderson Springs and Whispering Pines.

The sequence of photographs in Figures 6.1-1, 6.1-2, and 6.1-3 shows plume behavior for the 230° and 210° wind directions at speeds of 6.2 and 9.4 m/s for each direction with exit velocities of 20.6, 63.1, and 111.7 m/s. Only the higher wind speed cases were considered to offer a general comparison between changes in stack height (i.e. between 0 and 30.5 m prototype).

From the figures, it appears that increased exit velocities do not significantly increase the effective plume altitude. This is probably due to the fact that the plume is released at ground level within a small canyon and by the time the plume reaches the canyon top, it has lost much of its momentum.

Complete sets of still photographs supplement this report. Color motion pictures have been arranged into titled sequences and the sets available are summarized by run number in Table 6.1-1.

6.2 Concentration Measurements

The diffusion of gaseous effluent emitted from three surface stack releases were studied for two wind directions (230° and 210° azimuth), and two wind speeds (6.2 and 9.4 m/s) for the 210° direction and one wind speed (9.4 m/s) for the 230° direction.

The surface stack releases differ from the surface release in that the effluent is emitted through a circular tube of varying diameter to simulate varying exit velocity. Propane concentrations at ground level were measured at distances from 1200 to 4000 meters downwind.

For each wind direction studied, thirty-four gas samples were collected at ground level. The sampling arrays for the two wind directions are shown in Figures 3.2-4 and 3.2-5. The prototype locations for all sampling points are summarized in Table 3.2-1 with north and east as positive directions. The zero coordinate is the center of the terrain which was mounted on the turntable. This point is represented by the base of the north arrow in all figures.

All concentration data have been reported as H_2S concentrations and as dimensionless coefficients as explained in Section 3.4.

The results for the wind directions and speeds studied are presented in Tables 6.2-1 through 6.2-9. Sample locations in the tabels are defined in Table 3.2-1 and Figures 3.2-4 and 3.2-5.

In order to visually and quantitatively assess the effect of wind direction and wind speed on ground level concentration patterns, Figures 6.2-1 through 6.2-9 were prepared. These figures show isopleths of H_2S concentration for the wind directions and speeds studied. For the 230° wind direction (9.4 m/s wind speed), these figures show a decrease in maximum concentration with increased exit velocity. For the 210° wind direction (6.2 and 9.4 m/s), the isopleth patterns appear to be rather insensitive to wind speed and exit velocity, although the peak concentrations appear to be closer to the high wind speed case (9.4 m/s).

The maximum H_2S concentration (for the wind directions considered) near Anderson Springs of 2.2 ppb was observed to occur with a 230° wind direction at 9.4 m/s. Figure 6.2-2 shows the isopleth pattern for this case. At this speed and direction, it is evident that the plume is mixed rapidly to the ground after emission and follows the terrain confluences down close to Anderson Springs.

The highest H_2S concentration near Whispering Pines of 9.8 ppb was observed to occur with a 210° wind direction at 6.2 m/s.

7.0 TEST RESULTS - VELOCITY MEASUREMENTS

This section discusses the results of the velocity measurements. Techniques for data collection are described in Section 3.5. Both the mean value and the root mean square of wind speed were measured in the wind tunnel.

The turbulence intensities $(\frac{V_{rms}}{V})$ are plotted versus height in Figure 7-1 for the meteorological station and the Aminoil test site (Site 4). As a general trend, the turbulence intensity is higher near the ground. The values of the root mean square of the velocity appear to be about 1.5 times higher at the Aminoil test site than at the meteorological station from the surface to 772 m over the terrain (0.23 m model). At higher levels, the effect of the terrain appears to be negligible and the two sites have nearly the same root mean square value of wind velocity. The two sites have nearly the same turbulence intensity above 0.23 m from the ground (this corresponds to 442 m from the ground in the prototype). It is clear in Figure 7-1 that the Aminoil test site possesses higher turbulence intensity from the ground up to 0.23 m.

Figure 7-2 shows the mean wind velocity profiles at the Aminoil test site and the meteorological station. The mean velocity at the low levels ($z \leq 0.17$ m model or 326 m prototype) appears to have higher values at the meteorological station than at Site 4. Table 7-1 enumerates the mean wind speed at the two sites for various levels relatively close to the ground. The wind speeds at meteorological tower height (10 m prototype) are also listed.

Figure 7-3 illustrates the power law fit to the following equation for the three locations:

$$\frac{V}{V_g} = \left(\frac{z}{z_g}\right)^{1/n}$$

The plots show the following values for $(\frac{1}{n})$:

$\frac{1}{n} \cong 0.12$ Meteorological Station

$\frac{1}{n} \cong .158$ Aminoil Site (Site 4)

Figure 7-4 (showing constant velocity lines over the terrain) illustrates the acceleration of the velocity on the top and downwind side of the ridge. Also evident is the general down-motion which greatly affects plume transport.

The smoke wire visualization at three different levels on the downwind side of the ridge are shown in Figure 7-5 for a low wind velocity of 0.13 m/s in the model (corresponding to 2.15 m/s in the prototype). The three profiles in each photograph represent three intervals of time (each is 0.5 seconds long). The higher intensities of turbulence and irregular velocity profiles at the low levels with respect to the terrain are evident. It is also clear that the turbulence is three-dimensional and has a vertical fluctuating component.

8.0 DISCUSSION AND SUMMARY OF RESULTS

The primary purpose of this study is to define the H_2S concentration levels through wind tunnel modeling in the vicinity of Anderson Springs and Whispering Pines which are expected to result from the steam venting of Unit 13 assuming a 100 ppm H_2S source strength. Other source strengths may be considered by simply multiplying the results presented here by the new source strength divided by 100 ppm. The overall maximum concentrations and maxima near Anderson Springs or Whispering Pines are summarized in Table 8.1 for each case studied.

One general point that is obvious from the table is the change in location of maximum concentration with ambient wind speed. This result indirectly shows the influence of the wind speed on plume rise since different plume trajectories would result in a change of location of the maximum concentration. The maximum values presented in the table should not be viewed as the highest possible values for the given simulated conditions. The wind tunnel sampling grid did not cover locations close or very far from the plant site. Hence the values in the table should be considered as the highest values observed within the wind tunnel sampling grid. The implications of the results presented in Table 8.1 will now be discussed in more detail.

Surface release - For the 100 percent volume flow cases (12.7 m/s exit velocity) maximum ground level concentrations increase with increasing wind speed. The rate of increase is slowest between 6.2 and 9.4 m/s wind speeds. The maximum ground level concentrations for the 21 percent volume flow (2.5 m/s exit velocity) cases decrease with wind speed. In order to interpolate between wind speeds and volume flow rates further analysis of the surface release test data was undertaken.

Dimensional analysis and plume rise theory leads to the following relation:

$$\frac{\chi V_a D^2}{\Lambda} = f\left(\frac{g\Lambda}{V_a^3}\right)$$

Using regression analysis the following equation was found to fit the experimental data:

$$\ell n \frac{\chi V_a D^2}{\Lambda} = A'\left(\frac{g\Lambda}{V_a^3}\right)^{n'}$$

where A' and n' were different for each wind direction studied and $2.03 < \frac{g\Lambda}{V_a^3} < 56$. If χ is set equal to 30 ppb, then a new relation between Λ and V_a is determined which gives the maximum allowable volume flow for a fixed wind speed. The equation is:

$$\Lambda^{-n} + \frac{V_a^{-3n} \ell n \Lambda}{B} = \frac{V_a^{-3n}}{B}[7.47 + \ell n V_a]$$

where n' and B are given in the following Table:

Wind Direction	n'	B
250	0.08	3.52
230	0.07	3.25
210	0.04	2.62

The above equation was solved numerically and the results are plotted in Figure 8.1. The two nearly vertical curves represent the cut-off lines for which the regression analysis does not apply. The lines labeled with the wind direction represent solutions to the above equation. For a given wind speed the volume flow must be less than the value on the solid line so that $\chi < 30$ ppb for any location studied in the wind tunnel. As can be seen in the figure for the 210° wind direction the plant can operate at 100 percent flow for all applicable

wind speeds. For 250 and 230° wind direction the allowable volume flow is below 100 percent for all indicated wind speeds.

Stack releases - This series of tests was conducted to assess the effect of increased stack height (30 m) and increased exit velocity for a 100 percent flow upon ground level concentrations. From Table 8.1 it is evident that the maximum concentration increases with wind speed for a fixed exit velocity. For a 3.1 m/s wind speed the maximum concentrations decrease with increasing exit velocity for all wind directions studied. As the wind velocity increases, the effect of exit velocity on ground level concentrations is not as apparent. For the 6.2 and 9.4 m/s cases the maximum concentrations decrease when the exit velocity changes from 20.6 to 63.1 m/s and increase when the exit velocity changes from 63.1 to 111.7 m/s. This result may indicate a change in dispersion characteristics of the plume with extremely high exit velocities. Upon comparing these results with the surface release results it appears that the highest values occur with the stack release. This is probably due to the fact that the surface release is spread more in the horizontal due to the irregular flow field in the canyon where the surface release point is located. The stack on the other hand releases the effluent above the canyon and hence the initial mixing is less.

Surface Stack Releases - These tests were similar in scope to the stack release tests except the stack height was zero and only a limited number of wind tunnel tests were run. The results in Table 8.1 show a general decrease in concentration with increased exit velocity. The exceptions to the rule are explained by the fact that the sampling grid was finite and true maximum values may have occurred in between

grid points. Overall, the values compare closely with corresponding stack release values.

In summary the following conclusion may be drawn from this study:

- With the exception of the 2.5 m/s exit velocity cases (surface release) the maximum ground level impact was observed to occur most frequently with 9.4 m/s wind velocity regardless of wind direction or source configuration. For the 2.5 m/s exit velocity cases (surface release) the maximum concentrations occurred with a 3.1 m/s wind velocity.
- The maximum concentrations for the stack release and a 3.1 m/s wind velocity are less than the maxima for the corresponding surface release cases. However for the 9.4 m/s cases the maxima for the corresponding stack, surface stack and surface release tests were not significantly different.
- The maximum concentration near Anderson Springs was observed to be 104 ppb with a 250° wind direction, 9.4 m/s wind velocity and 20.6 m/s exist velocity from a 30 m stack release.
- The maximum concentration near Whispering Pines was observed to be 12.5 ppb with a 210° wind direction, 6.2 m/s wind velocity and a 12.7 m/s exit velocity from a surface release.
- The results show that the use of stacks (30m or less) and/or increased exit velocity will not significantly reduce and in fact may increase the expected maximum H_2S concentration levels for Unit 13. The 30m stack would reduce the concentration levels under light winds (3.1 m/s). However the maximum concentration levels occurred under the strong wind conditions.

REFERENCES

Cermak, J. E. and J. Peterka, "Simulation of Wind Fields Over Point Arguello, California, by Wind-Tunnel Flow Over a Topographical model," Final Report, U.S. Navy Contract N126(61756)34361 A(PMR), Colorado State University, CER65Jec-JAP64, December 1966.

Cermak, J. E., "Laboratory Simulation of the Atmospheric Boundary Layer," AIAA Jl., Vol. 9, No. 9, pp. 1746-1754, September, 1971.

Cermak, J. E., "Applications of Fluid Mechanics to Wind Engineering," 1974 Freeman Scholar Lecture, ASME Journal of Fluids Engineering, Vol. 97, Series 1, No. 1, March 1975, CEP 74-75JEC7.

Halitsky, J., J. Golden, P. Halpern, and P. Wu, "Wind Tunnel Tests of Gas Diffusion From a Leak in the Shell of a Nuclear Power Reactor and From a Nearby Stack," Geophysical Sciences Laboratory Report No. 63-2, New York University, April 1963.

Halitsky, J., "Gas Diffusion Near Buildings," Geophysical Sciences Laboratory Report No. 63-3, New York University, February 1963.

Hino, M., "Maximum Ground-Level Concentration and Sampling Time," Atmospheric Environment, Vol. 2, pp. 149-165, 1968.

Martin, J. E., "The Correlation of Wind Tunnel and Field Measurements of Gas Diffusion Using Kr-85 as a Tracer," Ph.D. Thesis, MMPP 272, University of Michigan, June 1965.

Schlichting, H., Boundary Layer Theory, McGraw-Hill, New York, 1960.

Singer, I. A., I. Kazukiko and G. D. Roman, "Peak to Mean Pollutant Concentration Ratios for Various Terrain and Vegetative Cover," Journal of APCA, Vol. 13, No. 1, p. 40, 1963.

Singer, I. A. and M. E. Smith, "The Relation of Gustiness to Other Meteorological Parameters," Journal of Meteorology, Vol. 10, No. 2, 1953.

APPENDIX A

ADDITIONAL WIND TUNNEL TESTS

Additional Wind Tunnel Tests

Since the wind tunnel tests were carried out with cooling tower source parameters, additional experiments were conducted to assess the effect of added buoyancy due to steam venting on the test results. The additional tests were carried out using the surface release test conditions described in Tables 2.1 and 2.2 and the steam venting conditions described in Table A-1. Consequently, identical wind and exit velocities were simulated and the gas density was varied.

Since the steam vented plume from Unit 13 is less dense than the cooling tower plume, one would intuitively expect the concentration levels from the steam venting to be less than those using the cooling tower source parameters. Figures A-1, A-2 and A-3 substantiate this hypothesis. Each figure shows a plot of the H_2S concentrations observed for the same simulated wind and exit velocity using the steam venting versus cooling tower source parameters. As can be seen from the figures, the steam venting would have resulted in lower concentrations. The figures also show that at the lighter wind speeds (3.4 and 6.5 m/s) the reduction in ground level concentrations due to the added buoyancy for the steam venting ranged from 65 to 72 percent. For the higher wind (9.4 m/s) this factor was less (36 percent), which can be explained by the fact that as the wind increases to a critical value the added rise due to buoyancy is diminished. The critical wind speed is when downwash first occurs and for this study appears to be between 6.5 and 9.8 m/s.

Table A-1 Model and Prototype Parameters for Unit 13 - Aminoil Surface Release (Steam Venting)

Parameter	Prototype	Model
A. Surface Release		
1. length (ℓ)	24.4 m	1.27 cm
2 width (w)	2.4 m	0.13 cm
3 exit velocity	2.5, 12.7 m/s	0.068, 0.34 m/s
4. volumetric emission	148.6, 743.0 m^3/s	1.09×10^{-6}, 5.46×10^{-6} m^3/s
5. hydraulic diameter (D_e^*)	8.62 m	0.419 cm
B. Exit Temperature	427.6°K	293°K
C. Gas Density	0.46 kg/m^3	0.22 kg/m^3
D. Ambient Density	1.12 kg/m^3	1.02 kg/m^3
E. Ambient Pressure	900 mb	850 mb
F. Ambient Temperature	283°K	293°K
G. Wind Speed at Meteorological Tower Height	3.4, 6.5, 9.8	0.09, 0.17, 0.26 m/s
H. z_o/H	4.8×10^{-3}	3.6×10^{-3}
I. D_e/H	8.62	0.082
J. $R = \frac{U_s}{U_a}$	3.74, 1.95, 1.28	3.78, 2.00, 1.30
K. $Fr = \frac{\rho_a U_a^2}{g(\rho_a - \rho_s) D_e^*}$	0.23, 0.85, 1.97	0.24, 0.84, 1.97
L. $\gamma = \frac{\rho_a - \rho_s}{\rho_a}$	0.59	0.78

*Hydraulic Diameter = $\frac{\ell w}{2(1+w)} = 8.62$

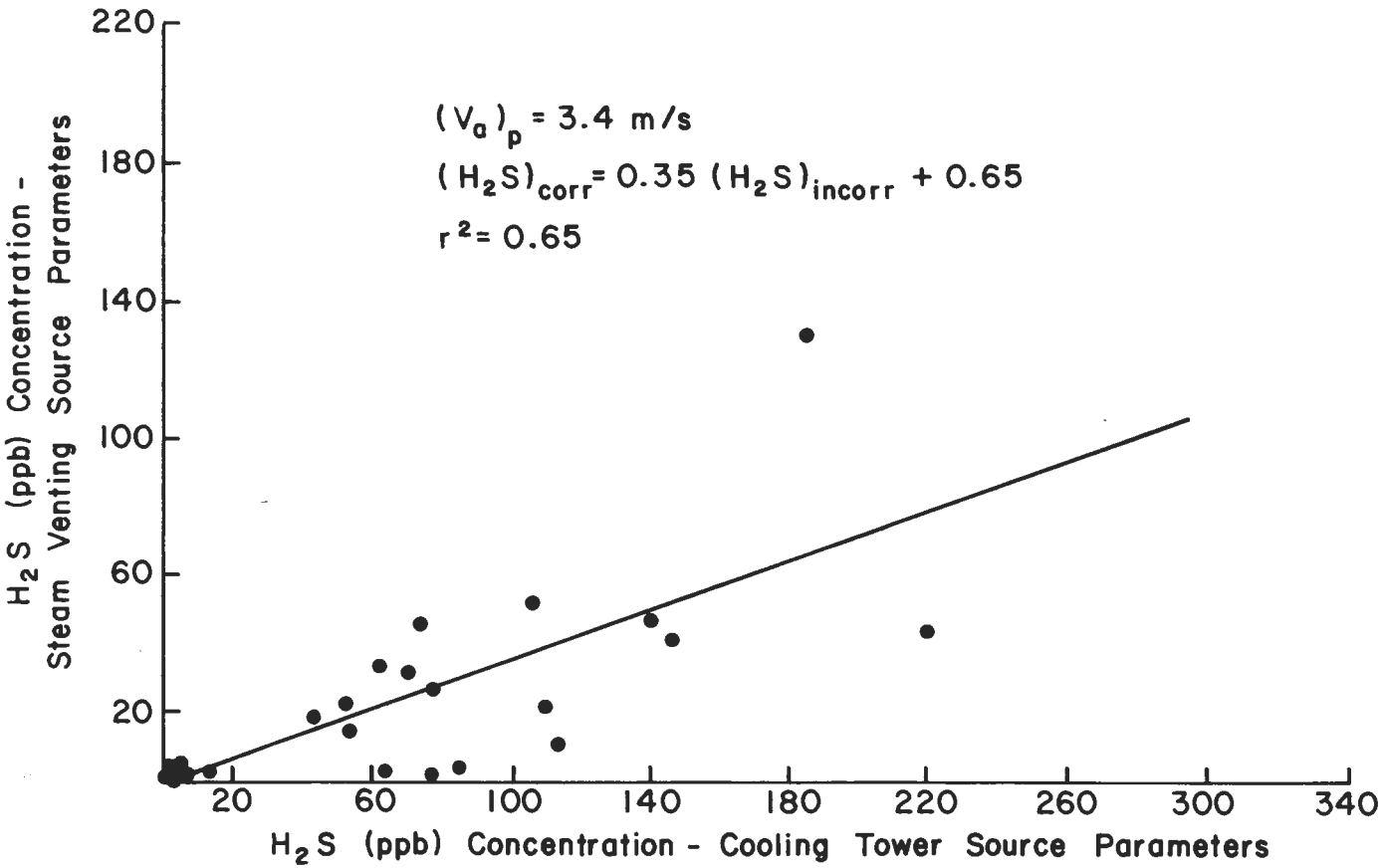

Figure A-1 H_2S Concentrations Using the Steam Venting Versus Cooling Tower Source Parameters and an Ambient Wind Speed of 3.4 m/s

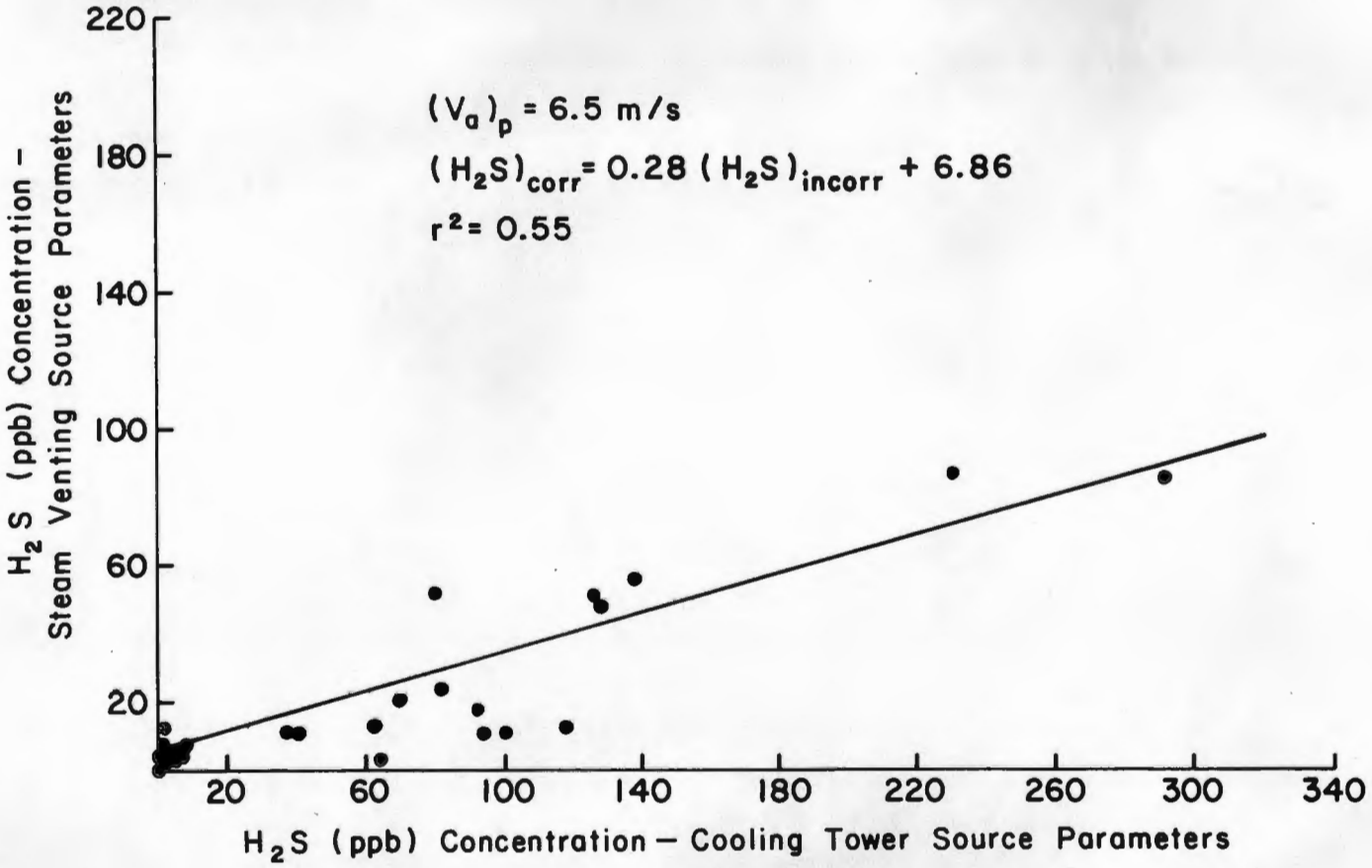

Figure A-1 H_2S Concentrations Using the Steam Venting Versus Cooling Tower Source Parameters and an Ambient Wind Speed of 6.5 m/s

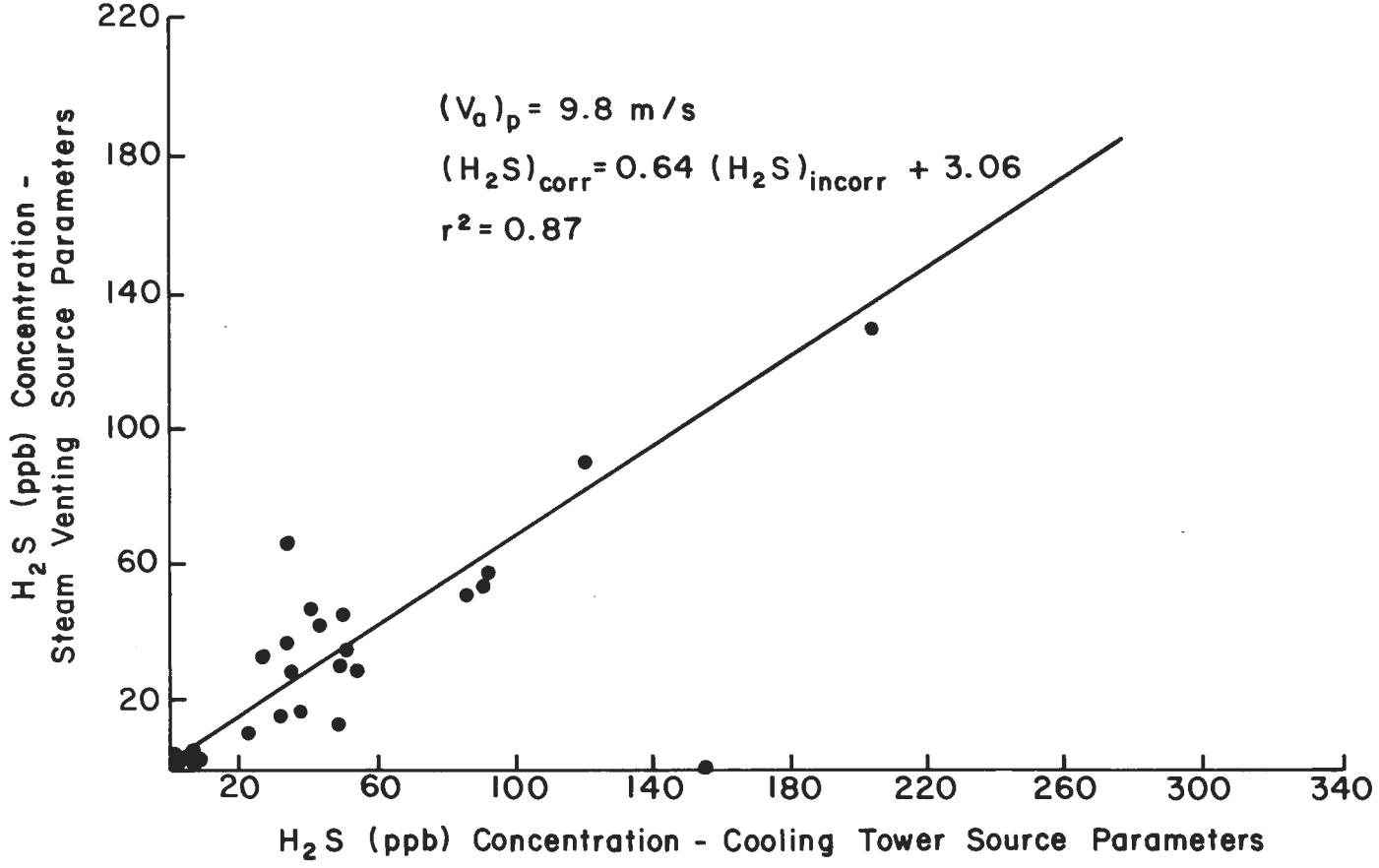

Figure A-3 H_2S Concentrations Using Steam Venting Versus Incorrect Cooling Tower Source Parameters and an Ambient Wind Speed of 9.8 m/s

TABLES

Table 2.1 Model and Prototype Dimensional Parameters for Unit 13 - Aminoil

Parameter	Prototype	Model
A. Surface Release		
1. length(ℓ)	24.4 m	1.27 cm
2. width (w)	2.4 m	0.13 cm
3. exit velocity (m/s)	2.5, 12.7	0.17, 0.79
4. volumetric emission (Λ)	172.3, 816.2 m^3/s	2.8×10^{-6} 1.3×10^{-5} m^3/s
5. equivalent diameter (D_e)	8.62 m	0.449 cm
B. Stack & Surface Stack Release		
1. height (h)	30.5, 0 m	1.59 m
2. diameter (D)	7.1, 4.06, 3.05	0.37, 0.21, 0.16
3. exit velocity (V_s)	20.6, 63.1, 111.7	1.32, 4.05, 7.16 m/s
4. volumetric emission (Λ)	816.2 m^3/s	1.3×10^{-5} m^3/s
C. Exit Temperature (T_s)	319°K	293°K
D. Gas Density (ρ_s)	.97 Kg/m^3	0.21 Kg/m^3
E. Ambient Density (ρ_a)	1.08 Kg/m^3	1.02 Kg/m^3
F. Ambient Pressure (P_a)	900 mb	850 mb
G. Ambient Temperature	293°K	293°K
H. Wind Speed at Meteorological Tower Height (V_a)	3.1, 6.2, 9.4 m/s	0.2, 0.4, 0.6 m/s
I. Wind Speed at Reference Height (V_r)	5.3, 10.8, 16.1 m/s	0.34, 0.69, 1.03 m/s
J. Reference Height Above Met Station (Z_r)	878 m	0.46 m
K. Ridge Height Elevation (H)	105 m	0.055 m
L. Surface Roughness (Z_o)	0.5 m	0.02 m

Table 2.2 Model and Prototype Dimensionless Parameters for Unit 13 - Aminoil

Parameter	Prototype	Model
$\frac{z_o}{H}$	4.8×10^{-3}	3.6×10^{-3}
$\frac{D}{H}$	8.2×10^{-2}	8.2×10^{-2}
$\frac{L}{H}$	0.29	0.29
$R = \frac{U_s}{U_a}$	1.4, 2.0, 4.1	1.4, 2.0, 4.0
$Fr = \frac{\rho_a U_a^2}{g(\rho_a - \rho_s)D}$	1.1, 4.6, 10.5	1.1, 4.6, 10.5
$\gamma = \frac{\rho_a - \rho_s}{\rho_a}$	.10	.79

Table 3.2-1 Prototype Sampling Location Key

Location #	x (m)	y (m)	z (m, MSL)	Location #	x (m)	y (m)	z (m, MSL)
1	-132.88	810.77	597.4	39	2029.97	804.67	402.3
2	195.07	804.67	524.3	40	2103.12	548.64	390.1
3	512.06	640.08	499.9	41	2151.89	292.61	487.7
4	755.09	304.8	609.6	42	2157.98	-201.17	499.9
5	816.86	-30.48	621.8	43	1194.82	2682.24	585.2
6	682.75	420.62	560.8	44	1450.85	2554.	536.4
7	-79.25	1286.26	597.4	45	1694.69	2401.8	499.9
8	109.73	1280.16	548.6	46	1914.14	2218.9	499.9
9	304.8	1255.78	517.44	47	2109.22	2036.1	463.3
10	487.68	1188.72	463.3	48	2304.29	1816.6	426.7
11	664.46	1097.28	451.1	49	2462.78	1591.1	402.3
12	816.86	987.55	426.7	50	2596.9	1353.3	402.3
13	999.74	816.86	438.9	51	2718.82	1060.7	402.3
14	1103.38	646.18	451.1	52	2810.26	780.3	451.1
15	1188.72	475.49	536.4	53	2877.31	530.4	560.8
16	1249.68	280.42	621.8	54	2926.08	-97.5	621.8
17	1280.16	85.34	548.6	56	-97.54	1755.6	597.4
18	1243.58	-298.7	463.3	57	-499.87	1676.4	609.6
19	304.8	1731.26	548.6	58	391.38	2170.2	633.9
20	524.26	1676.4	560.8	59	97.5	2182.4	646.2
21	707.14	1609.34	573	60	-396.2	2158.0	682.8
22	935.74	1493.52	536.4	61	938.8	2779.8	573.0
23	1097.28	137.16	499.9	62	658.4	2865.1	597.4
24	1243.84	1243.58	487.7	63	60.96	2926.1	719.3
25	1402.08	1054.61	426.7	64	670.56	3596.6	670.6
26	1536.19	847.34	390.1	70	-670.56	2072.6	737.6
27	1627.63	646.18	438.9	71	-1798.3	2255.5	722.4
28	1694.69	402.34	438.9	73	-487.68	2804.2	725.4
29	1743.46	170.69	438.9	74	914.4	2804.2	749.8
30	1725.17	-268.22	499.9	75	61.0	4389.1	731.5
31	573.02	2115.31	609.6	76	487.7	4937.8	792.5
32	804.67	2029.97	560.8	77	121.9	3657.6	765.0
33	1024.13	1926.34	524.3				
34	1243.58	1786.13	512.1				
35	1444.75	1633.73	475.5				
36	1597.15	1475.23	463.3				
37	1767.84	1267.97	426.7	Met Station	-2011.7	786.4	1005.8
38	1914.14	1024.13	402.3				

* All locations are with respect to the point represented by the base of the north arrow in Figure 1.1

Table 4.1-1 Summary of Photographs Taken for Aminoil Surface Release

Run #	Photo #	Wind Direction	Wind Speed (m/s)	Exit Velocity (m/s)
1	1	250	3.1	2.5
2	6	250	6.2	2.5
3	11	250	9.4	2.5
4	2	250	3.1	12.7
5	7	250	6.2	12.7
6	12	250	9.4	12.7
7	1A	230	3.1	2.5
8	2A	230	3.1	12.7
9	6A	230	6.2	2.5
10	7A	230	6.2	12.7
11	11A	230	9.4	2.5
12	12A	230	9.4	12.7
13	19A	210	3.1	2.5
14	20A	210	6.2	2.5
15	21A	210	9.4	2.5
16	22A	210	3.1	12.7
17	23A	210	6.2	12.7
18	24A	210	9.4	12.7

Table 4.2-1 Hydrogen Sulfide Concentrations and Nondimensional Concentration Coefficient for a 250° Wind Direction, a 3.1 m/s Wind Speed and a 2.5 m/s Exit Velocity--Aminoil Surface Releases

LOCATION NO.	NON DIMENSIONAL COEFF(K)	H2S CONCENTRATION(PPB)
1	.1121E-03	8.3854
2	.1525E-03	11.4041
7	.8970E-05	.6708
8	.1345E-04	1.0062
9	.4036E-04	3.0187
10	.4036E-04	3.0187
11	.2422E-03	18.1125
12	.2422E-03	18.1125
13	.6727E-05	.5031
14	.6727E-05	.5031
19	.8970E-05	.6708
20	.8970E-05	.6708
21	.8970E-05	.6708
22	.1345E-04	1.0062
23	.8970E-05	.6708
24	.1121E-04	.8385
25	.3364E-04	2.5156
26	.3364E-04	2.5156
31	.8970E-05	.6708
32	.8970E-05	.6708
33	.8970E-05	.6708
34	.1345E-04	1.0062
35	.2242E-04	1.6771
36	.1345E-04	1.0062
37	.8970E-05	.6708
38	0.	0.0000
43	.1570E-04	1.1740
44	.2242E-04	1.6771
45	.4485E-05	.3354
46	.1121E-04	.8385
47	.6727E-05	.5031
48	.1794E-04	1.3417
49	.4485E-05	.3354
50	.1121E-04	.8385

Table 4.2-2 Hydrogen Sulfide Concentrations and Nondimensional Concentration Coefficient for a 250° Wind Direction, a 6.2 m/s Wind Speed and a 2.5 m/s Exit Velocity--Aminoil Surface Releases

LOCATION NO.	NON DIMENSIONAL COEFF(K)	H2S CONCENTRATION(PPB)
1	.2063E-03	7.7146
2	.3005E-03	11.2364
7	.6727E-04	2.5156
8	.5830E-04	2.1802
9	.3588E-03	13.4166
10	.1839E-03	6.8760
11	.4171E-03	15.5968
12	.2915E-03	10.9010
13	.1794E-04	.6708
14	.2242E-04	.8385
19	.2691E-04	1.0062
20	.1794E-04	.6708
21	.1794E-04	.6708
22	.3588E-04	1.3417
23	.1794E-04	.6708
24	.2242E-04	.8385
25	.7624E-04	2.8510
26	.8970E-05	.3354
31	.2691E-04	1.0062
32	.4485E-05	.1677
33	.2691E-04	1.0062
34	.2691E-04	1.0062
35	.4933E-04	1.8448
36	.1525E-03	5.7021
37	.5382E-04	2.0125
38	.4485E-05	.1677
43	.3588E-04	1.3417
44	.2691E-04	1.0062
45	.3139E-04	1.1740
46	.1794E-04	.6708
47	.8970E-05	.3354
48	0.	0.0000
49	.2242E-04	.8385
50	0.	0.0000

Table 4.2-3 Hydrogen Sulfide Concentrations and Nondimensional Concentration Coefficient for a 250° Wind Direction, a 9.4 m/s Wind Speed and a 2.5 m/s Exit Velocity--Aminoil Surface Releases

LOCATION NO.	NON DIMENSIONAL COEFF(K)	H2S CONCENTRATION(PPB)
1	.2826E-03	6.9688
2	.6526E-03	16.0946
7	.2691E-04	.6637
8	.2691E-04	.6637
9	.8746E-04	2.1570
10	.8746E-04	2.1570
11	.3364E-03	8.2962
12	.4306E-03	1[illegible].6191
13	.6727E-05	.1659
14	.1345E-04	.3318
19	.2018E-04	.4978
20	.6727E-05	.1659
21	.2018E-04	.4978
22	.2691E-04	.6637
23	.6727E-05	.1659
24	.1345E-04	.3318
25	.8073E-04	1.9911
26	.6727E-04	1.6592
31	.2018E-04	.4978
32	.2018E-04	.4978
33	.2018E-04	.4978
34	.4036E-04	.9955
35	.4036E-04	.9955
36	.3364E-04	.8296
37	.3364E-04	.8296
38		
43	.2691E-04	.6637
44	.3364E-04	.8296
45	.2018E-04	.4978
46	.3364E-04	.8296
47	.2018E-04	.4978
48	.3364E-04	.8296
49	.6727E-05	.1659
50	.3364E-04	.8296

Table 4.2-4 Hydrogen Sulfide Concentrations and Nondimensional Concentration Coefficient for a 250° Wind Direction, a 3.1 m/s Wind Speed and a 12.7 m/s Exit Velocity--Aminoil Surface Releases

LOCATION NO.	NON DIMENSIONAL COEFF(K)	H2S CONCENTRATION(PPB)
1	.4895E-04	17.3413
2	.4721E-04	16.7256
7	.3765E-05	1.3339
8	.1834E-05	.6499
9	.1245E-04	4.4123
10	.1014E-04	3.5914
11	.6314E-04	22.3692
12	.3080E-04	10.9110
13	.8689E-06	.3078
14	.1834E-05	.6499
19	.1834E-05	.6499
20	.2800E-05	.9919
21	.2800E-05	.9919
22	.3765E-05	1.3339
23	.2800E-05	.9919
24	.3765E-05	1.3339
25	.8593E-05	3.0441
26	.5696E-05	2.0180
31	.3283E-05	1.1629
32	.3765E-05	1.3339
33	.3765E-05	1.3339
34	.5696E-05	2.0180
35	.1632E-04	5.7804
36	.1342E-04	4.7543
37	.5696E-05	2.0180
38	.3765E-05	1.3339
43	.3186E-05	1.1287
44	.3862E-06	.1368
45	.7627E-05	2.7021
46	.3765E-05	1.3339
47	.1834E-05	.6499
48	.2800E-05	.9919
49	.1834E-05	.6499
50	.1352E-05	.4789

Table 4.2-5 Hydrogen Sulfide Concentrations and Nondimensional Concentration Coefficient for a 250° Wind Direction, a 6.2 m/s Wind Speed and a 12.7 m/s Exit Velocity--Aminoil Surface Releases

LOCATION NO.	NON DIMENSIONAL COEFF(K)	H2S CONCENTRATION(PPB)
1	.1477E-03	26.1658
2	.1448E-03	5.0526
7	.8303E-04	14.7076
8	.7531E-04	13.3394
9	.3398E-03	60.1985
10	.1564E-03	27.7050
11	.2259E-03	40.0183
12	.1525E-03	27.0209
13	.5793E-05	1.0261
14	.4827E-05	.8551
19	.7724E-05	1.3681
20	.5793E-05	1.0261
21	.3862E-05	.6841
22	.7724E-05	1.3681
23	.5793E-05	1.0261
24	.4827E-05	.8551
25	.8206E-04	14.5366
26	.3283E-04	5.8146
31	.5793E-05	1.0261
32	.7724E-05	1.3681
33	.9655E-05	1.7102
34	.2124E-04	3.7624
35	.1014E-03	17.9569
36	.2607E-04	4.6175
37		
38		
43	.1931E-04	3.4204
44	.1448E-04	2.5653
45	.7724E-05	1.3681
46	.4827E-05	.8551
47	.2896E-05	.5131
48	.4827E-05	.8551
49	.1776E-04	3.1467
50	.2896E-04	5.1306

Table 4.2-6 Hydrogen Sulfide Concentrations and Nondimensional Concentration Coefficient for a 250° Wind Direction, a 9.4 m/s Wind Speed and a 12.7 m/s Exit Velocity--Aminoil Surface Releases

LOCATION NO.	NON DIMENSIONAL COEFF(K)	H2S CONCENTRATION(PPB)
1	.4342E-03	50.7259
2	.5222E-03	61.0132
7	.2781E-04	3.2486
8	.4229E-04	4.9406
9	.1477E-03	17.2583
10	.1214E-03	14.1789
11	.4263E-03	49.8122
12	.4122E-03	48.1541
13	.1448E-05	.1692
14	0.	0.0000
19	.5793E-05	.6768
20	.2896E-05	.3384
21	.5793E-05	.6768
22	.5793E-05	.6768
23	.2896E-05	.3384
24	0.	0.0000
25	.8747E-04	10.2196
26	.8284E-04	9.6782
31	.1448E-05	.1692
32	.2896E-05	.3384
33	0.	0.0000
34	.1970E-04	2.3011
35	.6430E-04	7.5124
36	.5445E-04	6.3619
37	.1159E-04	1.3536
38	.2636E-04	3.0794
43	.1634E-03	19.0857
44	.4605E-04	5.3805
45	.5213E-04	6.0912
46	.4460E-04	5.2113
47	.3707E-04	4.3315
48	.4171E-04	4.8729
49	.4345E-05	.5076
50	.4345E-05	.5076

Table 4.2-7 Hydrogen Sulfide Concentrations and Nondimensional Concentration Coefficient for a 230° Wind Direction, a 3.1 m/s Wind Speed and a 2.5 m/s Exit Velocity-- Aminoil Surface Releases

LOCATION NO.	NON DIMENSIONAL COEFF(K)	H2S CONCENTRATION(PPB)
1	.5380E-05	.4024
2	.1883E-04	1.4083
7	.3331E-03	24.9136
8	.2654E-03	19.8504
9	.1354E-03	10.1264
10	.9057E-04	6.7733
11	.1031E-04	.7712
13	.2690E-05	.2012
57	.6277E-05	.4694
56	.1031E-04	.7712
19	.9415E-05	.7042
20	.1529E-03	11.4341
21	.8070E-05	.6036
22	.1838E-04	1.3748
23	.1480E-04	1.1065
25	.4932E-05	.3688
60	.4484E-06	.0335
59	.4932E-05	.3688
58	.1793E-05	.1341
31	.2556E-04	1.9113
32	.7174E-05	.5365
33	.7622E-05	.5700
34	.1793E-05	.1341
35	.8967E-06	.0671
37	.9864E-05	.7377
63	.2690E-05	.2012
62	.4484E-06	.0335
61	.3138E-05	.2347
43	.4484E-06	.0335
45	.1793E-05	.1341
46	.2690E-05	.2012
47	.2690E-05	.2012
49	.2690E-05	.2012
64	.1121E-04	.8383

Table 4.2-8 Hydrogen Sulfide Concentrations and Nondimensional Concentration Coefficient for a 230° Wind Direction, a 6.2 m/s Wind Speed and a 2.5 m/s Exit Velocity--Aminoil Surface Releases

LOCATION NO.	NON DIMENSIONAL COEFF(K)	H2S CONCENTRATION(PPB)
1	.3587E-05	.1341
2	.3138E-04	1.1736
7	.3605E-03	13.4795
8	.2331E-03	8.7181
9	.7891E-04	2.9507
10	.6905E-04	2.5819
11	.4484E-05	.1677
13	.2690E-05	.1006
57	.1255E-04	.4694
56	.3228E-04	1.2071
19	.1103E-03	4.1243
20	.2618E-03	9.7911
21	.5291E-04	1.9783
22	.1255E-04	.4694
23	.7174E-05	.2682
25	.4484E-05	.1677
60	0.	0.0000
59	.9864E-05	.3688
58	.7174E-05	.2682
31	.3587E-04	1.3412
32	.2690E-04	1.0059
33	.4484E-05	.1677
34	.4484E-05	.1677
35	.4484E-05	.1677
37	.8967E-06	.0335
63	.8967E-06	.0335
62	.2690E-05	.1006
61		
43	.3587E-05	.1341
45	.2511E-04	.9389
46	.2690E-05	.1006
47	.8967E-05	.3353
49	.2690E-05	.1006
64	.1076E-04	.4024

Table 4.2-9 Hydrogen Sulfide Condentrations and Nondimensional Concentration Coefficient for a 230° Wind Direction, a 9.4 m/s Wind Speed and a 2.5 m/s Exit Velocity-- Aminoil Surface Releases

LOCATION NO.	NON DIMENSIONAL COEFF(K)	H2S CONCENTRATION(PPB)
1	.4119E-05	.1016
2	.1922E-04	.4741
7	.4847E-03	11.9539
8	.3958E-03	9.7866
9	.2005E-03	4.9441
10	.1098E-03	2.7091
11	.1785E-04	.4402
13	.2746E-05	.0677
57	0.	0.0000
56	.2197E-04	.5418
19	.1661E-03	4.0975
20	.2444E-03	6.0277
21	.1002E-03	2.4720
22	.3844E-04	.9482
23	.2883E-04	.7111
25	.2746E-05	.0677
60	.1648E-04	.4064
59	.1373E-05	.0339
58	.1373E-05	.0339
31	.3707E-04	.9143
32	.1510E-04	.3725
33	.6865E-05	.1693
34	.1373E-05	.0339
35		
37		
63	.1510E-04	.3725
62	.1510E-04	.3725
61	.2197E-04	.5418
43	.1236E-04	.3048
45	.9748E-04	2.4043
46	.1648E-04	.4064
47	.3570E-04	.8805
49	.2746E-05	.0677
64		

Table 4.2-10 Hydrogen Sulfide Concentrations and Nondimensional Concentration Coefficient for a 230° Wind Direction, a 3.1 m/s Wind Speed and a 12.7 m/s Exit Velocity--Aminoil Surface Releases

LOCATION NO.	NON DIMENSIONAL COEFF(K)	H2S CONCENTRATION(PPB)
1	.1158E-05	.4103
2	.6080E-05	2.1542
7	.4980E-04	17.6436
8	.4131E-04	14.6346
9	.1786E-04	6.3257
10	.1091E-04	3.8638
11	.1834E-05	.6497
13	.5791E-06	.2052
57	.5791E-06	.2052
56	.2220E-05	.7864
19	.7625E-05	2.7012
20	.3079E-04	10.9076
21	.1322E-04	4.6844
22	.6467E-05	2.2909
23	.1737E-05	.6155
25	.1062E-05	.3761
60	.1158E-05	.4103
59	.1158E-05	.4103
58	.1255E-05	.4445
31	.3185E-05	1.1284
32	.1834E-05	.6497
33	.1834E-05	.6497
34	.8686E-06	.3077
35	.7721E-06	.2735
37	.1158E-05	.4103
63	.1930E-06	.0684
62	0.	0.0000
61	0.	0.0000
43	.1930E-06	.0684
45	.5694E-05	2.0174
46	.3861E-06	.1368
47	.2413E-05	.8548
49	.5791E-06	.2052
64	.6756E-06	.2394

Table 4.2-11 Hydrogen Sulfide Concentrations and Nondimensional Concentration Coefficient for a 230° Wind Direction, a 6.2 m/s Wind Speed and a 12.7 m/s Exit Velocity--Aminoil Surface Releases

LOCATION NO.	NON DIMENSIONAL COEFF(K)	H2S CONCENTRATION(PPB)
1	0.	0.0000
2	.7142E-05	1.2651
7	.1141E-03	20.2080
8	.1181E-03	20.9261
9	.3783E-04	6.7018
10	.2394E-04	4.2399
11	.1544E-05	.2735
13	.9652E-06	.1710
57	.6949E-05	1.2309
56	.8879E-05	1.5729
19	.1023E-04	1.8122
20	.1562E-03	27.6621
21	.1621E-04	2.8722
22	.1062E-04	1.8806
23	.3668E-05	.6497
25	.7721E-06	.1368
60	.1544E-05	.2735
59	.9652E-06	.1710
58	.5598E-05	.9916
31	.6949E-05	1.2309
32	.8879E-05	1.5729
33	.2895E-05	.5129
34	.1737E-05	.3077
35	.2702E-05	.4787
37	.2316E-05	.4103
63	.2316E-05	.4103
62	.1930E-05	.3419
61	.1120E-04	1.9832
43	.3668E-05	.6497
45	.1158E-04	2.0516
46	.1158E-05	.2052
47	.1930E-06	.0342
49	.1351E-05	.2394
64	.4440E-05	.7864

Table 4.2-12 Hydrogen Sulfide Concentrations and Nondimensional Concentration Coefficient for a 230° Wind Direction, a 9.4 m/s Wind Speed and a 12.7 m/s Exit Velocity--Aminoil Surface Releases

LOCATION NO.	NON DIMENSIONAL COEFF(K)	H2S CONCENTRATION(PPB)
1	.4528E-05	.5290
2	.1479E-04	1.7281
7	.3601E-03	42.0734
8	.3607E-03	42.1439
9	.1841E-03	21.5128
10	.9750E-04	11.3912
11	.2415E-04	2.8213
13	.2113E-05	.2469
57	.4830E-05	.5643
56	.1721E-04	2.0102
19	0.	0.0000
20	.1941E-03	22.6766
21	.6037E-06	.0705
22	.3351E-04	3.9146
23	.2626E-04	3.0682
25	.3320E-05	.3879
60	.3924E-05	.4585
59	.2415E-05	.2821
58	.8150E-05	.9522
31	.1509E-05	.1763
32	.5131E-05	.5995
33	.6037E-06	.0705
34	.1509E-05	.1763
35	.2415E-05	.2821
37	.1992E-04	2.3276
63	.1449E-04	1.6928
62	.3924E-05	.4585
61		
43	.5735E-05	.6701
45	.4528E-05	.5290
46	.6037E-05	.7053
47	.1298E-04	1.5165
49	.2415E-05	.2821
64	.3834E-04	4.4789

Table 4.2-13 Hydrogen Sulfide Concentrations and Nondimensional Concentration Coefficient for a 210° Wind Direction, a 3.1 m/s Wind Speed and a 2.5 m/s Exit Velocity--Aminoil Surface Releases

LOCATION NO.	NON DIMENSIONAL COEFF(K)	H2S CONCENTRATION(PPB)
7	.3439E-05	.2572
8	.2675E-05	.2000
9	.3057E-05	.2286
10	.2675E-05	.2000
11	.1528E-05	.1143
13	.3057E-05	.2286
57	.1960E-03	14.6594
56	.7642E-05	.5715
19	.3821E-05	.2858
20	.5349E-05	.4001
21	.6496E-05	.4858
22	.4967E-05	.3715
25	.8024E-05	.6001
70	.4279E-04	3.2005
71	.9552E-05	.7144
60	.1456E-03	10.8874
59	.2675E-05	.2000
58	.4585E-05	.3429
31	.7642E-05	.5715
32	.8788E-05	.6572
33	.5349E-05	.4001
35	.1337E-04	1.0002
73	.7642E-06	.0572
74	0.	0.0000
63	.2216E-04	1.6574
62	.1108E-04	.8287
61	.4585E-05	.3429
43	.7642E-05	.5715
44	.1910E-05	.1429
47	.4203E-05	.3143
64	.3821E-05	.2858
75	.2522E-04	1.8860
76	.1796E-04	1.3431
77	.1528E-05	.1143

Table 4.2-14 Hydrogen Sulfide Concentrations and Nondimensional Concentration Coefficient for a 210° Wind Direction, a 6.2 m/s Wind Speed and a 2.5 m/s Exit Velocity--Aminoil Surface Releases

LOCATION NO.	NON DIMENSIONAL COEFF(K)	H2S CONCENTRATION(PPB)
7	.6113E-05	.2286
8	0.	0.0000
9	.7642E-05	.2858
10	.1223E-04	.4572
11	.3821E-05	.1429
13	.9170E-05	.3429
57	.8865E-04	3.3148
56	.5349E-05	.2000
19	.6113E-05	.2286
20	.1223E-04	.4572
21	.1299E-04	.4858
22	.1452E-04	.5429
25	.1146E-04	.4286
70	.1528E-03	5.7152
71	.3439E-04	1.2859
60	.1353E-03	5.0579
59	.1605E-04	.6001
58	.1070E-04	.4001
31	.1528E-04	.5715
32	.1910E-04	.7144
33	.1681E-04	.6287
35	.2369E-04	.8858
73	.1376E-04	.5144
74	.6878E-05	.2572
63	.3362E-04	1.2573
62	.1223E-04	.4572
61	.1605E-04	.6001
43	.1605E-04	.6001
44	.1910E-04	.7144
47	.1299E-04	.4858
64	.6113E-05	.2286
75	.3210E-04	1.2002
76	.9629E-04	3.6005
77	.2827E-04	1.0573

Table 4.2-15 Hydrogen Sulfide Concentrations and Nondimensional Concentration Coefficient for a 210° Wind Direction, a 9.4 m/s Wind Speed and a 2.5 m/s Exit Velocity--Aminoil Surface Releases

LOCATION NO.	NON DIMENSIONAL COEFF(K)	H2S CONCENTRATION(PPB)
7	.8024E-05	.1979
8	0.	0.0000
9	.4585E-05	.1131
10	.1146E-04	.2827
11	0.	0.0000
13	.8024E-05	.1979
57	.1536E-03	3.7884
56	.1146E-04	.2827
19	.6878E-05	.1696
20	.9170E-05	.2262
21	.1376E-04	.3393
22	.1146E-04	.2827
25	.1490E-04	.3675
70	.1158E-03	2.8555
71	.2063E-04	.5089
60	.2291E-03	5.6261
59	.1146E-04	.2827
58	.1834E-04	.4523
31	.2063E-04	.5089
32	.2407E-04	.5937
33	.2522E-04	.6220
35	.2865E-04	.7068
73	.1032E-04	.2544
74	.8024E-05	.1979
63	.3897E-04	.9612
62	.8024E-05	.1979
61	.1834E-04	.4523
43	.2522E-04	.6220
44	.2178E-04	.5372
47	.2293E-04	.5654
64	.5731E-05	.1414
75	.2751E-04	.6785
76	.5273E-04	1.3005
77	.9170E-05	.2262

Table 4.2-16 Hydrogen Sulfide Concentrations and Nondimensional Concentration Coefficient for a 210° Wind Direction, a 3.1 m/s Wind Speed and a 12.7 m/s Exit Velocity--Aminoil Surface Releases

LOCATION NO.	NON DIMENSIONAL COEFF(K)	H2S CONCENTRATION(PPB)
7	0.	0.0000
8	.8225E-07	.0291
9	.1645E-06	.0583
10	.6580E-06	.2331
11	.1645E-06	.0583
13	.4113E-06	.1457
57	.3389E-04	12.0056
56	.1234E-05	.4371
19	.1645E-06	.0583
20	.4113E-06	.1457
21	.5758E-06	.2040
22	.1234E-05	.4371
25	.9048E-06	.3205
70	.2797E-05	.9908
71	.9048E-06	.3205
60	.3529E-04	12.5010
59	.3290E-06	.1166
58	.1645E-06	.0583
31	.1152E-05	.4080
32	.1481E-05	.5245
33	.1234E-05	.4371
35	.3043E-05	1.0782
73	.9048E-06	.3205
74	.4935E-06	.1748
63	.5840E-05	2.0689
62	.1481E-05	.5245
61	.9870E-06	.3497
43	.1645E-05	.5828
44	.1645E-05	.5828
47	.1234E-05	.4371
64	.1069E-05	.3788
75	.8061E-05	2.8557
76	.2468E-05	.8742
77	.1069E-05	.3788

Table 4.2-17 Hydrogen Sulfide Concentrations and Nondimensional Concentration Coefficient for a 210° Wind Direction, a 6.2 m/s Wind Speed and a 12.7 m/s Exit Velocity--Aminoil Surface Releases

LOCATION NO.	NON DIMENSIONAL COEFF(K)	H2S CONCENTRATION(PPB)
7	.6580E-06	.1166
8	.9870E-06	.1748
9	.8225E-06	.1457
10	.6580E-06	.1166
11	0.	0.0000
13	.3290E-06	.0583
57	.5330E-04	9.4413
56	.6580E-06	.1166
19	.9870E-06	.1748
20	.1316E-05	.2331
21	.1316E-05	.2331
22	.1481E-05	.2623
25	.1810E-05	.3205
70	.4277E-04	7.5764
71	.2418E-04	4.2836
60	.1153E-03	2[illegible] 270
59	.3290E-06	. 583
58	.4935E-06	. 974
31	.8225E-06	.1457
32	.1810E-05	.3205
33	.2139E-05	.3788
35	.3619E-05	.6411
73	.2303E-05	.4080
74	.8225E-06	.1457
63	.2155E-04	3.8173
62	.2139E-05	.3788
61	.3126E-05	.5537
43	.1810E-05	.3205
44	.3290E-05	.5828
47	.1645E-06	.0291
64	.2632E-05	.4662
75	.2040E-04	3.6133
76	.7041E-04	12.4719
77	.1332E-04	2.3603

Table 4.2-18 Hydrogen Sulfide Concentrations and Nondimensional Concentration Coefficient for a 210° Wind Direction, a 9.4 m/s Wind Speed and a 12.7 m/s Exit Velocity--Aminoil Surface Releases

LOCATION NO.	NON DIMENSIONAL COEFF(K)	H2S CONCENTRATION(PPB)
7	0.	0.0000
8	.2468E-06	.0288
9	.2468E-06	.0288
10	.2961E-05	.3460
11	.2468E-05	.2883
13	.4935E-06	.0577
57	.1323E-03	15.4528
56	.9870E-06	.1153
19	.9870E-06	.1153
20	.1481E-05	.1730
21	.1481E-05	.1730
22	.2714E-05	.3171
25	.2961E-05	.3460
70	.3331E-04	3.8920
71	.5182E-05	.6054
60	.2055E-03	24.0153
59	.1234E-05	.1441
58	.2468E-05	.2883
31	.3701E-05	.4324
32	.3208E-05	.3748
33	.6662E-05	.7784
35	.7403E-05	.8649
73	.5429E-05	.6343
74	.2468E-05	.2883
63	.3479E-04	4.0650
62	.3948E-05	.4613
61	.5675E-05	.6631
43	.3208E-05	.3748
44	.8883E-05	1.0379
47	.4442E-05	.5189
64	.6416E-05	.7496
75	.2295E-04	2.6812
76	.3726E-04	4.3533
77	.4195E-05	.4901

Table 5.1-1 Summary of Photographs Taken for Aminoil Stack Release

Run #	Photo #	Wind Direction	Wind Speed (m/s)	Exit Velocity (m/s)
1	3	250°	3.1	20.6
2	8	250°	6.2	20.6
3	13	250°	9.4	20.6
4	4	250°	3.1	63.1
5	9	250°	6.2	63.1
6	14	250°	9.4	63.1
7	5	250°	3.1	111.7
8	10	250°	6.2	111.7
9	15	250°	9.4	111.7
10	3A	230°	3.1	20.6
11	4A	230°	3.1	63.1
12	5A	230°	3.1	111.7
13	8A	230°	6.2	20.6
14	9A	230°	6.2	63.1
15	10A	230°	6.2	111.7
16	13A	230°	9.4	20.6
17	14A	230°	9.4	63.1
18	15A	230°	9.4	111.7
19	31A	210°	3.1	20.6
20	32A	210°	6.2	20.6
21	33A	210°	9.4	20.6
22	34A	210°	3.1	63.1
23	35A	210°	6.2	63.1
24	36A	210°	9.4	63.1
25	37A	210°	3.1	111.7
26	38A	210°	6.2	111.7
27	39A	210°	9.4	111.7

Table 5.2-1 Hydrogen Sulfide Concentrations and Nondimensional Concentration Coefficient for a 250° Wind Direction, a 3.1 m/s Wind Speed and a 20.6 m/s Exit Velocity--Aminoil Stack Releases

LOCATION NO.	NON DIMENSIONAL COEFF(K)	H2S CONCENTRATION(PPB)
1	.2657E-05	1.3861
2	.1328E-05	.6931
7	.8856E-06	.4620
8	0.	0.0000
9	.9289E-05	4.8514
10	.1771E-05	.9241
11	.1240E-04	6.4686
12	.1771E-05	.9241
13	.8856E-06	.4620
14	.8856E-06	.4620
19	.1771E-05	.9241
20	.1328E-05	.6931
21	.1328E-05	.6931
22	.2214E-05	1.1551
23	.1771E-05	.9241
24	.1328E-05	.6931
25	.1328E-05	.6931
26	.8856E-06	.4620
31	.2657E-05	1.3861
32	.1328E-05	.6931
33	.1328E-05	.6931
34	.1771E-05	.9241
35	.3543E-05	1.8482
36	.1771E-05	.9241
37	.8856E-06	.4620
38		
43	.2657E-05	1.3861
44	.1328E-05	.6931
45	0.	0.0000
46	0.	0.0000
47	0.	0.0000
48	0.	0.0000
49	0.	0.0000

Table 5.2-2 Hydrogen Sulfide Concentrations and Nondimensional Concentration Coefficient for a 250° Wind Direction, a 6.2 m/s Wind Speed and a 20.6 m/s Exit Velocity--Aminoil Stack Releases

LOCATION NO.	NON DIMENSIONAL COEFF(K)	H2S CONCENTRATION(PPB)
1	.7085E-05	1.8482
2	.1328E-04	3.4653
7	.6996E-04	18.2506
8	.4428E-04	11.5510
9	.2249E-03	58.6790
10	.6554E-04	17.0955
11	.4428E-04	11.5510
12	.2303E-04	6.0065
13	.3188E-05	.8317
14	.3543E-05	.9241
19	.3543E-05	.9241
20	.3543E-05	.9241
21	.1771E-05	.4620
22	.1771E-05	.4620
23	.8856E-06	.2310
24	.5314E-06	.1386
25	.2657E-05	.6931
26	.8856E-06	.2310
31	.1771E-05	.4620
32	.8856E-06	.2310
33	.9742E-05	2.5412
34	.8856E-05	2.3102
35	.8148E-04	21.2538
36	.2303E-04	6.0065
37	.5314E-05	1.3861
38	0.	0.0000
43	.5314E-05	1.3861
44	.1771E-05	.4620
45	0.	0.0000
46	0.	0.0000
47		
48		
49	0.	0.0000

Table 5.2-3 Hydrogen Sulfide Concentrations and Nondimensional Concentration Coefficient for a 250° Wind Direction, a 9.4 m/s Wind Speed and a 20.6 m/s Exit Velocity--Aminoil Stack Releases

LOCATION NO.	NON DIMENSIONAL COEFF(K)	H2S CONCENTRATION(PPB)
1	.5091E-03	87.5902
2	.3558E-03	61.2117
7	.7135E-04	12.2761
8	.2752E-04	4.7346
9	.7646E-04	13.1493
10	.1091E-03	18.7693
11	.2713E-03	46.6697
12	.2516E-03	43.2878
13	.3774E-03	64.9317
14	.2555E-04	4.3964
19	.2555E-04	4.3964
20	.1966E-04	3.3819
21	.5897E-05	1.0146
22	.6880E-05	1.1837
23	.7862E-05	1.3527
24	.5897E-05	1.0146
25	.1022E-03	17.5857
26	.2162E-04	3.7200
31	.2555E-04	4.3964
32	.8845E-05	1.5218
33	.3145E-04	5.4110
34	.1199E-03	20.6293
35	.3440E-04	5.9183
36	.2752E-04	4.7346
37	.7469E-04	12.8511
38	.4717E-04	8.1165
43	.4128E-04	7.1019
44	.3342E-04	5.7492
45	.3833E-04	6.5946
46	.2948E-04	5.0728
47	.9238E-04	15.8947
48	.6054E-03	104.1613
49	.5897E-05	1.0146

Table 5.2-4 Hydrogen Sulfide Concentrations and Nondimensional Concentration Coefficient for a 250° Wind Direction, a 3.1 m/s Wind Speed and a 63.1 m/s Exit Velocity--Aminoil Stack Releases

LOCATION NO.	NON DIMENSIONAL COEFF(K)	H2S CONCENTRATION(PPB)
1	.2853E-06	.4620
2	.5706E-06	.9241
7	0.	0.0000
8	.2853E-06	.4620
9	.1141E-05	1.8482
10	.8559E-06	1.3861
11	.2568E-05	4.1584
12	.1425E-05	2.3102
13	.1426E-06	.2310
14	.2853E-06	.4620
19	.4279E-06	.6931
20	.5706E-06	.9241
21	.2853E-06	.4620
22	.7132E-06	1.1551
23	.2853E-06	.4620
24	.4279E-06	.6931
25	0.	0.0000
26	.2853E-06	.4620
31	.5706E-06	.9241
32	.2853E-06	.4620
33	.1569E-05	2.5412
34	.8559E-06	1.3861
35	.2425E-05	3.9273
36	.2853E-06	.4620
37	0.	0.0000
38		
43	.2853E-06	.4620
44	0.	0.0000
45	0.	0.0000
46	.5706E-06	.9241
47	0.	0.0000
48	.1426E-06	.2310
49		

Table 5.2-5 Hydrogen Sulfide Concentrations and Nondimensional Concentration Coefficient for a 250° Wind Direction, a 6.2 m/s Wind Speed and a 63.1 m/s Exit Velocity--Aminoil Stack Releases

LOCATION NO.	NON DIMENSIONAL COEFF(K)	H2S CONCENTRATION(PPB)
1	.2853E-05	2.3102
2	.2853E-05	2.3102
7	.8559E-05	6.9306
8	.3423E-05	2.7722
9	.2511E-04	20.3297
10	.1027E-04	8.3167
11	.1598E-04	12.9371
12	.6847E-05	5.5445
13	.1141E-05	.9241
14	.1141E-05	.9241
19	.1141E-05	.9241
20	.1141E-05	.9241
21	.1141E-05	.9241
22	.1141E-05	.9241
23	.5706E-06	.4620
24	.8559E-06	.6931
25	.5706E-06	.4620
26	.5706E-06	.4620
31	.1141E-05	.9241
32		
33	.2282E-05	1.8482
34	.1712E-05	1.3861
35	.1655E-04	13.3991
36	.1141E-05	.9241
37	.1141E-05	.9241
38		
43	0.	0.0000
44	0.	0.0000
45	.5706E-06	.4620
46	.2853E-06	.2310
47		
48	.8559E-06	.6931
49	0.	0.0000

Table 5.2-6 Hydrogen Sulfide Concentrations and Nondimensional Concentration Coefficient for a 250° Wind Direction, a 9.4 m/s Wind Speed and a 63.1 m/s Exit Velocity--Aminoil Stack Releases

LOCATION NO.	NON DIMENSIONAL COEFF(K)	H2S CONCENTRATION(PPB)
1	.1615E-04	8.6237
2	.8991E-04	48.0224
7	.2849E-05	1.5218
8	.4749E-05	2.5364
9	.2564E-04	13.6965
10	.1266E-04	6.7637
11	.7377E-04	39.3987
12	.4622E-05	2.4688
13	.1266E-05	.6764
14	.2849E-05	1.5218
19	.2849E-05	1.5218
20	.2849E-05	1.5218
21	.3166E-06	.1691
22	.6332E-05	3.3819
23	0.	0.0000
24	.3166E-06	.1691
25	.5699E-05	3.0437
26	.1583E-05	.8455
31	.5382E-05	2.8746
32	.1266E-05	.6764
33	.2533E-05	1.3527
34	.9498E-05	5.0728
35	.1045E-04	5.5801
36	.2216E-05	1.1837
37	.2216E-05	1.1837
38	.3514E-04	18.7693
43	.1805E-04	9.6383
44	.3388E-04	18.0929
45	.1583E-05	.8455
46	.3166E-06	.1691
47	.1900E-05	1.0146
48	.1583E-05	.8455
49	.2216E-05	1.1837

Table 5.2-7 Hydrogen Sulfide Concentrations and Nondimensional Concentration Coefficient for a 250° Wind Direction, a 3.1 m/s Wind Speed and a 111.7 m/s Exit Velocity--Aminoil Stack Releases

LOCATION NO.	NON DIMENSIONAL COEFF(K)	H2S CONCENTRATION(PPB)
1	0.	0.0000
2	.8281E-07	.2310
7	.8281E-07	.2310
8	.8281E-07	.2310
9	.2484E-06	.6931
10	.1656E-06	.4620
11	.4968E-06	1.3861
12	.4968E-06	1.3861
13	.1656E-06	.4620
14	.1656E-06	.4620
19	.1656E-06	.4620
20	.3312E-06	.9241
21	.3312E-06	.9241
22	.4140E-06	1.1551
23	.1656E-06	.4620
24	.1656E-06	.4620
25	.1656E-06	.4620
26	.1656E-06	.4620
31	.8281E-07	.2310
32	.1656E-06	.4620
33	.1656E-06	.4620
34	.3312E-06	.9241
35	.3312E-06	.9241
36	.4968E-06	1.3861
37	.3312E-06	.9241
38		
43		
44	.4140E-06	1.1551
45	.1656E-06	.4620
46		
47	.1656E-06	.4620
48	0.	0.0000
49	.8281E-07	.2310

Table 5.2-8 Hydrogen Sulfide Concentrations and Nondimensional Concentration Coefficient for a 250° Wind Direction, a 6.2 m/s Wind Speed and a 111.7 m/s Exit Velocity--Aminoil Stack Releases

LOCATION NO.	NON DIMENSIONAL COEFF(K)	H2S CONCENTRATION(PPB)
1	.5962E-05	8.3167
2	.3643E-05	5.0824
7	.6624E-06	.9241
8	.2319E-05	3.2343
9	.6293E-05	8.7788
10	.6624E-05	9.2408
11	.6956E-05	9.7028
12	.3312E-05	4.6204
13	.9937E-06	1.3861
14	.6624E-06	.9241
19	.3312E-06	.4620
20	.1822E-05	2.5412
21	0.	0.0000
22	.8281E-06	1.1551
23	0.	0.0000
24	.3312E-06	.4620
25	.9937E-06	1.3861
26	.2981E-06	.4158
31	0.	0.0000
32	.3312E-06	.4620
33	.1656E-05	2.3102
34	.4306E-05	6.0065
35	.4637E-05	6.4686
36	.6624E-06	.9241
37	.1557E-04	21.7159
38	.1987E-05	2.7722
43		
44		
45		
46	.9937E-06	1.3861
47	.9937E-06	1.3861
48	.3312E-02	
49		

Table 5.2-9 Hydrogen Sulfide Concentrations and Nondimensional Concentration Coefficient for a 250° Wind Direction, a 9.4 m/s Wind Speed and a 111.7 m/s Exit Velocity--Aminoil Stack Releases

LOCATION NO.	NON DIMENSIONAL COEFF(K)	H2S CONCENTRATION(PPB)
1	.2733E-04	25.1418
2	.5167E-04	47.5409
7	.9142E-04	84.1109
8	.1267E-04	11.6567
9	.3950E-04	36.3414
10	.1987E-04	18.2850
11	.4347E-04	39.9984
12	.6682E-04	61.4832
13	.6956E-05	6.3997
14	.7204E-05	6.6283
19	.2559E-04	23.5419
20	.3031E-04	27.8846
21	.3478E-05	3.1999
22	.1936E-04	17.8278
23	.1490E-05	1.3714
24	.2981E-05	2.7427
25	.2981E-05	2.7427
26	.1987E-05	1.8285
31	.2186E-04	20.1135
32	.1490E-05	1.3714
33	.9937E-05	9.1425
34	.1689E-04	15.5422
35	.4968E-05	4.5712
36	.3975E-05	3.6570
37	.2931E-04	26.9703
38	.6459E-05	5.9426
43		
44		
45	0.	0.0000
46	.1043E-04	9.5996
47	.5962E-05	5.4855
48	.4968E-05	4.5712
49		

Table 5.2-10 Hydrogen Sulfide Concentrations and Nondimensional Concentration Coefficient for a 230° Wind Direction, a 3.1 m/s Wind Speed and a 20.6 m/s Exit Velocity--Aminoil Stack Releases

LOCATION NO.	NON DIMENSIONAL COEFF(K)	H2S CONCENTRATION(PPB)
1	.5899E-06	.3077
2	.1835E-05	.9574
7	.1180E-04	6.1547
8	.1186E-04	6.1889
9	.5899E-05	3.0774
10	.5440E-05	2.8380
11	.9176E-06	.4787
13	.3277E-06	.1710
57	.4588E-06	.2394
56	.7865E-06	.4103
19	.5505E-05	2.8722
20	.1055E-04	5.5051
21	.2228E-05	1.1626
22	.2359E-05	1.2309
23	.1180E-05	.6155
25	.9831E-06	.5129
60	.3932E-06	.2052
59	.2622E-06	.1368
58	.5899E-06	.3077
31	.1311E-05	.6839
32	.1442E-05	.7522
33	.7209E-06	.3761
34	.3932E-06	.2052
35	.3277E-06	.1710
37	.3932E-06	.2052
63	.6554E-07	.0342
62	0.	0.0000
61	.8520E-06	.4445
43	.9176E-06	.4787
45	.1966E-05	1.0258
46	.7865E-06	.4103
47	.1835E-05	.9574
49	.6554E-06	.3419
64	.1114E-05	.5813

Table 5.2-11 Hydrogen Sulfide Concentrations and Nondimensional Concentration Coefficient for a 230° Wind Direction, a 6.2 m/s Wind Speed and a 20.6 m/s Exit Velocity--Aminoil Stack Releases

LOCATION NO.	NON DIMENSIONAL COEFF(K)	H2S CONCENTRATION(PPB)
1		
2	.5193E-05	1.3546
7	.8117E-04	21.1738
8	.5780E-04	15.0783
9	.1735E-04	4.5271
10	.9566E-05	2.4952
11	.1367E-05	.3565
13	.1367E-05	.3565
57	.6559E-05	1.7110
56	.2583E-04	6.7371
19	.4318E-04	11.2642
20	.1015E-03	26.4850
21	.1503E-05	.3921
22	.4373E-05	1.1407
23	.5466E-06	.1426
25	0.	0.0000
60	.2733E-06	.0713
59	.1367E-06	.0356
58	.1503E-05	.3921
31	.1230E-05	.3208
32	.1776E-05	.4634
33	.1093E-05	.2852
34	.6833E-06	.1782
35	.1093E-05	.2852
37	.8199E-06	.2139
63		
62	.8199E-06	.2139
61	.2596E-05	.6773
43	.2050E-05	.5347
45	.8336E-05	2.1744
46	.1230E-05	.3208
47	.3416E-05	.8912
49	.6833E-06	.1782
64	.8199E-06	.2139

Table 5.2-12 Hydrogen Sulfide Concentrations and Nondimensional Concentration Coefficient for a 230° Wind Direction, a 9.4 m/s Wind Speed and a 20.6 m/s Exit Velocity--Aminoil Stack Releases

LOCATION NO.	NON DIMENSIONAL COEFF(K)	H2S CONCENTRATION(PPB)
1	.9438E-05	1.6238
2	.3264E-04	5.6156
7	.2418E-03	41.6099
8	.1985E-03	34.1675
9	.9713E-04	16.7114
10	.4522E-04	7.7807
11	.9241E-05	1.5900
13	.6095E-05	1.0487
57	.4129E-05	.7104
56	.1514E-04	2.6048
19	.5702E-05	.9810
20	.1625E-03	27.9767
21	.5309E-05	.9134
22	.1848E-04	3.1799
23	.1317E-04	2.2666
25	.2949E-05	.5074
60	.3343E-05	.5751
59	0.	0.0000
58	.2163E-05	.3721
31	.4916E-05	.8457
32	.3932E-05	.5766
33	.2163E-05	.3721
34	.2556E-05	.4398
35	.4522E-05	.7781
37	.1022E-04	1.7591
63	.6292E-05	1.0825
62	.4129E-05	.7104
61	.6292E-05	1.0825
43	.5309E-05	.9134
45	.5309E-05	.9134
46	.4326E-05	.7442
47	.8258E-05	1.4208
49	.1180E-05	.2030
64	.5309E-05	.9134

Table 5.2-13 Hydrogen Sulfide Concentrations and Nondimensional Concentration Coefficient for a 230° Wind Direction, a 3.1 m/s Wind Speed and a 63.1 m/s Exit Velocity--Aminoil Stack Releases

LOCATION NO.	NON DIMENSIONAL COEFF(K)	H2S CONCENTRATION(PPB)
1	.1056E-06	.1710
2	.3167E-06	.5129
7	.1858E-05	3.0090
8	.1309E-05	2.1200
9	.5067E-06	.8206
10	.3167E-06	.5129
11	.1267E-06	.2052
13	.1267E-06	.2052
57	.1056E-06	.1710
56	.3378E-06	.5471
19	.4434E-06	.7181
20	.1478E-05	2.3935
21	.4011E-06	.6497
22	.3378E-06	.5471
23	.2534E-06	.4103
25	.2111E-06	.3419
60	.1689E-06	.2735
59	.2111E-07	.0342
58	.2111E-06	.3419
31	.6545E-06	1.0600
32	.4856E-06	.7864
33		
34	.6334E-07	.1026
35	.2534E-06	.4103
37	.2745E-06	.4445
63	.1689E-06	.2735
62	.8445E-07	.1368
61	0.	0.0000
43	.6334E-07	.1026
45	.3800E-06	.6155
46	.8445E-07	.1368
47	0.	0.0000
49	.1056E-06	.1710
64		

Table 5.2-14 Hydrogen Sulfide Concentrations and Nondimensional Concentration Coefficient for a 230° Wind Direction, a 6.2 m/s Wind Speed and a 63.1 m/s Exit Velocity--Aminoil Stack Releases

LOCATION NO.	NON DIMENSIONAL COEFF(K)	H2S CONCENTRATION(PPB)
1	.2111E-06	.1710
2	.4223E-06	.3419
7	.6080E-05	4.9238
8	.1790E-04	14.4978
9	.5276E-05	4.2741
10	.3378E-05	2.7354
11	.6334E-06	.5129
13		
57	0.	0.0000
56	.5489E-06	.4445
19	.3125E-05	2.5303
20	.2322E-05	1.8806
21	.6334E-06	.5129
22		
23	.4223E-06	.3419
25	.2111E-06	.1710
60	.4223E-06	.3419
59	.2111E-06	.1710
58	.2111E-06	.1710
31	.1267E-06	.1026
32	.2956E-06	.2394
33	0.	0.0000
34	0.	0.0000
35	.2111E-06	.1710
37	.5912E-06	.4787
63	.6334E-06	.5129
62	.5489E-06	.4445
61	.1562E-05	1.2651
43	.4223E-06	.3419
45	.2449E-05	1.9832
46	.6334E-06	.5129
47	.9712E-06	.7864
49	.5067E-06	.4103
64	.1056E-05	.8548

Table 5.2-15 Hydrogen Sulfide Concentrations and Nondimensional Concentration Coefficient for a 230° Wind Direction, a 9.4 m/s Wind Speed and a 63.1 m/s Exit Velocity--Aminoil Stack Releases

LOCATION NO.	NON DIMENSIONAL COEFF(K)	H2S CONCENTRATION(PPB)
1	.7924E-06	.4232
2	.8584E-05	4.5847
7	.8194E-04	43.7662
8	.7336E-04	39.1815
9	.3579E-04	19.1146
10	.1809E-04	9.6631
11	.4358E-05	2.3276
13	.3962E-06	.2116
57	.7263E-06	.3879
56	.4820E-05	2.5745
19	.1010E-04	5.3958
20	.4662E-04	24.8984
21	.6009E-05	3.2093
22	.8518E-05	4.5494
23	.5018E-05	2.6803
25	.5943E-06	.3174
60	.1321E-05	.7053
59	.7263E-06	.3879
58	.2377E-05	1.2696
31		
32	.1255E-05	.6701
33	.1519E-05	.8111
34	.5282E-06	.2821
35	.9904E-06	.5290
37		
63	.1585E-05	.8464
62	.9904E-06	.5290
61	.2377E-05	1.2696
43	.7263E-06	.3879
45	.2047E-05	1.0933
46	.1056E-05	.5643
47	.1519E-05	.8111
49	.5282E-06	.2821
64	.1981E-05	1.0580

Table 5.2-16 Hydrogen Sulfide Concentrations and Nondimensional Concentration Coefficient for a 230° Wind Direction, a 3.1 m/s Wind Speed and a 111.7 m/s Exit Velocity--Aminoil Stack Releases

LOCATION NO.	NON DIMENSIONAL COEFF(K)	H2S CONCENTRATION(PPB)
1	0.	0.0000
2	.6128E-07	.1710
7	.6005E-06	1.6755
8	.3064E-06	.8548
9	.1716E-06	.4787
10	.2083E-06	.5813
11	.1348E-06	.3761
13	.1226E-06	.3419
57	.1593E-06	.4445
56	.1593E-06	.4445
19	.3432E-06	.9574
20	.7721E-06	2.1542
21	.2819E-06	.7864
22	.2329E-06	.6497
23	.2206E-06	.6155
25	.2206E-06	.6155
60	.8579E-07	.2394
59	.1961E-06	.5471
58	.9805E-07	.2735
31	.3922E-06	1.0942
32	.2329E-06	.6497
33	.2329E-06	.6497
34	.2206E-06	.6155
35	.1716E-06	.4787
37	.1593E-06	.4445
63	.9805E-07	.2735
62	.1103E-06	.3077
61	.4902E-07	.1368
43	.9805E-07	.2735
45	.1716E-06	.4787
46	.1348E-06	.3761
47	.1103E-06	.3077
49	.9805E-07	.2735
64		

Table 5.2-17 Hydrogen Sulfide Concentrations and Nondimensional Concentration Coefficient for a 230° Wind Direction, a 6.2 m/s Wind Speed and a 111.7 m/s Exit Velocity--Aminoil Stack Releases

LOCATION NO.	NON DIMENSIONAL COEFF(K)	H2S CONCENTRATION(PPB)
1	.4412E-06	.6155
2	.6863E-06	.9574
7	.1405E-04	19.5926
8	.8498E-05	11.7282
9	.2696E-05	3.7612
10	.1814E-05	2.5303
11	.7354E-07	.1026
13	.1226E-06	.1710
57	.1961E-06	.2735
56	.1814E-05	2.5303
19	.1789E-05	2.4961
20	.1354E-04	18.9429
21	.9314E-06	1.2993
22	.4902E-06	.6839
23	.7354E-07	.1026
25	.9805E-07	.1368
60	.1226E-06	.1710
59	.6863E-06	.9574
58	.9805E-07	.1368
31	.4157E-06	.5813
32	.5393E-06	.7522
33	.1961E-06	.2735
34		
35	0.	0.0000
37	.2696E-06	.3761
63	.1961E-06	.2735
62	.1716E-06	.2394
61	.4412E-06	.6155
43	.1226E-06	.1710
45	.1138E-05	1.5729
46	.1961E-06	.2735
47	.2941E-06	.4103
49	.2451E-06	.3419
64	.5883E-06	.8206

Table 5.2-18 Hydrogen Sulfide Concentrations and Nondimensional Concentration Coefficient for a 230° Wind Direction, a 9.4 m/s Wind Speed and a 111.7 m/s Exit Velocity--Aminoil Stack Releases

LOCATION NO.	NON DIMENSIONAL COEFF(K)	H2S CONCENTRATION(PPB)
1	.6884E-06	.6334
2	.4130E-05	3.8001
7	.2574E-04	23.6804
8	.1656E-04	15.2357
9	.6845E-05	6.2964
10	.3939E-05	3.6242
11	.6119E-06	.5630
13	.6119E-06	.5630
57	.6884E-06	.6334
56	.2868E-05	2.6390
19	.1568E-05	1.4426
20	.2295E-04	21.1118
21	.1071E-05	.9852
22	.1530E-06	.1407
23	.2295E-06	.2111
25	0.	0.0000
60	.2295E-06	.2111
59	.2295E-06	.2111
58	.2295E-06	.2111
31	.4207E-06	.3870
32	.4972E-06	.4574
33	0.	0.0000
34	0.	0.0000
35	.4207E-06	.3870
37	.4207E-06	.3870
63	.4207E-06	.3870
62	.2295E-06	.2111
61	.1109E-05	1.0204
43	.4207E-06	.3870
45	.9561E-06	.8797
46	0.	0.0000
47	.5354E-06	.4926
49	0.	0.0000
64	.8413E-06	.7741

Table 5.2-19 Hydrogen Sulfide Concentrations and Nondimensional Concentration Coefficient for a 210° Wind Direction, a 3.1 m/s Wind Speed and a 20.6 m/s Exit Velocity--Aminoil Stack Releases

LOCATION NO.	NON DIMENSIONAL COEFF(K)	H2S CONCENTRATION(PPB)
7	0.	0.0000
8	.5450E-07	.0284
9	.1635E-06	.0853
10	.5995E-06	.3128
11	.4360E-06	.2275
13	.5995E-06	.3128
57	.2060E-04	10.7478
56	.3325E-05	1.7344
19	.6540E-06	.3412
20	.5450E-06	.2843
21	.1036E-05	.5402
22		
25	.5450E-07	.0284
70	.1363E-05	.7108
71	.6540E-06	.3412
60	.7794E-05	4.0659
59	.1853E-05	.9667
58	.1145E-05	.5971
31	.1199E-05	.6255
32	.1853E-05	.9667
33	.1363E-05	.7108
35	.3325E-05	1.7344
73	.8175E-06	.4265
74	.1526E-05	.7961
63		
62	.4905E-06	.2559
61	.3815E-06	.1990
43	.7085E-06	.3696
44	.1635E-05	.8530
47	.3815E-06	.1990
64	.6540E-06	.3412
75	.2725E-05	1.4217
76	.1199E-05	.6255
77	.4360E-06	.2275

Table 5.2-20 Hydrogen Sulfide Concentrations and Nondimensional Concentration Coefficient for a 210° Wind Direction, a 6.2 m/s Wind Speed and a 20.6 m/s Exit Velocity--Aminoil Stack Releases

LOCATION NO.	NON DIMENSIONAL COEFF(K)	H2S CONCENTRATION(PPB)
7	.3706E-05	.9667
8	.3270E-05	.8530
9	.2616E-05	.6824
10	0.	0.0000
11	.3488E-05	.9099
13	.3379E-05	.8814
57	.2474E-04	6.4543
56	.3052E-05	.7961
19	.3597E-05	.9383
20	.2834E-05	.7393
21	.3924E-05	1.0236
22	.6540E-06	.1706
25	.3488E-05	.9099
70	.3630E-04	9.4683
71		
60	.4000E-04	10.4350
59	.2725E-05	.7108
58	.2398E-05	.6255
31	.3161E-05	.8246
32	.3488E-05	.9099
33	.5014E-05	1.3079
35	.4687E-05	1.2226
73	.3052E-05	.7961
74	.4251E-05	1.1089
63	.1057E-04	2.7580
62	.4251E-05	1.1089
61	.3488E-05	.9099
43		
44	.2180E-05	.5687
47	.3706E-05	.9667
64	.2725E-05	.7108
75	.1068E-04	2.7865
76	.3291E-04	8.5584
77	.1014E-04	2.6443

Table 5.2-21 Hydrogen Sulfide Concentrations and Nondimensional Concentration Coefficient for a 210° Wind Direction, a 9.4 m/s Wind Speed and a 20.6 m/s Exit Velocity--Aminoil Stack Releases

LOCATION NO.	NON DIMENSIONAL COEFF(K)	H2S CONCENTRATION(PPB)
7	.1962E-05	.3376
8	.1635E-05	.2813
9	.8175E-06	.1407
10	.8175E-06	.1407
11	.1962E-05	.3376
13	.1962E-05	.3376
57	.1056E-03	18.1724
56	.2943E-05	.5064
19	.2616E-05	.4501
20	.3270E-05	.5626
21	.4742E-05	.8158
22	0.	0.0000
25	.2780E-05	.4782
70	.3123E-04	5.3730
71	.3761E-05	.6470
60	.8633E-04	14.8530
59	.4742E-05	.8158
58	.2943E-05	.5064
31	.3597E-05	.6189
32	.2943E-05	.5064
33	.4251E-05	.7314
35	.6867E-05	1.1815
73	.4905E-05	.8439
74	.5559E-05	.9564
63	.2371E-04	4.0790
62	.5069E-05	.8721
61	.7194E-05	1.2378
43	.4088E-05	.7033
44	.5232E-05	.9002
47		
64	.2126E-05	.3657
75	.9320E-05	1.6035
76	.1308E-04	2.2505
77	.1243E-04	2.1379

Table 5.2-22 Hydrogen Sulfide Concentrations and Nondimensional Concentration Coefficient for a 210° Wind Direction, a 3.1 m/s Wind Speed and a 63.1 m/s Exit Velocity--Aminoil Stack Releases

LOCATION NO.	NON DIMENSIONAL COEFF(K)	H2S CONCENTRATION(PPB)
7	.3511E-07	.0569
8	.1229E-06	.1990
9	.1053E-06	.1706
10	.1229E-06	.1990
11	.1580E-06	.2559
13	.2985E-06	.4834
57	.1246E-05	2.0188
56	.6320E-06	1.0236
19	.1756E-06	.2843
20	0.	0.0000
21	.2242E-06	.3696
22	.2107E-06	.3412
25	.2809E-06	.4549
70	.2458E-06	.3981
71	.4389E-06	.7108
60	.3687E-06	.5971
59	.5969E-06	.9667
58	.2809E-06	.4549
31	.2458E-06	.3981
32	.4214E-06	.6824
33	.4038E-06	.6540
35	.7023E-06	1.1373
73	.1931E-06	.3128
74	.2458E-06	.3981
63	.4214E-06	.6824
62	.6145E-06	.9952
61	.6145E-06	.9952
43	.2282E-06	.3696
44	.3687E-06	.5971
47	.1756E-06	.2843
64	.1580E-06	.2559
75	.5618E-06	.9099
76	.1053E-06	.1706
77	.1053E-06	.1706

Table 5.2-23 Hydrogen Sulfide Concentrations and Nondimensional Concentration Coefficient for a 210° Wind Direction, a 6.2 m/s Wind Speed and a 63.1 m/s Exit Velocity--Aminoil Stack Releases

LOCATION NO.	NON DIMENSIONAL COEFF(K)	H2S CONCENTRATION(PPB)
7	.3998E-06	.3237
8	.5088E-06	.4120
9	.1090E-06	.0883
10	.1090E-06	.0883
11	.7269E-07	.0589
13	0.	0.0000
57	.7342E-05	5.9450
56	.1890E-05	1.5304
19	.4725E-06	.3826
20	0.	0.0000
21	.5452E-06	.4415
22		
25	.2544E-06	.2060
70	.1127E-05	.9124
71	.1272E-05	1.0301
60	.5961E-05	4.8267
59	.1090E-06	.0883
58	.1454E-06	.1177
31	.3998E-06	.3237
32	.5452E-06	.4415
33	.8359E-06	.6769
35	.1381E-05	1.1184
73	.6179E-06	.5003
74	.7269E-06	.5886
63	.1090E-05	.8829
62	.6179E-06	.5003
61	.6542E-06	.5298
43	.8359E-06	.6769
44	.8359E-06	.6769
47	.6542E-06	.5298
64	.7269E-06	.5886
75	.2181E-05	1.7659
76	.3889E-05	3.1491
77	.7269E-06	.5886

Table 5.2-24 Hydrogen Sulfide Concentrations and Nondimensional Concentration Coefficient for a 210° Wind Direction, a 9.4 m/s Wind Speed and a 63.1 m/s Exit Velocity--Aminoil Stack Releases

LOCATION NO.	NON DIMENSIONAL COEFF(K)	H2S CONCENTRATION(PPB)
7	.2159E-06	.1153
8	.1943E-05	1.0379
9	.1619E-06	.0865
10	0.	0.0000
11		
13	.2159E-06	.1153
57	.2181E-04	11.6473
56	.3239E-06	.1730
19	0.	0.0000
20	.1403E-05	.7496
21	.1511E-05	.8072
22		
25	.2969E-05	1.5856
70	.1457E-04	7.7841
71	.1619E-05	.8649
60	.2715E-04	14.5014
59	.1619E-06	.0865
58	.2213E-05	1.1820
31	.1026E-05	.5478
32	.2591E-05	1.3838
33	.2969E-05	1.5856
35	.3778E-05	2.0181
73	.1781E-05	.9514
74	.9716E-06	.5189
63	.6364E-05	3.4019
62	.9176E-06	.4901
61	.7017E-06	.3748
43	.5393E-07	.0288
44	.1511E-05	.8072
47	.1134E-05	.6054
64	.1970E-04	10.5229
75	.3832E-05	2.0469
76	.6531E-05	3.4884
77	0.	0.0000

Table 5.2-25 Hydrogen Sulfide Concentrations and Nondimensional Concentration Coefficient for a 210° Wind Direction, a 3.1 m/s Wind Speed and a 111.7 m/s Exit Velocity--Aminoil Stack Releases

LOCATION NO.	NON DIMENSIONAL COEFF(K)	H2S CONCENTRATION(PPB)
7	.8356E-07	.2331
8	.2089E-07	.0583
9	.3133E-07	.0874
10	.7311E-07	.2040
11		
13	.6261E-07	.1748
57	.3969E-06	1.1073
56	.3342E-06	.9325
19	0.	0.0000
20	.2611E-06	.7285
21	.2507E-06	.6994
22	.1671E-06	.4662
25	.2716E-06	.7576
70	.1253E-06	.3497
71	.2089E-06	.5828
60	.1128E-05	3.1471
59	.6267E-07	.1748
58	.1358E-06	.3788
31	.1253E-06	.3497
32	.2089E-06	.5828
33	.3133E-06	.8742
35	.3447E-06	.9616
73	.1462E-06	.4080
74	.1358E-06	.3788
63		
62	.1671E-06	.4662
61	.2820E-06	.7868
43	.1253E-06	.3497
44	.1880E-06	.5245
47	.1253E-06	.3497
64	.9400E-07	.2623
75	.5013E-06	1.3987
76	.2089E-06	.5828
77	.2089E-07	.0583

Table 5.2-26 Hydrogen Sulfide Concentrations and Nondimensional Concentration Coefficient for a 210° Wind Direction, a 6.2 m/s Wind Speed and a 111.7 m/s Exit Velocity--Aminoil Stack Releases

LOCATION NO.	NON DIMENSIONAL COEFF(K)	H2S CONCENTRATION(PPB)
7	.2298E-06	.3205
8	.1253E-06	.1748
9	0.	0.0000
10	.6267E-07	.0874
11		
13	.6267E-07	.0874
57	.2757E-05	3.8465
56	.2089E-06	.2914
19	.1044E-06	.1457
20	.3342E-06	.4662
21	.4178E-06	.5828
22	.3551E-06	.4954
25	.4178E-06	.5828
70	.7478E-05	10.4321
71	.1295E-05	1.8067
60	.6016E-05	8.3923
59	.1671E-06	.2331
58	.1880E-06	.2623
31	.8356E-07	.1166
32	.4387E-06	.6119
33	.3342E-06	.4662
35	.8147E-06	1.1365
73	.1462E-06	.2040
74	.1880E-06	.2623
63	.1964E-05	2.7391
62	.8356E-07	.1166
61	.2716E-06	.3788
43	.8356E-07	.1166
44	.1253E-06	.1748
47	.4178E-07	.0583
64	.1253E-06	.1748
75	.1838E-05	2.5643
76	.8899E-05	12.4136
77	.1253E-05	1.7484

Table 5.2-27 Hydrogen Sulfide Concentrations and Nondimensional Concentration Coefficient for a 210° Wind Direction, a 9.4 m/s Wind Speed and a 111.7 m/s Exit Velocity--Aminoil Stack Releases

LOCATION NO.	NON DIMENSIONAL COEFF(K)	H2S CONCENTRATION(PPB)
7	.3133E-06	.2883
8	.4073E-06	.3748
9	.9400E-07	.0865
10	.9400E-07	.0865
11	0.	0.0000
13	.2820E-06	.2595
57	.1354E-04	12.4545
56	.4700E-06	.4324
19	.2193E-06	.2018
20	.4073E-06	.3748
21	.3447E-06	.3171
22	.6893E-06	.6343
25	.2820E-06	.2595
70	.7959E-05	7.3228
71	.2820E-06	.2595
60	.2052E-04	18.8836
59	.3760E-06	.3460
58	.6267E-06	.5766
31	.9714E-06	.8937
32	.1347E-05	1.2397
33	.7834E-06	.7207
35	.1535E-05	1.4127
73	.3760E-06	.3460
74	.7520E-06	.6919
63	.3885E-05	3.5749
62	.2507E-06	.2306
61	.9087E-06	.8361
43	.3133E-06	.2883
44	.5953E-06	.5478
47	.2193E-06	.2018
64	.4073E-06	.3748
75	.3102E-05	2.8542
76	.3760E-05	3.4596
77	.6267E-07	.0577

Table 6.1-1 Summary of Photographs Taken for Aminoil Surface Stack Releases

Run #	Photo #	Wind Direction	Wind Speed (m/s)	Exit Velocity (m/s)
1	16A	230°	9.4	20.6
2	17A	230°	9.4	63.1
3	18A	230°	9.4	111.7
4	25A	210°	9.4	20.6
5	26A	210°	9.4	63.1
6	27A	210°	9.4	111.7
7	28A	210°	6.2	20.6
8	29A	210°	6.2	63.1
9	30A	210°	6.2	111.7

Table 6.2-1 Hydrogen Sulfide Concentrations and Nondimensional Concentration Coefficient for a 230° Wind Direction, a 9.4 m/s Wind Speed and a 20.6 m/s Exit Velocity--Aminoil Surface Stack Releases

LOCATION NO.	NON DIMENSIONAL COEFF(K)	H2S CONCENTRATION(PPB)
1	.5931E-05	1.0204
2	.3743E-04	6.4391
7	.3593E-03	61.8224
8	.2317E-03	39.8661
9	.1039E-03	17.8747
10	.4867E-04	8.3743
11	.6749E-05	1.1611
13	.1636E-05	.2815
57	.1043E-04	1.7945
56	.1554E-04	2.6742
19	.1636E-05	.2815
20	.1078E-03	18.5432
21	.4295E-05	.7389
22	.1268E-04	2.1816
23	.1227E-04	2.1112
25	.1841E-05	.3167
60	.6135E-06	.1056
59	0.	0.0000
58	.6135E-06	.1056
31	.1227E-05	.2111
32	0.	0.0000
33	0.	0.0000
34	0.	0.0000
35	0.	0.0000
37		
63	.4704E-05	.8093
62	.6135E-06	.1056
61	.3886E-05	.6685
43	.6135E-06	.1056
45	.5317E-05	.9148
46	0.	0.0000
47	.4704E-05	.8093
49	.7567E-05	1.3019
64	.8180E-05	1.4075

Table 6.2-2 Hydrogen Sulfide Concentrations and Nondimensional Concentration Coefficient for a 230° Wind Direction, a 9.4 m/s Wind Speed and a 63.1 m/s Exit Velocity--Aminoil Surface Stack Releases

LOCATION NO.	NON DIMENSIONAL COEFF(K)	H2S CONCENTRATION(PPB)
1	.1449E-05	.7741
2	.8894E-05	4.7502
7	.4625E-04	24.7008
8	.7326E-04	39.1272
9	.2134E-04	11.4004
10	.1687E-04	9.0077
11	.4150E-05	2.2167
13	.5929E-06	.3167
57	.5270E-06	.2815
56	.1383E-05	.7389
19	.6522E-05	3.4834
20	.1285E-04	6.8613
21	.4480E-05	2.3927
22	.9223E-06	.4926
23	.6588E-06	.3519
25	.6588E-06	.3519
60	.5270E-06	.2815
59	.6588E-06	.3519
58	0.	0.0000
31	.4612E-06	.2463
32	.6588E-06	.3519
33	.2635E-06	.1407
34	.4612E-06	.2463
35	0.	0.0000
37	.1647E-05	.8797
63	.9882E-06	.5278
62	.6588E-06	.3519
61	.6588E-06	.3519
43	.9882E-06	.5278
45	.3426E-05	1.8297
46	.2306E-05	1.2315
47	.6588E-06	.3519
49	.6588E-06	.3519
64	.1120E-05	.5982

Table 6.2-3 Hydrogen Sulfide Concentrations and Nondimensional Concentration Coefficient for a 230° Wind Direction, a 9.4 m/s Wind Speed and a 111.7 m/s Exit Velocity--Aminoil Surface Stack Releases

LOCATION NO.	NON DIMENSIONAL COEFF(K)	H2S CONCENTRATION(PPB)
1	.3824E-06	.3519
2	.2065E-05	1.9001
7	.7649E-05	7.0373
8	.2444E-04	22.4841
9	.6234E-05	5.7354
10	.4474E-05	4.1168
11	.2677E-06	.2463
13	.3824E-07	.0352
57	.1147E-06	.1056
56	.2295E-06	.2111
19	.2868E-05	2.6390
20	.2103E-05	1.9352
21	.6884E-06	.6334
22	.2600E-05	2.3927
23	.4207E-06	.3870
25	.7649E-07	.0704
60	.7649E-07	.0704
59	.1530E-06	.1407
58	.1147E-06	.1056
31	.3059E-06	.2815
32	.2677E-06	.2463
33	.1912E-06	.1759
34	.1530E-06	.1407
35	.1147E-06	.1056
37	.9561E-06	.8797
63	.7649E-07	.0704
62	.1530E-06	.1407
61	.1147E-06	.1056
43	.3442E-06	.3167
45	.2677E-05	2.4630
46	.2792E-05	2.5686
47	.4972E-06	.4574
49	.7649E-07	.0704
64	.4972E-06	.4574

Table 6.2-4 Hydrogen Sulfide Concentrations and Nondimensional Concentration Coefficient for a 210° Wind Direction, a 9.4 m/s Wind Speed and a 20.6 m/s Exit Velocity--Aminoil Surface Stack Releases

LOCATION NO.	NON DIMENSIONAL COEFF(K)	H2S CONCENTRATION(PPB)
7	0.	0.0000
8	.9810E-06	.1688
9	.1635E-06	.0281
10	.1635E-06	.0281
11	.6377E-05	1.0971
13	.1308E-05	.2250
57	.6998E-04	12.0399
56	.1145E-05	.1969
19	0.	0.0000
20	.1145E-05	.1969
21	.1799E-05	.3094
22	0.	0.0000
25	.4905E-06	.0844
70	.4071E-04	7.0045
71	.1079E-04	1.8566
60	.6769E-04	11.6461
59	.1308E-05	.2250
58	.2126E-05	.3657
31	.1799E-05	.3094
32	.2453E-05	.4220
33	.2943E-05	.5064
35	.9810E-05	1.6878
73	.3107E-05	.5345
74	.1030E-04	1.7722
63	.1373E-04	2.3630
62	.4415E-05	.7595
61	.1962E-05	.3376
43	.6704E-05	1.1534
44	.2616E-05	.4501
47	.4415E-05	.7595
64	.4578E-05	.7877
75	.8175E-05	1.4065
76	.6867E-05	1.1815
77	.3597E-05	.6189

Table 6.2-5 Hydrogen Sulfide Concentrations and Nondimensional Concentration Coefficient for a 210° Wind Direction, a 9.4 m/s Wind Speed and a 63.1 m/s Exit Velocity--Aminoil Surface Stack Releases

LOCATION NO.	NON DIMENSIONAL COEFF(K)	H2S CONCENTRATION(PPB)
7	.1001E-05	.5345
8	.5267E-06	.2813
9	.6320E-06	.3376
10	.6320E-06	.3376
11	.4214E-06	.2250
13	.7900E-06	.4220
57	.1643E-04	8.7768
56	.4214E-06	.2250
19	.2107E-06	.1125
20	.5267E-06	.2813
21	.1211E-05	.6470
22	.1053E-06	.0563
25	.8954E-06	.4782
70	.7374E-05	3.9383
71	.1106E-05	.5907
60	.1333E-04	7.1171
59	.5267E-06	.2813
58	.1211E-05	.6470
31	.5267E-06	.2813
32	.8954E-06	.4782
33	.1211E-05	.6470
35	.2107E-05	1.1252
73	.8954E-06	.4782
74	.1685E-05	.9002
63	.3002E-05	1.6035
62	.2633E-06	.1407
61		
43	.2423E-05	1.2940
44	.2107E-06	.1125
47	.5267E-07	.0281
64	.2633E-06	.1407
75	.1685E-05	.9002
76	.3213E-05	1.7160
77	.9480E-06	.5064

Table 6.2-6 Hydrogen Sulfide Concentrations and Nondimensional Concentration Coefficient for a 210° Wind Direction, a 9.4 m/s Wind Speed and a 111.7 m/s Exit Velocity--Aminoil Surface Stack Releases

LOCATION NO.	NON DIMENSIONAL COEFF(K)	H2S CONCENTRATION(PPB)
7	.4586E-06	.4220
8	.5809E-06	.5345
9	.4586E-06	.4220
10	.6726E-06	.6189
11	0.	0.0000
13	.1529E-06	.1407
57	.1520E-04	13.9810
56	.5809E-06	.5345
19	.1223E-06	.1125
20	.1223E-06	.1125
21	.4892E-06	.4501
22	.9784E-06	.9002
25	.3364E-06	.3094
70	.8652E-05	7.9610
71	.5809E-06	.5345
60	.1611E-04	14.8249
59	.7032E-06	.6470
58	.7338E-06	.6751
31	.7949E-06	.7314
32	.1101E-05	1.0127
33	.6115E-06	.5626
35	.5809E-06	.5345
73	.8867E-06	.8158
74	.1529E-06	.1407
63	.2935E-05	2.7005
62	.1223E-06	.1125
61	.6115E-07	.0563
43	.1223E-06	.1125
44	.4586E-06	.4220
47	.3057E-06	.2813
64	.4586E-06	.4220
75	.3210E-05	2.9537
76	.4280E-05	3.9383
77	.2721E-05	2.5036

Table 6.2-7 Hydrogen Sulfide Concentrations and Nodimensional Concentration Coefficient for a 210° Wind Direction, a 6.2 m/s Wind Speed and a 20.6 m/s Exit Velocity--Aminoil Surface Stack Releases

LOCATION NO.	NON DIMENSIONAL COEFF(K)	H2S CONCENTRATION(PPB)
7	.3052E-05	.7961
8	.2071E-05	.5402
9	.1635E-05	.4265
10	.7630E-06	.1990
11	.1090E-06	.0284
13	.1090E-06	.0284
57	.2899E-04	7.5632
56	.1526E-05	.3981
19	.1417E-05	.3696
20	.1199E-05	.3128
21	.3379E-05	.8814
22	.1308E-05	.3412
25	.3815E-05	.9952
70	.6540E-04	17.0599
71	.8938E-05	2.3315
60	.4055E-04	10.5772
59	.2507E-05	.6540
58	.2180E-05	.5687
31	.3052E-05	.7961
32	.2725E-05	.7108
33	.3161E-05	.8246
35		
73	.1853E-05	.4834
74	.3161E-05	.8246
63	.1079E-04	2.8149
62	.6540E-06	.1706
61	.7630E-06	.1990
43	.6540E-06	.1706
44	.7630E-06	.1990
47	.1526E-05	.3981
64	0.	0.0000
75	.7303E-05	1.9050
76	.1875E-04	4.8905
77	.3161E-05	.8246

Table 6.2-8 Hydrogen Sulfide Concentrations and Nondimensional Concentration Coefficient for a 210° Wind Direction, a 6.2 m/s Wind Speed and a 63.1 m/s Exit Velocity--Aminoil Surface Stack Releases

LOCATION NO.	NON DIMENSIONAL COEFF(K)	H2S CONCENTRATION(PPB)
7	.7725E-06	.6255
8	.9129E-06	.7393
9	.4214E-06	.3412
10	.9129E-06	.7393
11	.9480E-06	.7677
13	.8427E-06	.6824
57	.6777E-05	5.4876
56	.8778E-06	.7108
19	.5618E-06	.4549
20	.8076E-06	.6540
21	.1229E-05	.9952
22	.1159E-05	.9383
25	.5267E-06	.4265
70	.2205E-04	17.8561
71	.2704E-05	2.1894
60	.7479E-05	6.0563
59	.5267E-06	.4265
58	.3160E-06	.2559
31	.5969E-06	.4834
32	.7374E-06	.5971
33	.5969E-06	.4834
35	.1405E-05	1.1373
73	.8427E-06	.6824
74	.8427E-06	.6824
63		
62	.7023E-06	.5687
61	0.	0.0000
43	.1756E-06	.1422
44	.5618E-06	.4549
47	.7725E-06	.6255
64	.8076E-06	.6540
75	.2282E-05	1.8482
76	.9726E-05	7.8760
77	.2282E-05	1.8482

Table 6.2-9 Hydrogen Sulfide Concentrations and Nondimensional Concentration Coefficient for a 210° Wind Direction, a 6.2 m/s Wind Speed and a 111.7 m/s Exit Velocity--Aminoil Surface Stack Releases

LOCATION NO.	NON DIMENSIONAL COEFF(K)	H2S CONCENTRATION(PPB)
7	.4077E-06	.5687
8	.4484E-06	.6255
9	.3261E-06	.4549
10	.6115E-07	.0853
11		
13	.1223E-06	.1706
57	.3771E-05	5.2601
56	.2446E-06	.3412
19	0.	0.0000
20	.1019E-06	.1422
21	.3873E-06	.5402
22	0.	0.0000
25	.1631E-06	.2275
70	.9050E-05	12.6243
71	.6522E-06	.9099
60	.5014E-05	6.9946
59	.6319E-06	.8814
58	.7949E-06	1.1089
31	.7542E-06	1.0520
32	.8561E-06	1.1942
33	.8357E-06	1.1658
35	.9988E-06	1.3932
73	.6115E-06	.8530
74	.6726E-06	.9383
63	.9376E-06	1.3079
62	.3873E-06	.5402
61	.4484E-06	.6255
43	.5911E-06	.8246
44	.3261E-06	.4549
47	.5707E-06	.7961
64		
75	.8561E-06	1.1942
76	.7032E-05	9.8095
77	.9376E-06	1.3079

Table 7-1 The Wind Velocity (m/s) at Aminoil Test Site and the Meteorological Station for Three Heights Above Ground Level

Height Z Prototype	Aminoil Test Site		Meterological Station	
	Model m/s	Prototype m/s	Model m/s	Prototype m/s
Z = 10 m	0.67	10.93	0.73	11.95
Z = 20 m	0.76	12.4	0.86	14.0
Z = 40 m	0.85	13.87	0.92	15.2

Table 8.1 Summary of H_2S Concentrations for the Proposed Geothermal Plant Site (Unit 13)

Description	Wind Speed m/s	Wind Direction	Exit Velocity m/s	Maximum		Highest near Anderson Springs or Whispering Pines	
				X MAX (ppb)	Location	X MAX (ppb)	Location
Surface	3.1	250	2.5	18.1	12	18.1	12
Release	3.1	250	12.7	22.4	11	22.4	11
	3.1	230	2.5	24.9	7	0.8	64
	3.1	230	12.7	17.6	7	0.9	47
	3.1	210	2.5	14.7	57	1.9	75
	3.1	210	12.7	12.5	60	2.9	75
	6.2	250	2.5	15.6	11	15.6	11
	6.2	250	12.7	60.2	9	40.0	11
	6.2	230	2.5	13.5	7	0.4	64
	6.2	230	12.7	27.7	20	0.8	64
	6.2	210	2.5	5.7	70	3.6	76
	6.2	210	12.7	20.4	60	12.5	76
	9.4	250	2.5	16.1	2	10.6	12
	9.4	250	12.7	61.0	2	49.8	11
	9.4	230	2.5	12.0	7	2.4	45
	9.4	230	12.7	42.1	8	4.5	64
	9.4	210	2.5	5.6	60	1.3	76
	9.4	210	12.7	24.0	60	4.4	76
Surface	6.2	210	20.6	17.1	70	4.9	76
Stack	6.2	210	63.1	17.9	70	7.9	76
Release	6.2	210	111.7	12.6	70	9.8	76
	9.4	210	20.6	12.0	57	1.4	75
	9.4	210	63.1	8.8	57	1.7	76
	9.4	210	111.7	14.8	60	3.9	76
	9.4	230	20.6	61.8	7	1.2	11
	9.4	230	63.1	39.1	8	2.2	11
	9.4	230	111.7	22.5	8	0.5	64

Table 8.1 (continued)

Description	Wind Speed m/s	Wind Direction	Exit Velocity m/s	Maximum X MAX (ppb)	Maximum Location	Highest near Anderson Springs or Whispering Pines X MAX (ppb)	Highest near Anderson Springs or Whispering Pines Location
Stack (30m)	3.1	250	20.6	6.5	11	6.5	11
Release	3.1	250	63.1	4.2	11	4.2	11
	3.1	250	111.7	1.4	11	1.4	11
	3.1	230	20.6	6.2	8	1.0	47
	3.1	230	63.1	3.0	7	0.4	37
	3.1	230	111.7	2.2	20	[illegible].6	25
	3.1	210	20.6	10.8	57	0.6	76
	3.1	210	63.1	2.0	57	0.5	13
	3.1	210	111.7	3.1	60	0.8	25
	6.2	250	20.6	58.7	9	11.6	[illegible]1
	6.2	250	63.1	20.3	9	12.9	[illegible]1
	6.2	250	111.7	21.7	37	21.7	3[illegible]
	6.2	230	20.6	26.5	20	0.9	47
	6.2	230	63.1	14.5	8	0.8	64
	6.2	230	111.7	19.6	7	0.8	[illegible]
	6.2	210	20.6	10.4	60	8.6	[illegible]
	6.2	210	63.1	6.0	57	3.2	76
	6.2	210	111.7	12.4	76	12.4	76
	9.4	250	20.6	104.2	48	104.2	48
	9.4	250	63.1	48.0	2	39.4	11
	9.4	250	111.7	84.1	7	61.5	12
	9.4	230	20.6	41.6	7	1.8	37
	9.4	230	63.1	43.8	7	2.3	11
	9.4	230	111.7	23.7	7	3.8	2
	9.4	210	20.6	18.2	57	2.3	76
	9.4	210	63.1	14.5	60	10.5	64
	9.4	210	111.7	18.9	60	3.5	76

FIGURES

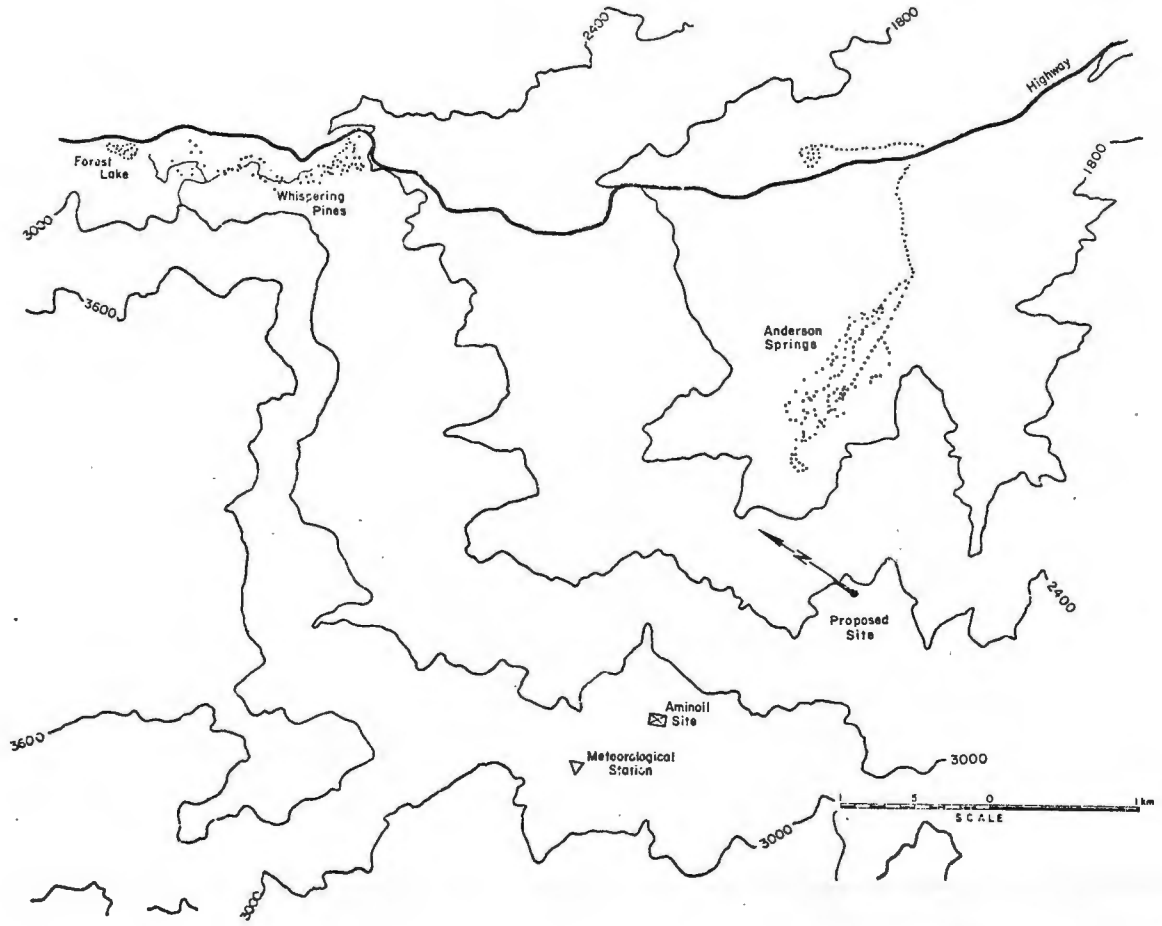

Figure 1.1 Map Showing Geyser Geothermal Area and Location of Proposed Aminoil Power Plant

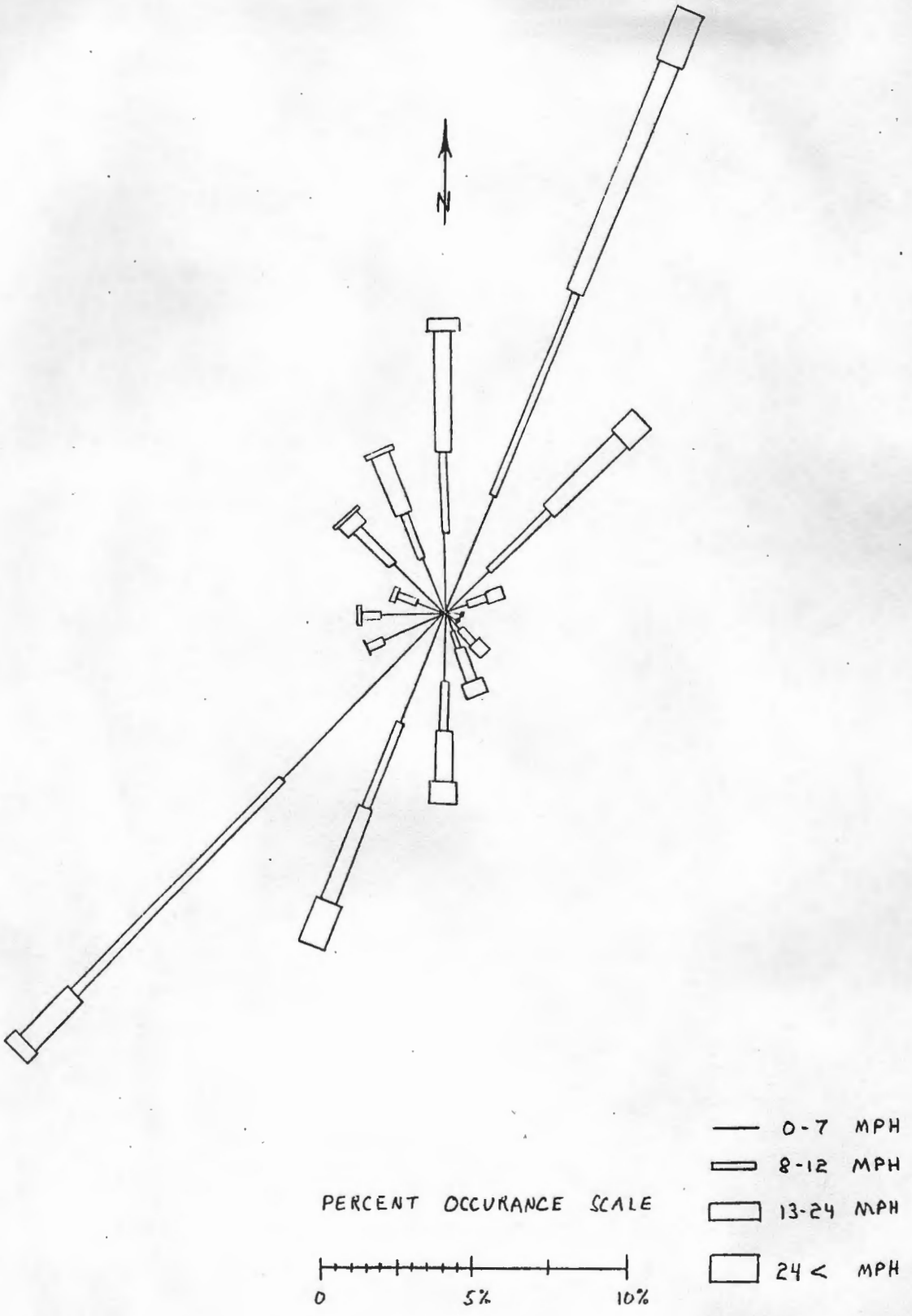

Figure 1.2 Wind Rose from Meteorological Station Located near Proposed Sites

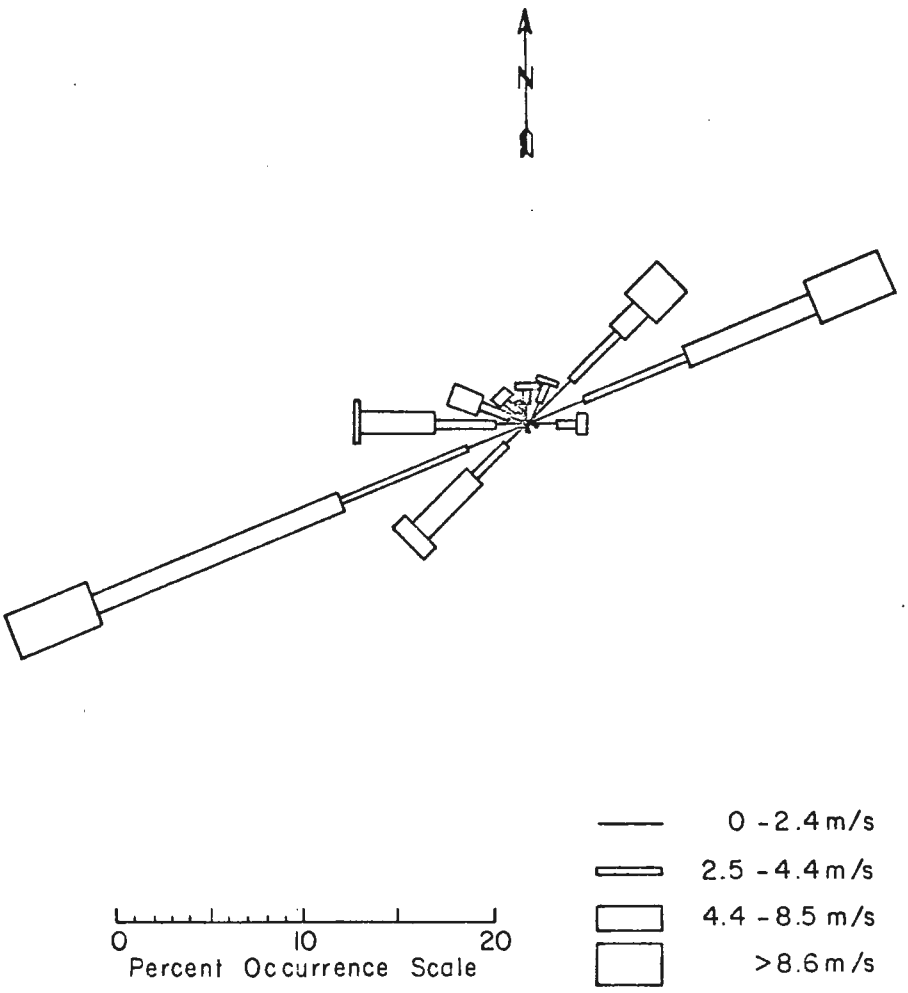

Figure 1.2b Wind Rose from Meteorological Station #2

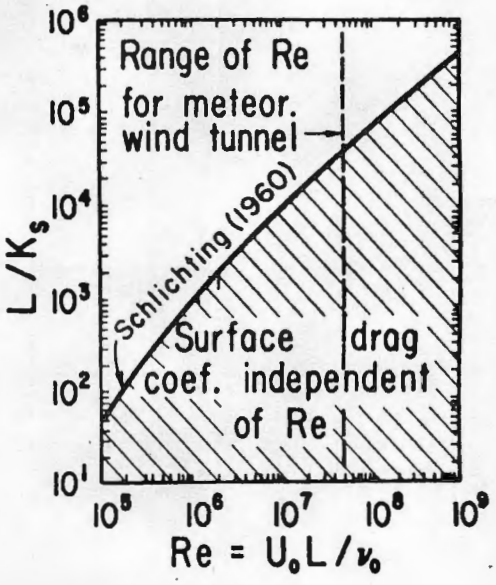

Figure 2.1 Reynolds Number at which Flow Becomes Independent of Reynolds Number for Prescribed Relative Roughness

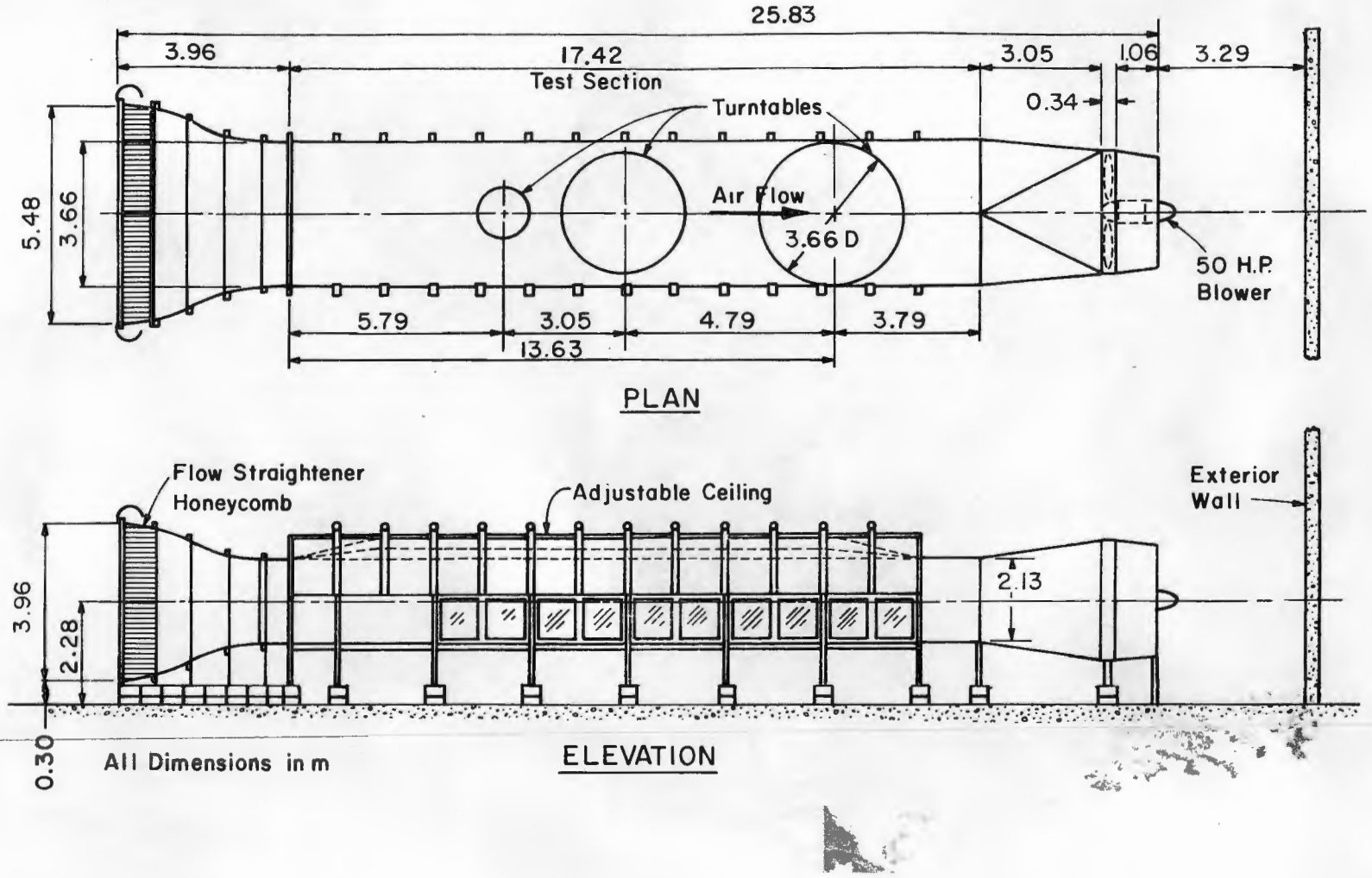

Figure 3.1-1 Environmental Wind Tunnel; Fluid Dynamics and Diffusion Laboratory, Colorado State University

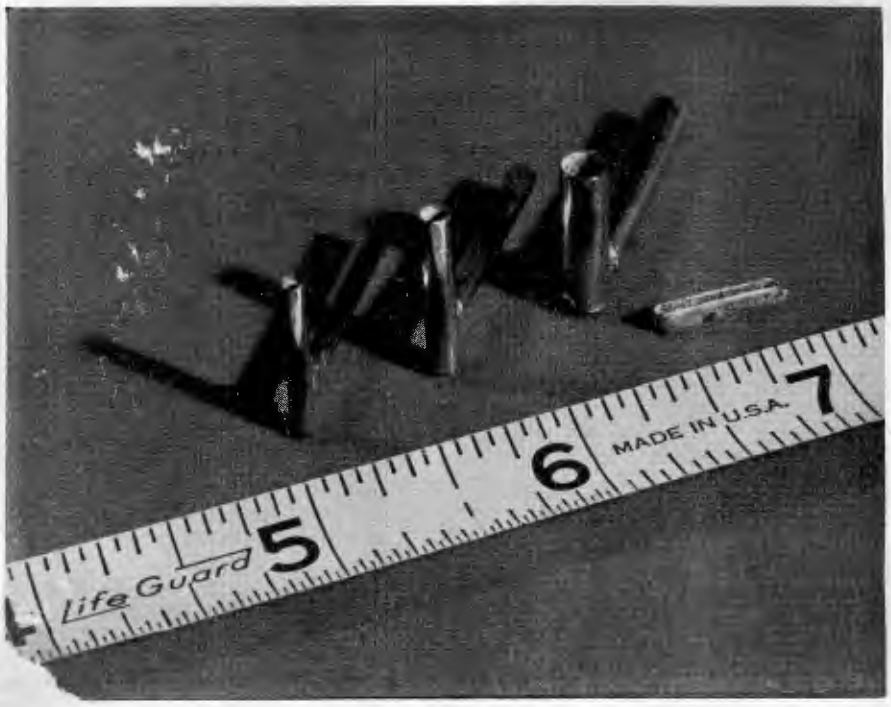

Figure 3.2-1 Photograph of Model Stacks and Area Source

Figure 3.2-2 Photograph of Terrain Model in the Environmental Wind Tunnel

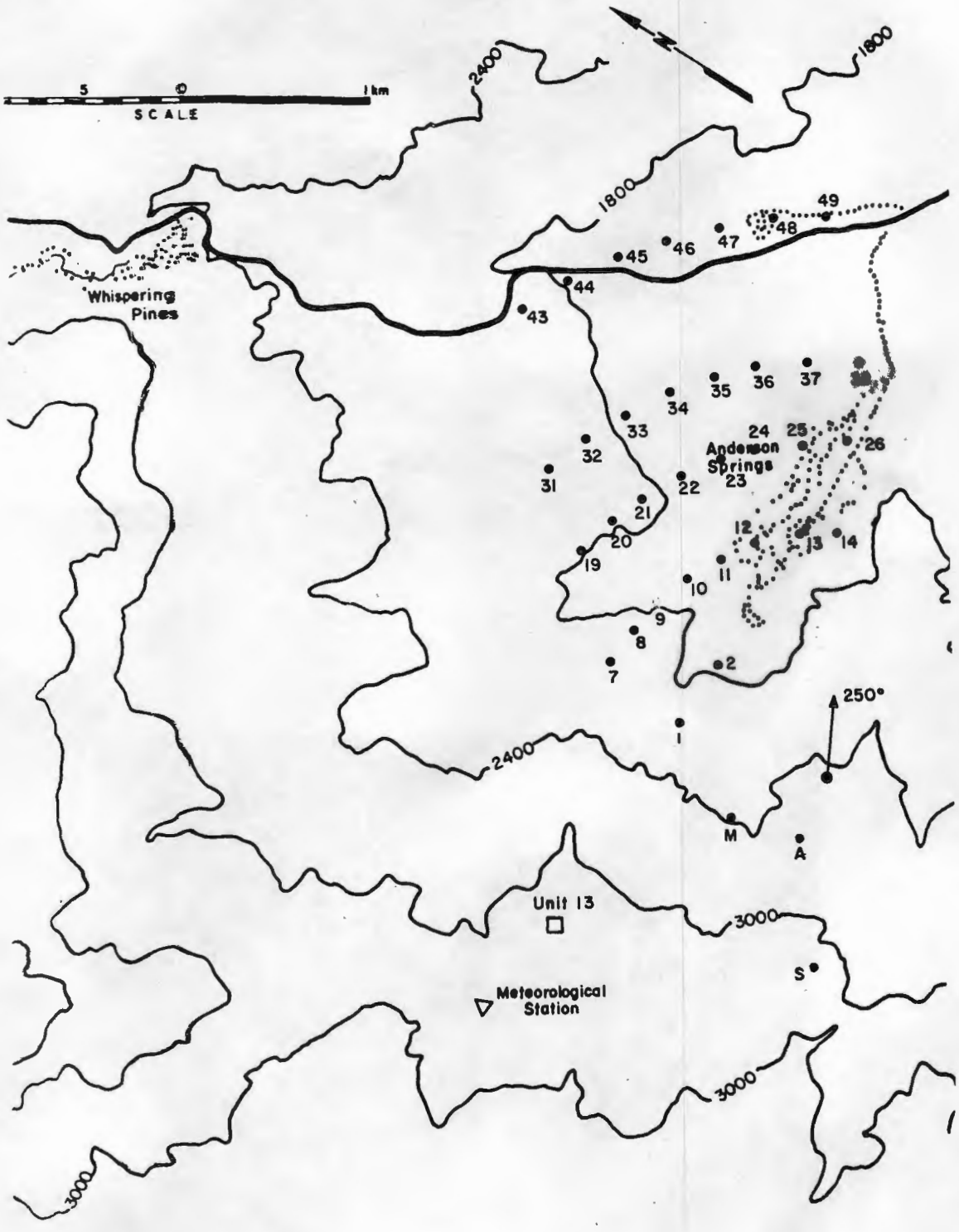

Figure 3.2-3 Basemap for the 250° Wind Direction

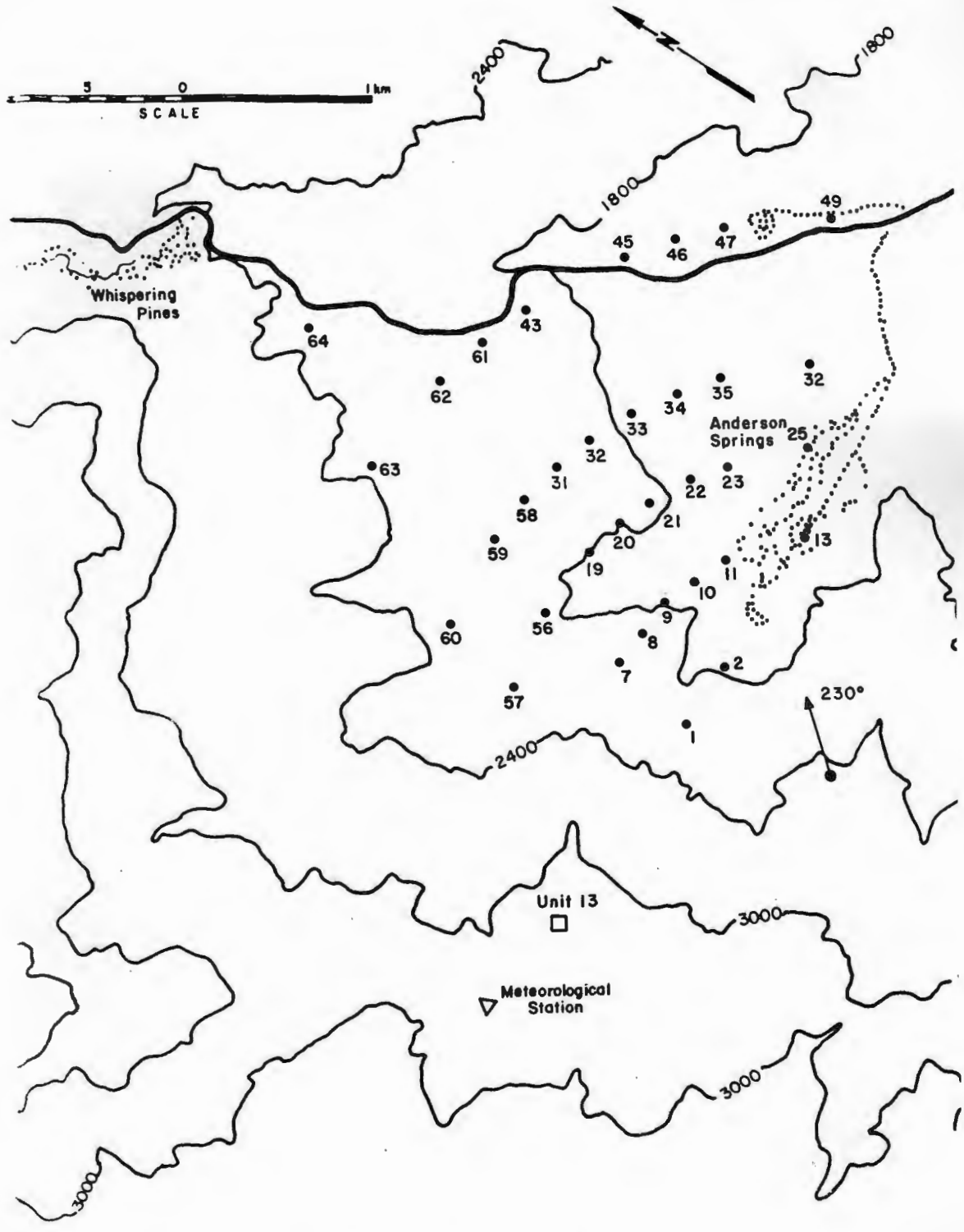

Figure 3.2-4 Basemap for the 230° Wind Direction

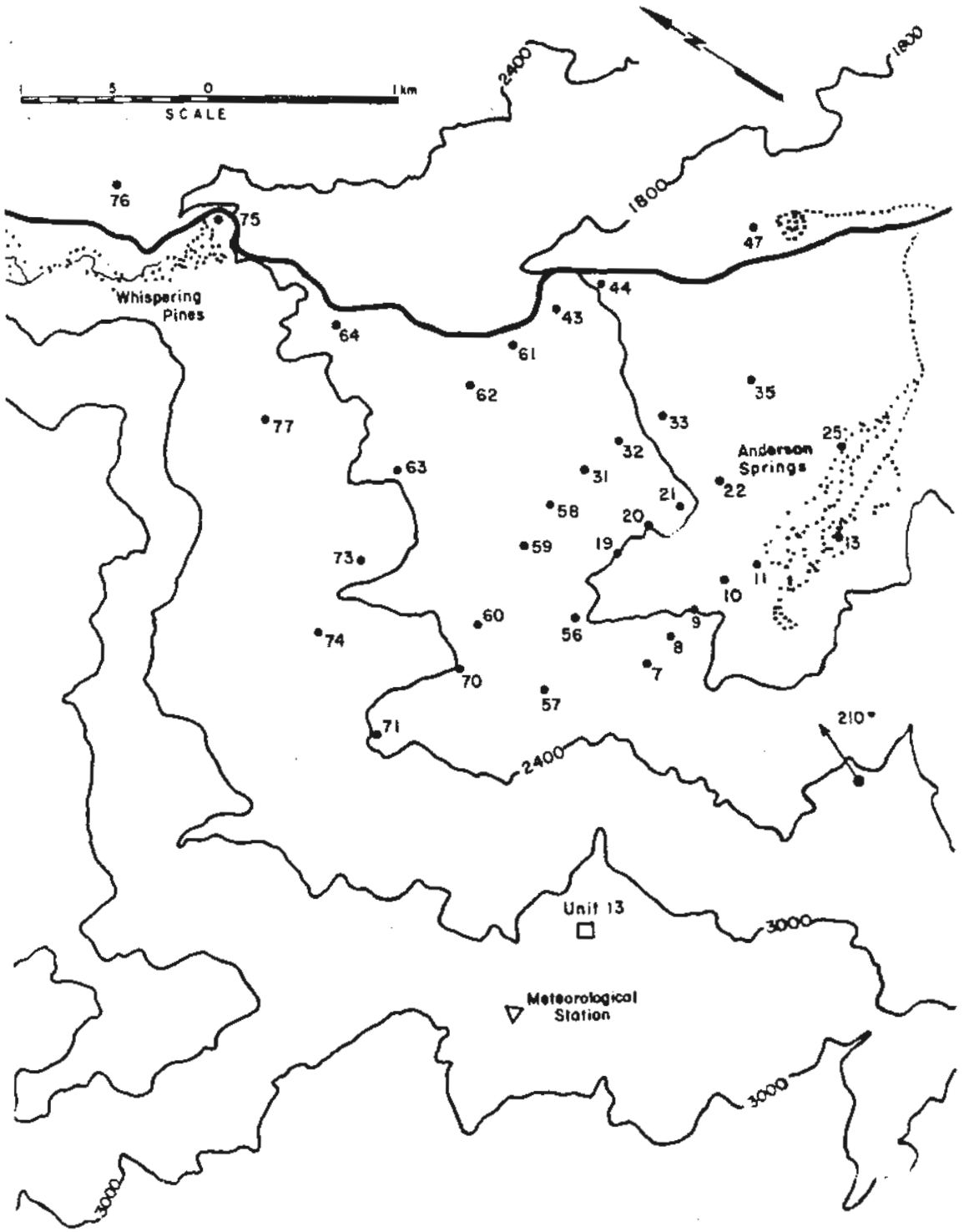

Figure 3.2-5 Basemap for the 210° Wind Direction

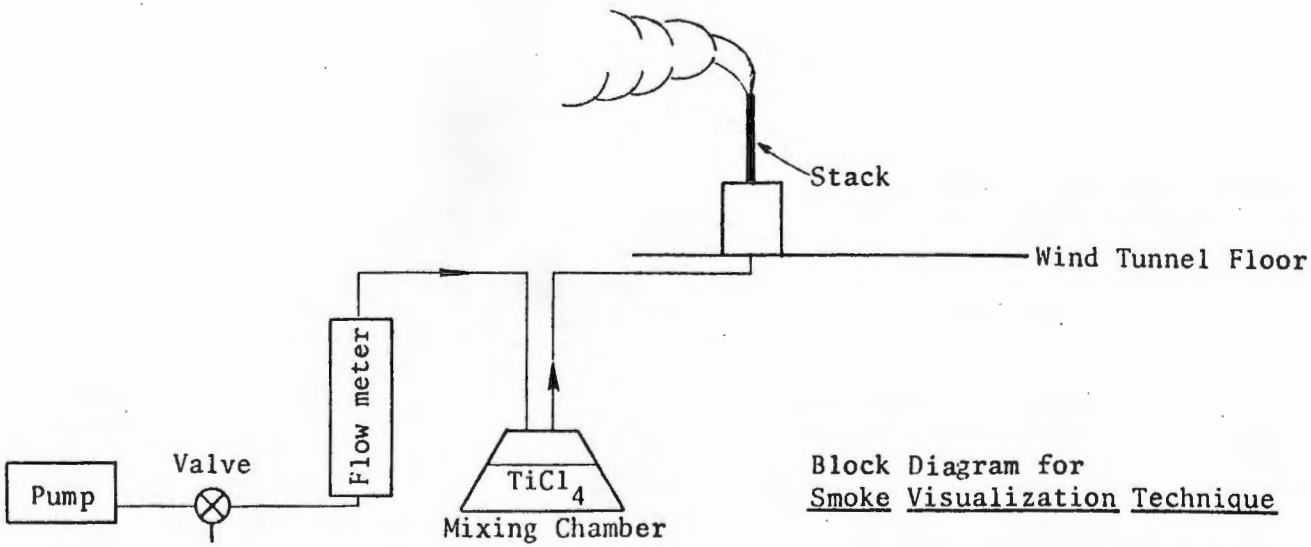

Figure 3.3-1 Schematic of Plume Visualization Equipment

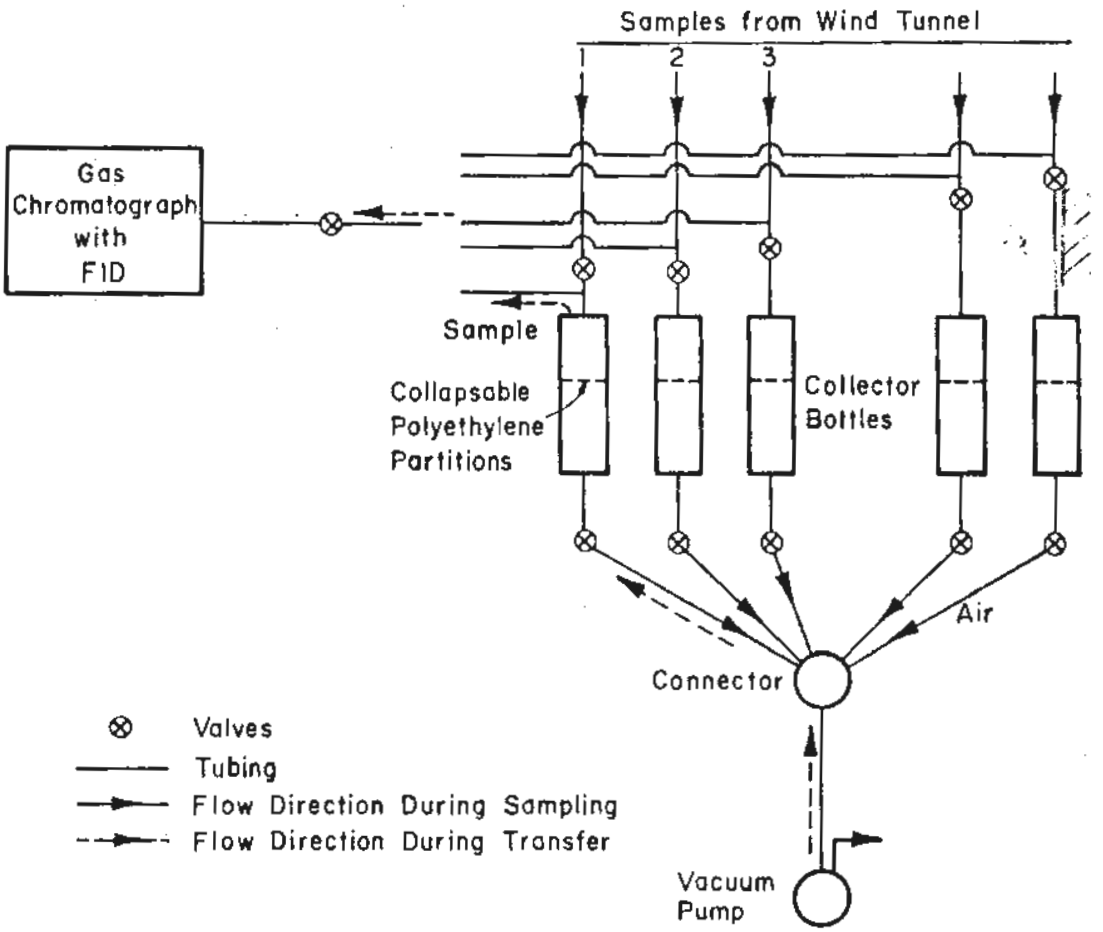

Figure 3.4-1 Schematic of Tracer Gas Sampling System

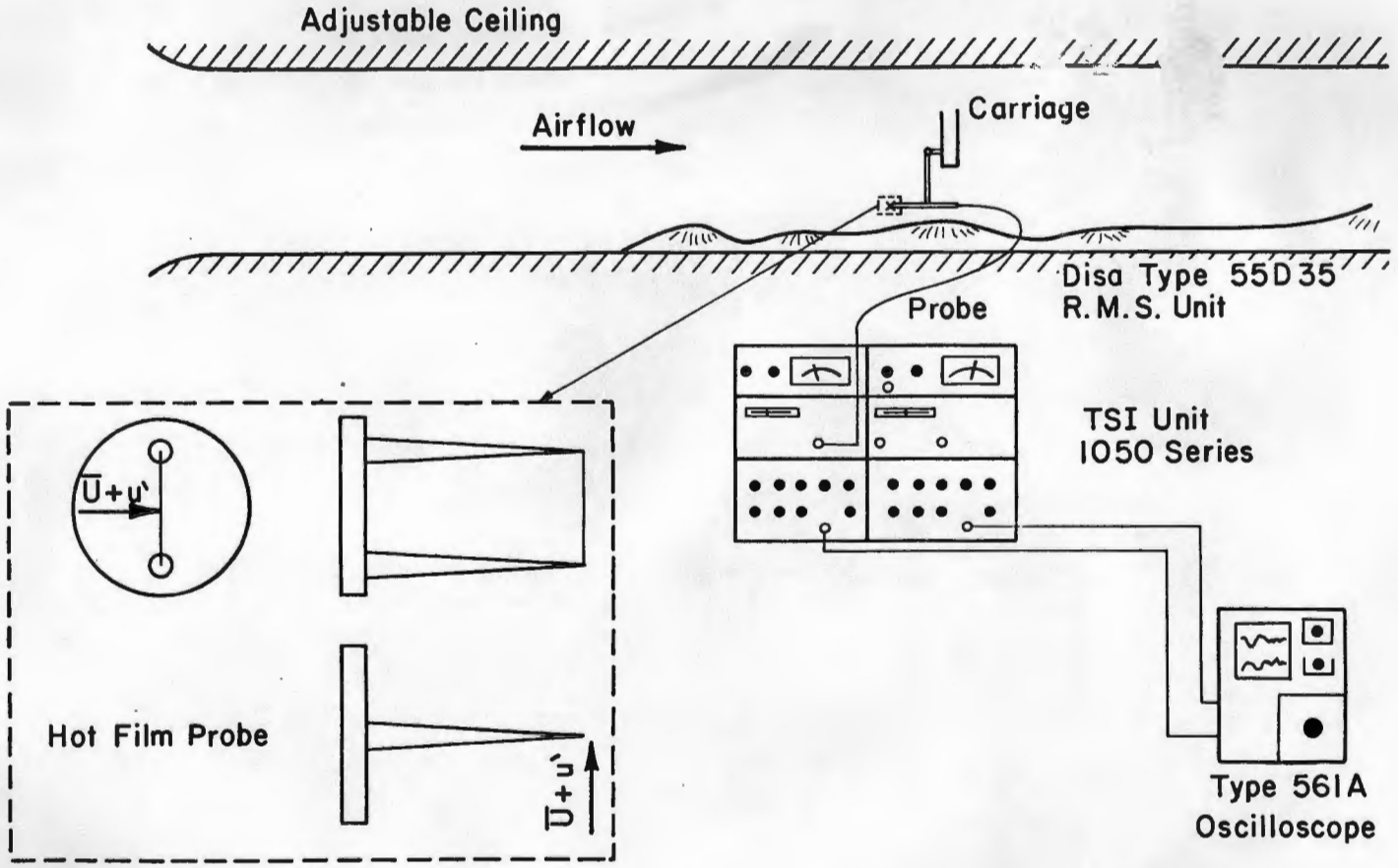

Figure 3.5-1 Laboratory Experimental Arrangement for Obtaining Turbulent Intensities and Mean Wind Velocities over the Terrain

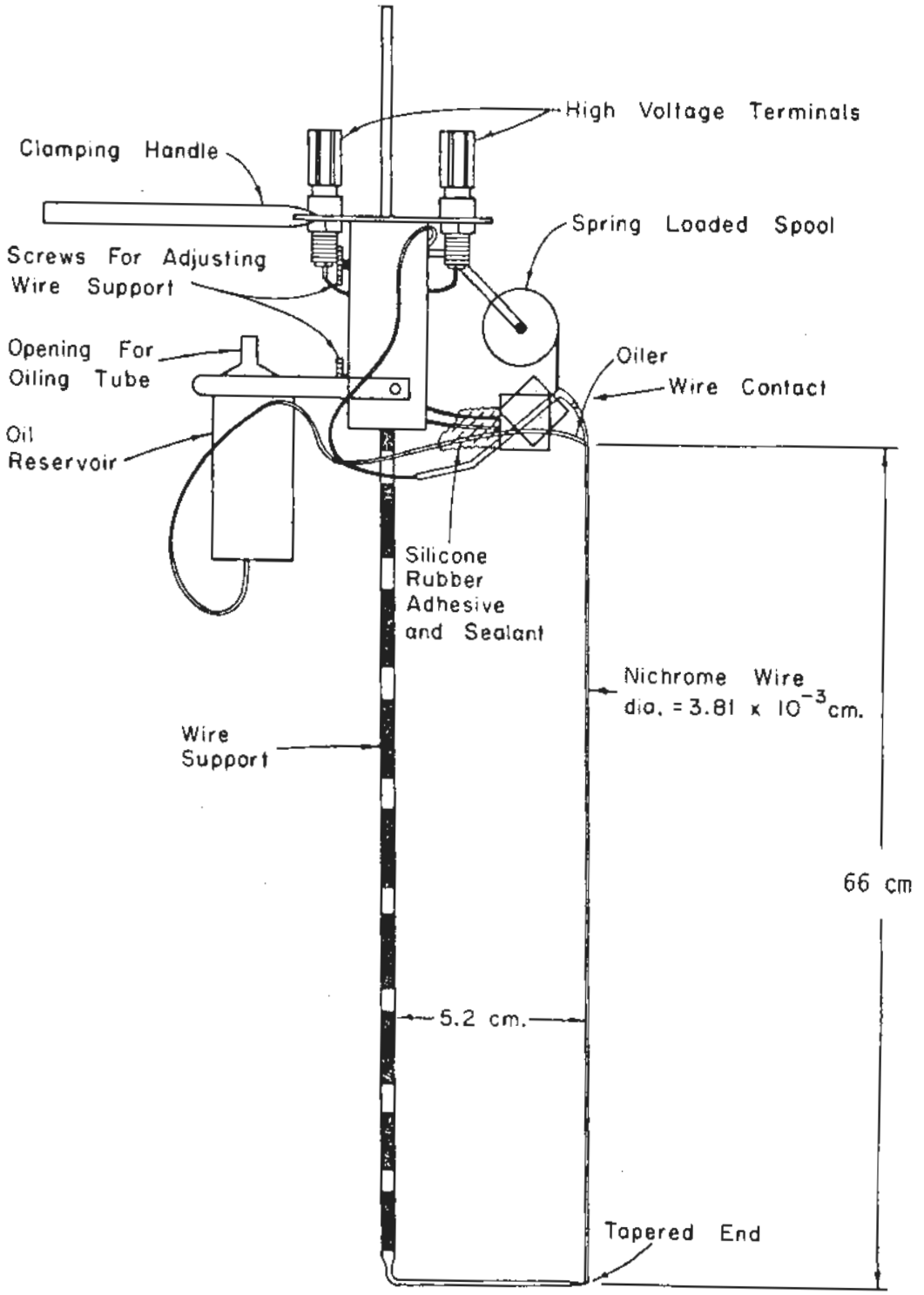

Figure 3.5-2 The Smoke-Wire Used to Visualize Wind Profiles over the Terrain

a) 3.1 m/s

b) 6.2 m/s

c) 9.4 m/s

Figure 4.1-1 Surface release plume visualization for a 12.7 m/s exit velocity, 250° wind direction and wind speeds of a) 3.1 m/s, b) 6.2 m/s, and c) 9.4 m/s.

a) 3.1 m/s

b) 6.2 m/s

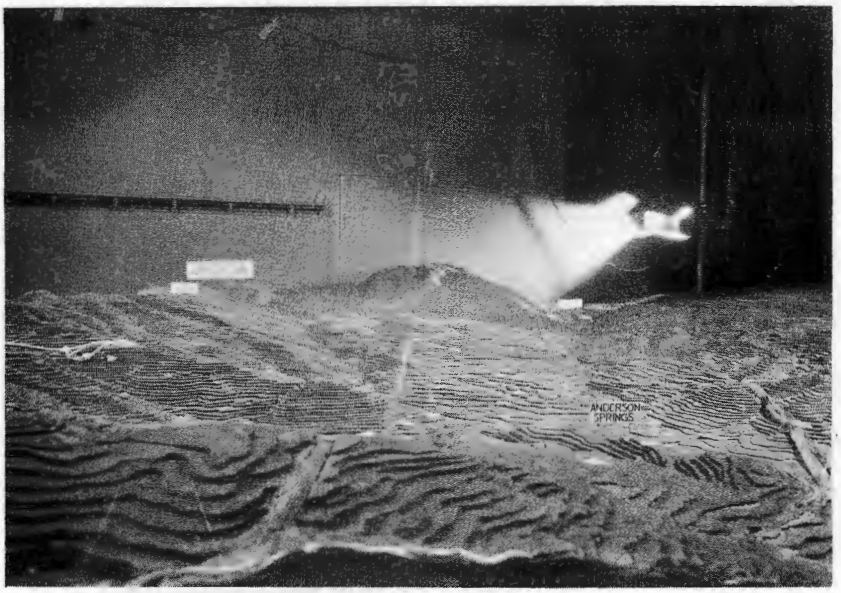

c) 9.4 m/s

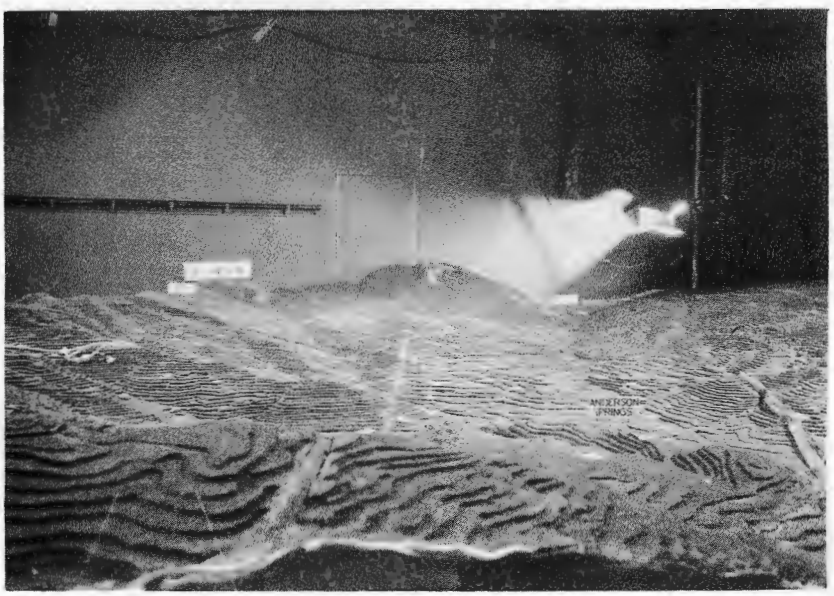

Figure 4.1-2 Surface release plume visualization for a 12.7 m/s exit velocity, 210° wind direction and wind speeds of a) 3.1 m/s, b) 6.2 m/s, and c) 9.4 m/s.

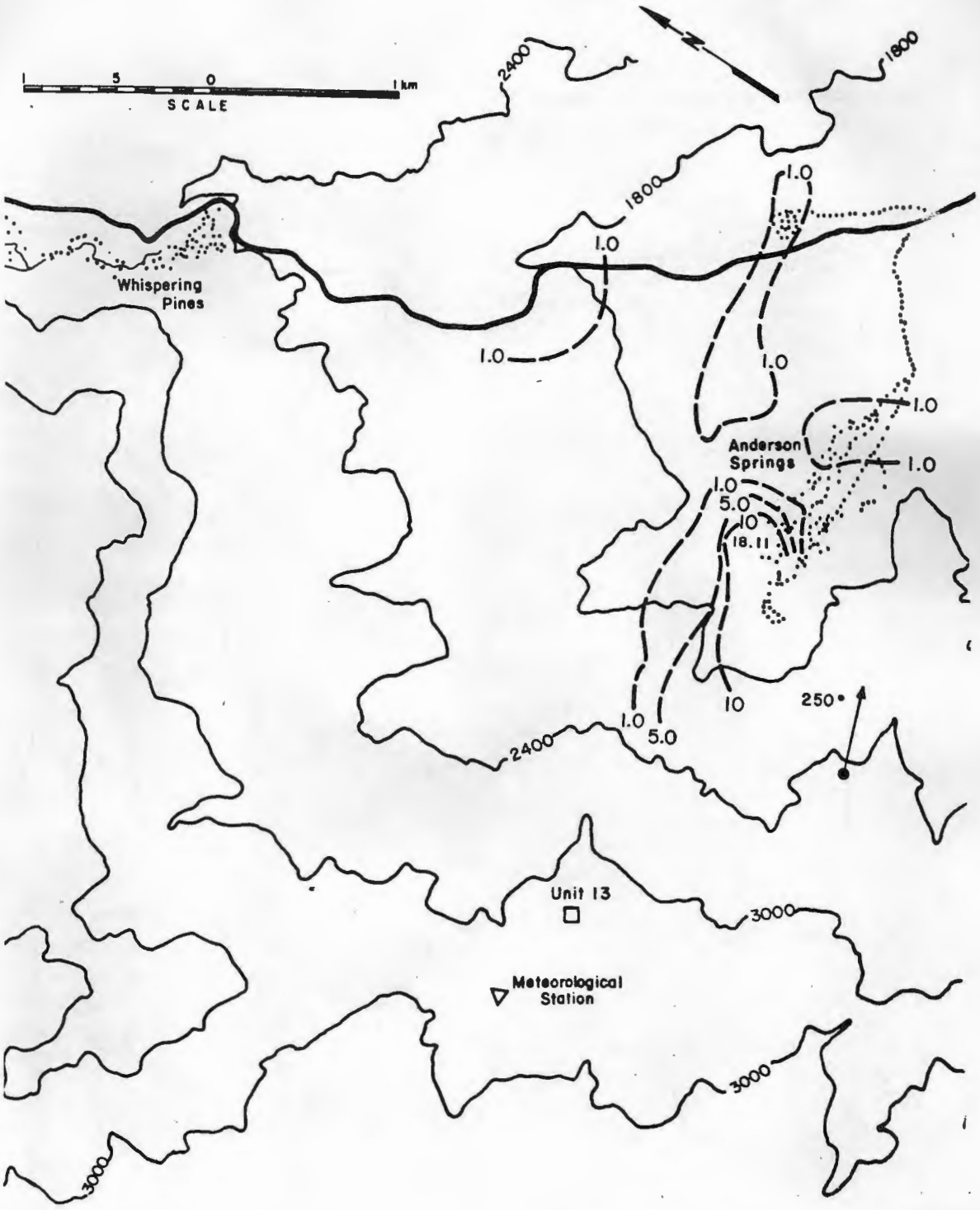

Figure 4.2-1 Isopleths of H_2S Concentrations for a 250° Wind Direction, a 3.1 m/s Wind Speed and a 2.5 m/s Exit Velocity-- Aminoil Surface Releases

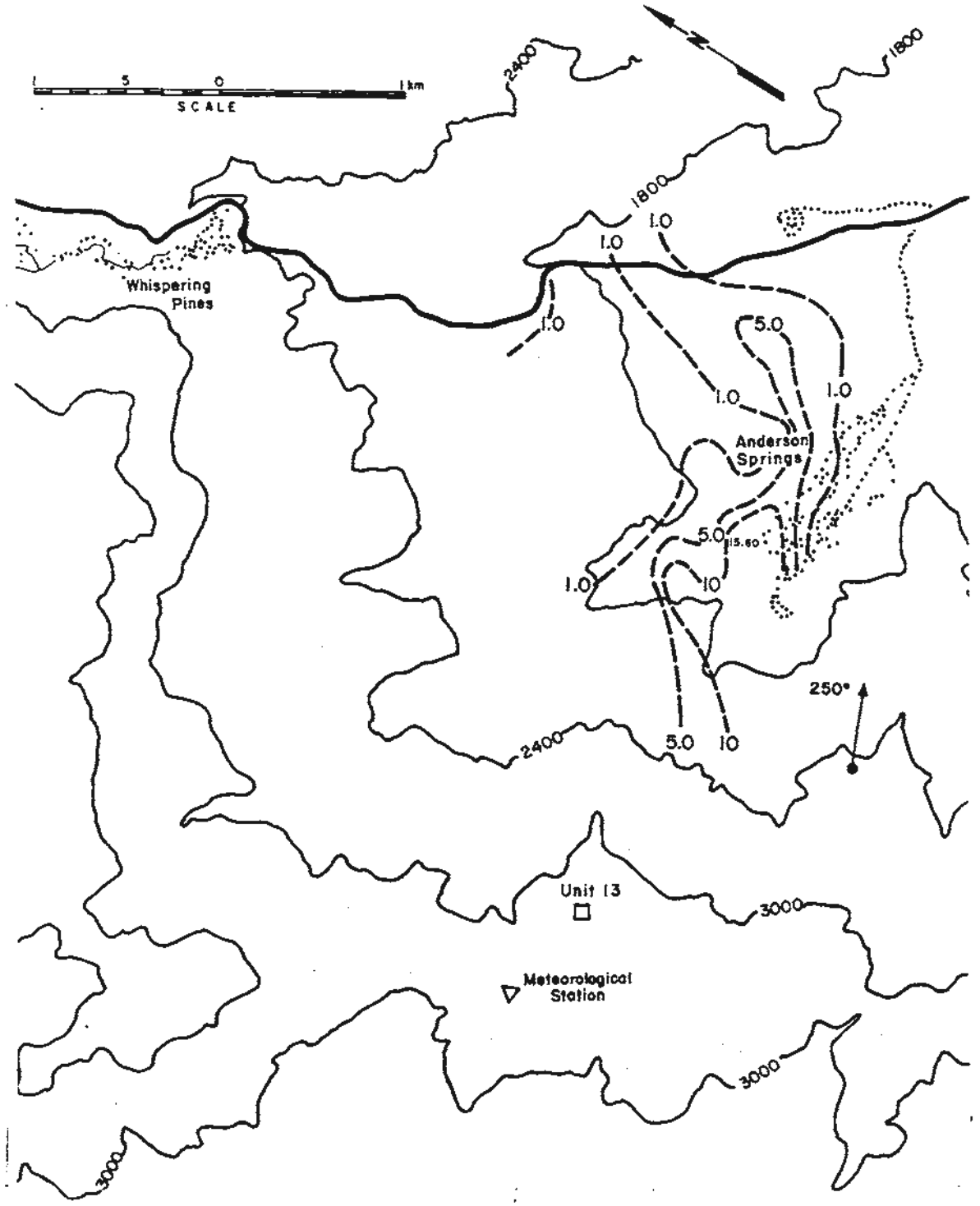

Figure 4.2-2 Isopleths of H_2S Concentrations for a 250° Wind Direction, a 6.2 m/s Wind Speed and a 2.5 m/s Exit Velocity--Aminoil Surface Releases

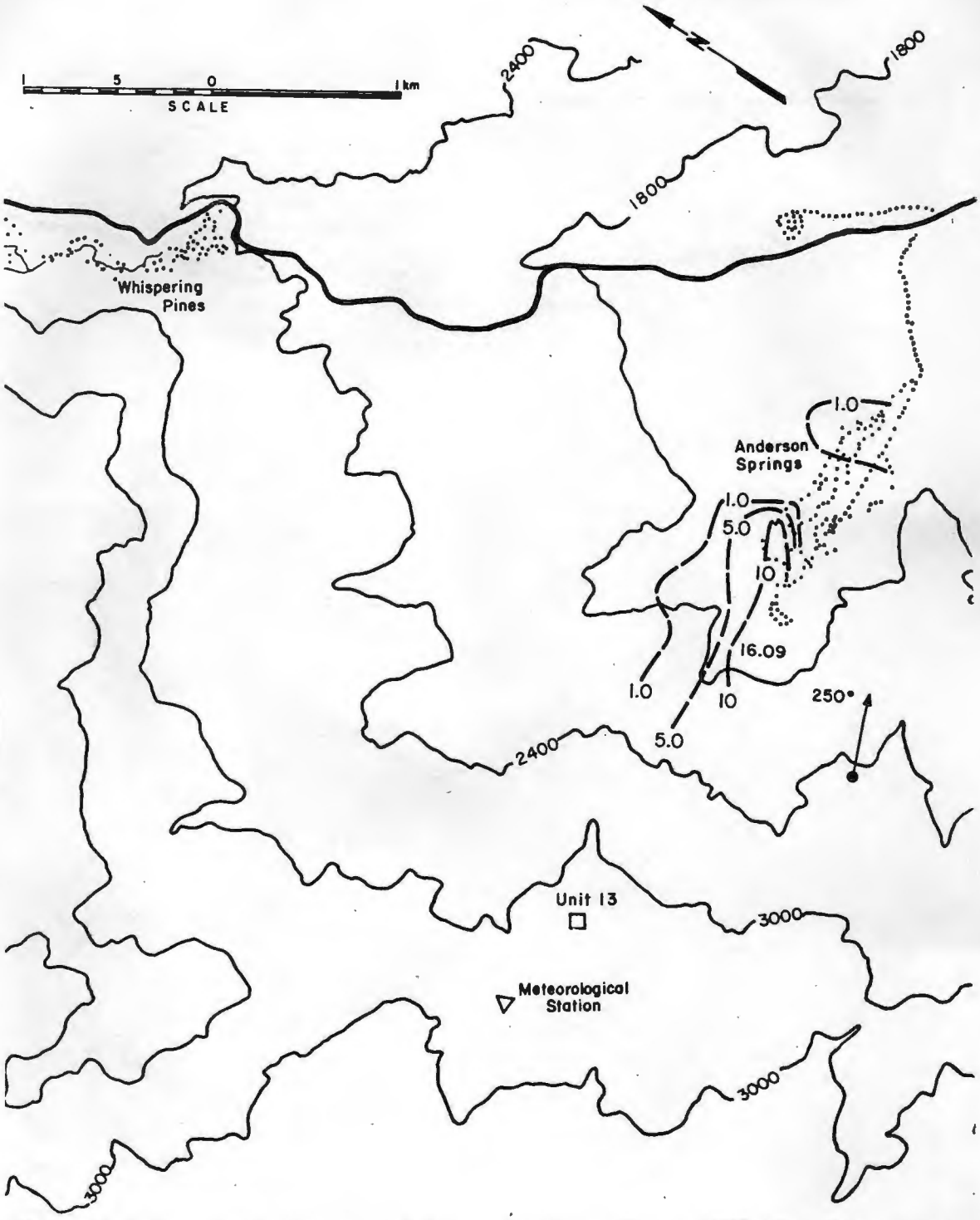

Figure 4.2-3 Isopleths of H_2S Concentrations for a 250° Wind Direction, a 9.4 m/s Wind Speed and a 2.5 m/s Exit Velocity--Aminoil Surface Releases

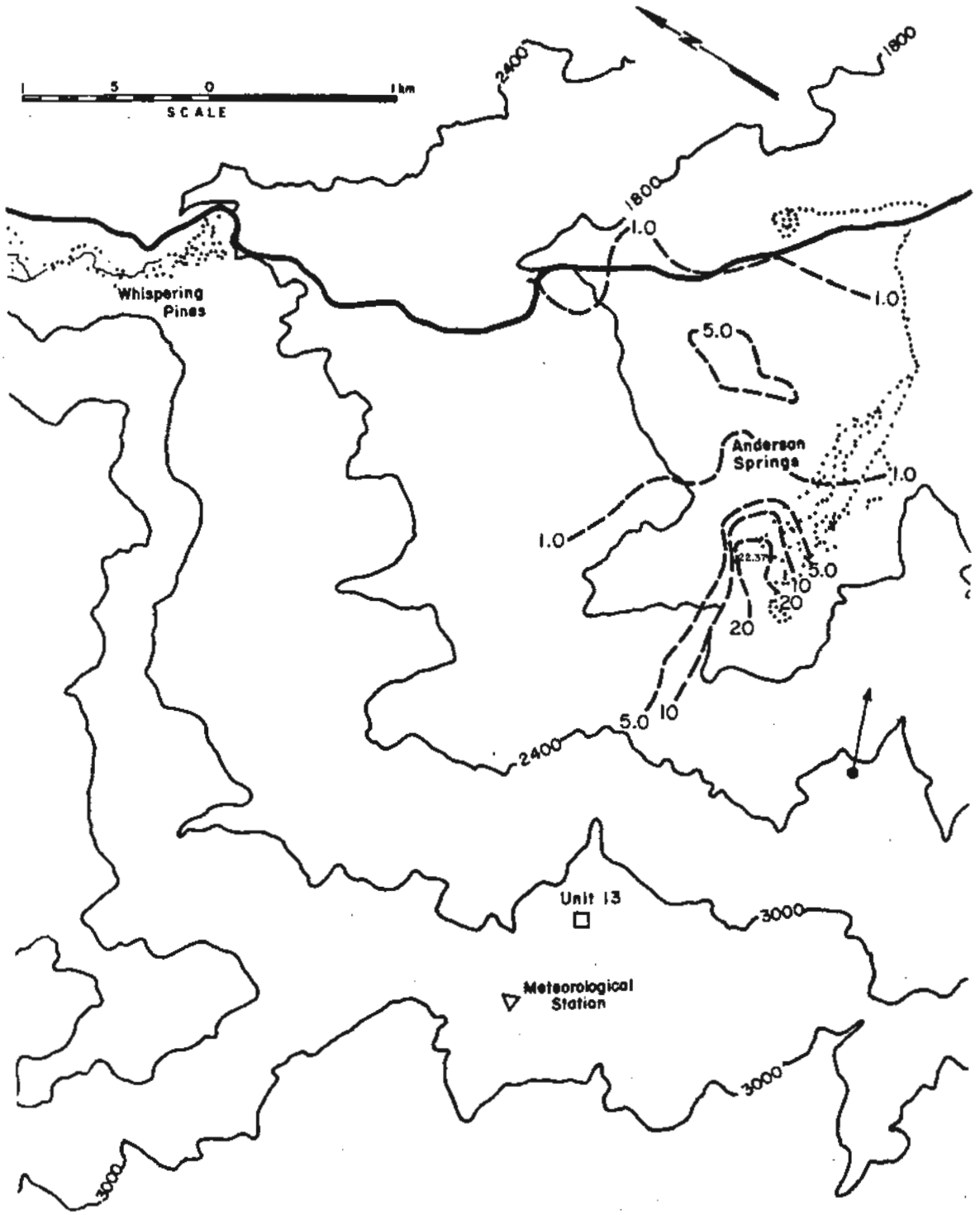

Figure 4.2-4 Isopleths of H_2S Concentrations for a 250° Wind Direction, a 3.2 m/s Wind Speed and a 12.7 m/s Exit Velocity--Aminoil Surface Releases

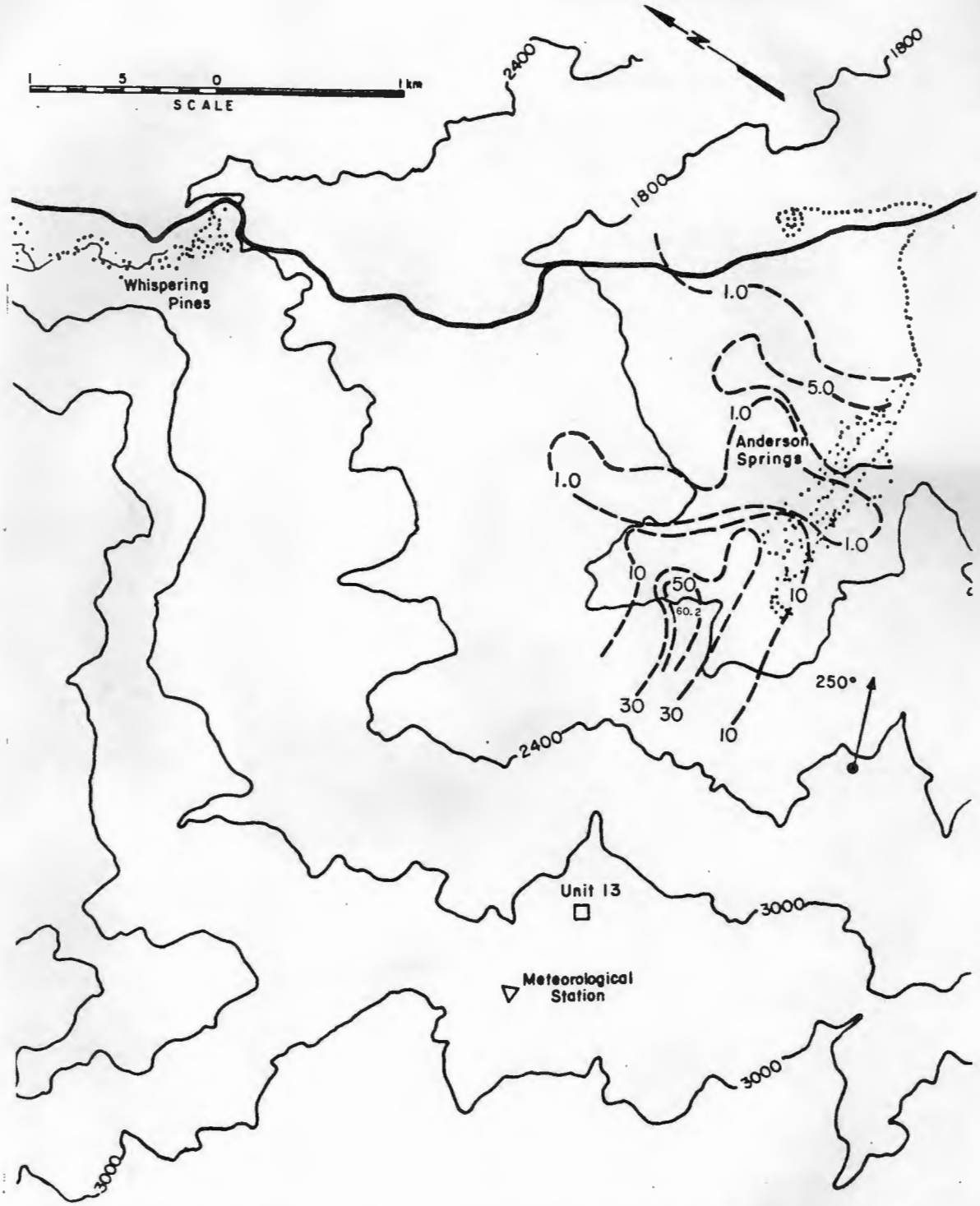

Figure 4.2-5 Isopleths of H_2S Concentrations for a 250° Wind Direction, a 6.2 m/s Wind Speed and a 12.7 m/s Exit Velocity-- Aminoil Surface Releases

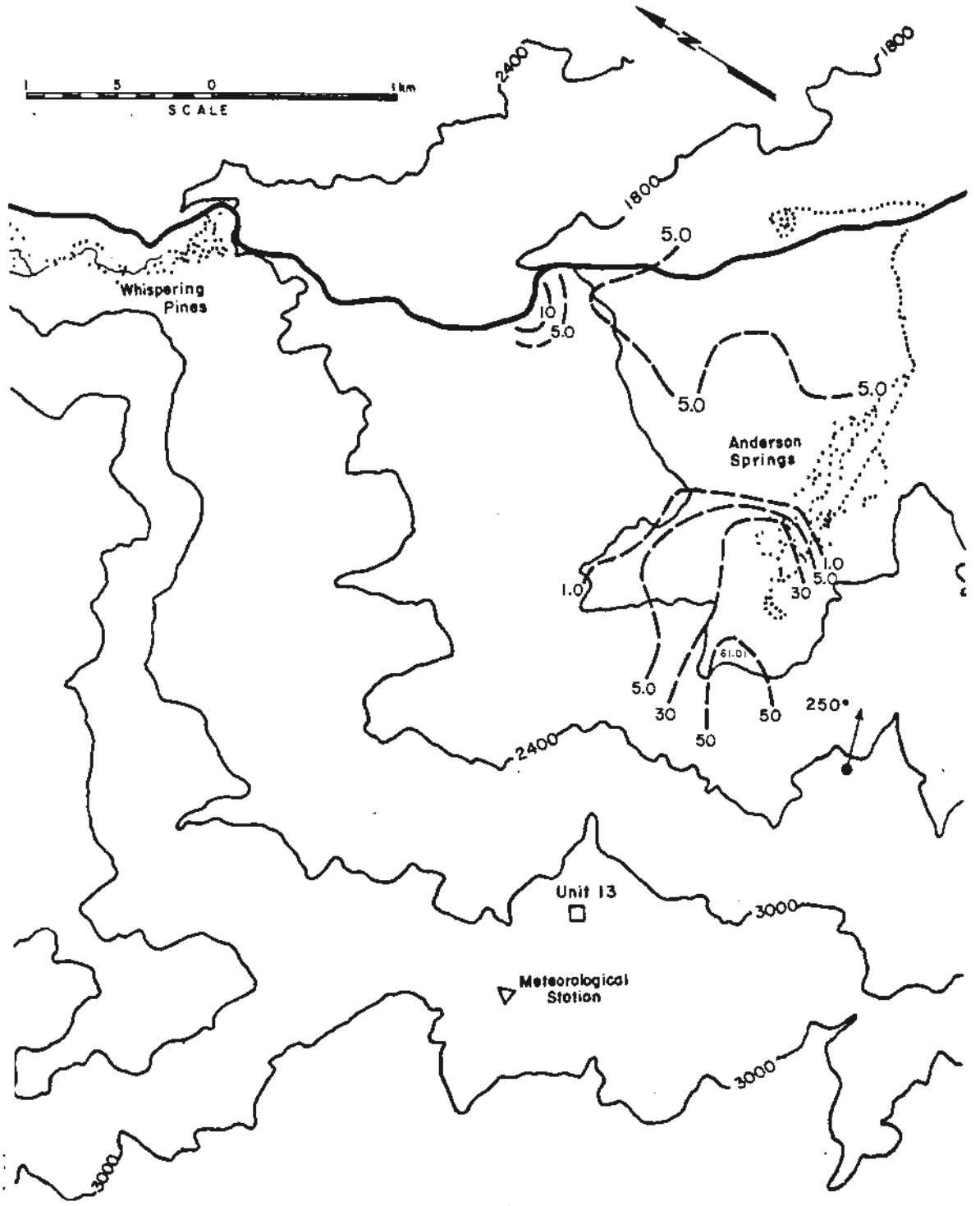

Figure 4.2-6 Isopleths of H_2S Concentrations for a 250° Wind Direction, a 9.4 m/s Wind Speed and a 12.7 m/s Exit Velocity--Aminoil Surface Releases

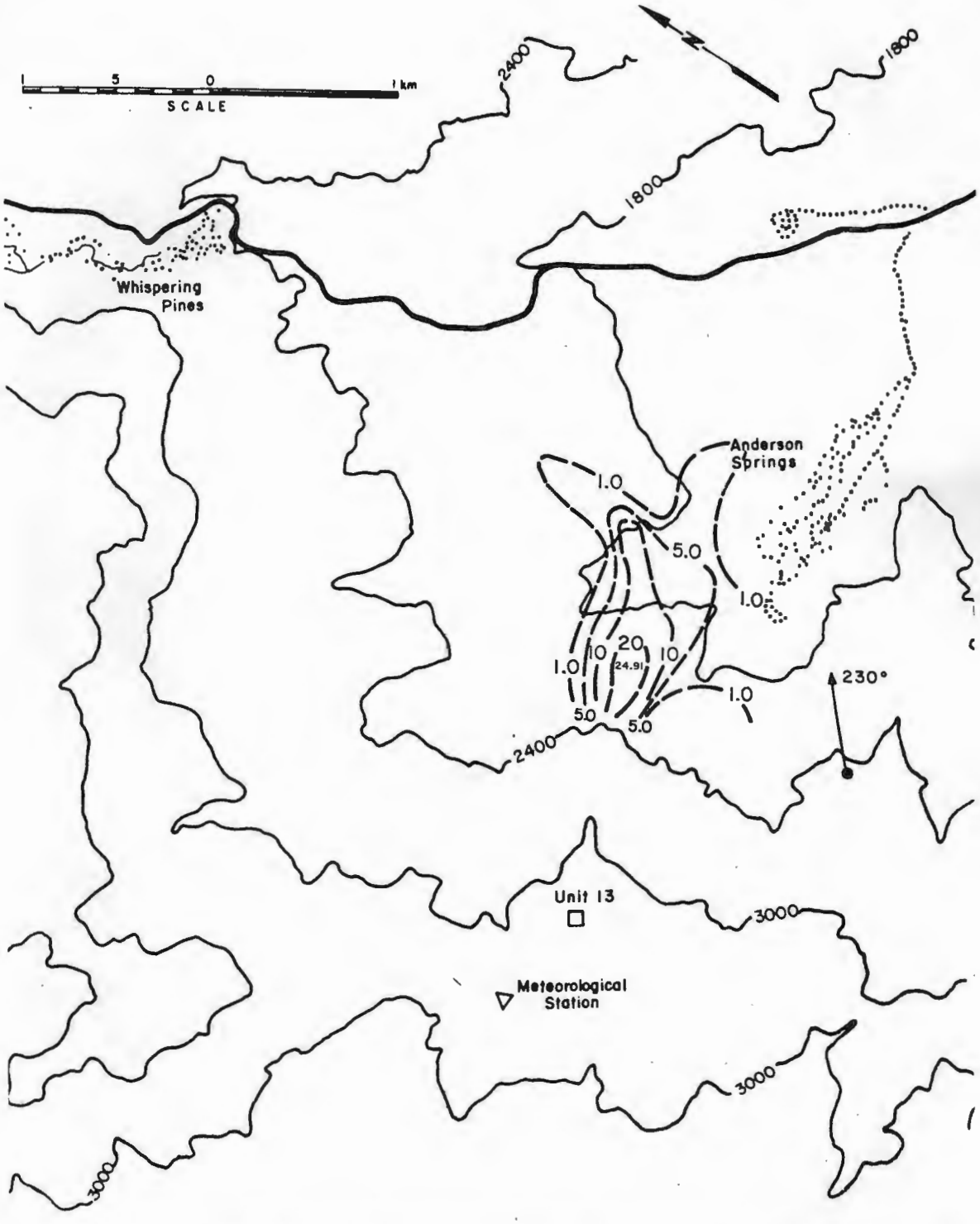

Figure 4.2-7 Isopleths of H_2S Concentrations for a 230° Wind Direction, a 3.1 m/s Wind Speed and a 2.5 m/s Exit Velocity-- Aminoil Surface Releases

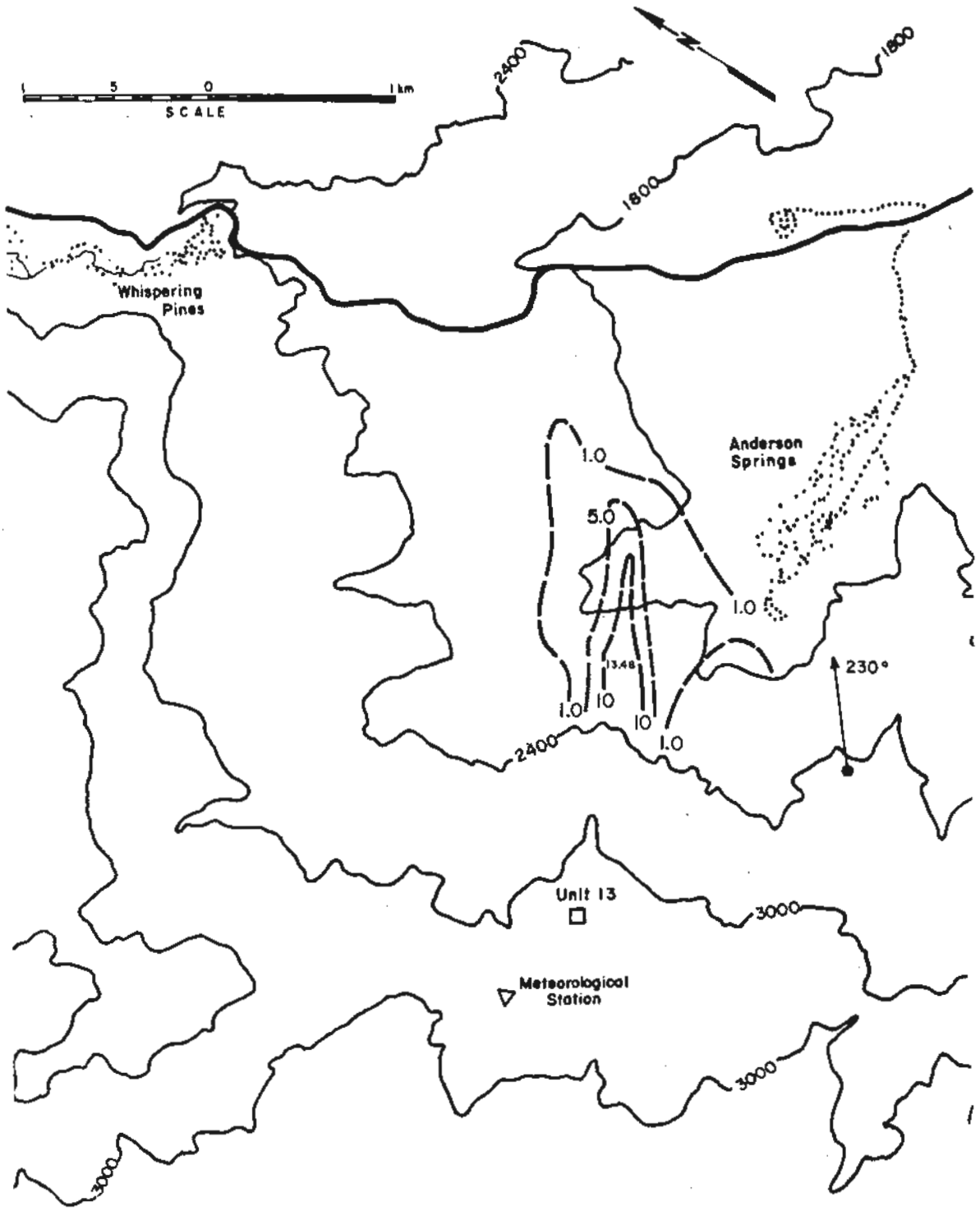

Figure 4.2-8 Isopleths of H_2S Concentrations for a 230° Wind Direction, a 6.2 m/s Wind Speed and a 2.5 m/s Exit Velocity--Aminoil Surface Releases

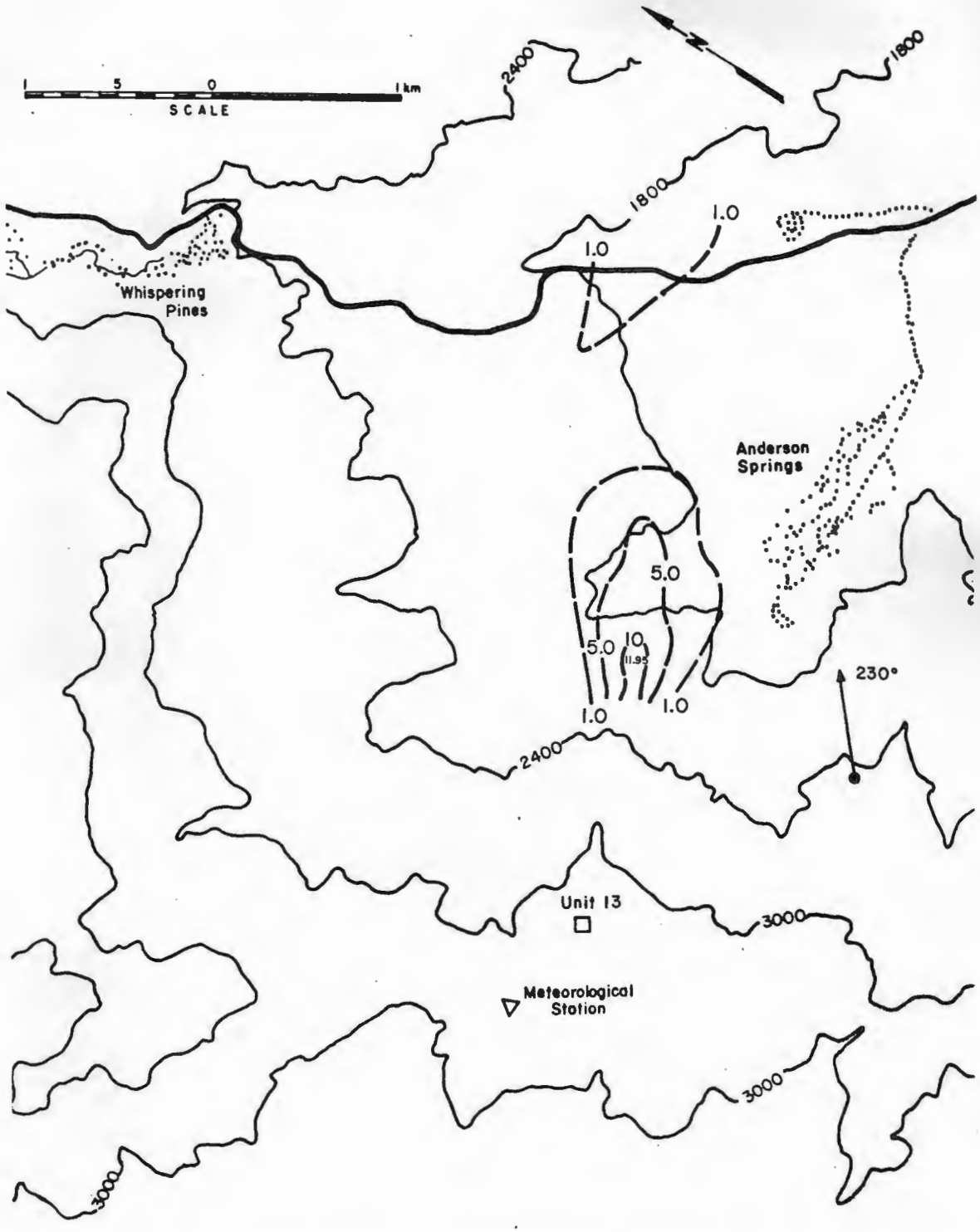

Figure 4.2-9 Isopleths of H_2S Concentrations for a 230° Wind Direction, a 9.4 m/s Wind Speed and a 2.5 m/s Exit Velocity--Aminoil Surface Releases

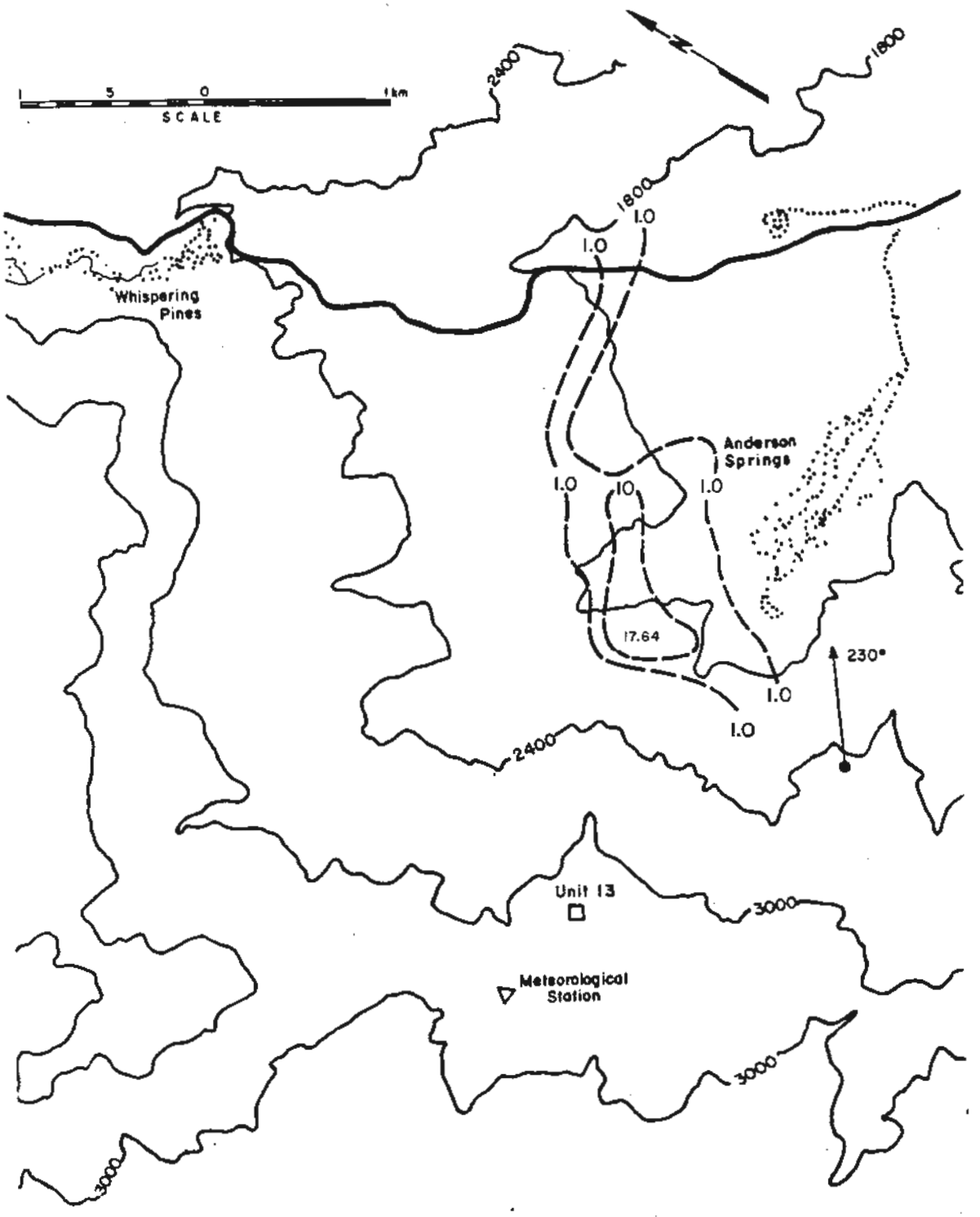

Figure 4.2-10 Isopleths of H_2S Concentrations for a 230° Wind Direction a 3.1 m/s Wind Speed and a 12.7 m/s Exit Velocity-- Aminoil Surface Releases

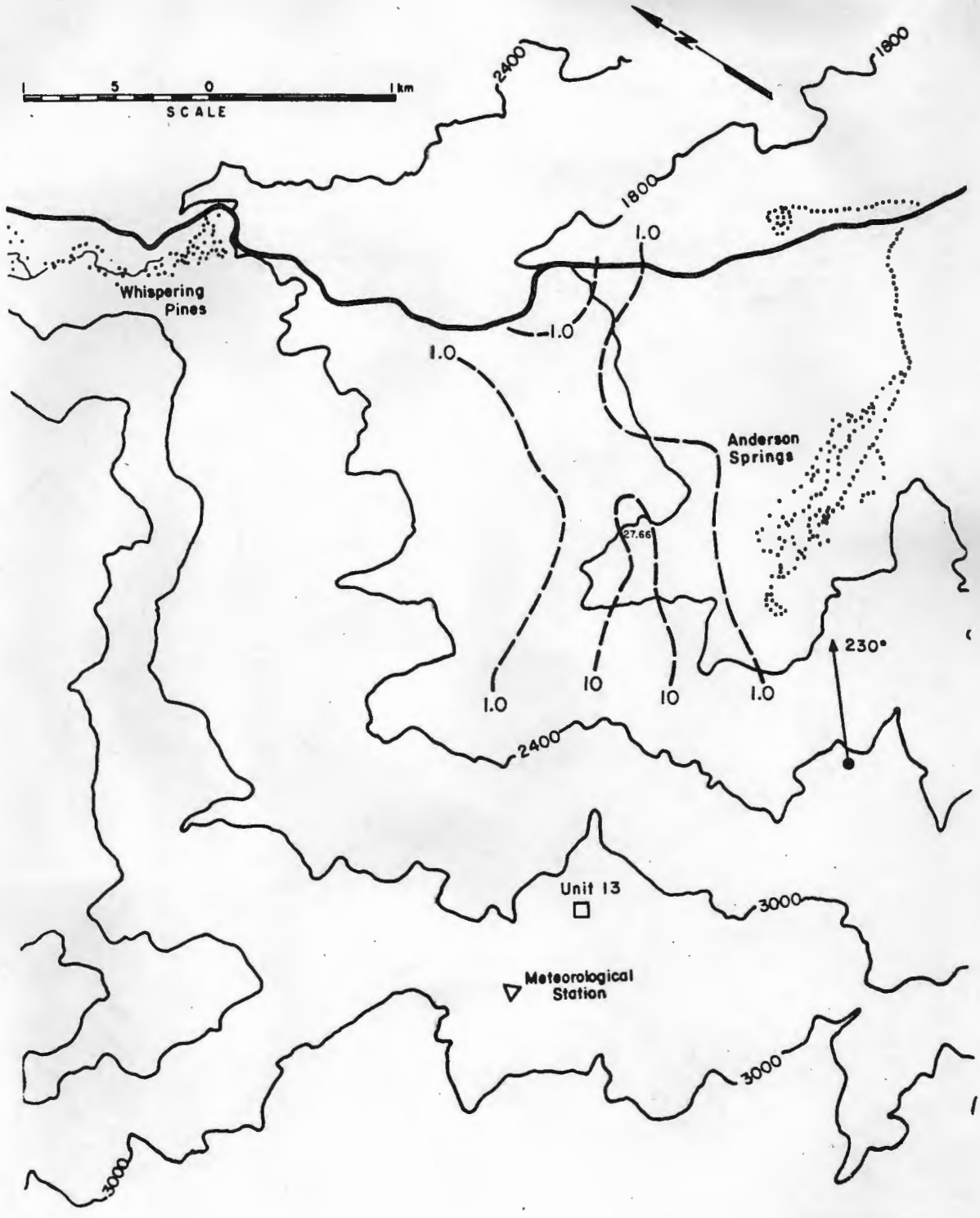

Figure 4.2-11 Isopleths of H_2S Concentrations for a 230° Wind Direction, a 6.2 m/s Wind Speed and a 12.7 m/s Exit Velocity--Aminoil Surface Releases

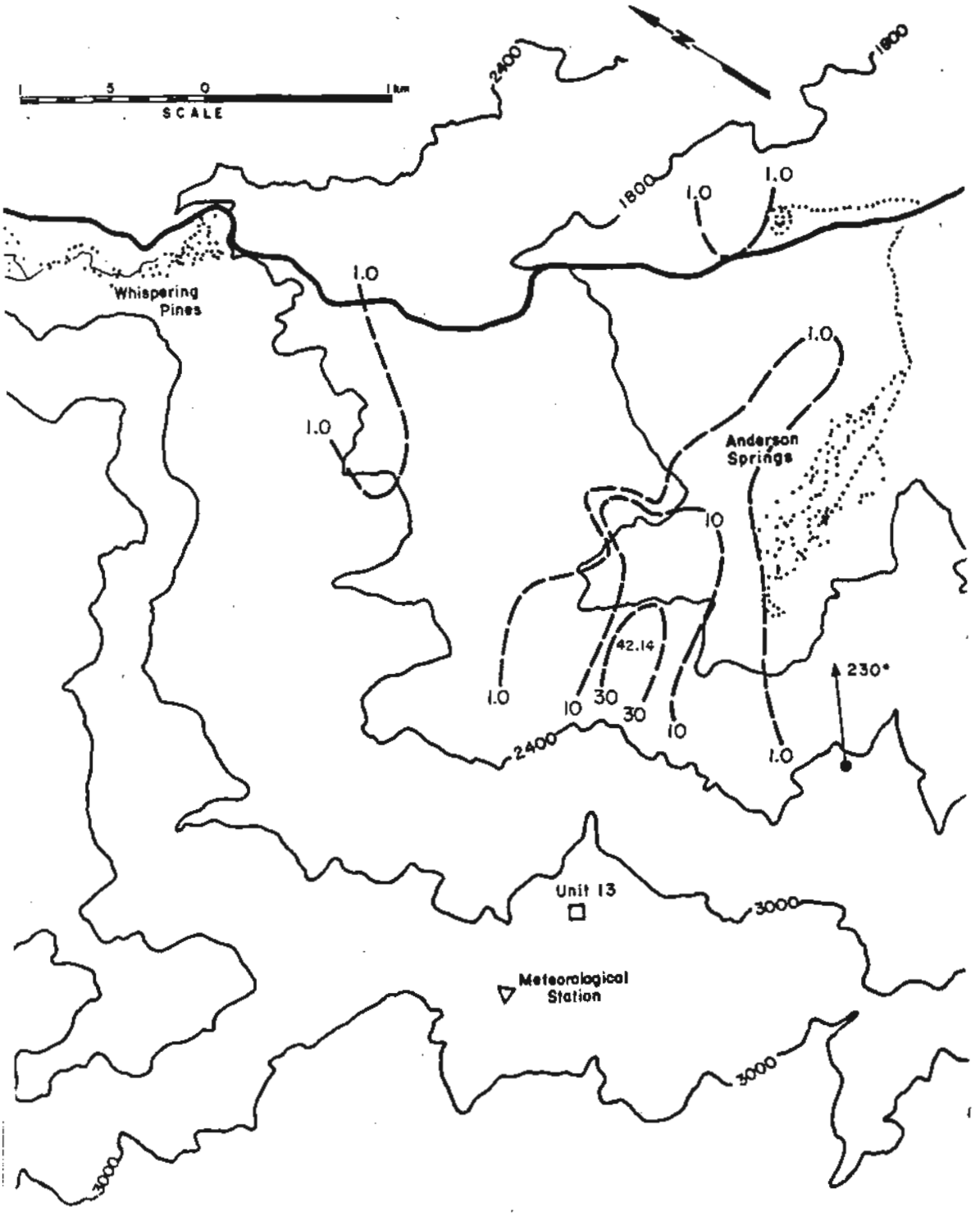

Figure 4.2-12 Isopleths of H_2S Concentrations for a 230° Wind Direction, a 9.4 m/s Wind Speed and a 12.7 m/s Exit Velocity--Aminoil Surface Releases

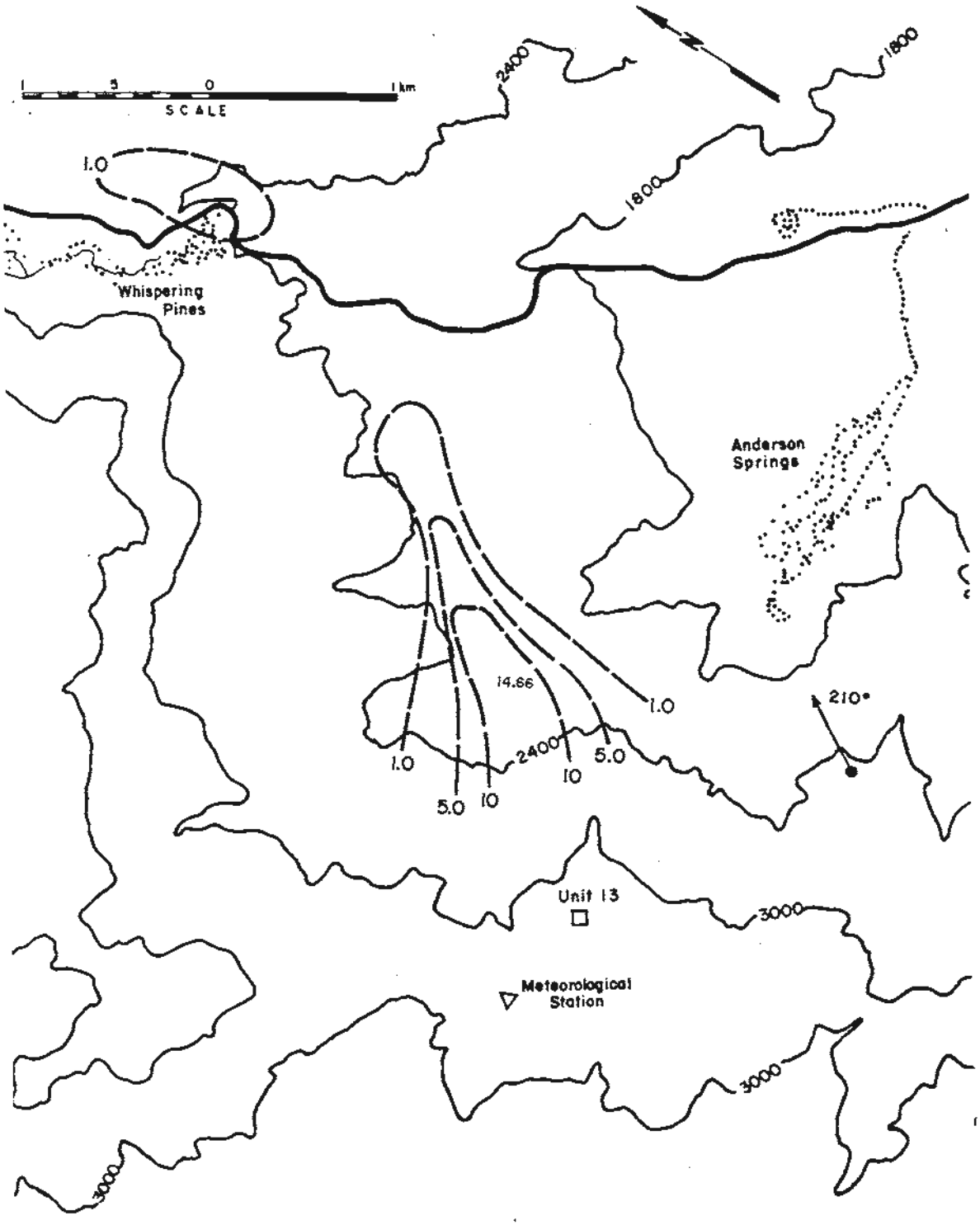

Figure 4.2-13 Isopleths of H_2S Concentrations for a 210° Wind Direction, a 3.1 m/s Wind Speed and a 2.5 m/s Exit Velocity--Aminoil Surface Releases

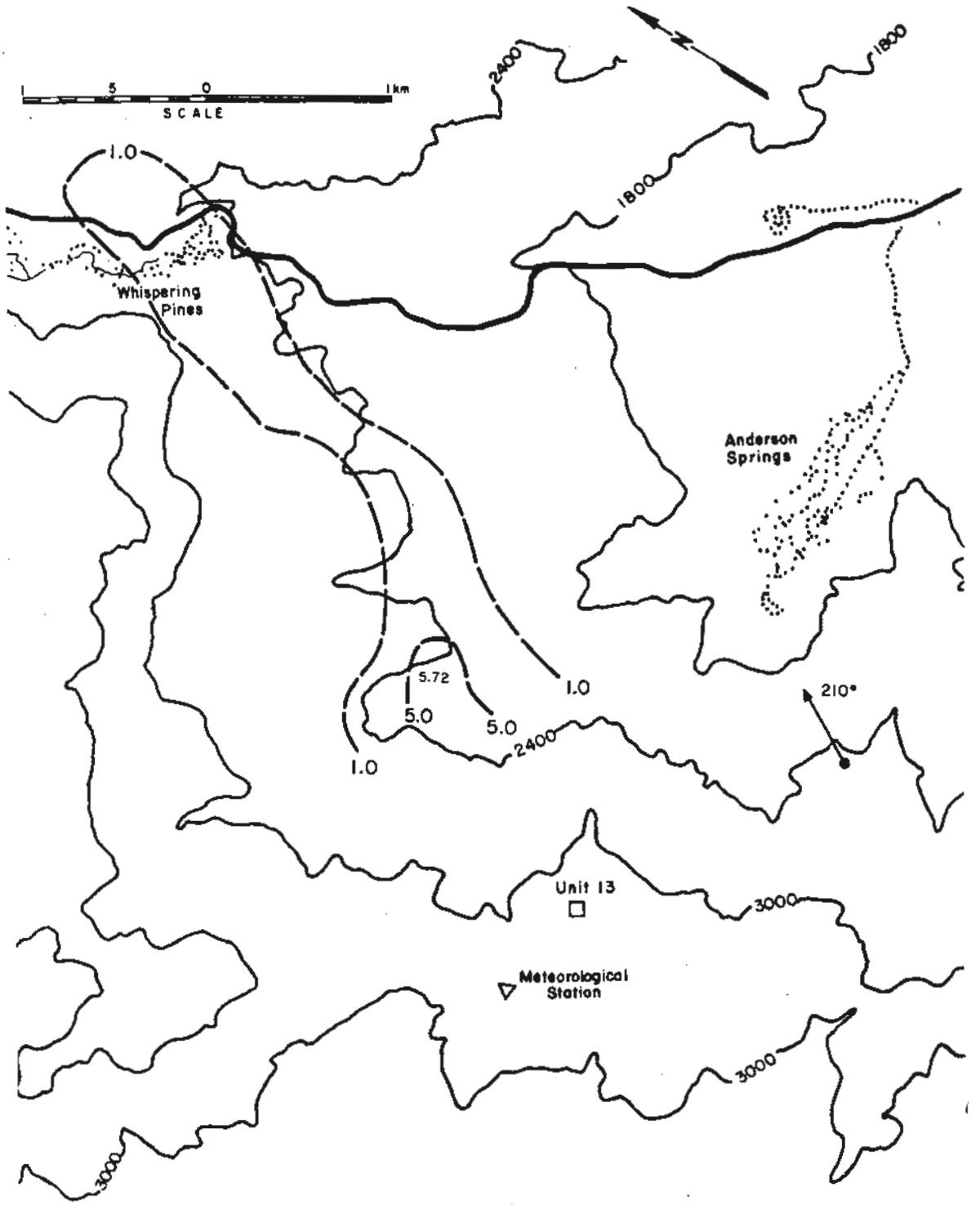

Figure 4.2-14 Isopleths of H_2S Concentrations for a 210° Wind Direction, a 6.2 m/s Wind Speed and a 2.5 m/s Exit Velocity-- Aminoil Surface Releases

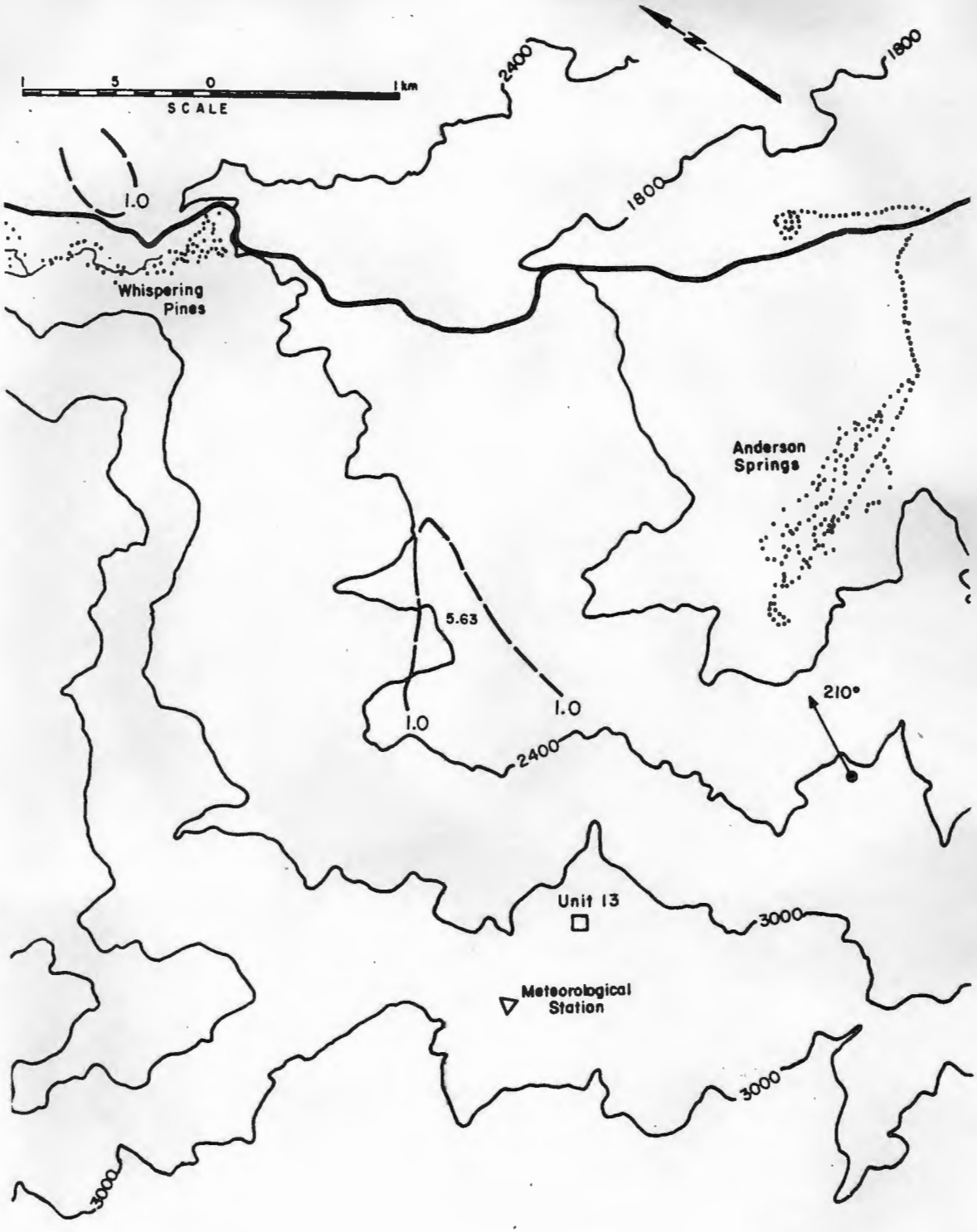

Figure 4.2-15 Isopleths of H_2S Concentrations for a 210° Wind Direction a 9.4 m/s Wind Speed and a 2.5 m/s Exit Velocity-- Aminoil Surface Releases

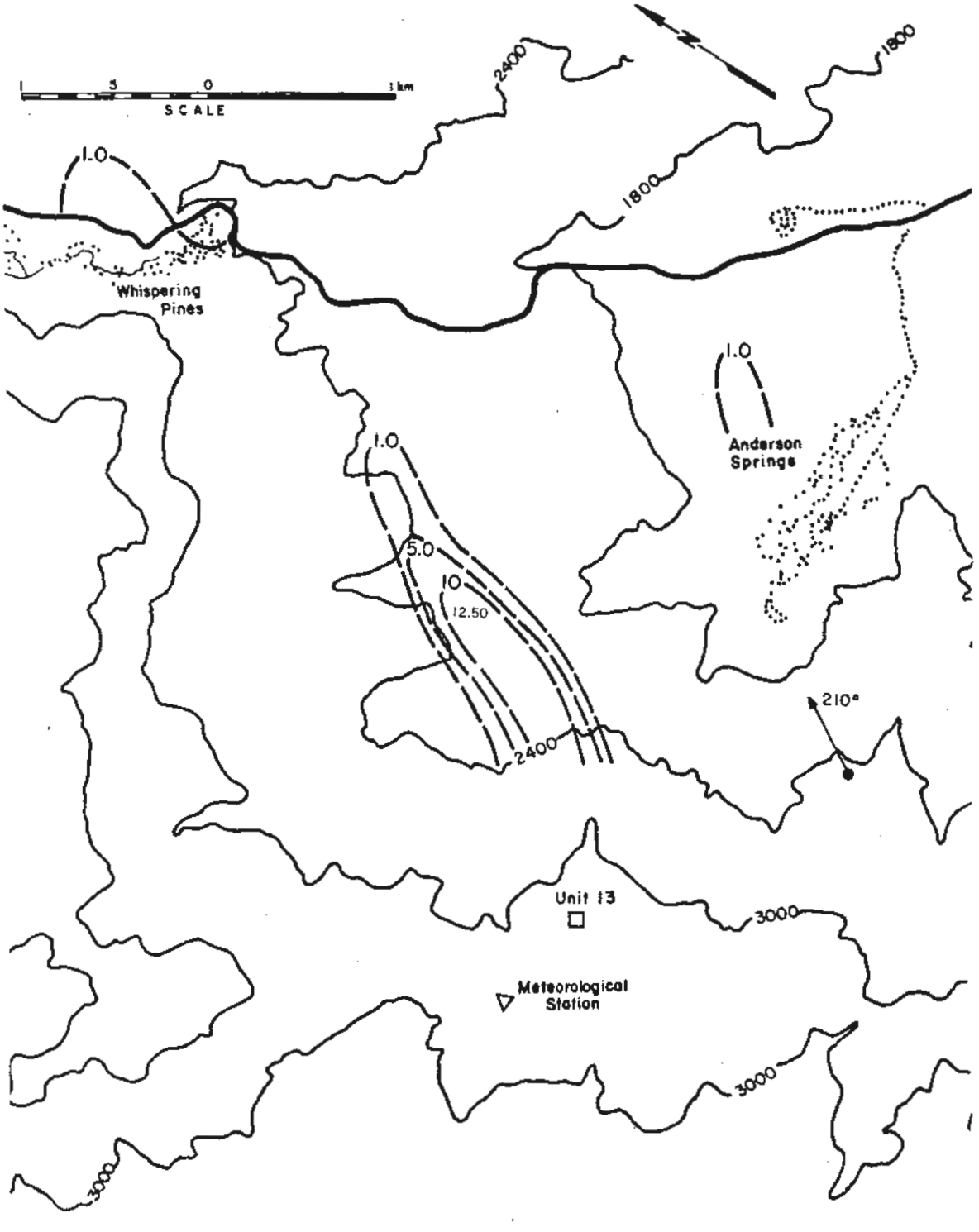

Figure 4.2-16 Isopleths of H_2S Concentrations for a 210° Wind Direction a 3.1 m/s Wind Speed and a 12.7 m/s Exit Velocity-- Aminoil Surface Releases

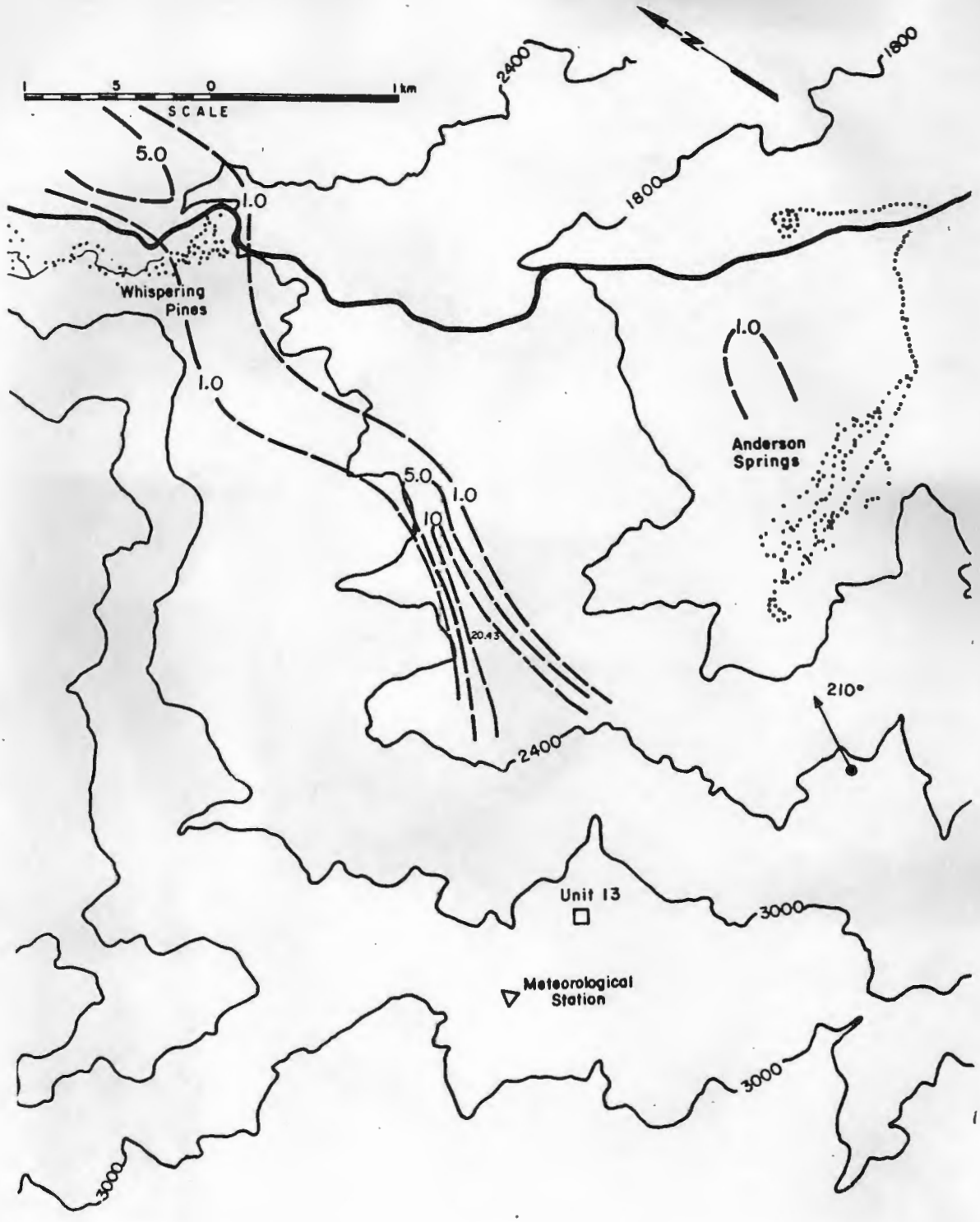

Figure 4.2-17 Isopleths of H_2S Concentrations for a 210° Wind Direction a 6.2 m/s Wind Speed and a 12.7 m/s Exit Velocity-- Aminoil Surface Releases

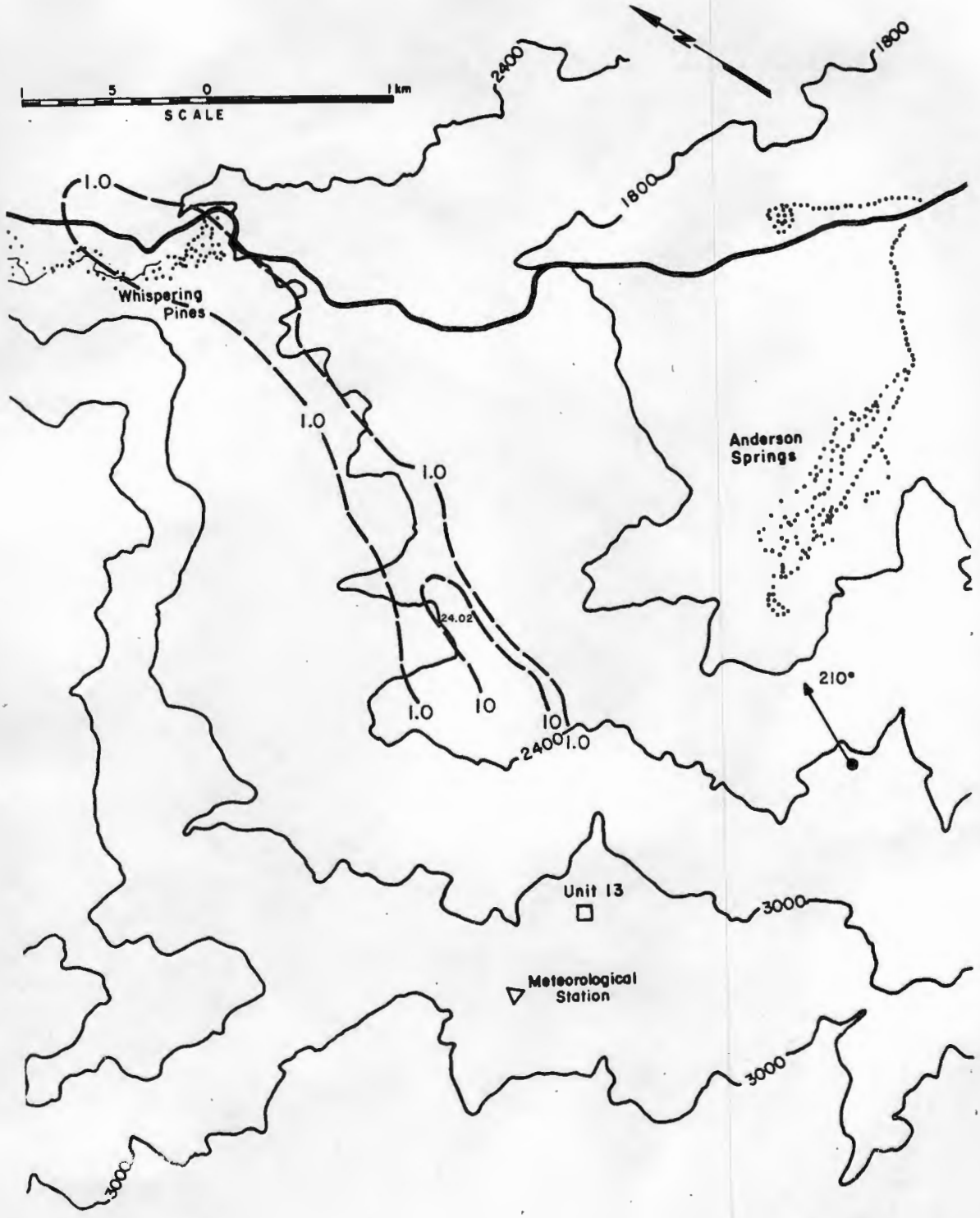

Figure 4.2-18 Isopleths of H_2S Concentrations for a 210° Wind Direction, a 9.4 m/s Wind Speed and a 12.7 m/s Exit Velocity-- Aminoil Surface Releases

a) 3.1 m/s

b) 6.2 m/s

c) 9.4 m/s

Figure 5.1-1 Stack release plume visualization for a 20.6 m/s exit velocity, 250° wind direction and wind speeds of a) 3.1 m/s, b) 6.2 m/s, and c) 9.4 m/s.

a) 3.1 m/s

b) 6.2 m/s

c) 9.4 m/s

Figure 5.1-2 Stack release plume visualization for a 63.1 m/s exit velocity, 250° wind direction and wind speeds of a) 3.1 m/s, b) 6.2 m/s, and c) 9.4 m/s.

a) 3.1 m/s

b) 6.2 m/s

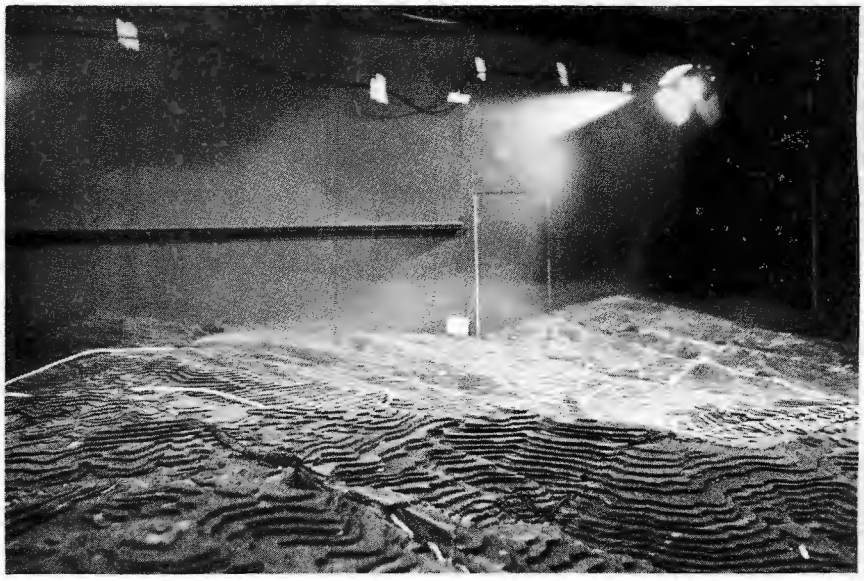

c) 9.4 m/s

Figure 5.1-3 Stack release plume visualization for a 111.7 m/s exit velocity, 250° wind direction and wind speeds of a) 3.1 m/s, b) 6.2 m/s, and c) 9.4 m/s.

a) 3.1 m/s

b) 6.2 m/s

c) 9.4 m/s

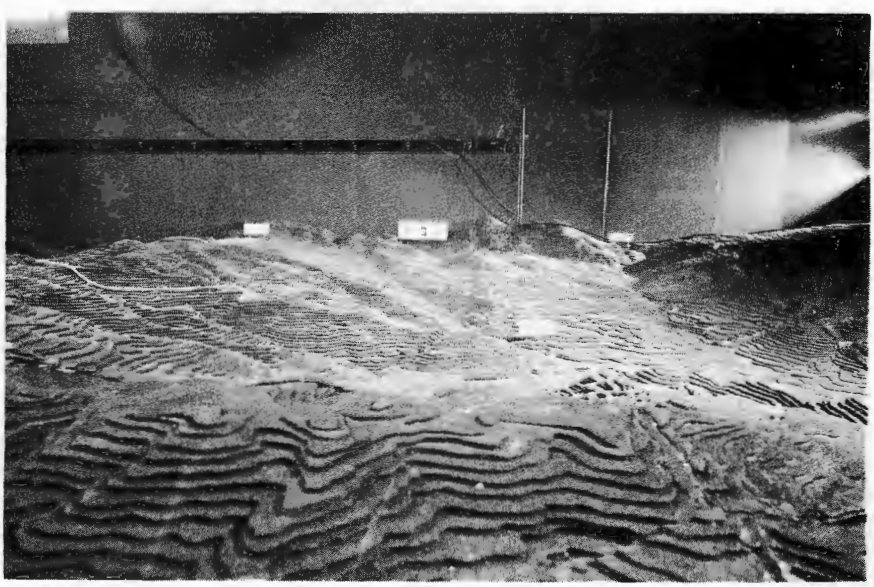

Figure 5.1-4 Stack release plume visualization for a 20.6 m/s exit velocity, 230° wind direction and wind speeds of a) 3.1 m/s, b) 6.2 m/s, and c) 9.4 m/s.

a) 3.1 m/s

b) 6.2 m/s

c) 9.4 m/s

Figure 5.1-5 Stack release plume visualization for a 63.1 m/s exit velocity, 230° wind direction and wind speeds of a) 3.1 m/s, b) 6.2 m/s, and c) 9.4 m/s.

a) 3.1 m/s

b) 6.2 m/s

c) 9.4 m/s

Figure 5.1-6 Stack release plume visualization for 111.7 m/s exit velocity, 230° wind direction and wind speeds of a) 3.1 m/s, b) 6.2 m/s, and c) 9.4 m/s.

a) 3.1 m/s

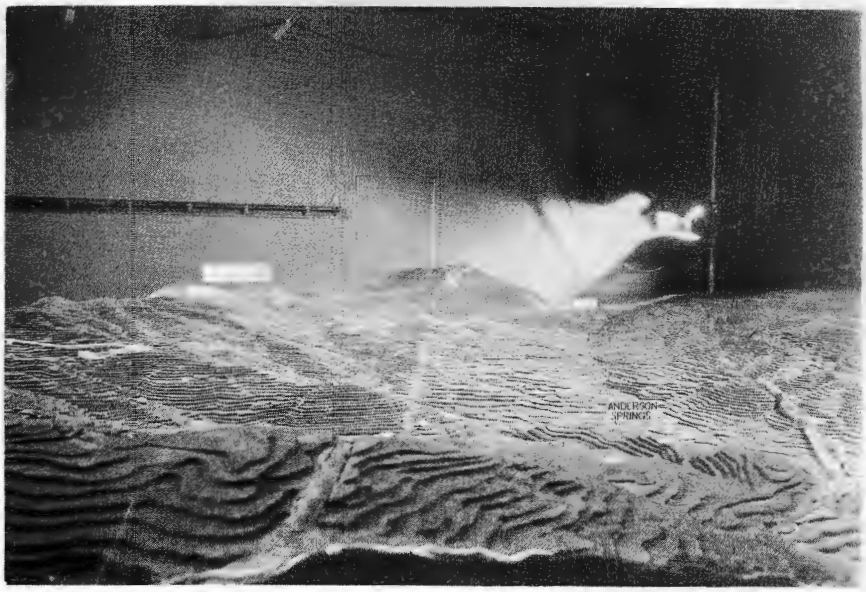

b) 6.2 m/s

c) 9.4 m/s

Figure 5.1-7 Stack release plume visualization for a 20.6 m/s exit velocity, 210° wind direction and wind speeds of a) 3.1 m/s, b) 6.2 m/s, and c) 9.4 m/s.

a) 3.1 m/s

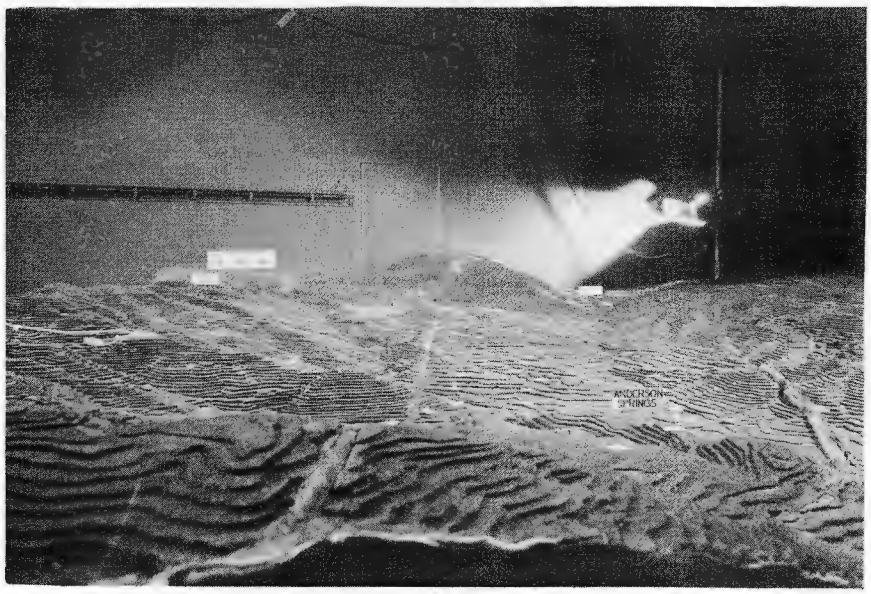

b) 6.2 m/s

c) 9.4 m/s

Figure 5.1-8 Stack release plume visualization for a 63.1 m/s exit velocity, 210° wind direction and wind speeds of a) 3.1 m/s, b) 6.2 m/s, and c) 9.4 m/s.

a) 3.1 m/s

b) 6.2 m/s

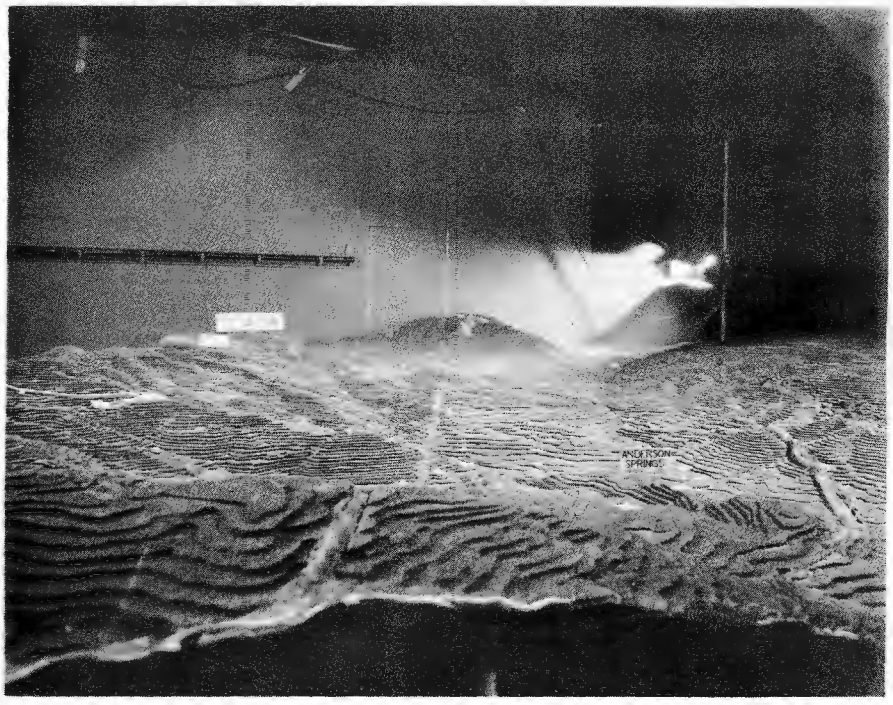

Figure 5.1-9 Stack release plume visulization for a 111.7 m/s exit velocity, 210° wind direction and wind speeds of a) 3.1 m/s and b) 6.2 m/s.

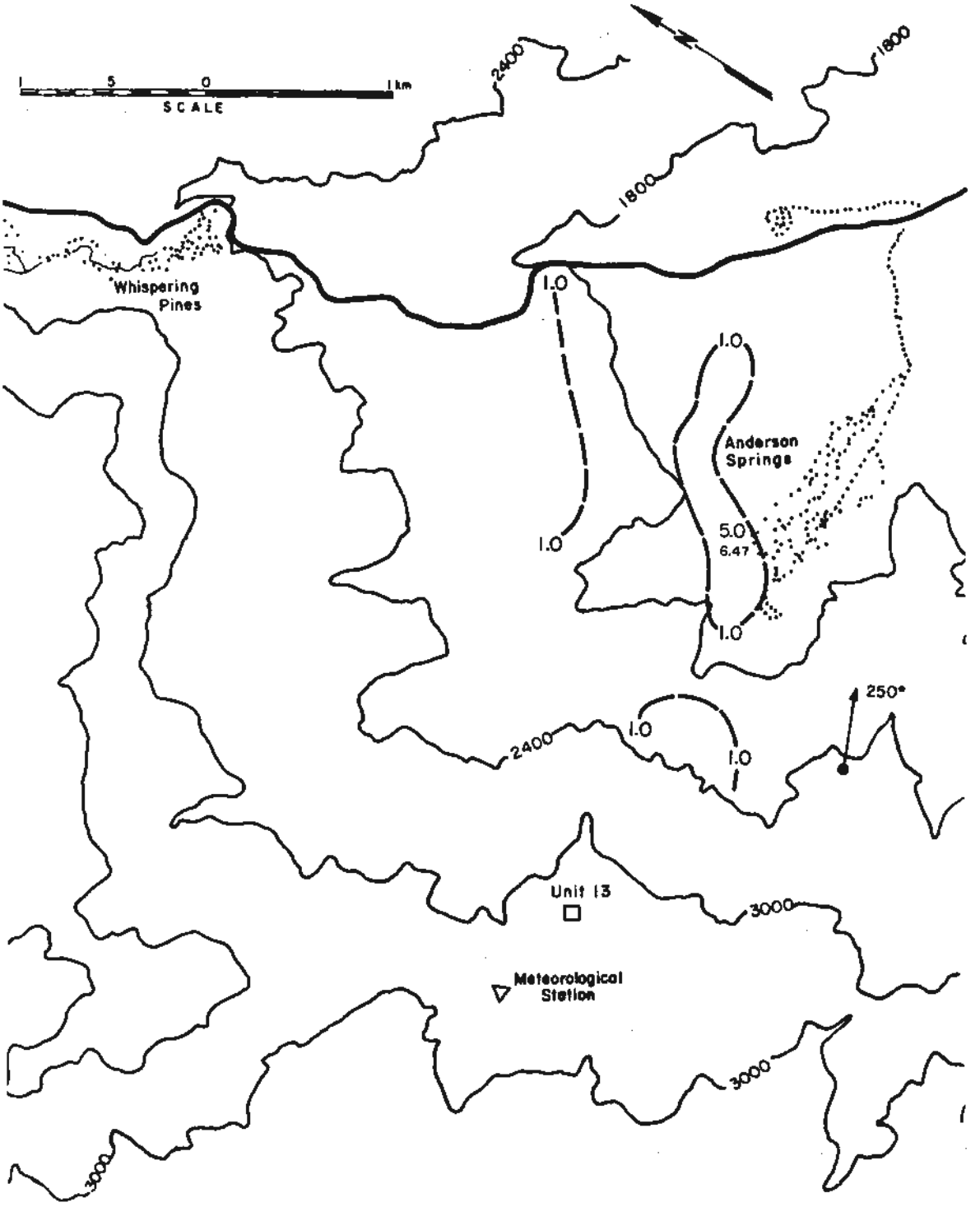

Figure 5.2-1 Isopleths of H_2S Concentrations for a 250° Wind Direction, a 3.1 m/s Wind Speed and a 20.6 m/s Exit Velocity--Aminoil Stack Release

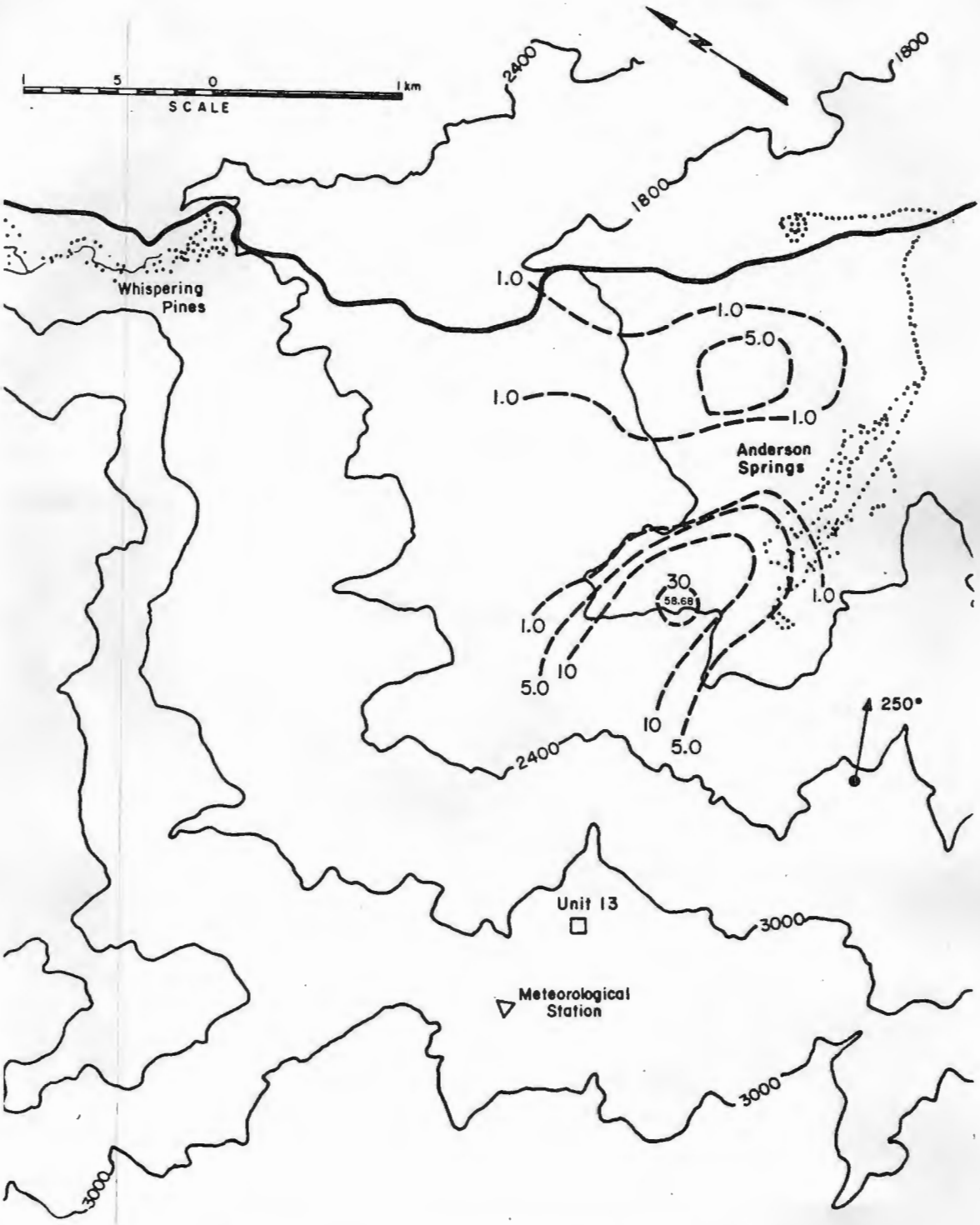

Figure 5.2-2 Isopleths of H_2S Concentrations for a 250° Wind Direction, a 6.2 m/s Wind Speed and a 20.6 m/s Exit Velocity--Aminoil Stack Release

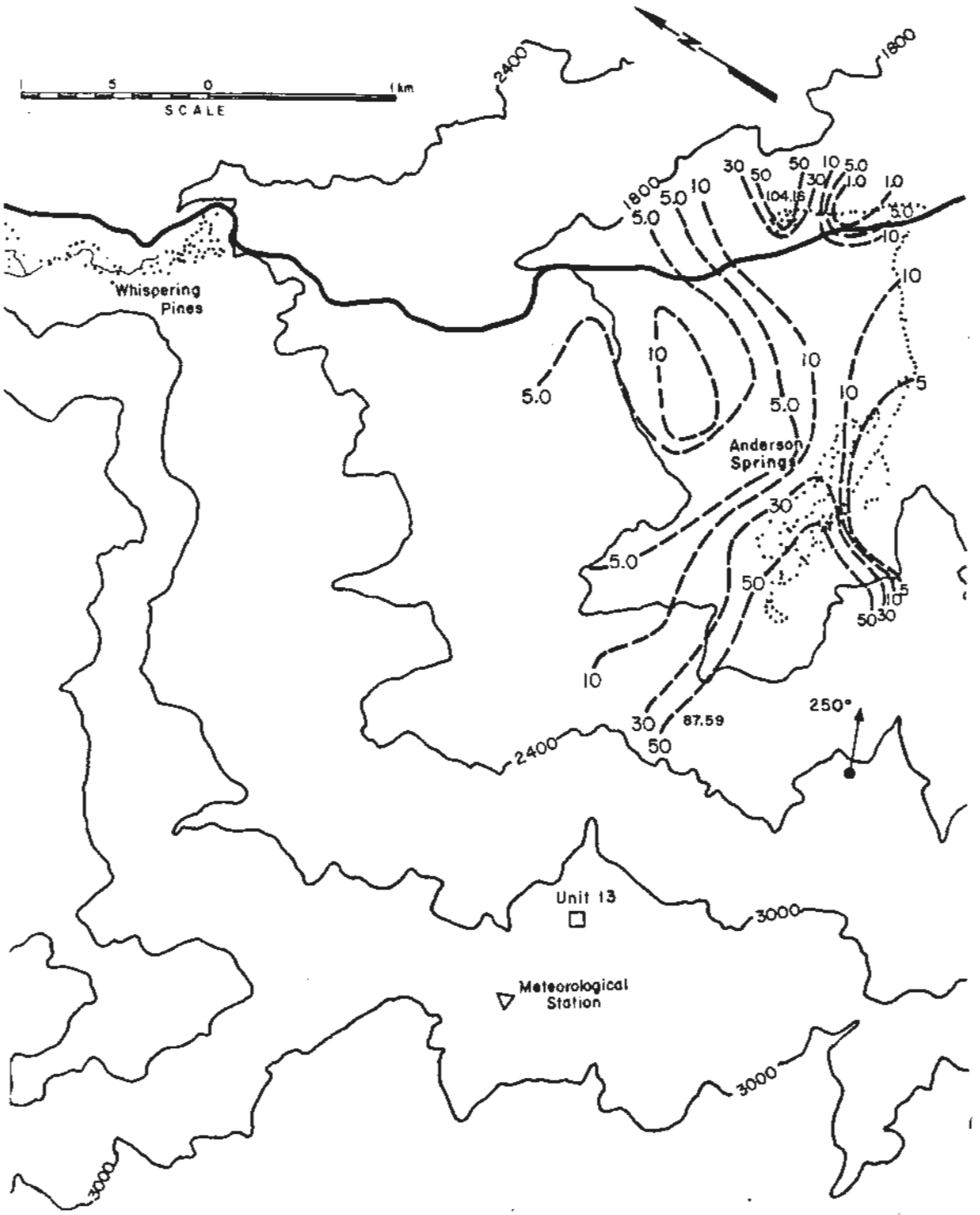

Figure 5.2-3 Isopleths of H_2S Concentrations for a 250° Wind Direction, a 9.4 m/s Wind Speed and a 20.6 m/s Exit Velocity--Aminoil Stack Release

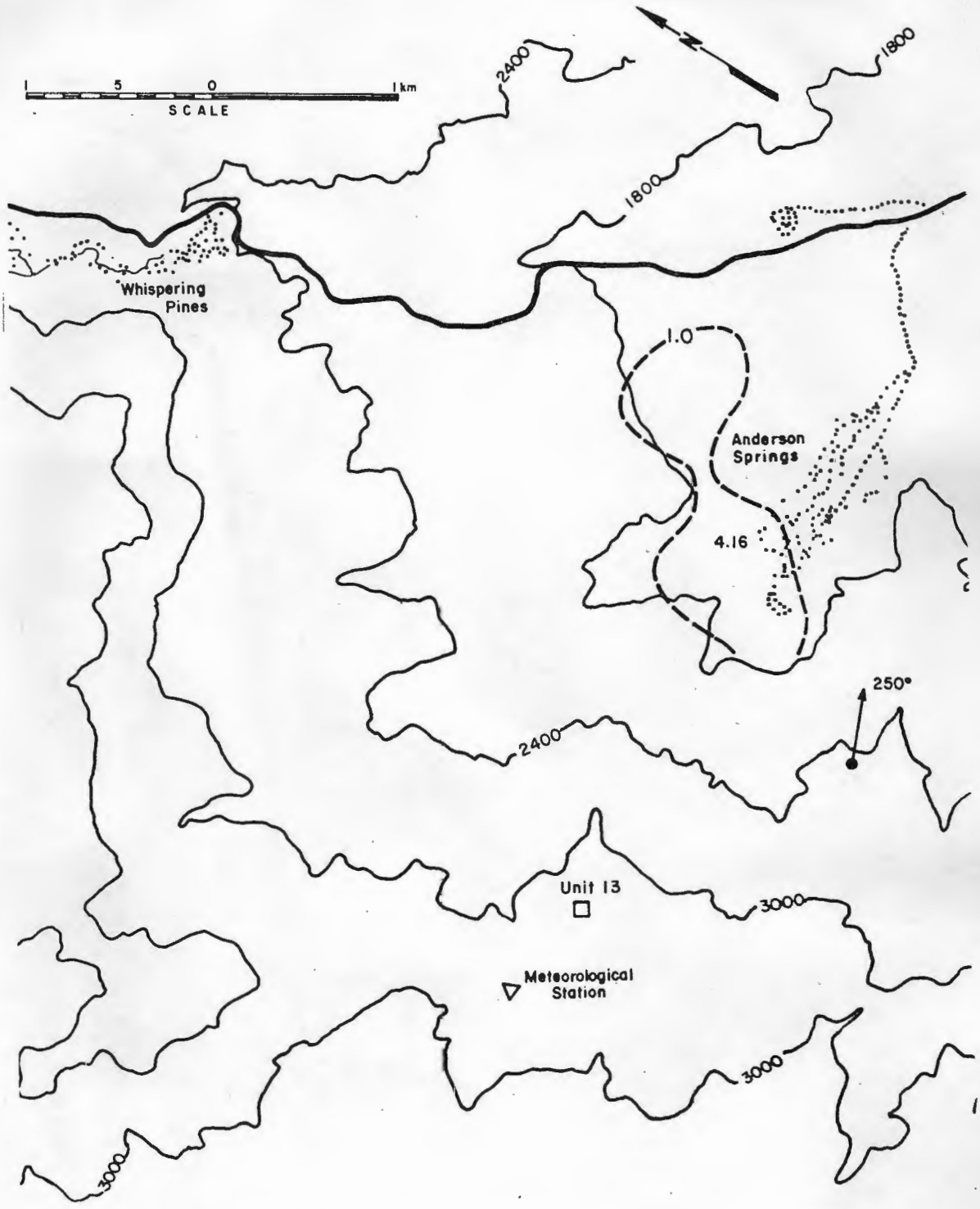

Figure 5.2-4 Isopleths of H_2S Concentrations for a 250° Wind Direction, a 3.1 m/s Wind Speed and a 63.1 m/s Exit Velocity--Aminoil Stack Release

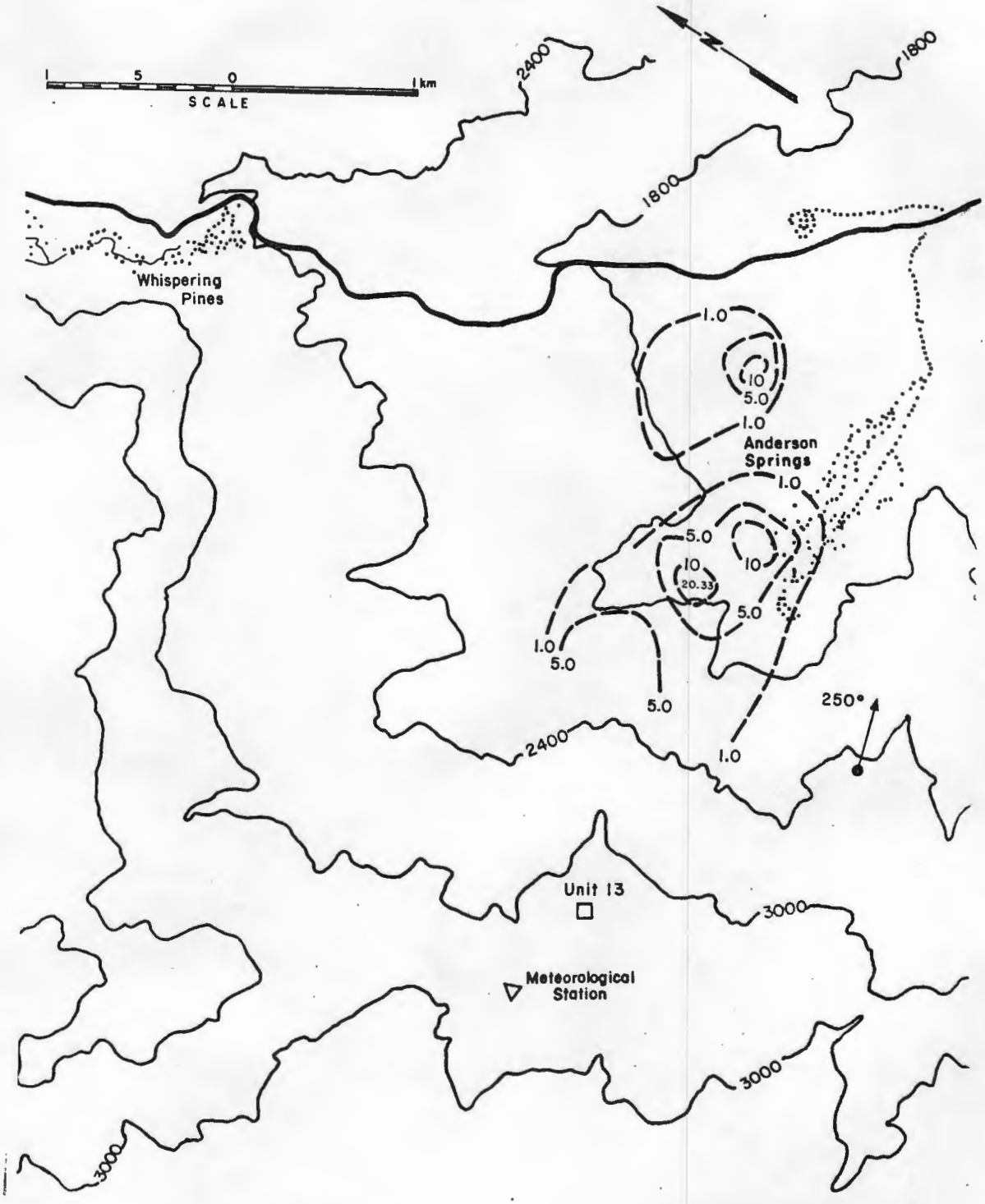

Figure 5.2-5 Isopleths of H_2S Concentrations for a 250° Wind Direction, a 6.2 m/s Wind Speed and a 63.1 m/s Exit Velocity--Aminoil Stack Release

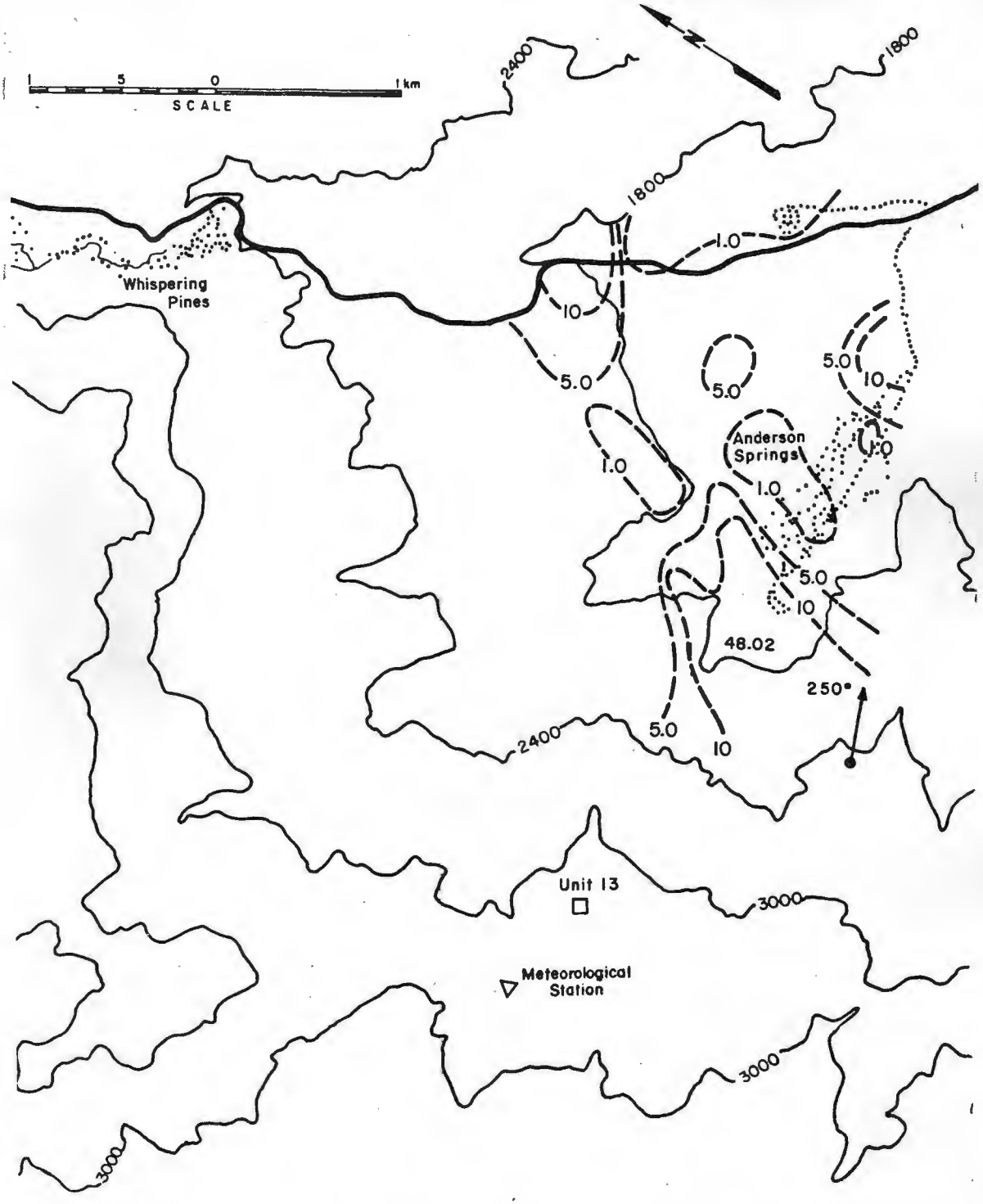

Figure 5.2-6 Isopleths of H_2S Concentrations for a 250° Wind Direction, a 9.4 m/s Wind Speed and a 63.1 m/s Exit Velocity--Aminoil Stack Release

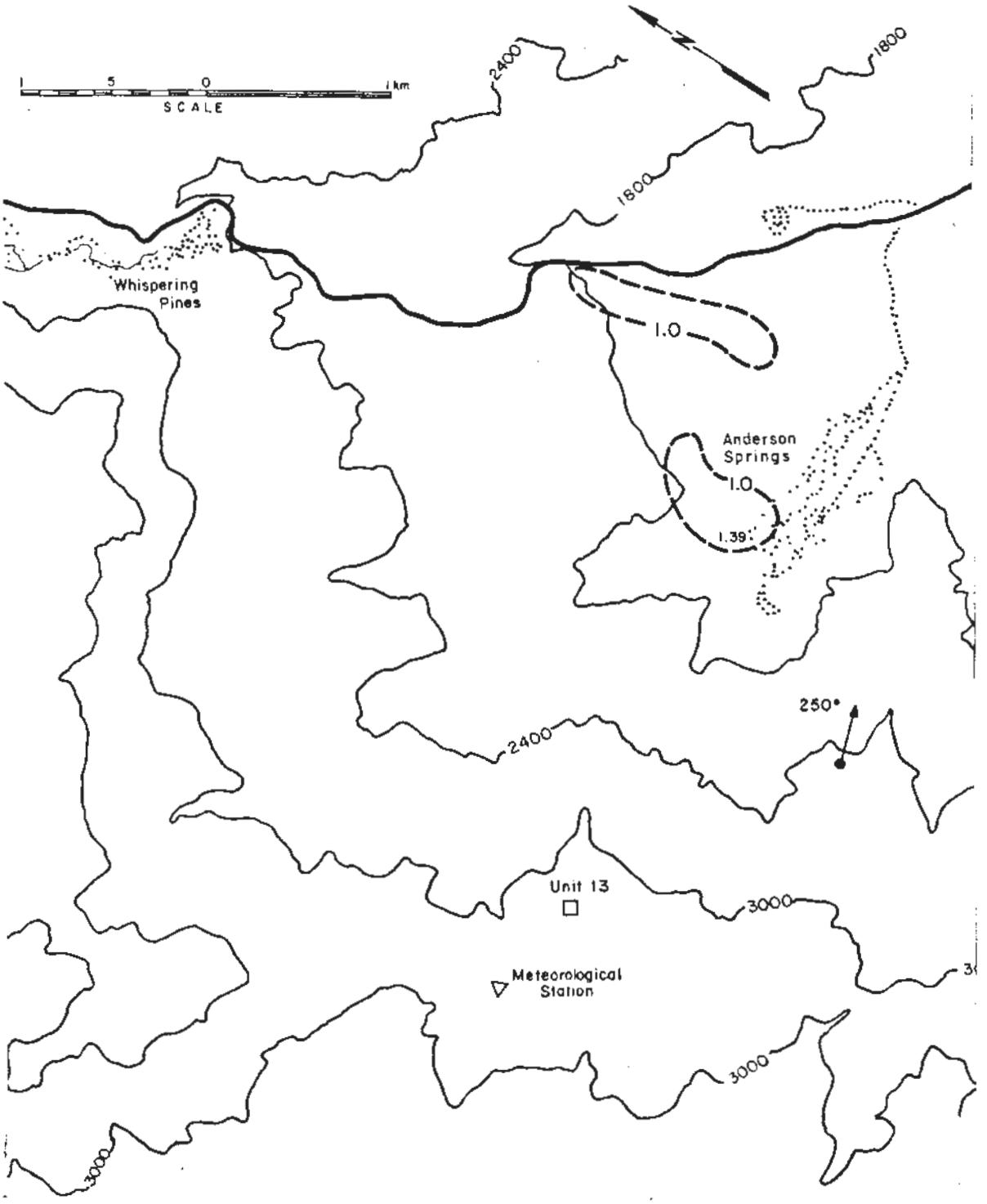

Figure 5.2-7 Isopleths of H_2S Concentrations for a 250° Wind Direction, a 3.1 m/s Wind Speed and a 111.7 m/s Exit Velocity--Aminoil Stack Release

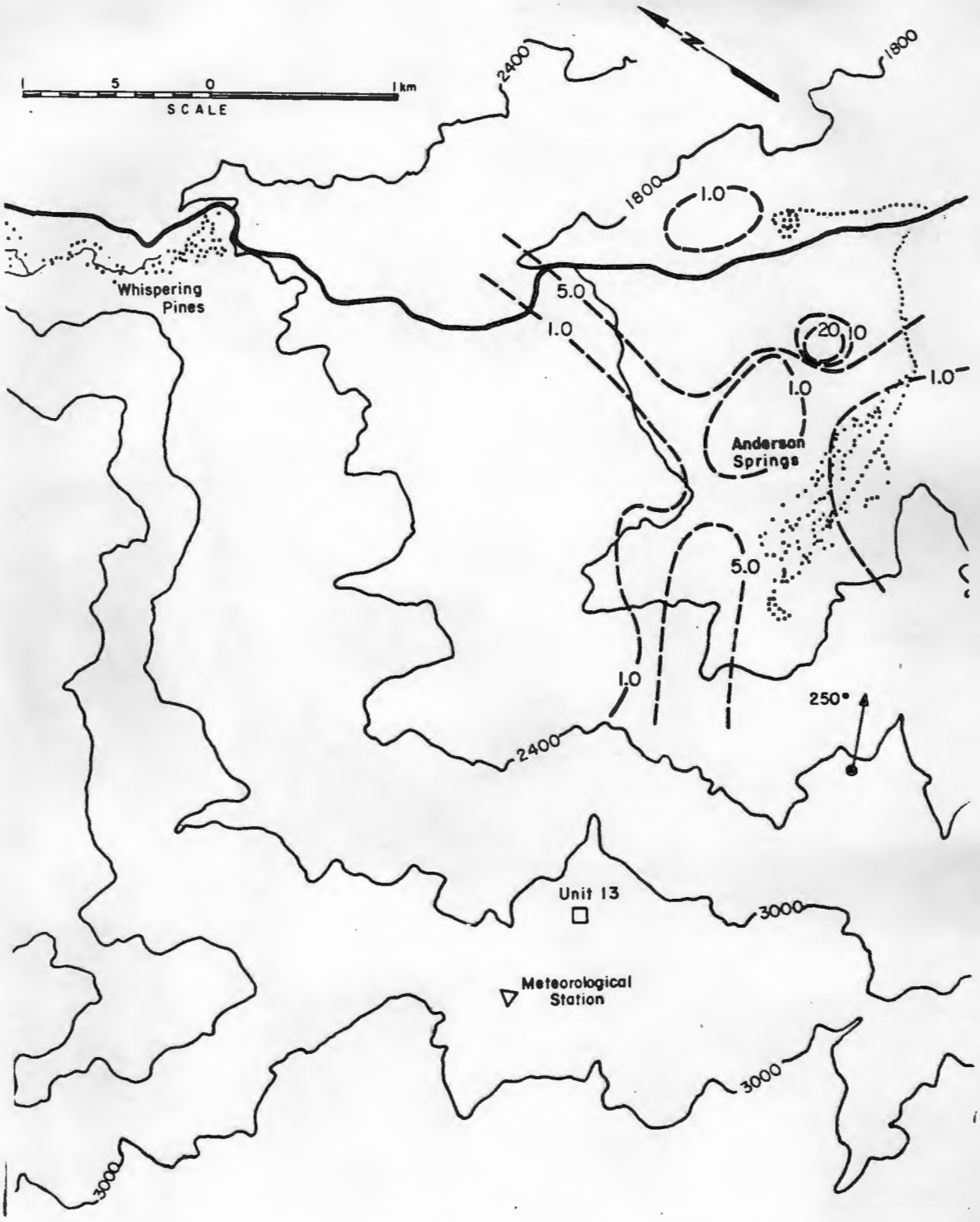

Figure 5.2-8 Isopleths of H_2S Concentrations for a 250° Wind Direction, a 6.2 m/s Wind Speed and a 111.7 m/s Exit Velocity--Aminoil Stack Release

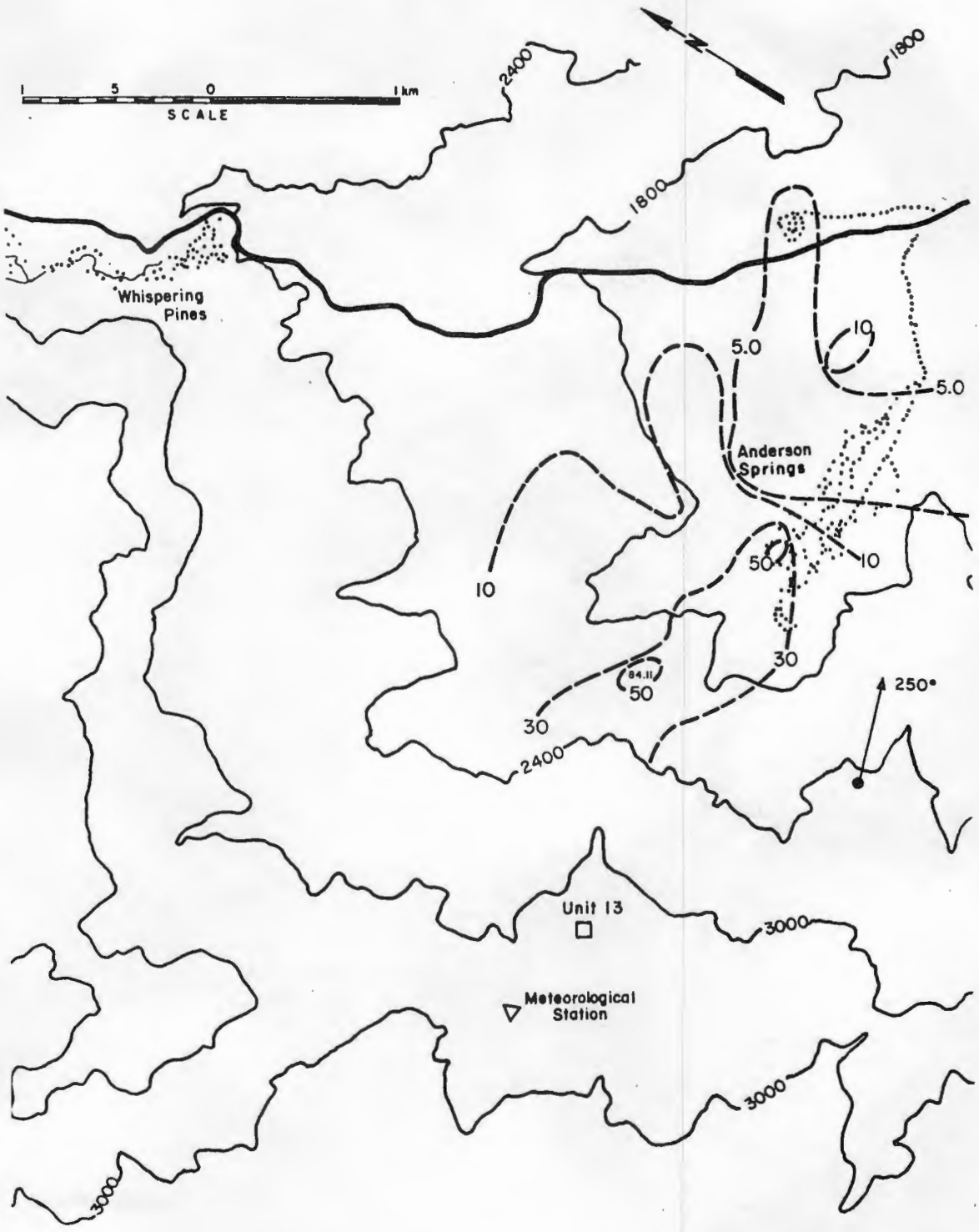

Figure 5.2-9 Isopleths of H_2S Concentrations for a 250° Wind Direction, a 9.4 m/s Wind Speed and a 111.7 m/s Exit Velocity--Aminoil Stack Release

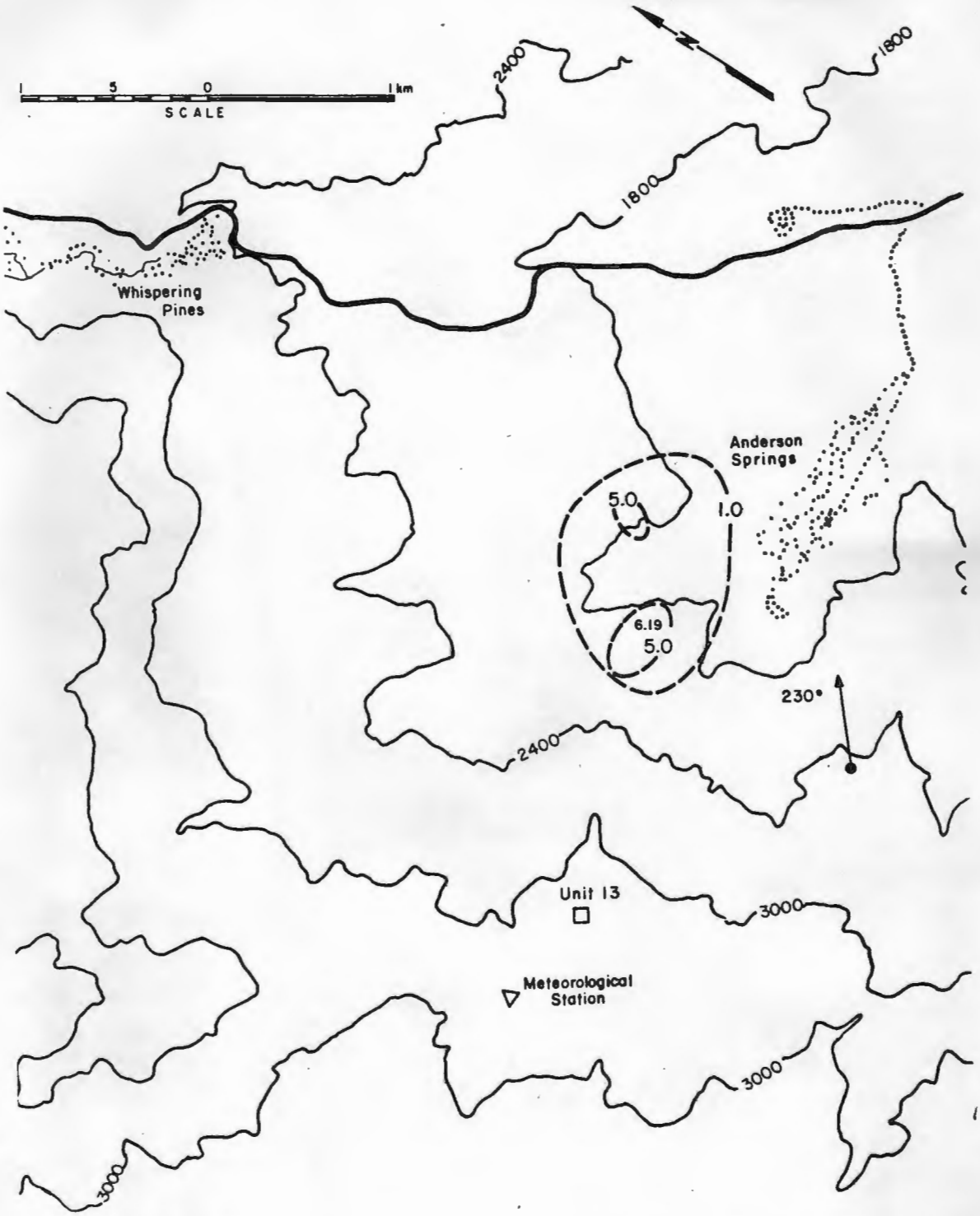

Figure 5.2-10 Isopleths of H_2S Concentrations for a 230° Wind Direction, a 3.1 m/s Wind Speed and a 20.6 m/s Exit Velocity--Aminoil Stack Release

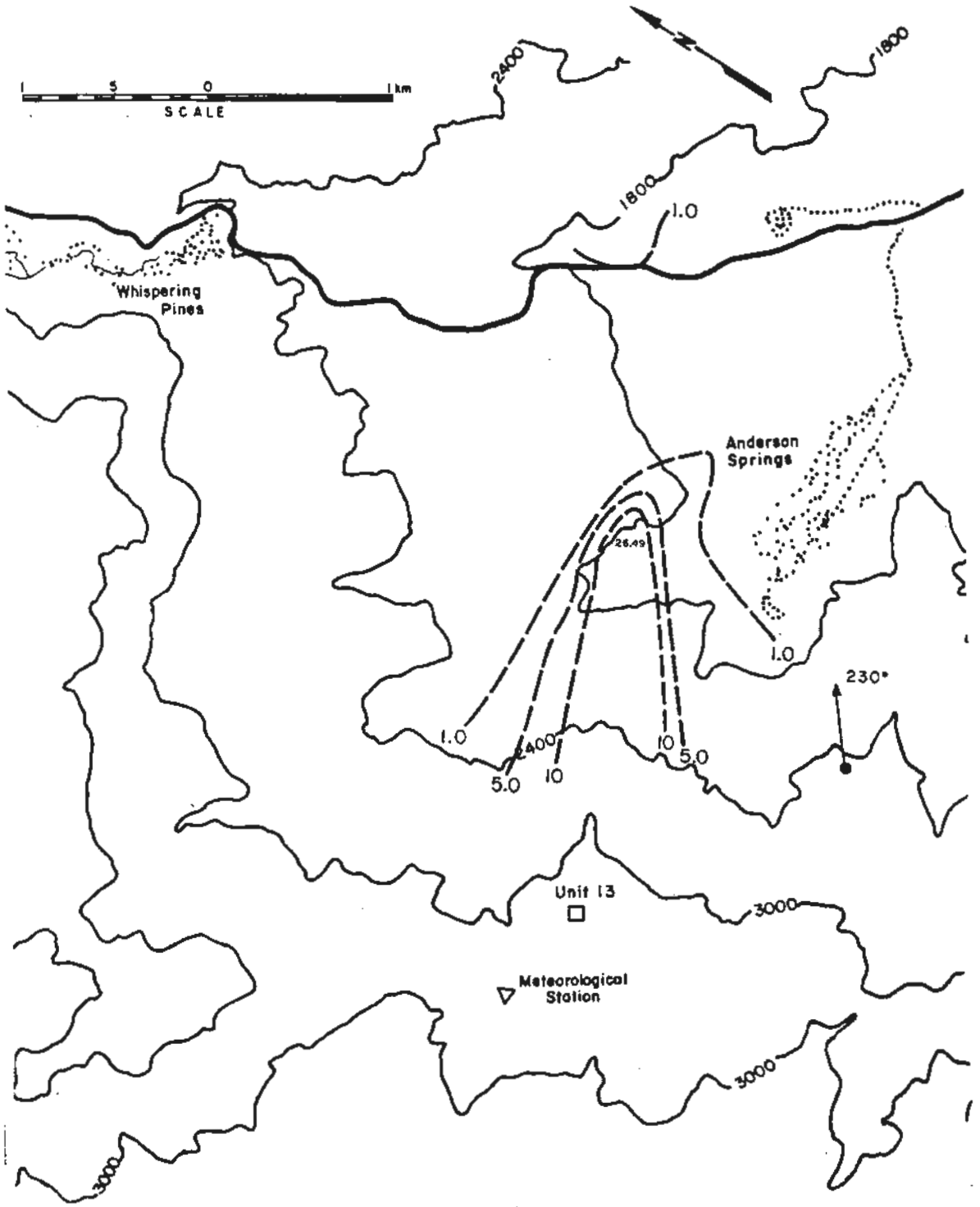

Figure 5.2-11 Isopleths of H_2S Concentrations for a 230° Wind Direction, a 6.2 m/s Wind Speed and a 20.6 m/s Exit Velocity--Aminoil Stack Release

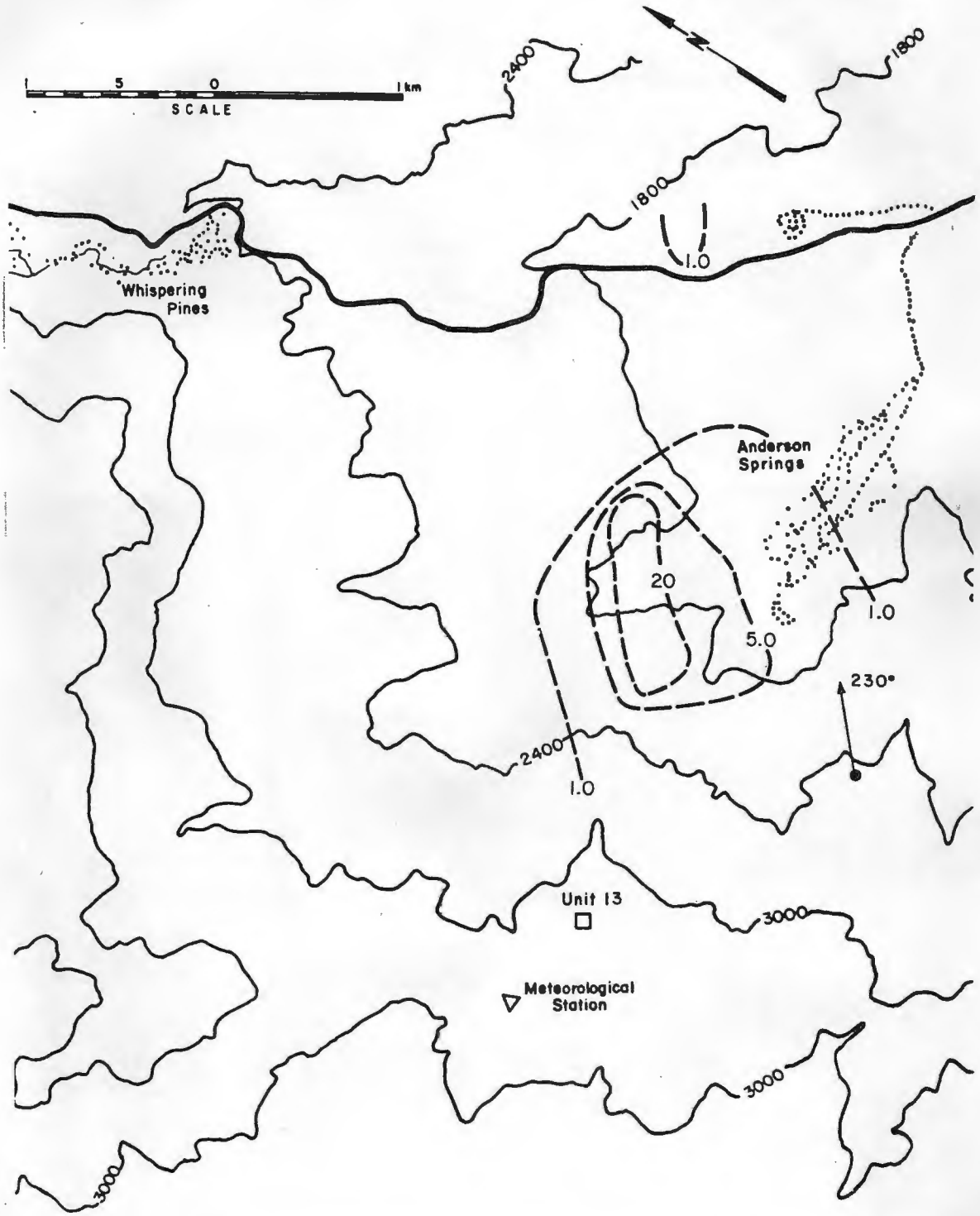

Figure 5.2-12 Isopleths of H_2S Concentrations for a 230° Wind Direction, a 9.4 m/s Wind Speed and a 20.6 m/s Exit Velocity--Aminoil Stack Release

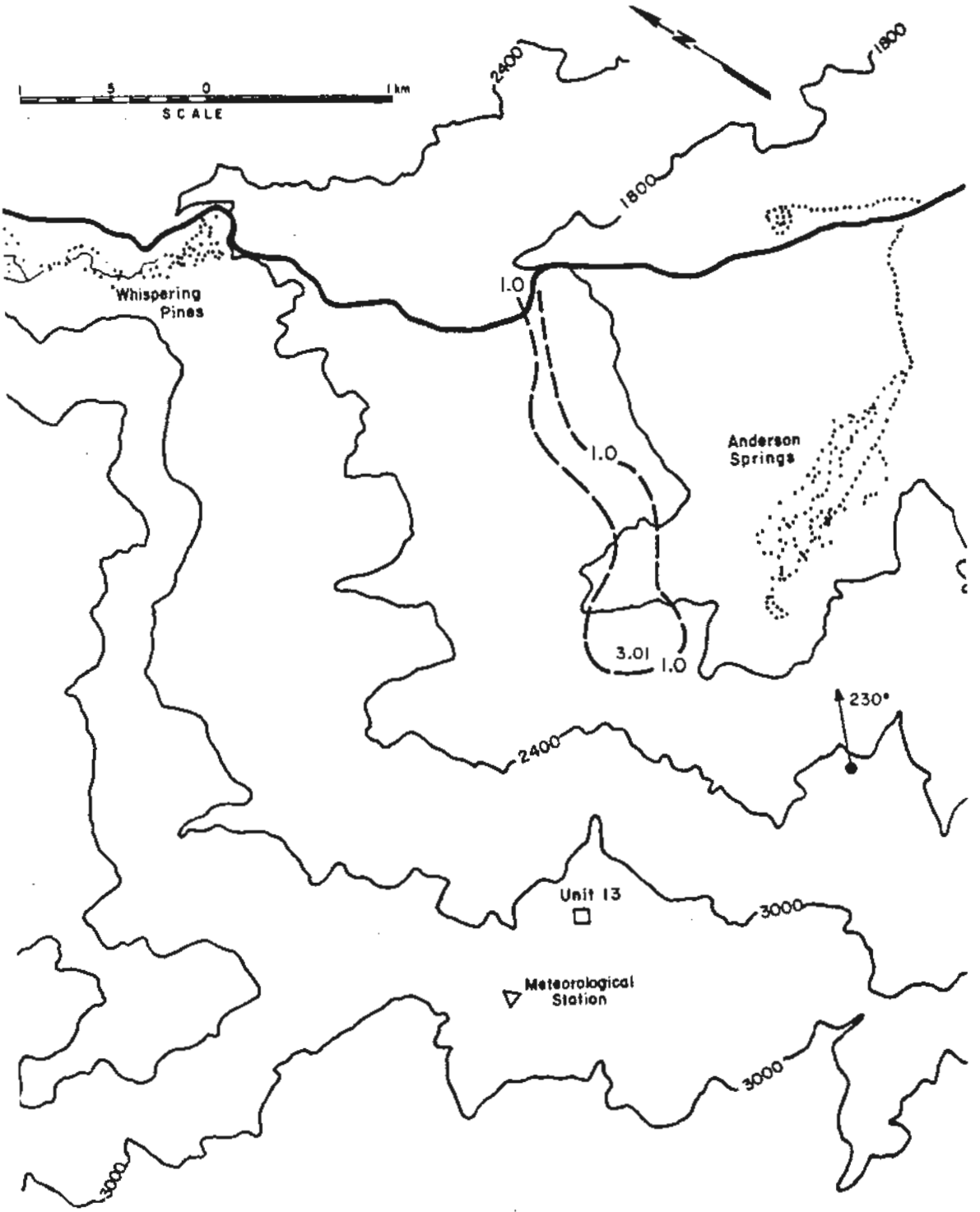

Figure 5.2-13 Isopleths of H_2S Concentrations for a 230° Wind Direction, a 3.1 m/s Wind Speed and a 63.1 m/s Exit Velocity--Aminoil Stack Release

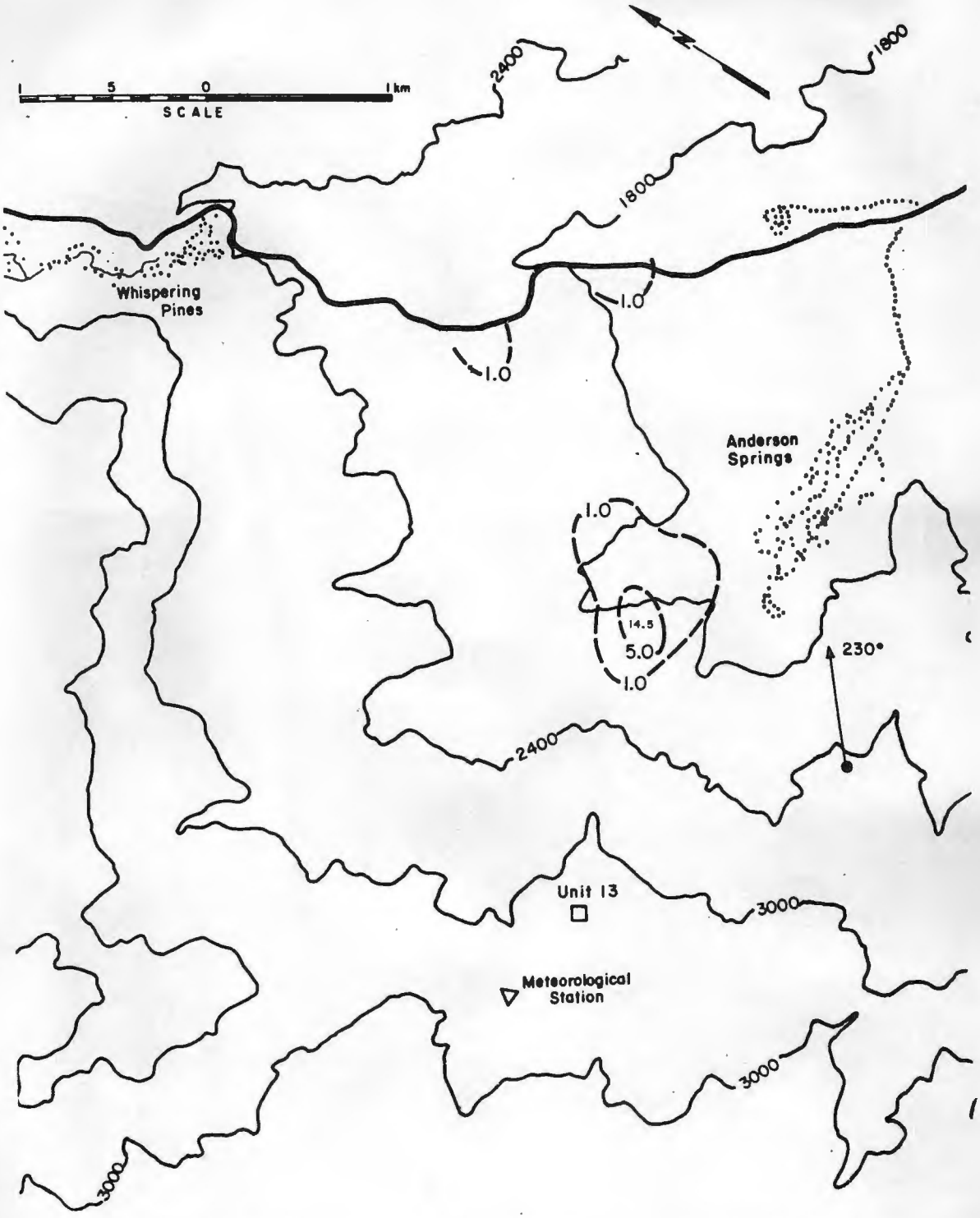

Figure 5.2-14 Isopleths of H_2S Concentrations for a 230° Wind Direction, a 6.2 m/s Wind Speed and a 63.1 m/s Exit Velocity--Aminoil Stack Release

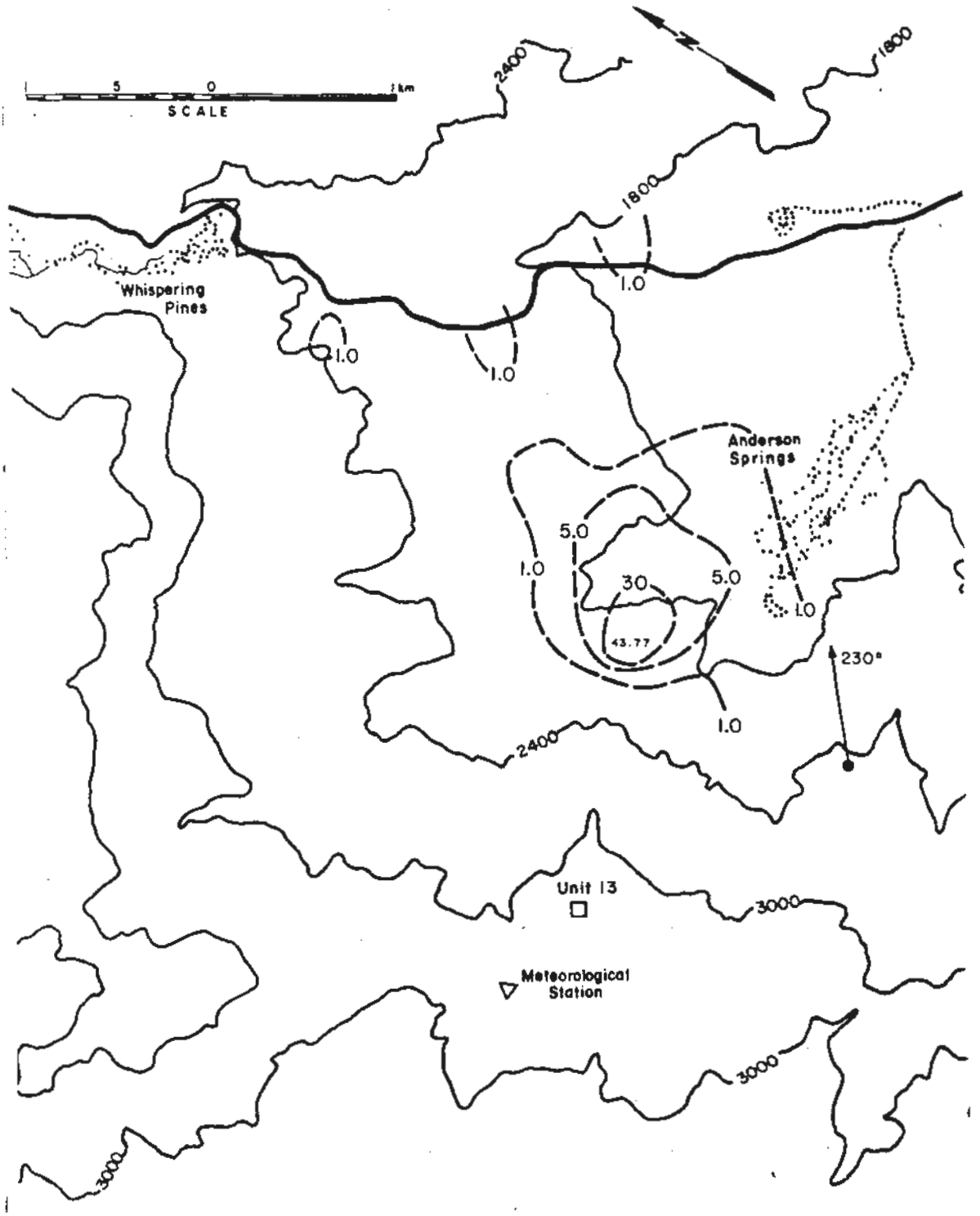

Figure 5.2-15 Isopleths of H_2S Concentrations for a 230° Wind Direction, a 9.4 m/s Wind Speed and a 63.1 m/s Exit Velocity--Aminoil Stack Release

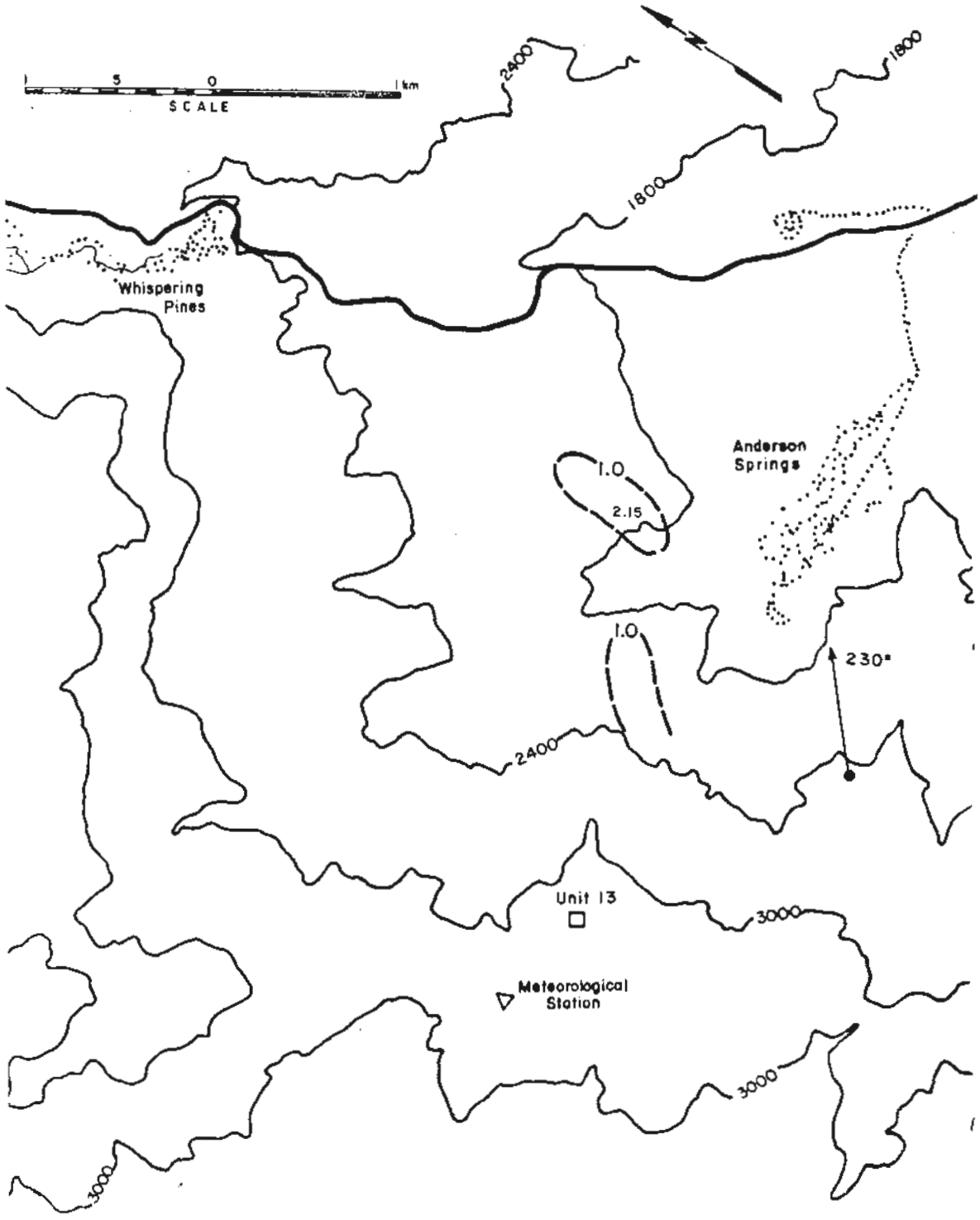

Figure 5.2-16 Isopleths of H_2S Concentrations for a 230° Wind Direction, a 3.1 m/s Wind Speed and a 111.7 m/s Exit Velocity--Aminoil Stack Release

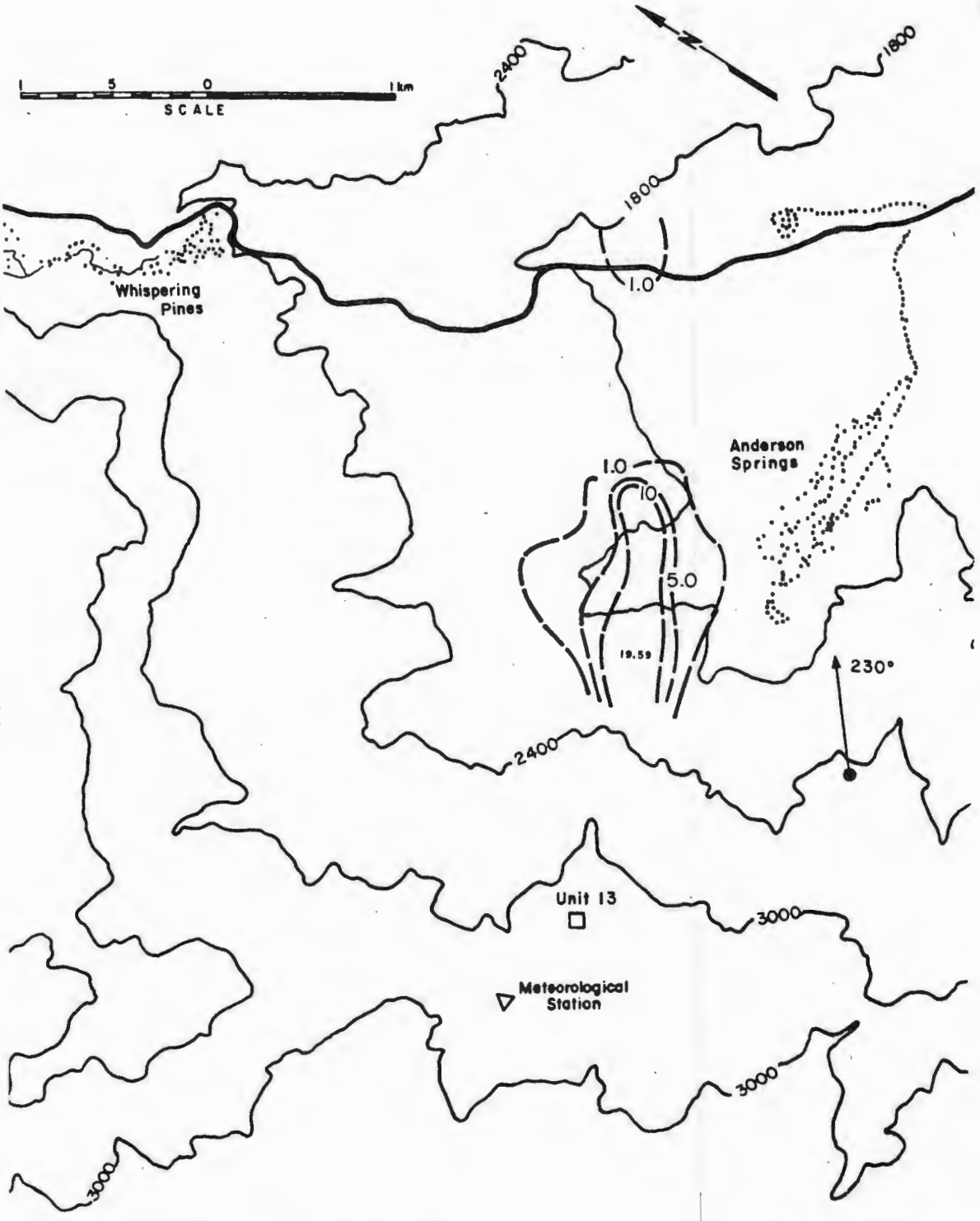

Figure 5.2-17 Isopleths of H_2S Concentrations for a 230° Wind Direction, a 6.2 m/s Wind Speed and a 111.7 m/s Exit Velocity--Aminoil Stack Release

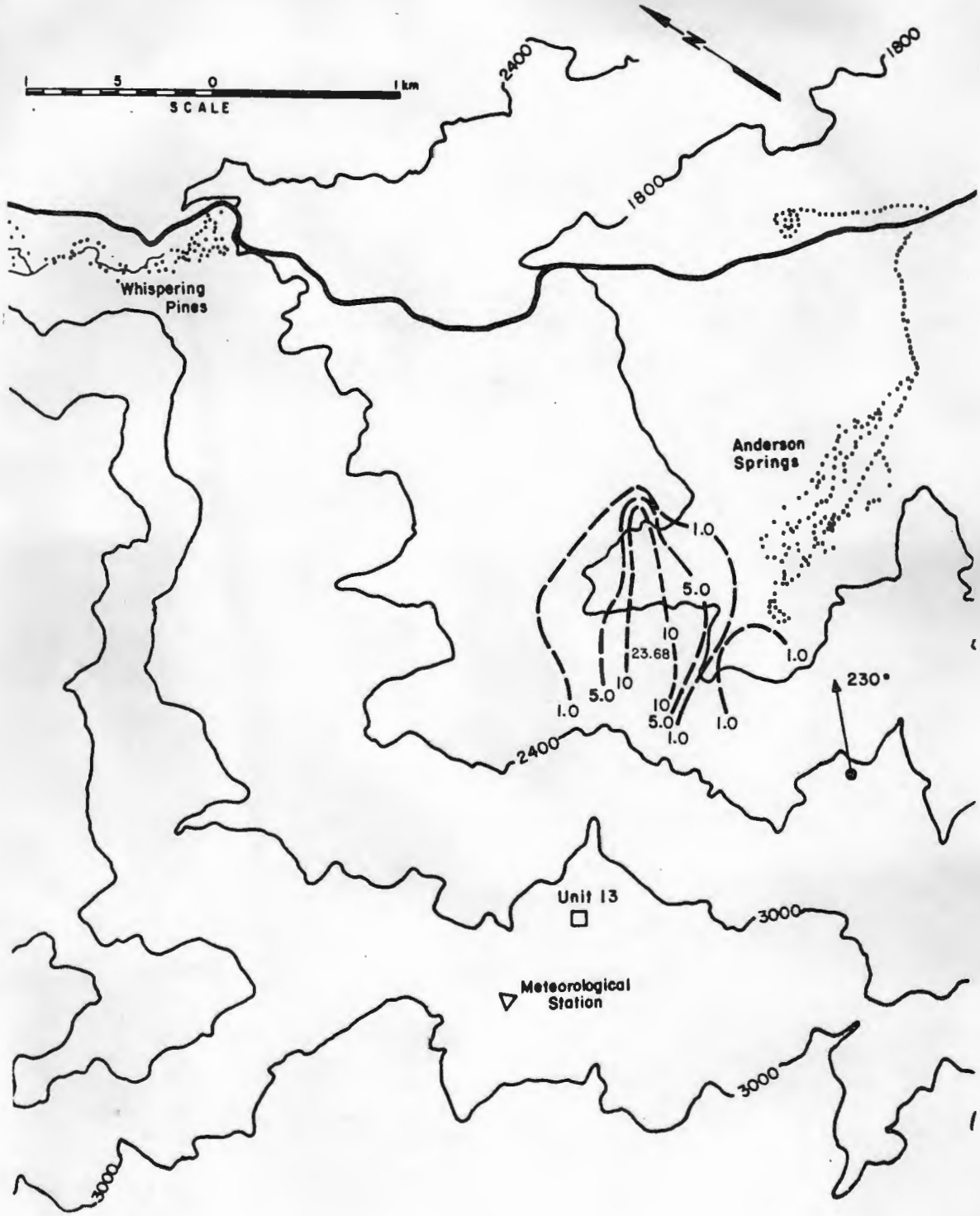

Figure 5.2-18 Isopleths of H_2S Concentrations for a 230° Wind Direction, a 9.4 m/s Wind Speed and a 111.7 m/s Exit Velocity--Aminoil Stack Release

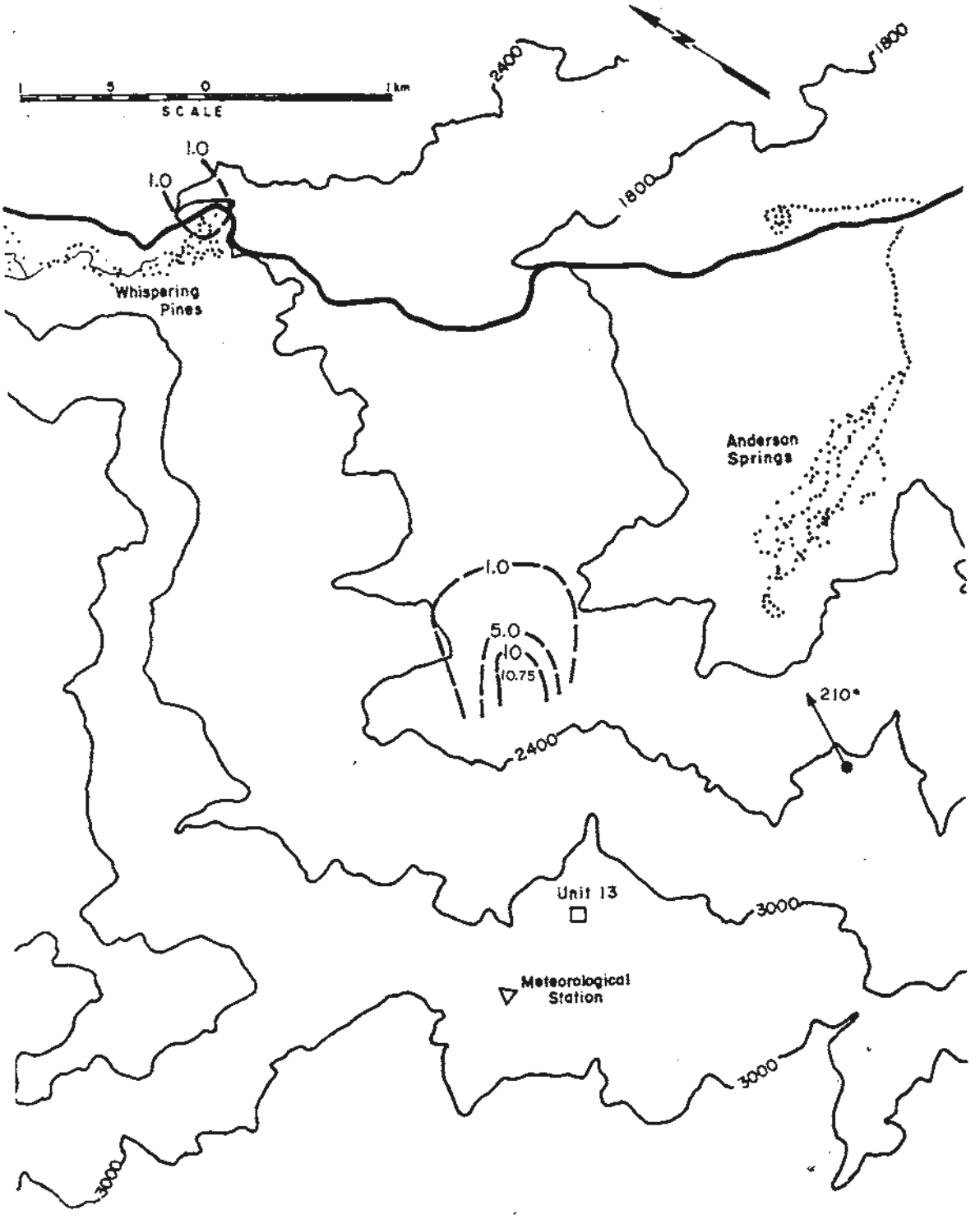

Figure 5.2-19 Isopleths of H_2S Concentrations for a 210° Wind Direction, a 3.1 m/s Wind Speed and a 20.6 m/s Exit Velocity--Aminoil Stack Release

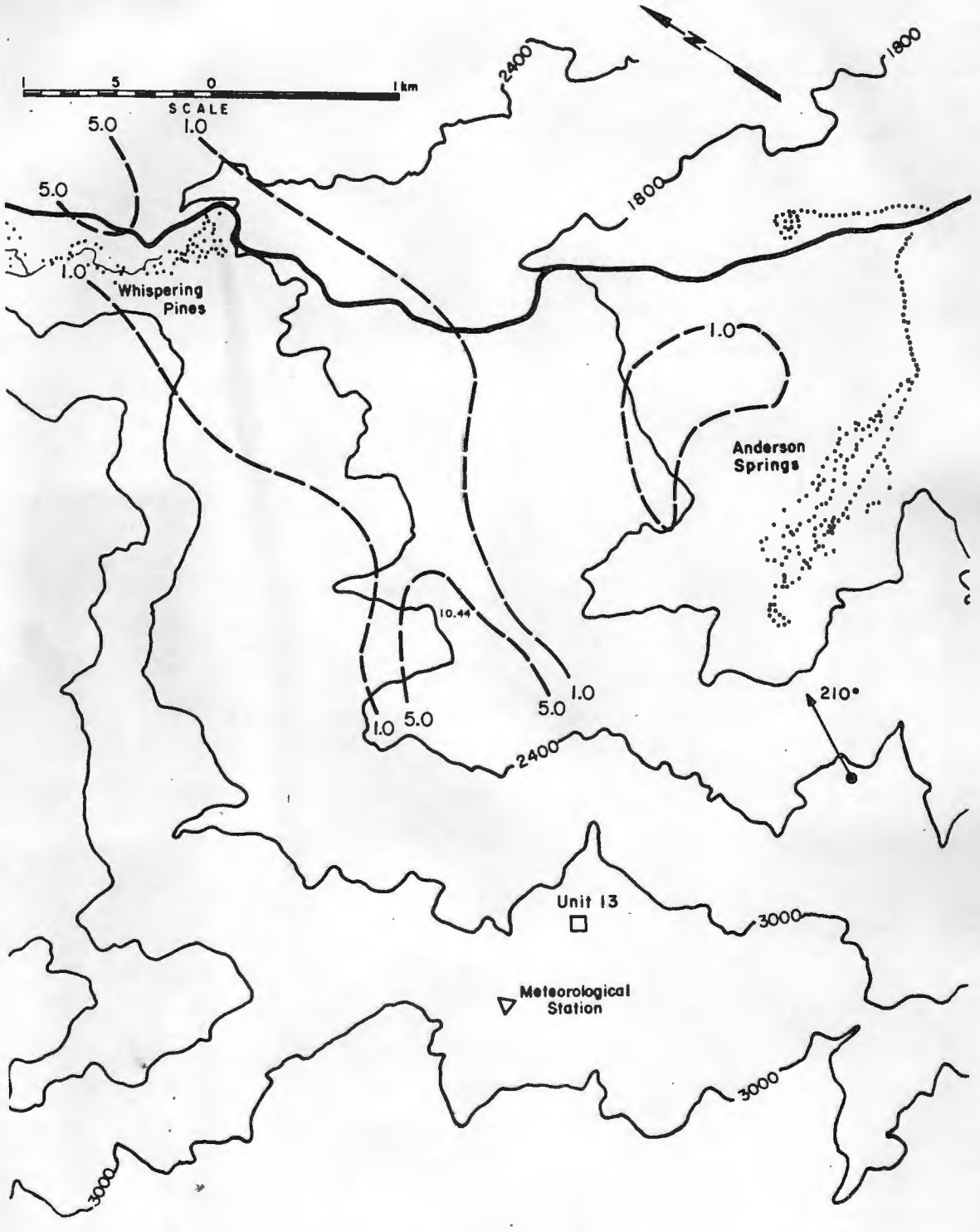

Figure 5.2-20 Isopleths of H_2S Concentrations for a 210° Wind Direction, a 6.2 m/s Wind Speed and a 20.6 m/s Exit Velocity--Aminoil Stack Release

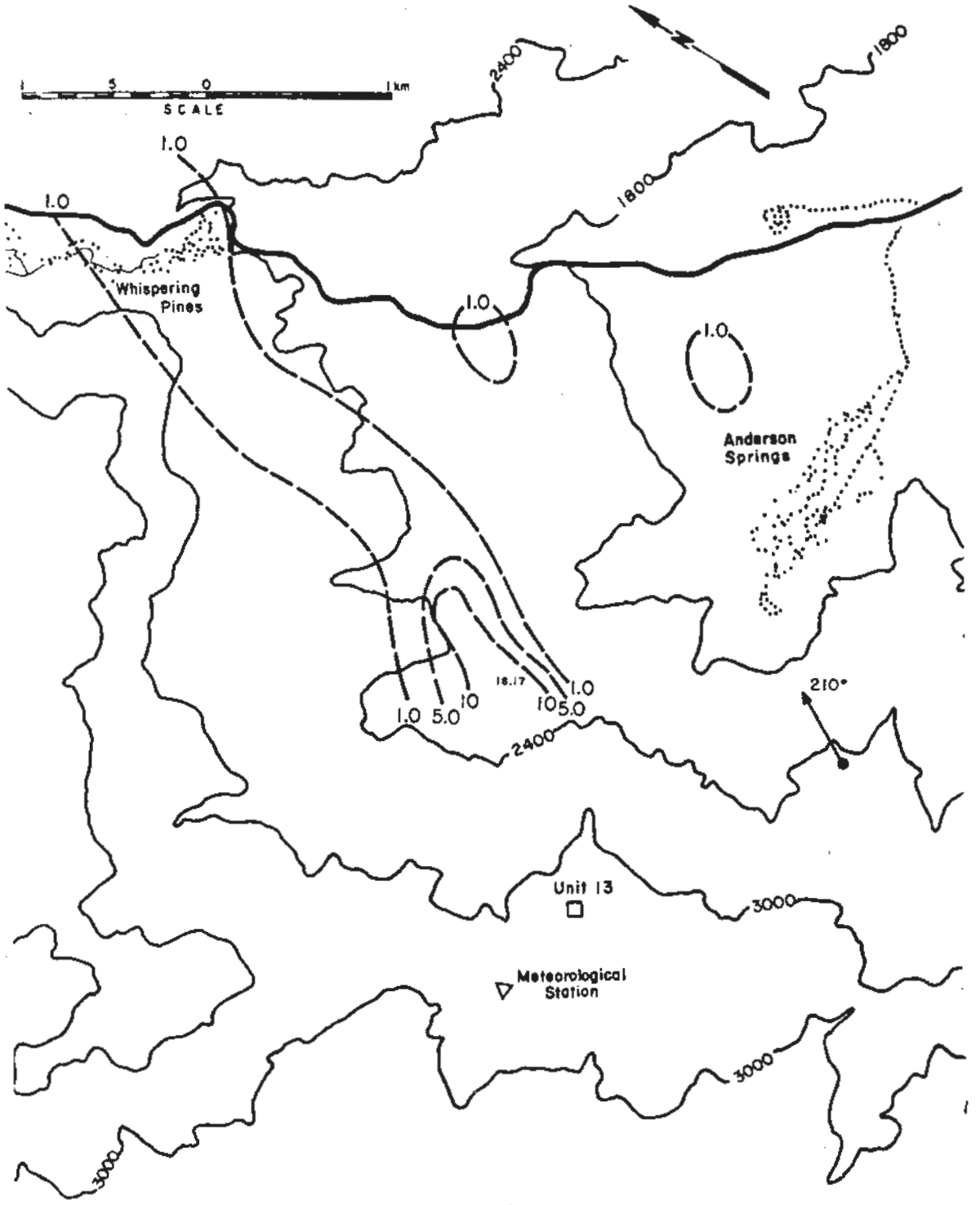

Figure 5.2-21 Isopleths of H_2S Concentrations for a 210° Wind Direction, a 9.4 m/s Wind Speed and a 20.6 m/s Exit Velocity--Aminoil Stack Release

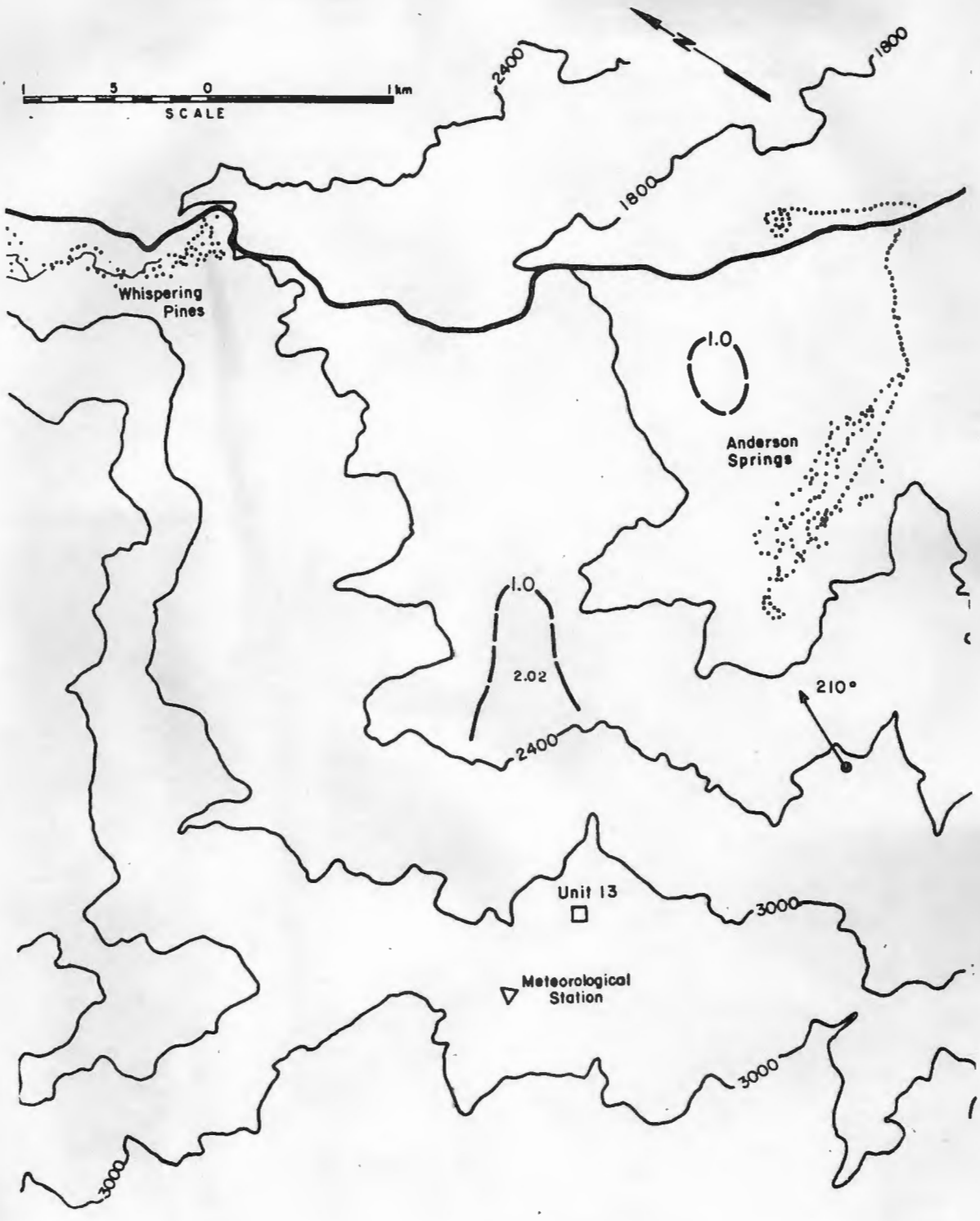

Figure 5.2-22 Isopleths of H_2S Concentrations for a 210° Wind Direction, a 3.1 m/s Wind Speed and a 63.1 m/s Exit Velocity--Aminoil Stack Release

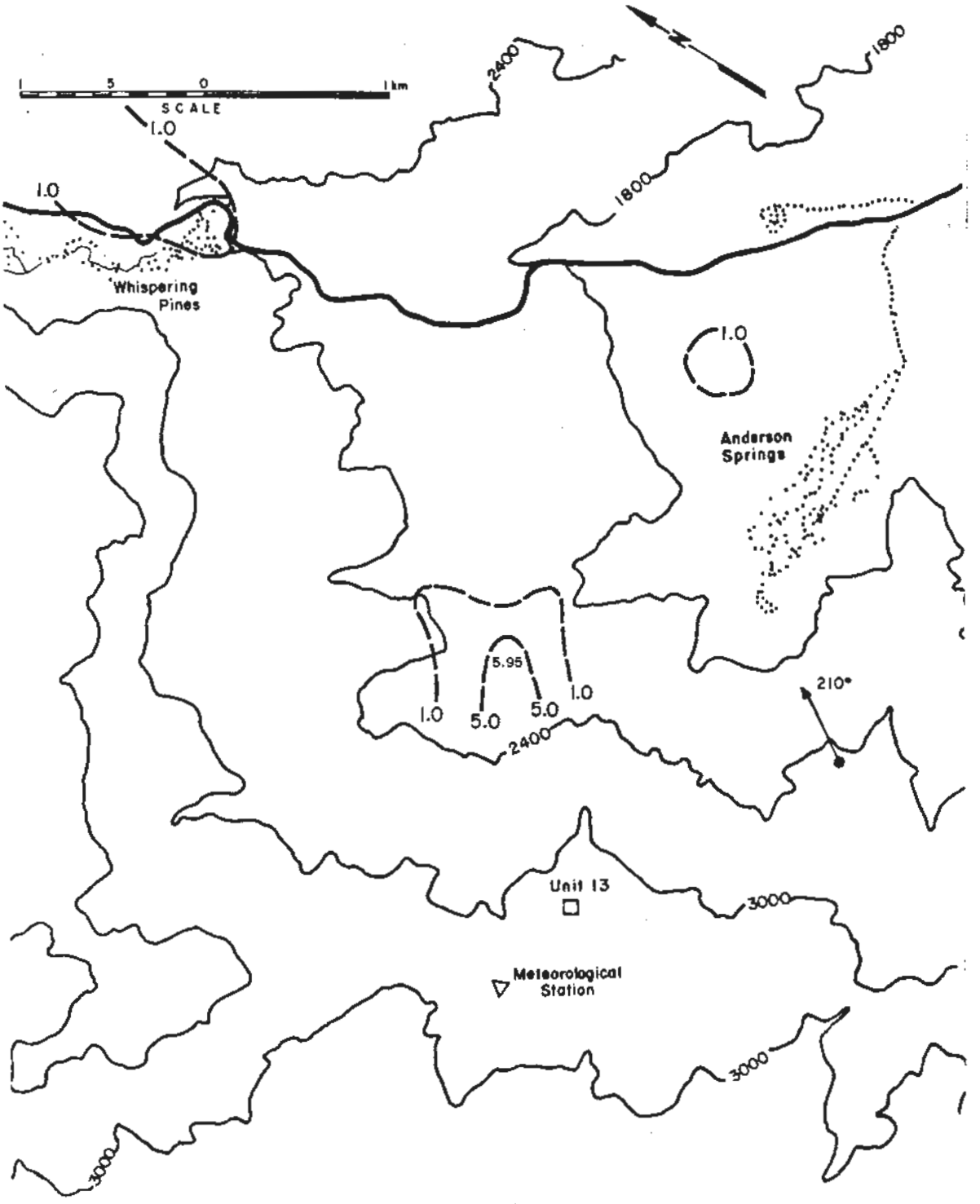

Figure 5.2-23 Isopleths of H_2S Concentrations for a 210° Wind Direction, a 6.2 m/s Wind Speed and a 63.1 m/s Exit Velocity--Aminoil Stack Release

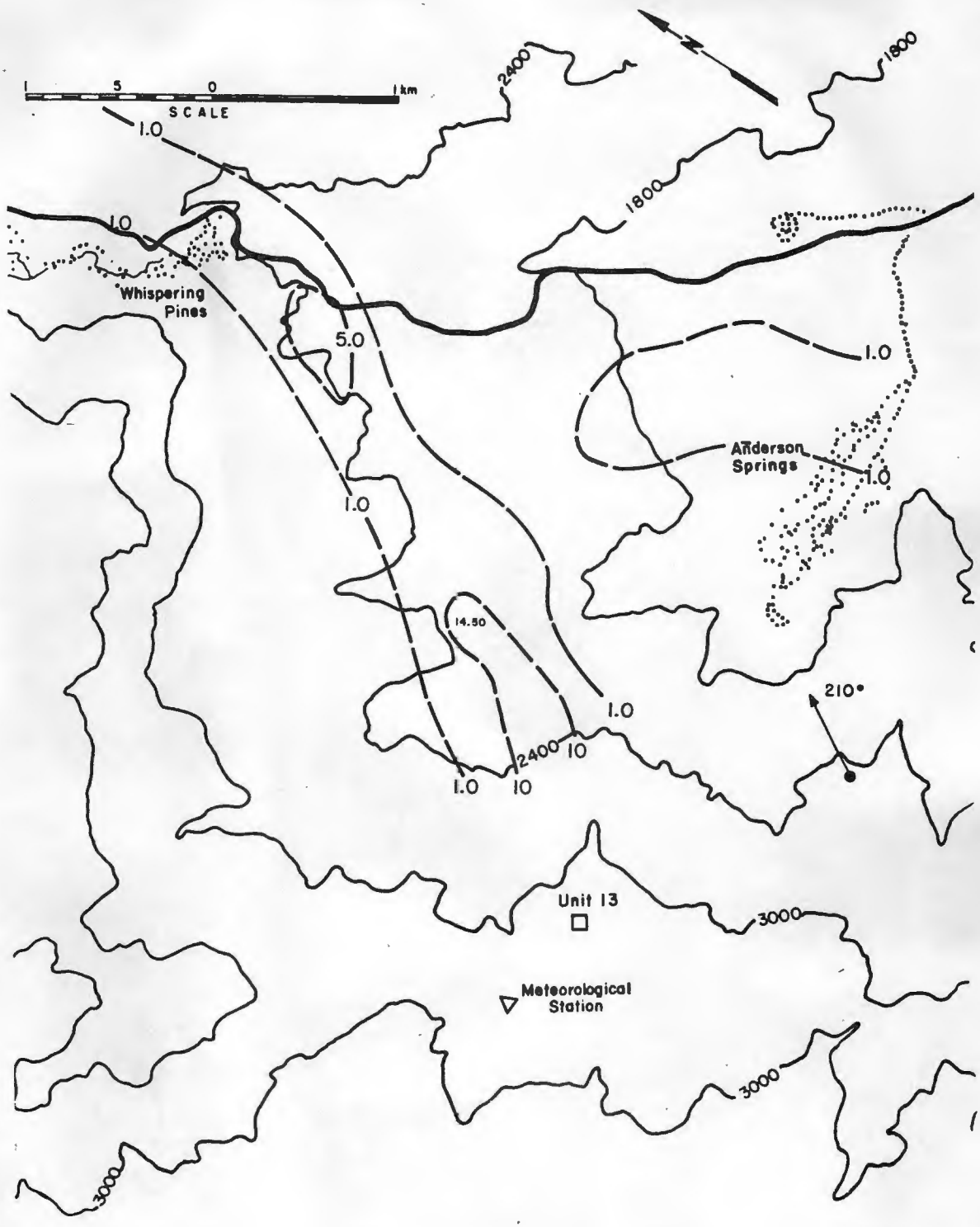

Figure 5.2-24 Isopleths of H_2S Concentrations for a 210° Wind Direction, a 9.4 m/s Wind Speed and a 63.1 m/s Exit Velocity--Aminoil Stack Release

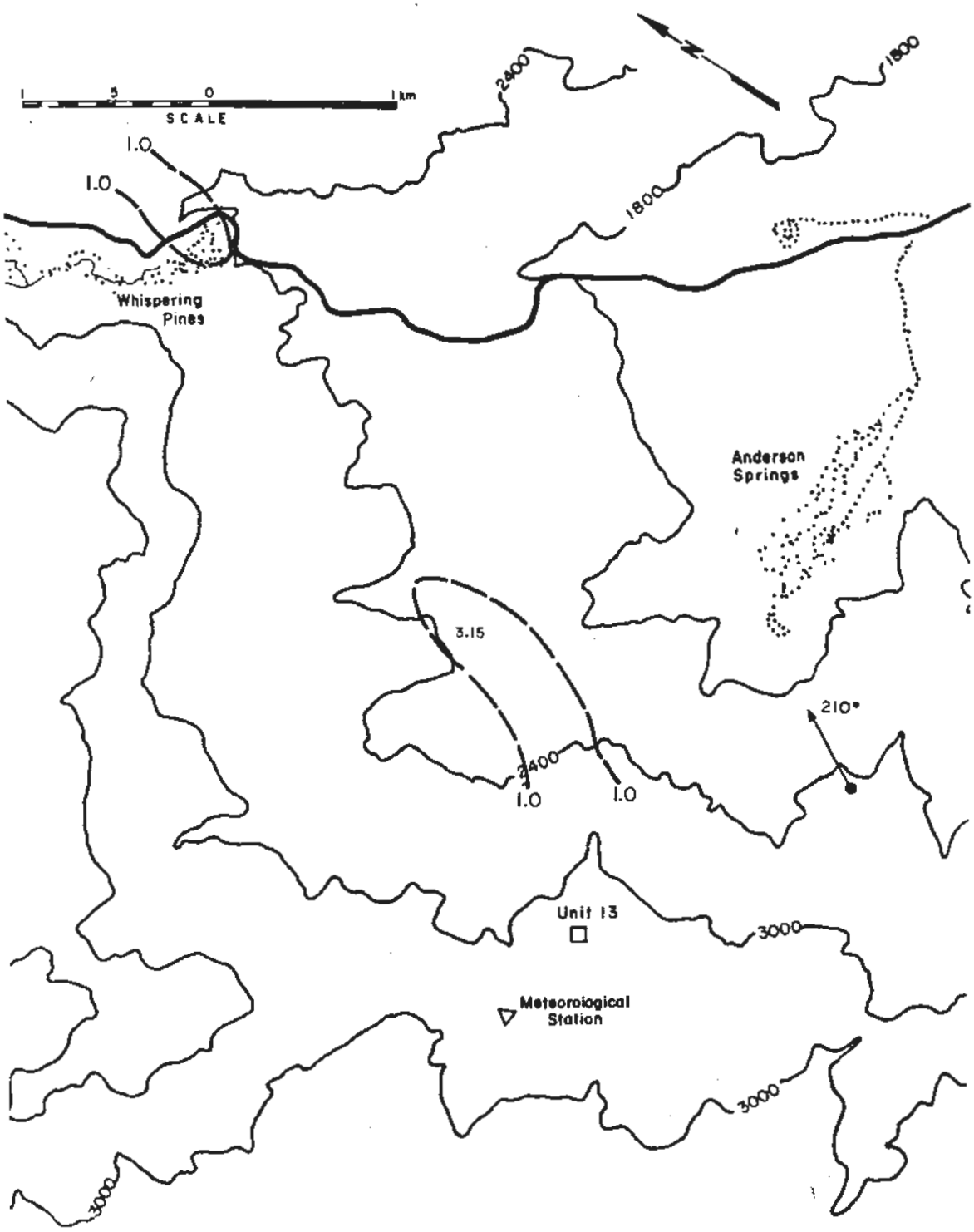

Figure 5.2-25 Isopleths of H_2S Concentrations for a 210° Wind Direction, a 3.1 m/s Wind Speed and a 111.7 m/s Exit Velocity--Aminoil Stack Release

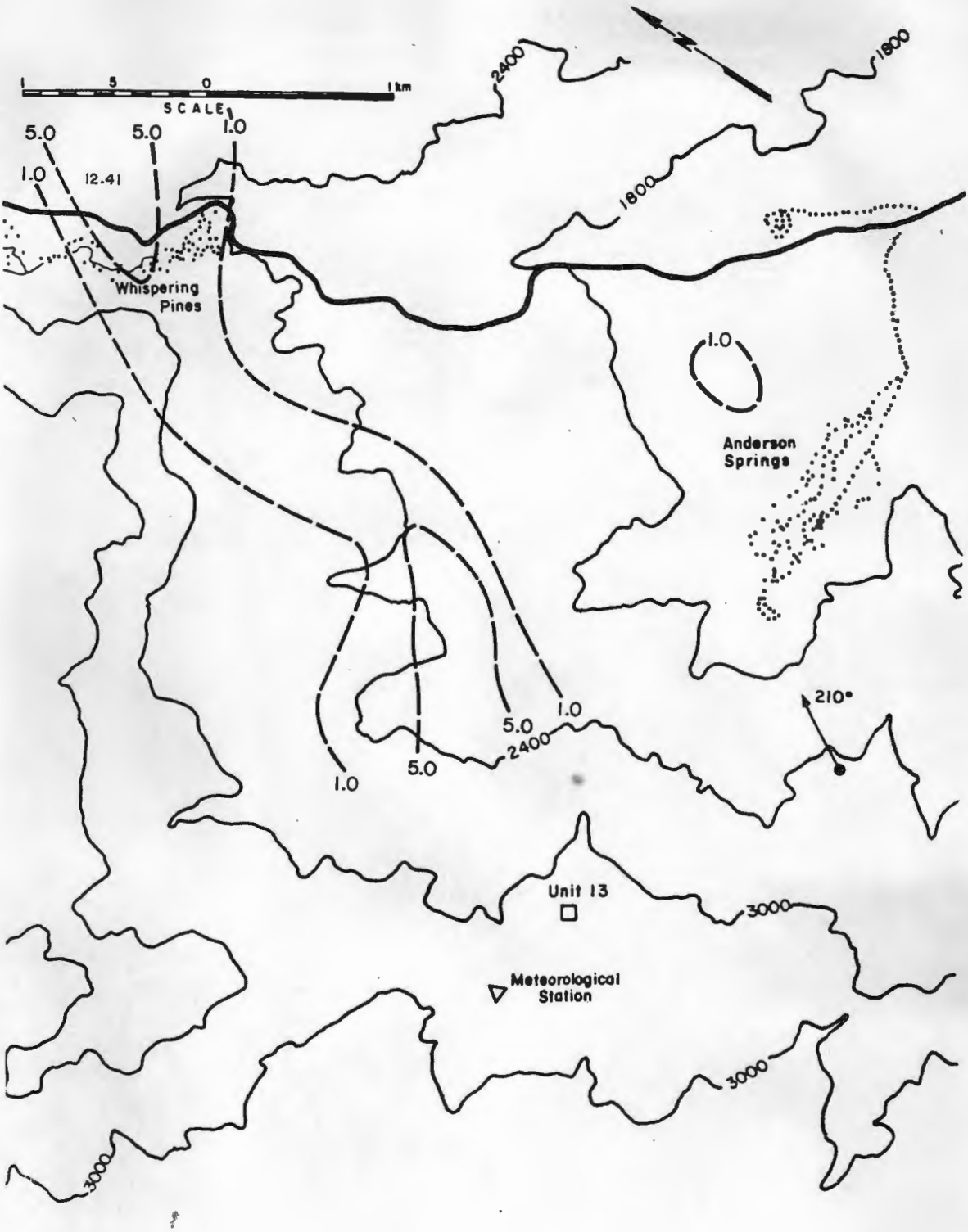

Figure 5.2-26 Isopleths of H_2S Concentrations for a 210° Wind Direction, a 6.2 m/s Wind Speed and a 111.7 m/s Exit Velocity--Aminoil Stack Release

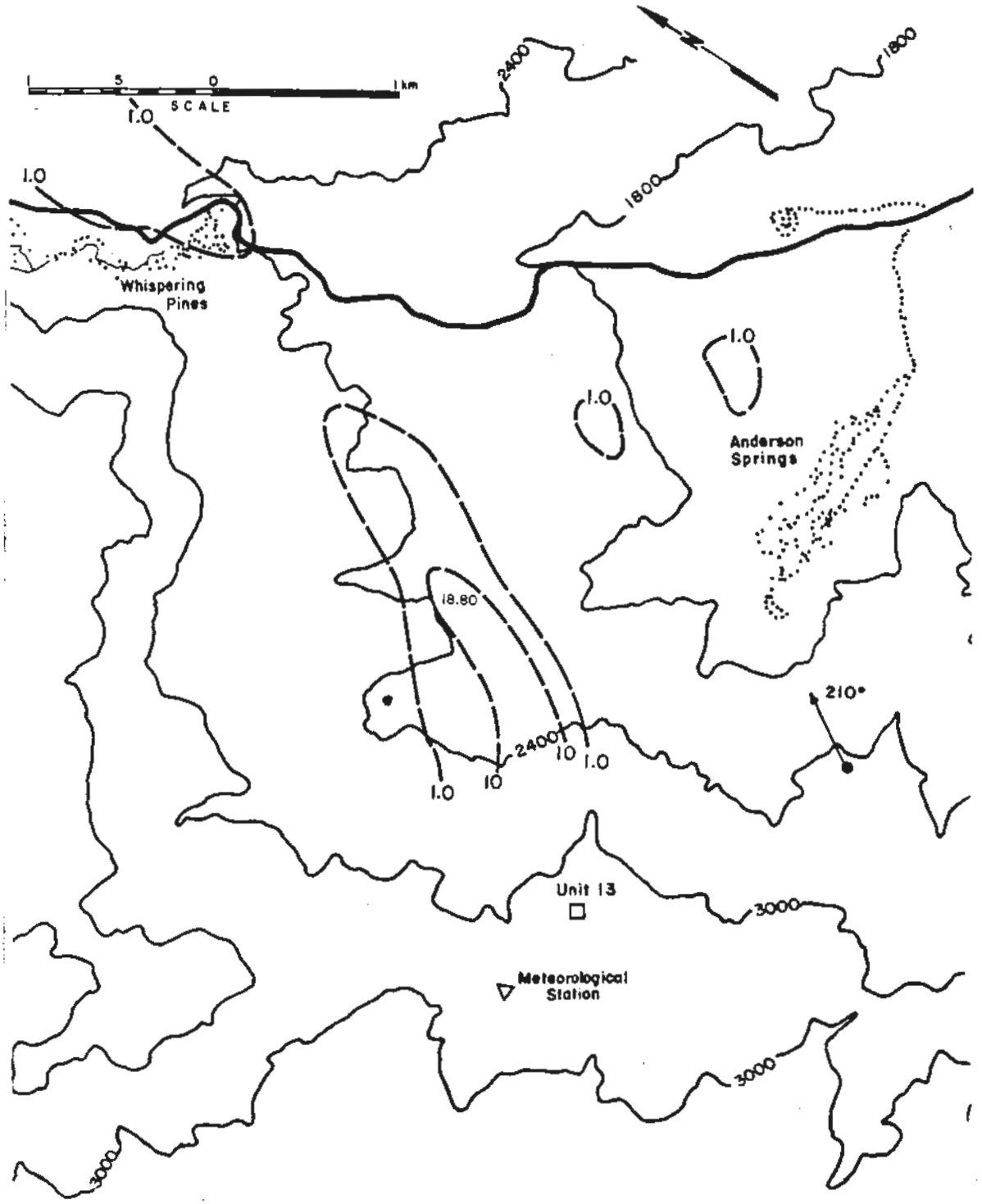

Figure 5.2-27 Isopleths of H_2S Concentrations for a 210° Wind Direction, a 9.4 m/s Wind Speed and a 111.7 m/s Exit Velocity--Aminoil Stack Release

a) 20.6 m/s

b) 63.1 m/s

c) 111.7 m/s

Figure 6.1-1 Surface stack release plume visualization for a 230° wind direction, 9.4 m/s wind speed and exit velocities of a) 20.6 m/s, b) 63.1 m/s, and c) 111.7 m/s.

a) 20.6 m/s

b) 63.1 m/s

c) 111.7 m/s

Figure 6.1-2 Surface stack release plume visualization for a 210° wind direction, 9.4 m/s wind speed and exit velocities of a) 20.6 m/s, b) 63.1 m/s, and c) 111.7 m/s.

a) 20.6 m/s

b) 63.1 m/s

c) 111.7 m/s

Figure 6.1-3 Surface stack release plume visualization for a 210° wind direction, 6.2 m/s wind speed and exit velocities of a) 20.6 m/s, b) 63.1, and c) 111.7 m/s.

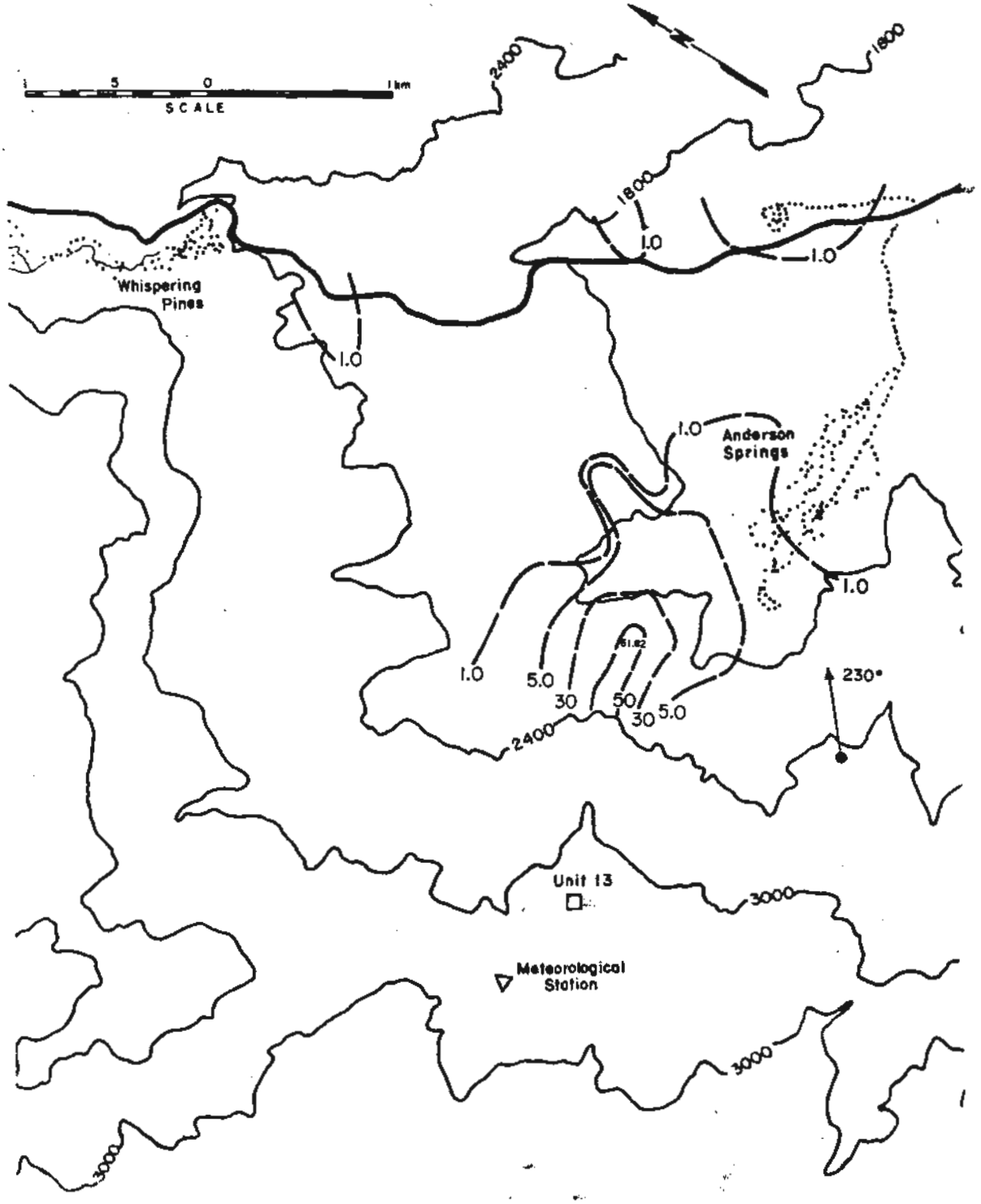

Figure 6.2-1 Isopleths of H_2S Concentrations for a 230° Wind Direction, a 9.4 m/s Wind Speed and a 20.6 m/s Exit Velocity--Aminoil Surface Releases

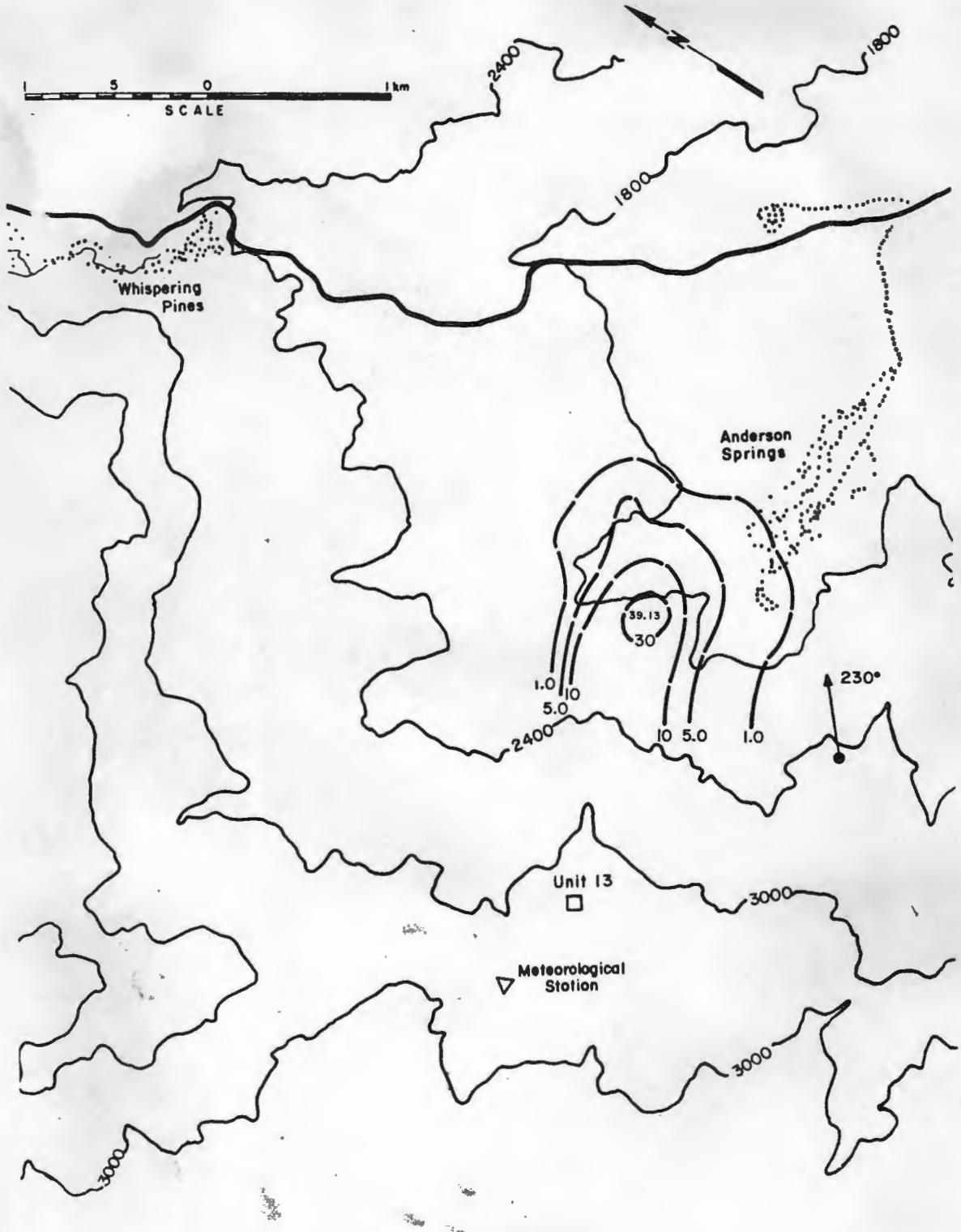

Figure 6.2-2 Isopleths of H_2S Concentrations for a 230° Wind Direction, a 9.4 m/s Wind Speed and a 63.1 m/s Exit Velocity--Aminoil Surface Releases

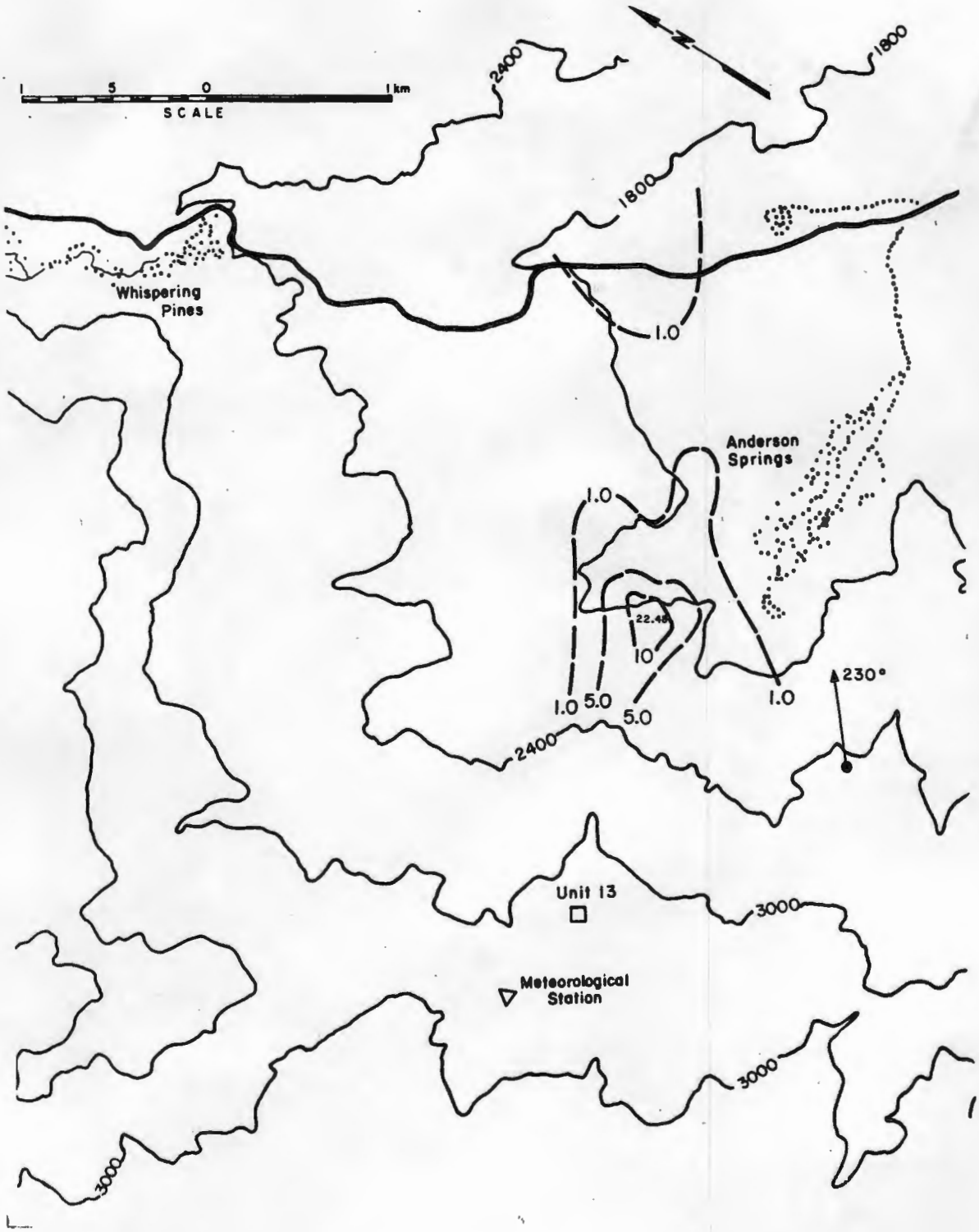

Figure 6.2-3 Isopleths of H_2S Concentrations for a 230° Wind Direction, a 9.4 m/s Wind Speed and a 111.7 m/s Exit Velocity--Aminoil Surface Stack Releases

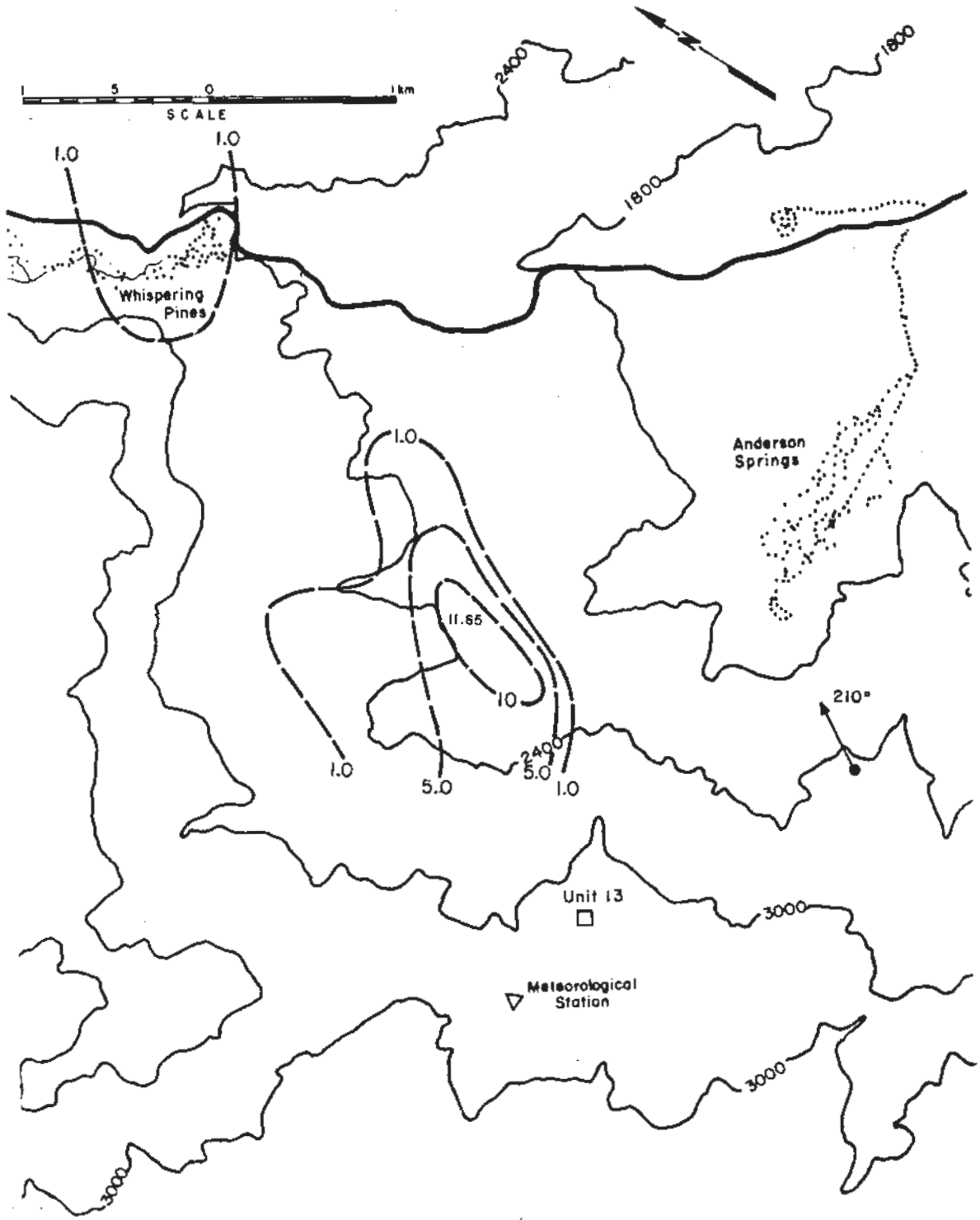

Figure 6.2-4 Isopleths of H_2S Concentrations for a 210° Wind Direction, a 9.4 m/s Wind Speed and a 20.6 m/s Exit Velocity-- Aminoil Surface Stack Releases

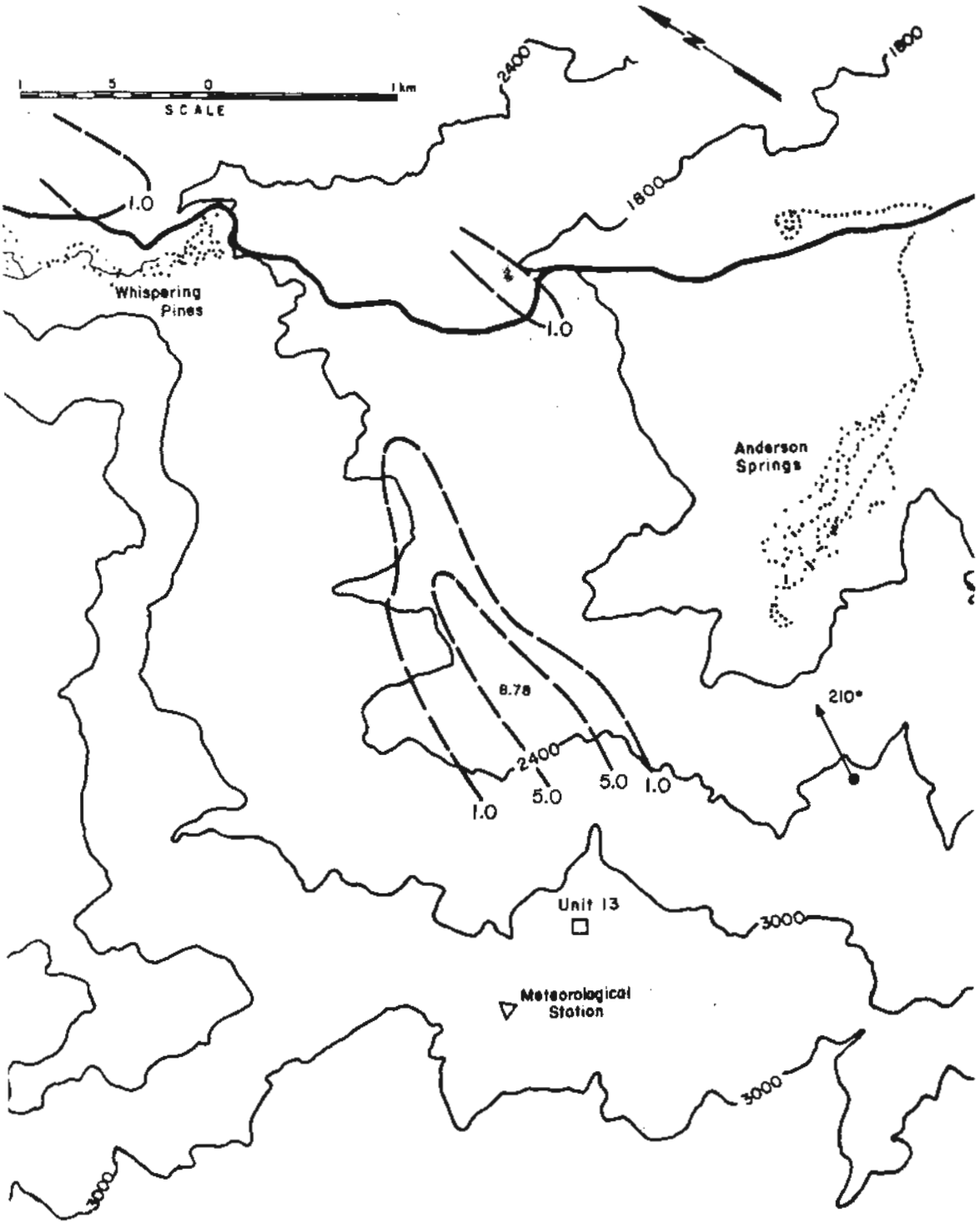

Figure 6.2-5 Isopleths of H_2S Concentrations for a 210° Wind Direction, a 9.4 m/s Wind Speed and a 63.1 m/s Exit Velocity-- Aminoil Surface Stack Releases

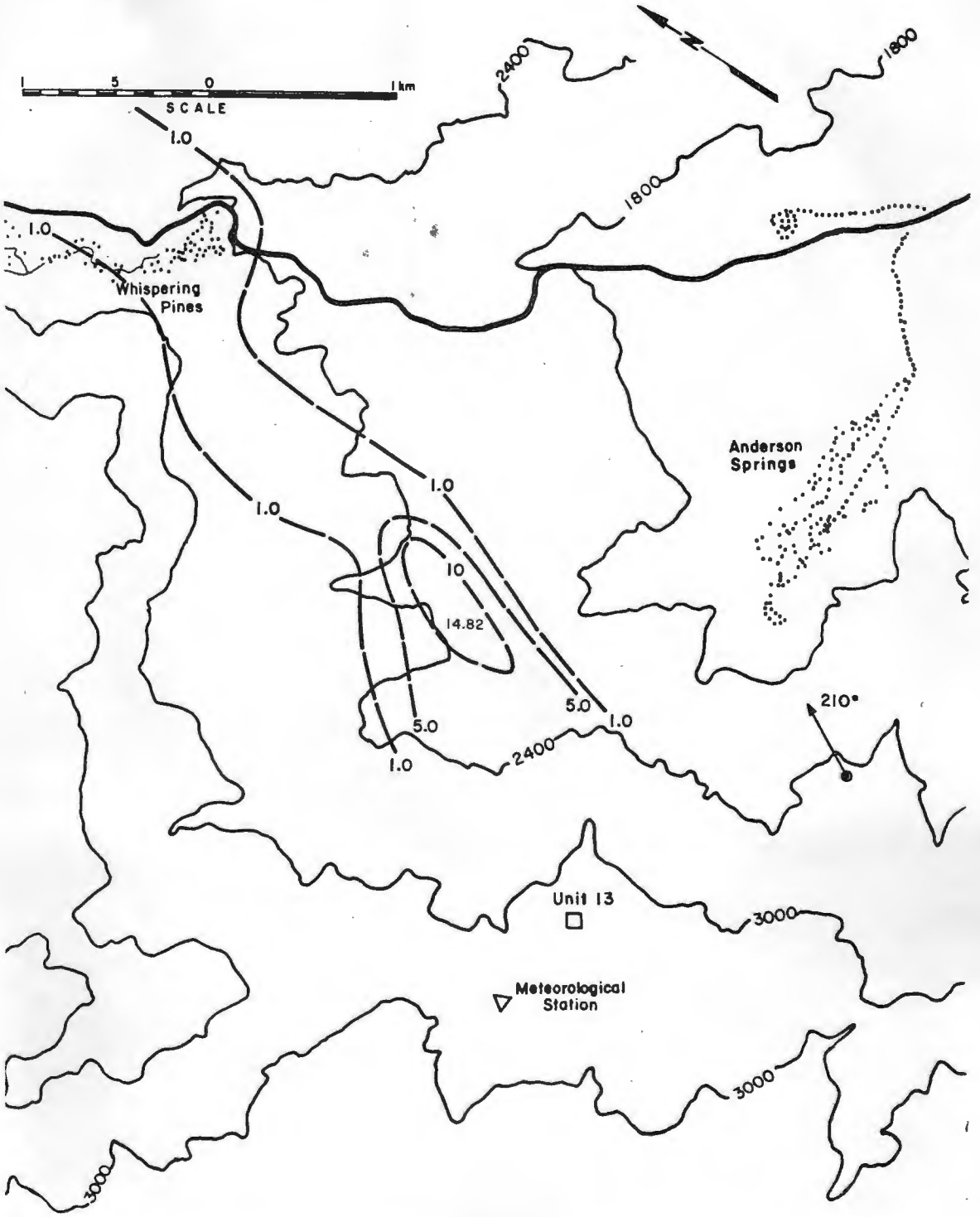

Figure 6.2-6 Isopleths of H_2S Concentrations for a 210° Wind Direction, a 9.4 m/s Wind Speed and a 111.7 m/s Exit Velocity--Aminoil Surface Stack Releases

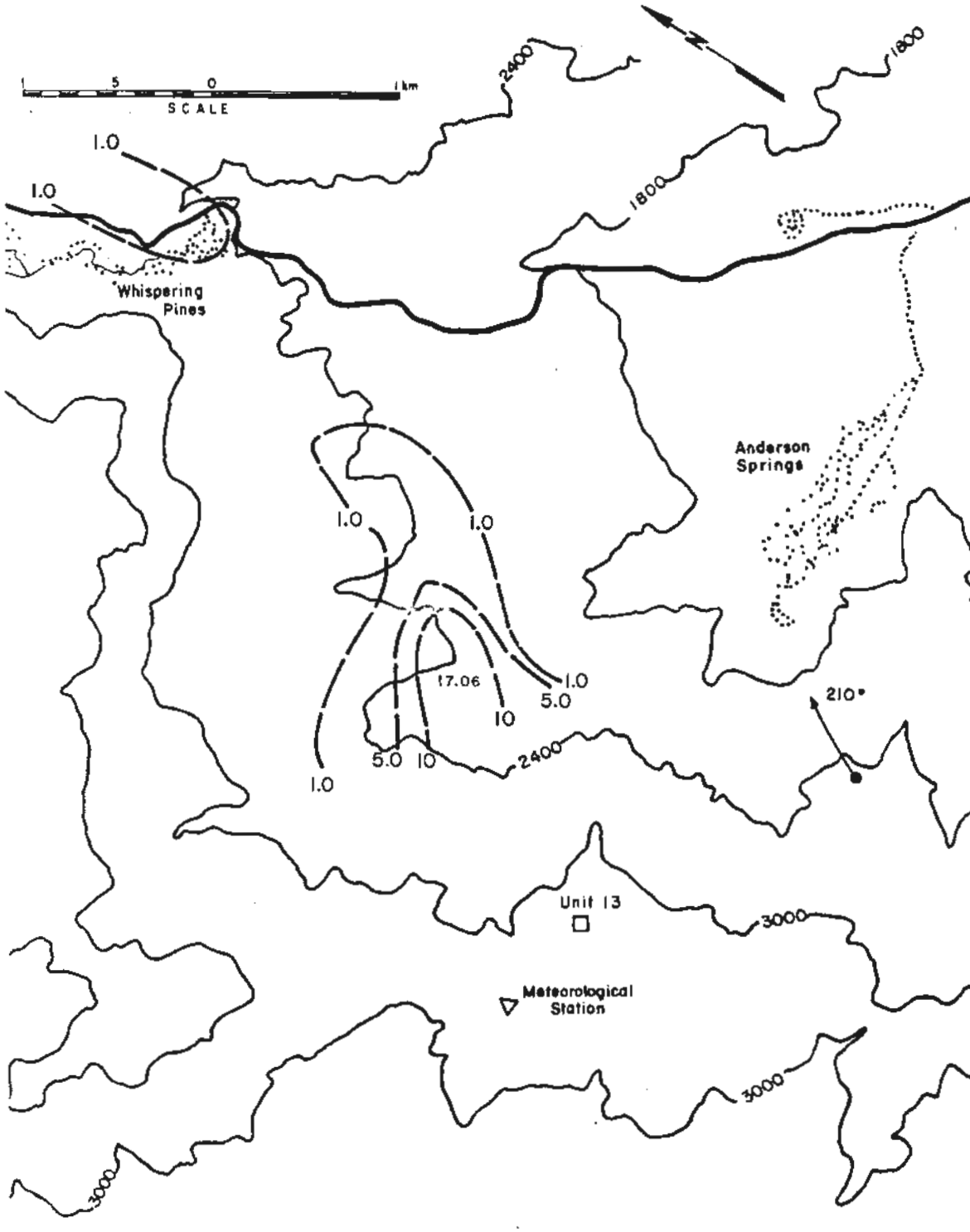

Figure 6.2-7 Isopleths of H_2S Concentrations for a 210° Wind Direction, a 6.2 m/s Wind Speed and a 20.6 m/s Exit Velocity--Aminoil Surface Stack Releases

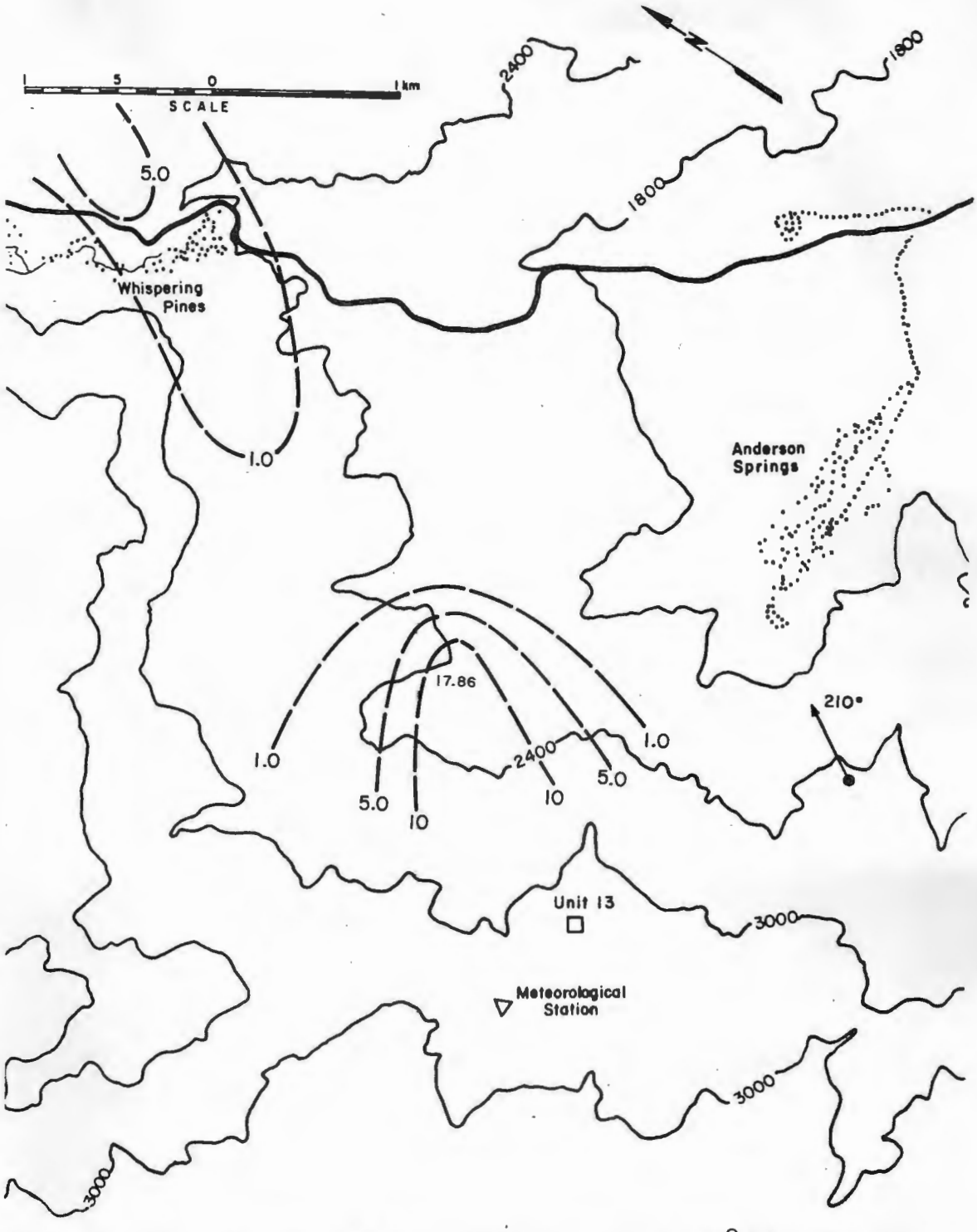

Figure 6.2-8 Isopleths of H_2S Concentrations for a 210° Wind Direction, a 6.2 m/s Wind Speed and a 63.1 m/s Exit Velocity--Aminoil Surface Stack Releases

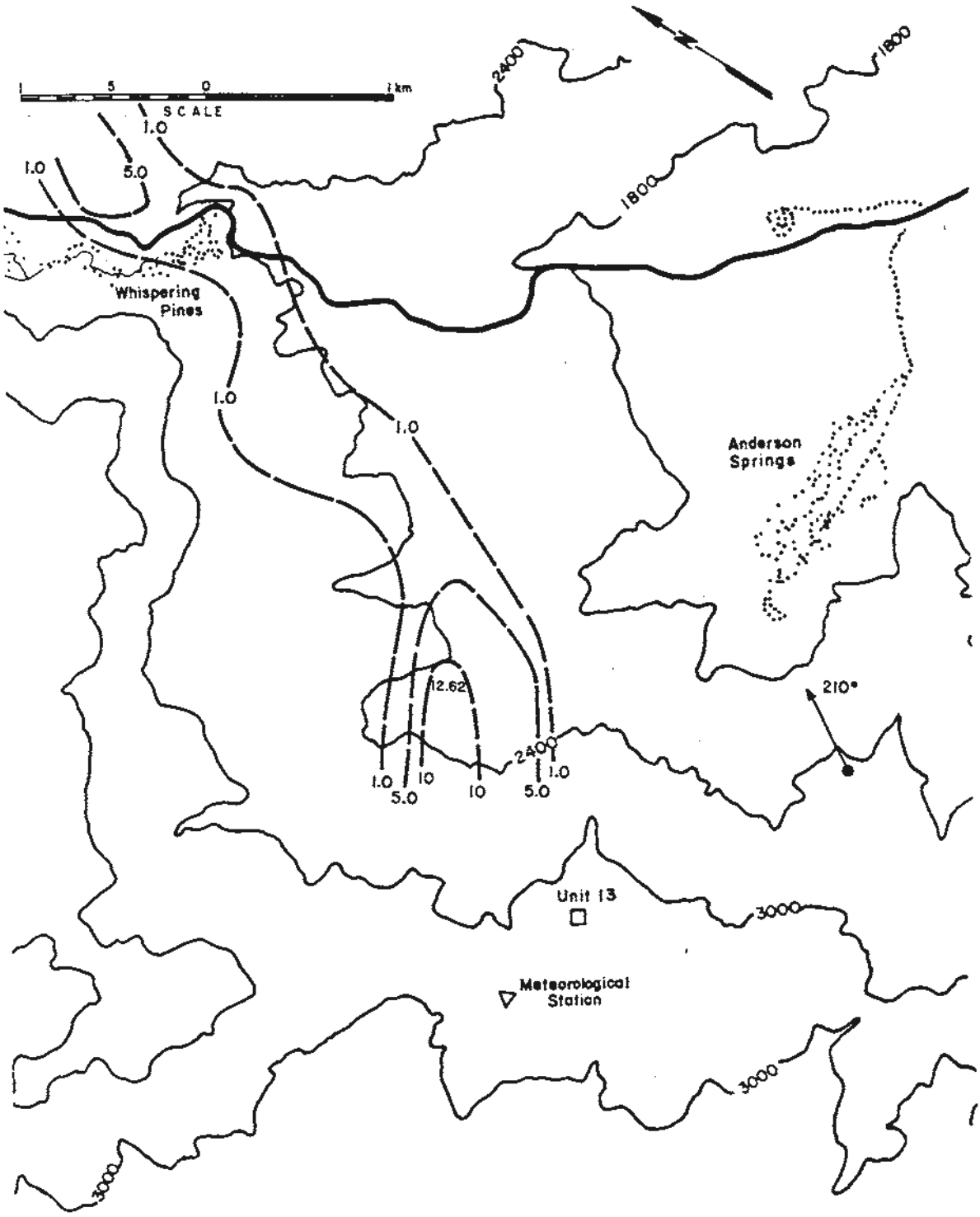

Figure 6.2-9 Isopleths of H_2S Concentrations for a 210° Wind Direction, a 6.2 m/s Wind Speed and a 111.7 m/s Exit Velocity-- Aminoil Surface Stack Releases

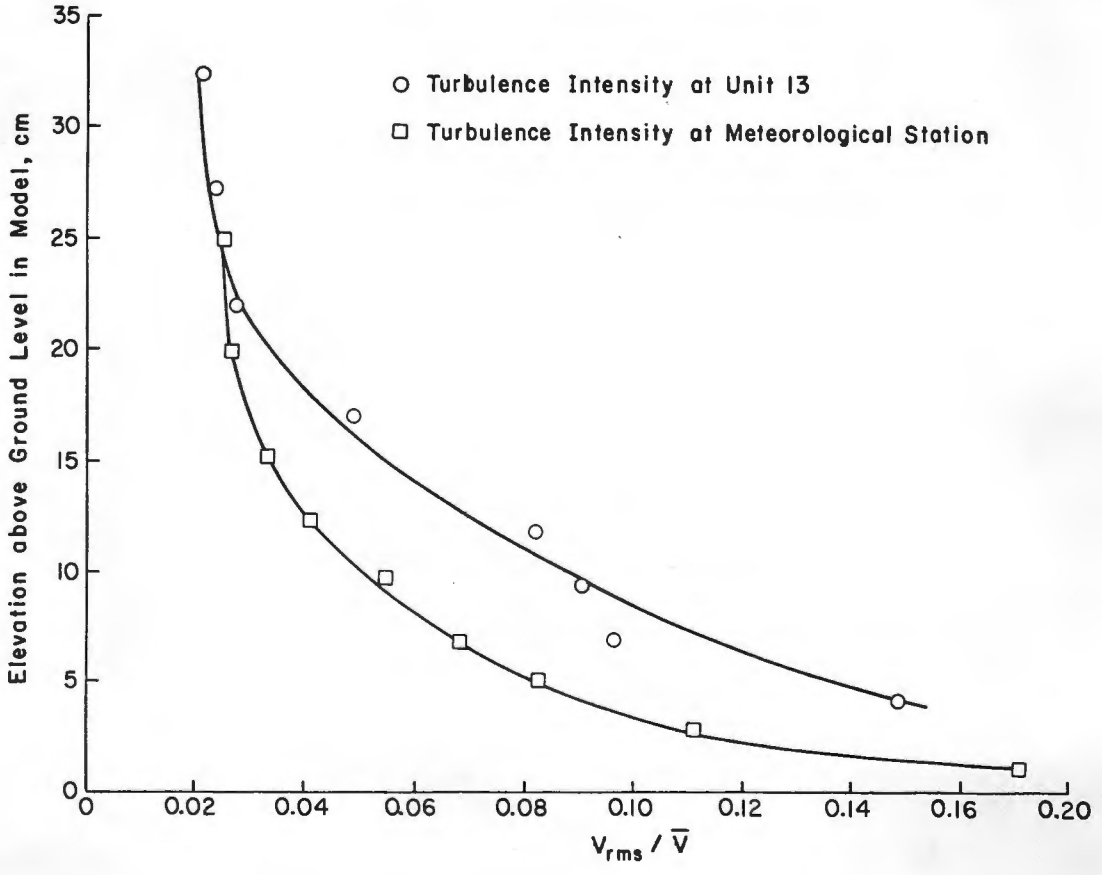

Figure 7.1 Turbulent Intensity at Aminoil Test Site (Unit 13) and Meteorological Station

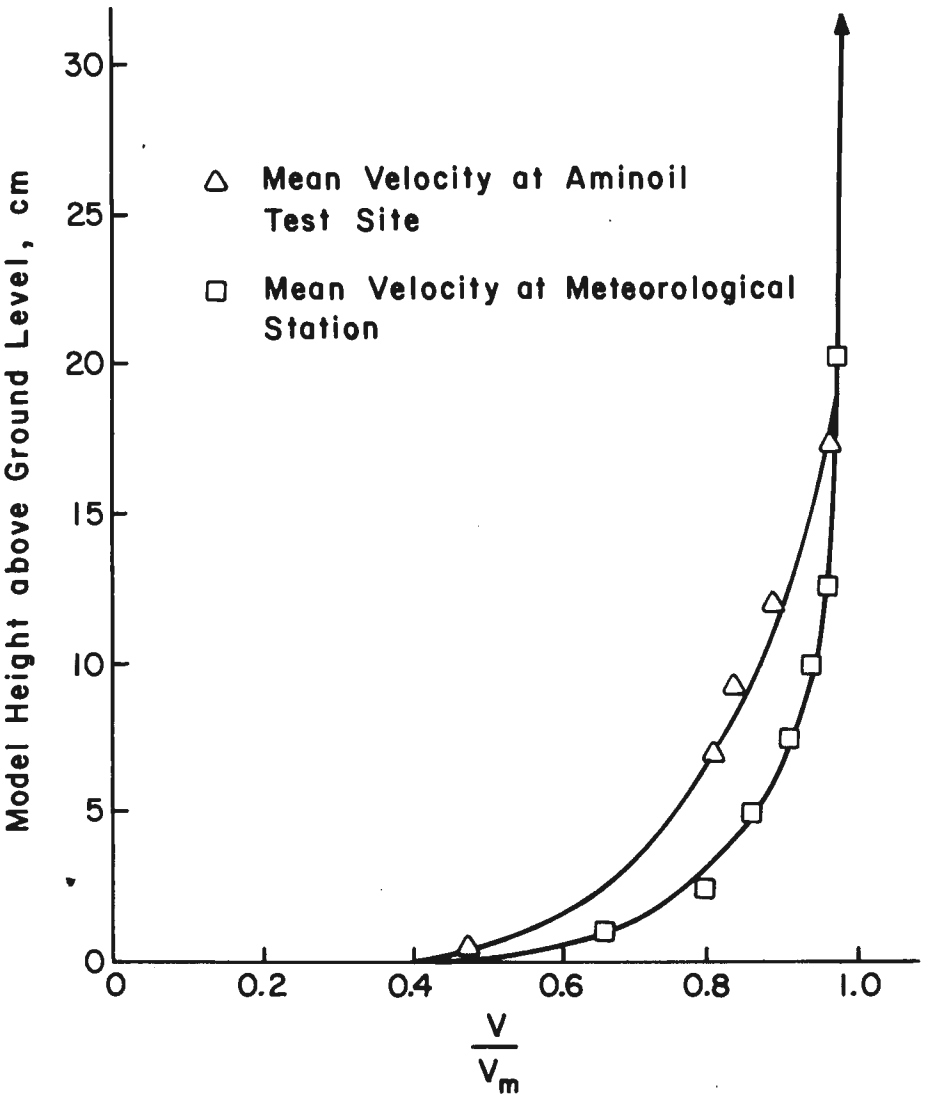

Figure 7.2 Comparison of Mean Wind Tunnel Velocity Profiles at the Aminoil Test Site and the Meteorological Station

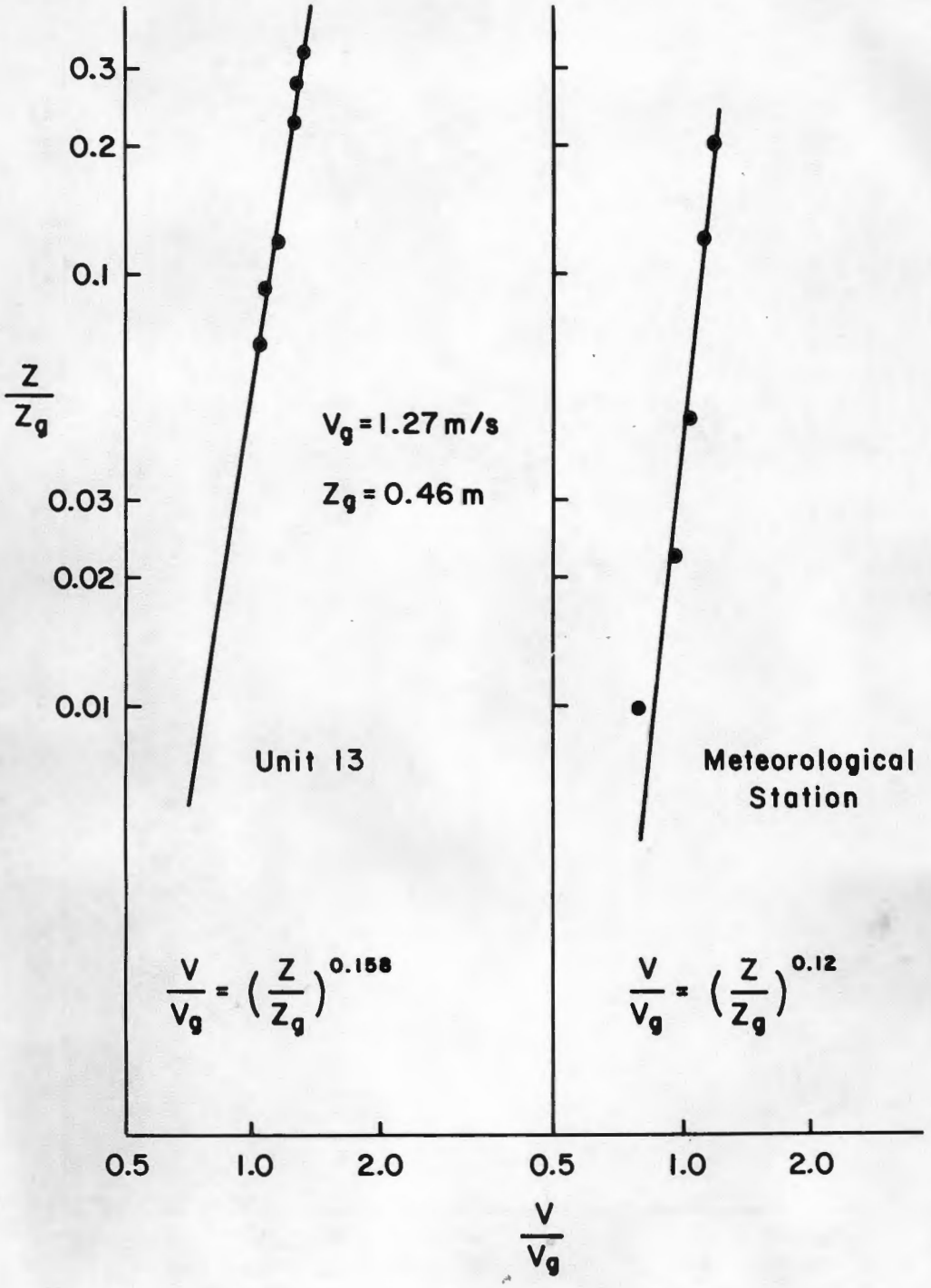

Figure 7.3 Comparison of the Power Laws fitted for the Mean Wind Velocity at the Meteorological Station and the Aminoil Test Site.

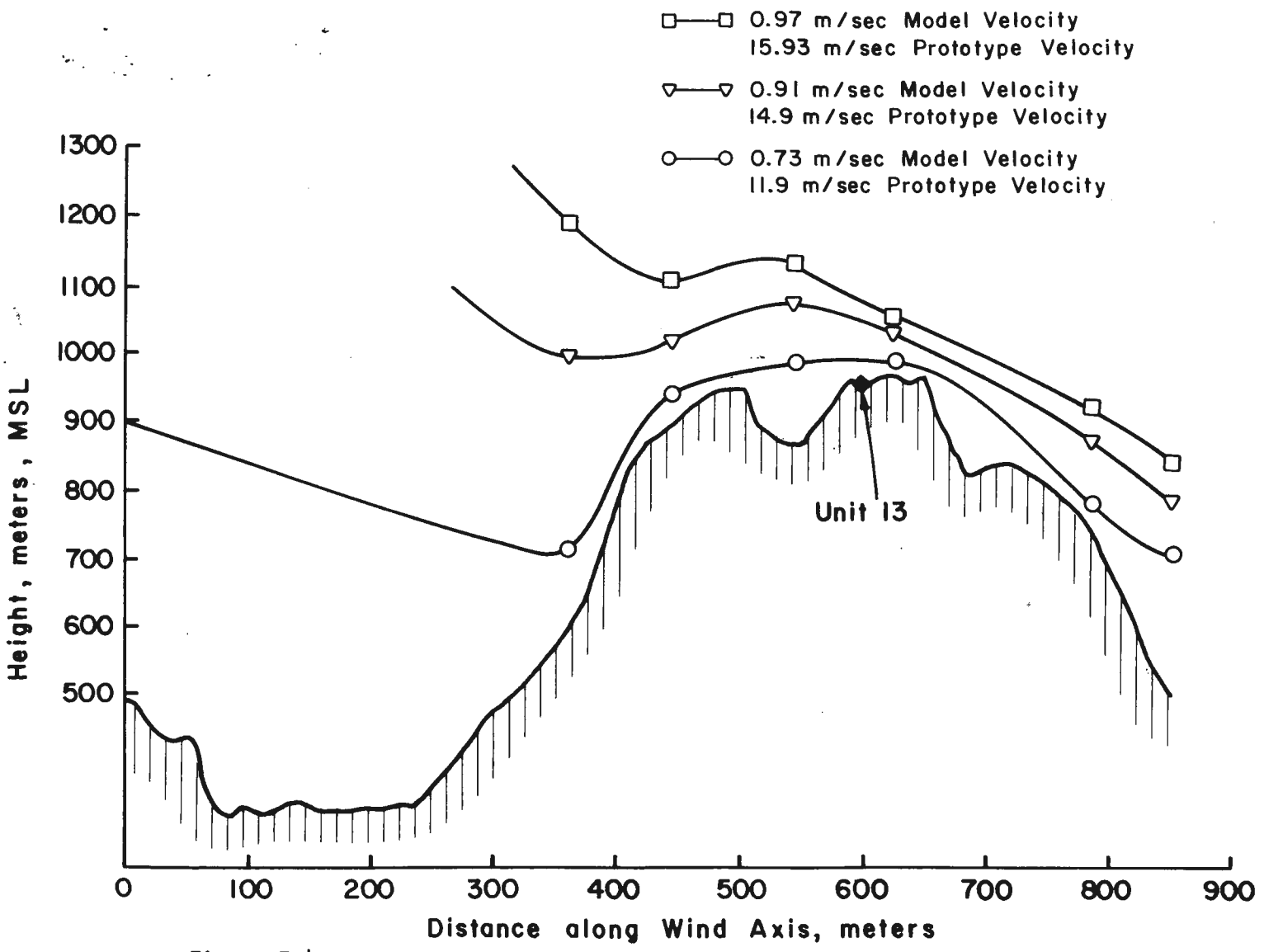

Figure 7.4 Constant Velocity Lines Over the Terrain

a

Figure 7.5 Smoke Wire Velocity Profiles (.05-second intervals) taken at three terrain heights in the Anderson Ridge Vicinity a) 975 m; b) 792 m; c) 719 m

b

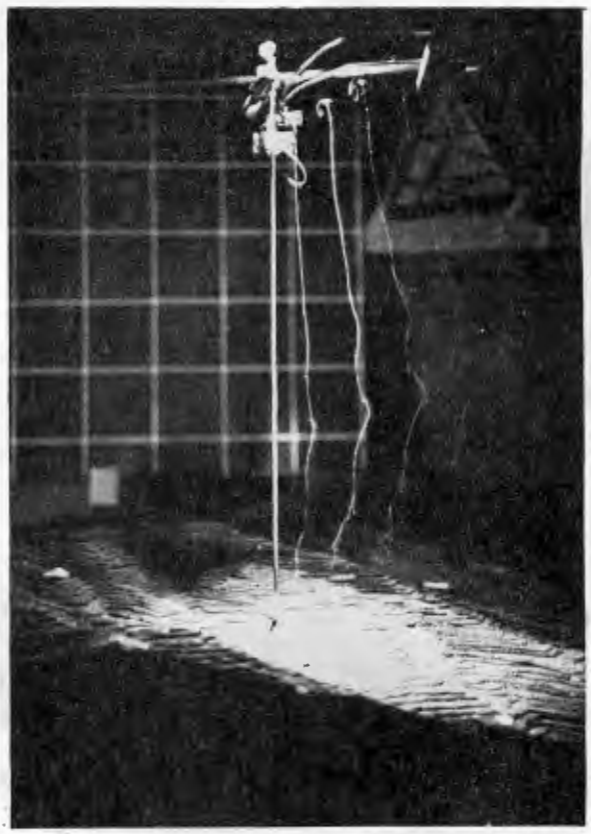

c

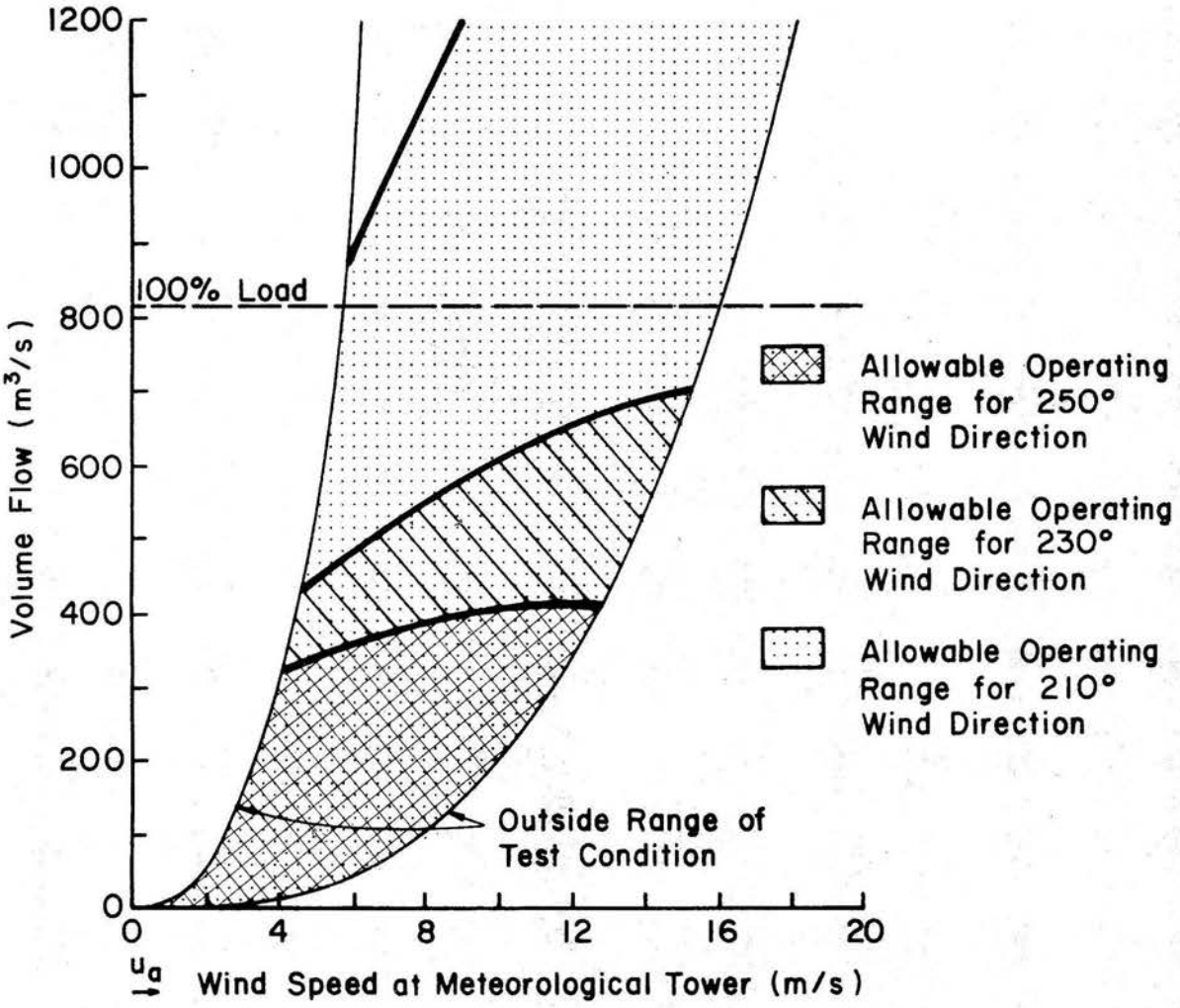

Figure 8.1 Graph Showing Allowable Operating Levels for Unit 13 Stream Venting and 210, 230 and 250° Wind Directions Based on Wind Tunnel Results